University of Torino

Doctoral School of Sciences and Innovative Technologies

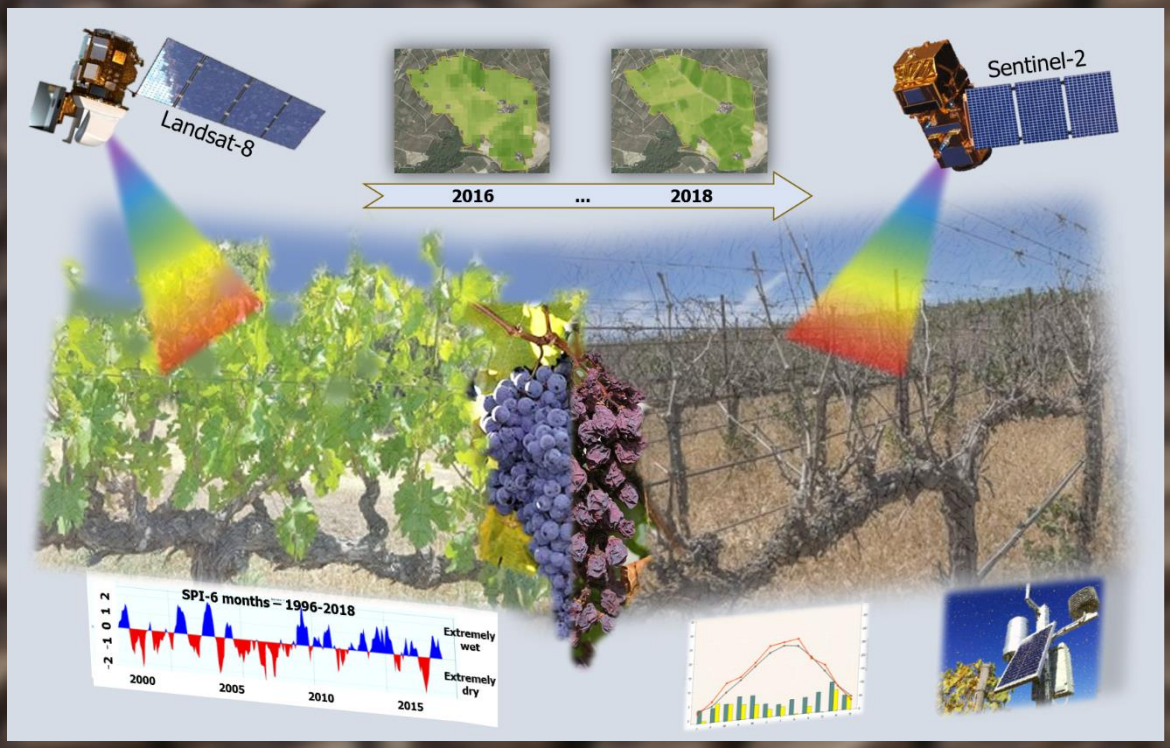

Multi-temporal analyses of drought and its effects on agriculture in different climatic environments using weather stations and satellite imagery

Simone FALZOI

DIPARTIMENTO DI SCIENZE DELLA TERRA
UNIVERSITÀ DEGLI STUDI DI TORINO

EARTH SCIENCES

University of Torino

Doctoral School of Sciences and Innovative Technologies

Doctorate in Earth Sciences
(XXXII Cycle)

Multi-temporal analyses of drought and its effects on agriculture in different climatic environments using weather stations and satellite imagery

Candidate: **Simone Falzoi**

Tutor: **Dott.ssa Simona Fratianni**

Co-Tutor: **Prof. Enrico Corrado Borgogno Mondino**

CONTENTS

ABSTRACT VI

ACKNOWLEDGEMENTS VII

INDEX OF TABLES VIII

INDEX OF FIGURES X

LIST OF ACRONYMS XIII

PUBLICATIONS AND PRESENTATIONS XVI

CHAPTER 1: INTRODUCTION 1

1.1. Context and Research Aims 1

1.1.1. Agriculture and drought 2

1.1.2. Agriculture and climate change 3

1.2. Study goal and focus regions 4

1.2.1. Viniculture, drought and climate change in Piedmont 5

1.2.2. Barbera cultivar 7

1.2.3. Moscato Bianco cultivar 8

1.2.4. Nebbiolo cultivar 8

1.2.5. Terroir 9

1.2.6. Grape Phenology 10

1.2.7. Agriculture, drought and climate change in Ireland 11

1.3. Remote sensing principles 13

1.4. Satellite characteristics 14

1.4.1. MODIS 14

1.4.2. Landsat 8 17

1.4.3. Sentinel-2 18

1.5. Study aims and objectives 21

1.6. Thesis Structure 22

CHAPTER 2: DROUGHT 25

2.1. Definition of Drought 25
2.2. Types of Drought 26
2.2.1. Meteorological drought 26
2.2.2. Agricultural drought 26
2.2.3. Hydrological drought 28
2.2.4. Socio-economic drought 28
2.3. Impact and vulnerability 29
2.4. Early warning system 31
2.5. Trend and Scenarios 32

CHAPTER 3: MATERIAL AND METHODS 35

3.1. Weather stations 35
3.1.1. Weather data: Piedmont 35
3.1.2. Weather data: Sardinia 36
3.1.3. Weather data: Republic of Ireland 37
3.1.4. Weather data: New Brunswick 38
3.2. Quality Control: *ClimPACT2* software 39
3.3. Drought indicators 39
3.3.1. Percent of Normal Index (PNI) 40
3.3.2. Standardised Precipitation Index (SPI) 40
3.3.3. Standardised Precipitation Evapotranspiration Index (SPEI) 40
3.3.4. Soil Moisture Deficit (SMD) 41
3.4. Evapotranspiration 41
3.4.1. Thornthwaite 42
3.4.2. Penman-Monteith 42
3.4.3. Hargreaves 42
3.5. Data production and grape varieties 43
3.6. Remote sensing data 44

3.7. Remote sensing indices 45
3.7.1. Enhanced Vegetation Index (EVI) 45
3.7.2. Normalized Difference Moisture Index (NDMI) 46
3.8. Random Forest missing data algorithm 46
3.9. Gross Primary Production 47

CHAPTER 4: APPLICATION OF *ClimPACT2* SOFTWARE IN TWO DIFFERENT CLIMATIC ENVIRONMENTS 49

4.1. Hydrological drought analysis in Continental Temperate and Mediterranean environment during the period 1981-2017 50
4.2. Introduction 50
4.3. Materials and methods 53
4.3.1. Study area 53
4.3.2. Meteorological data 54
4.3.3. Method 55
4.4. Results and discussion 58
4.5. Conclusion 63

CHAPTER 5: ANALYSIS OF THE SEVERE DROUGHT IN IRELAND IN 2018 65

5.1. Introduction 66
5.2. Datasets 69
5.2.1. Meteorological data 69
5.3. Drought indicators 71
5.3.1. Standardised Precipitation Index (SPI) 71
5.3.2. Percent of Normal Index (PNI) 72
5.3.3. Soil Moisture Deficit (SMD) 73
5.3.4. Enhanced Vegetation Index (EVI) 74
5.3.5. Spatial interpolation 75
5.4. Results 75

5.5. Discussion 79
5.6. Conclusion 80

CHAPTER 6: ANALYSIS OF DROUGHT IN NORTH-WESTERN ITALY AND ITS EFFECTS ON WINE PRODUCTION USING LANDSAT AND SENTINEL SATELLITE IMAGERY 81

6.1. Introduction 82
6.2. Materials and Methods 86
6.2.1. Study area 86
6.2.2. Weather data 87
6.2.3. Drought indices 90
6.2.4. Remote Sensing data 91
6.2.5. Gross Primary Production, GPP 93
6.2.6. Statistical analysis 94
6.3. Results 95
6.4. Discussion 100
6.5. Conclusions 103

CHAPTER 7: DISCUSSION AND CONCLUSIONS 105

7.1. Discussion of methods, findings, and limitations 106
7.1.1. Combining meteorological and satellite data to support decision-making 106
7.1.2. Strengthening tools for monitoring and analysing drought effects 107
7.1.3. Impact of drought on agriculture characterised by local variation 108
7.1.4. Limitations 109
7.2. Conclusions 112
7.2.1. The spatial and temporal distribution of major drought episodes in Continental Temperate, Mediterranean, and Temperate Oceanic climates 113

7.2.2. The effects of water shortage and drought on the productivity of grass pasture in Ireland 114

7.2.3. The effects of drought in vineyards in Piedmont and consequences of water shortage on production of Barbera Moscato Bianco and Nebbiolo grape varieties 114

7.2.4. Data collection and technology development for near-real-time decision support services for winemakers 115

7.3. Recommendations 116

REFERENCES 119

APPENDICES: Supplementary data 137

8.1. Appendix 1. Adaptation plan: New Brunswick 137

8.1.1. Adaptation plan to climate change in the Cocagne watershed, New Brunswick 137

8.1.2. Materials and Methods 138

8.1.3. Annual total precipitation 142

8.1.4. Number of very heavy rain days (10; 20; 30 mm) 145

8.1.5. Growing Degree Days 146

8.1.6. Growing Season Length 148

8.1.7. Heatwave: Number, Magnitude, Amplitude, Duration and Frequency 149

8.1.8. Drought indices, SPI and SPEI 150

8.1.9. Conclusion 152

8.2. Appendix 2. Meteorological Data 154

8.3. Appendix 3. Remote sensing imagery 160

8.3.1. MODIS imagery 160

8.3.2. Landsat 8 imagery 169

8.3.3. Sentinel-2 imagery 173

8.4. Appendix 4. 177

ABSTRACT

Drought is not an instantaneous phenomenon; its effects often take weeks or months to appear. Drought has the greatest consequences, compared to all other natural hazards, in terms of the number of people affected, both directly, i.e. by water scarcity, and indirectly, e.g. due to famine and consequent food shortages. Agricultural activity is inextricably linked with climate change, both as a contributing factor and an aspect of social activity that will be profoundly affected by changes in climate. The specific focus of this study was agricultural drought in the context of climate change, and the development of novel information sources and improvement of existing instruments to provide support for the management and detection of agricultural drought. The study aimed to analyse the effects of drought and water supply in four different climatic conditions represented by four distinct regions: Piedmont (Italy), Ireland (Republic of Ireland), Sardinia (Italy) and New Brunswick (Canada), by combining meteorological data and satellite imagery.

The drought analyses in Piedmont and Ireland regions highlighted the need for meteorological analysis on micro-, meso-, and macro-scales in order to accurately identify the incidence of drought at local and regional levels and analyse the impacts for specific crops. These analyses were strengthened using satellite data which enabled evaluation of the evolution of drought episodes.

In Sardinia and New Brunswick, the study assessed the application of the tools used to examine agricultural drought conditions, in the context of other water supply challenges, including hydrological drought (Sardinia) and flood risk (New Brunswick).

This study clearly showed the value of combining different geo-physical data sources, i.e. meteorological and satellite data, for the analysis of precipitation events and their impacts. This study contributed to the development of knowledge and techniques that can be applied to achieve near-real-time monitoring of drought impacts in agriculture, e.g. regional maps of drought evolution and crop-specific impacts. The findings provide improved decision-making support that can help farmers, agricultural technicians and advisory services, and policymakers to plan for and adapt to changing climatic conditions.

***Key words**: Enhanced Vegetation Index, Normalised Difference Moisture Index, Gross Primary Production, Drought indices, grape varieties, climate change adaptation.*

ACKNOWLEDGEMENTS

...so, another period ends, a beautiful and deep period, rich in experiences and encounters, mates and wonderful people who helped me to make it special.

I would like to sincerely thank several people who helped me along this PhD journey:

my supervisor, Prof. Simona Fratianni, for all her support, guidance, encouragement and motivation over the last three years, and especially for her empathy during a challenging time in my life.

Dr. Stuart Green and his Spatial Teagasc Group, from Dublin, for their advice on remote sensing, for their interest in this work, for the willingness to revise this dissertation and useful suggestions to improve it.

Dr. Emily Gleeson, from Research, Environment and Applications Division, Met Éireann, Dublin, for precious tips and advices on climate data.

Dr. Enrico Corrado Borgogno Mondino, Assistant Professor in Geomatics, Dept. of Agriculture, Forest and Food Sciences and Andrea Lessio for introducing me to the geomatics' world.

The 3a group: Massimo de Marziis, Emanuela Forni, Laura Alemanno, Gianmaurizio Menconi for their essential job to collect weather data, and, over all, for their friendship.

Dr. Federico Spanna, Irene Vercellino and Tiziana la Iacona from Piedmont Region, Phytosanitary Service, Agrometeorology Sector, for their suggestion about vineyard.

Dr. Guillaume Fortine for his suggestion on the research topic during the Canadian adventure.

My family and my grandparents who allowed me to reach this important result, thanks to their patience shown over these years and for all the moral and material support that they have always given me.

All my frieds, for being there.

The Irish people that always make me feel at home.

Last but not least, a really special thanks to Tracey (and the "pen") for the precious suggestions and tips, and for all her inexhaustible support.

INDEX OF TABLES

TABLE 1 MODIS SPECTRAL BANDS 16

TABLE 2 LIST OF SPECTRAL BANDS OF LANDSAT 8 OPERATIONAL LAND IMAGER (OLI) AND THERMAL INFRARED SENSOR (TIRS), WITH RANGE OF WAVELENGTH AND SPATIAL RESOLUTION. 18

TABLE 3 LIST OF SPECTRAL BANDS OF SENTINEL-2, WITH CENTRAL WAVELENGTH, BANDWIDTH AND SPATIAL RESOLUTION. 19

TABLE 4 CLASSIFICATION OF THE WET AND DROUGHT PERIODS OF SPI AND SPEI, ACCORDING TO MCKEE *ET AL*. (1993) AND VICENTE-SERRANO *ET AL*. (2010), RESPECTIVELY. SPI AND SPEI INDICES ARE DIMENSIONLESS. 57

TABLE 5 WEATHER STATIONS LIST ANALYSED IN PIEDMONT AND SARDINIA REGIONS FOR THE REFERENCE PERIOD 1981-2010, WITH THEIR VALUES OF ELEVATION (ALT. M A.S.L.), COORDINATES (LAT N; LON E), THE CALCULATED SPI AND SPEI ANNUAL TRENDS (YEAR^{-1}) AT 12 MONTHS, ANNUAL TOTAL WET-DAY (PRECTOT), TOTAL ANNUAL P FROM HEAVY RAIN DAYS (R95P), AMOUNT OF HOT DAYS (T_X90P), AND AMOUNT OF HOT NIGHTS (T_N90P) AT 12- MONTH TIME SCALE. STATISTICALLY SIGNIFICANT TRENDS WITH A P VALUE ≤ 0.05 ARE INDICATED IN BOLD. 59

TABLE 6 CLASSIFICATION OF WET AND DROUGHT PERIODS BASED ON SPI INDEX (MCKEE *ET AL*.,1993). 72

TABLE 7 CLASSIFICATION OF WET AND DROUGHT PERIODS BASED ON PNI INDEX, (WERICK *ET AL*., 1994). 73

TABLE 8 LIST OF VINEYARDS AND THEIR GRAPE VARIETY 89

TABLE 9 SPI AND SPEI CLASSIFICATION OF WET AND DROUGHT PERIODS ACCORDING TO MCKEE *ET AL*. (1993) AND VICENTE-SERRANO *ET AL*. (2010), RESPECTIVELY. SPI AND SPEI INDICES ARE DIMENSIONLESS. 91

TABLE 10 BLUE, RED, NEAR-INFRARED (NIR) AND SHORTWAVE INFRARED (SWIR) WAVELENGTH BANDS IN THE INSTRUMENTS CARRIED ON BOARD THE LANDSAT 8 (L8) AND SENTINEL-2 (S2) SATELLITES. 93

TABLE 11 LIST OF METEOROLOGICAL STATIONS (ID STATION) USED FOR THIS STUDY, DIVIDED BY PROVINCE (PROV.) NEW BRUNSWICK, NB, AND PRINCE EDWARD ISLAND, PEI; START DATE AND END DATE ARE THE DATE OF STARTING AND ENDING STATION ACTIVITY, RESPECTIVELY; NEW END DATE IS THE DATE AFTER JOINING DATA SET; TOT YEARS IS THE NUMBER OF YEARS RECORDED; AND DISTANCE FROM WATERSHED BORDER IN KM IS CALCULATED IN THE LAST COLUMN. 138

TABLE 12 PERCENTAGE OF MISSING DATA OF THE METEOROLOGICAL STATIONS (ID STATION) IN THE STUDY AREA, WHERE TOT % IS THE PERCENTAGE OF MISSING DATA OF THE WHOLE STATION DATASET, AND P %, T_X %, T_N % ARE THE PERCENTAGES OF MISSING DATA CONCERNING PRECIPITATION, MAXIMUM TEMPERATURE AND MINIMUM TEMPERATURE, RESPECTIVELY. 140

TABLE 13 METEOROLOGICAL STATIONS USED TO ANALYSE THE DROUGHT EPISODE DURING THE SUMMER 2018 IN IRELAND. 159

TABLE 14 INFORMATION AND METADATA ABOUT MODIS IMAGERY (SEE CHAPTER 5)..... 168

TABLE 15 LANDSAT 8 IMAGERY METADATA USED TO EVALUATE THE EFFECTS OF DROUGHT IN SOME OF THE MOST IMPORTANT VINEYARDS IN PIEDMONT (SEE CHAPTER 6)..... 172

TABLE 16 SENTINEL-2 IMAGERY METADATA USED TO EVALUATE THE EFFECTS OF DROUGHT IN SOME OF THE MOST IMPORTANT VINEYARDS IN PIEDMONT (SEE CHAPTER 6)..... 176

INDEX OF FIGURES

FIGURE 1 GENERAL SOIL TYPES MAP OF PIEDMONT REGION, SPATIAL RESOLUTION 250M. 7

FIGURE 2 GENERAL SOIL TYPES MAP OF IRELAND. 12

FIGURE 3 GLOBAL BROWSE IMAGE FOR MODIS 15

FIGURE 4 COMPARISON OF LANDSAT 8 AND LANDSAT 7 SPECTRAL BANDS WITH SENTINEL-2 SPECTRAL BANDS (NASA 2018) 20

FIGURE 5 DIAGRAM OF THESIS STRUCTURE 24

FIGURE 6 RELATIONSHIP BETWEEN VARIOUS TYPES OF DROUGHT AND DURATION OF DROUGHT EVENTS (WILHITE, 2000) 29

FIGURE 7 GRAPHICAL ABSTRACT OF THE STUDY IN CONTINENTAL TEMPERATE (ON THE LEFT) AND MEDITERRANEAN (ON THE RIGHT) ENVIRONMENTS. 50

FIGURE 8 STUDY AREA: PIEDMONT REGION ON THE LEFT, SARDINIA REGION ON THE RIGHT; WHITE DOTS INDICATE POSITIONS OF METEOROLOGICAL STATIONS. 54

FIGURE 9 THERMO-PLUVIOMETRIC DIAGRAM FOR TORINO DATA SERIES (ON THE LEFT) AND CAGLIARI/ELMAS (ON THE RIGHT) DURING THE PERIOD 1981-2017. 55

FIGURE 10 AVERAGE OF SPI (ON THE LEFT) AND SPEI (ON THE RIGHT) VALUES FOR THE STATIONS OF PIEDMONT REGION. THE YELLOW/BROWN AND BLUE/GREEN COLOURED LINES INDICATE THE CRITICAL VALUES OF THE INDICES IN DRY AND WET CONDITIONS, RESPECTIVELY. 60

FIGURE 11 AVERAGE OF SPI (ON THE LEFT) AND SPEI (ON THE RIGHT) VALUES FOR THE STATIONS IN SARDINIA REGION. THE YELLOW/BROWN AND BLUE/GREEN COLOURED LINES INDICATE THE CRITICAL VALUES OF THE INDICES IN DRY AND WET CONDITIONS, RESPECTIVELY. 61

FIGURE 12 SPI (ON THE LEFT) AND SPEI (ON THE RIGHT) VALUES FOR THE TORINO STATION IN PIEDMONT REGION, CALCULATED ON THE PERIOD OF 12, 24 MONTHS. 62

FIGURE 13 SPI (ON THE LEFT) AND SPEI (ON THE RIGHT) VALUES FOR THE CAGLIARI/ELMAS STATION IN SARDINIA REGION, CALCULATED ON THE PERIOD OF 12, 24 MONTHS. 63

FIGURE 14 GRAPHICAL ABSTRACT OF CHAPTER 5 65

FIGURE 15 EFFECTS OF DROUGHT IN CO. TIPPERARY 17TH JULY 2018 (PHOTO CREDIT: ALISON MALONEY, TEAGASC) 67

FIGURE 16 THE NASA TERRA SATELLITE MODIS TRUE COLOUR IMAGERY FOR THE (LEFT) 17TH JULY 2017 AND THE (RIGHT) 10TH JULY 2018 67

FIGURE 17 IMAGES WERE PRE-PROCESSED USING RADIOMETRIC CALIBRATION, SPECKLE FILTERING, AND TERRAIN CORRECTION. THE RESPECTIVE ACQUISITION DATES WERE THE 2ND AND 4TH AUGUST 2017 AND 2018 69

FIGURE 18 THE METEOROLOGICAL STATIONS USED FOR THE CALCULATION OF (A) SPI AND (B) PNI. 71

FIGURE 19 MONTHLY SPI (ROW 1), PNI (ROW 2) AND ANOMALIES OF MONTHLY GROWTH (2018 VS. (2000-2017) BASED ON MODIS-EVI (ROW 3) FOR (A) JANUARY TO APRIL 2018 AND (B), MAY TO AUGUST 2018. 77

FIGURE 20 THERMO-PLUVIOMETRIC DIAGRAM IN IRELAND FOR (A) 2018 AND (B) THE REFERENCE PERIOD 1981–2010. THE BLUE BARS REPRESENT THE MONTHLY AMOUNT OF PRECIPITATION, AND THE RED LINE SHOWS THE AVERAGE MONTHLY TREND..... 78

FIGURE 21 DAILY SOIL MOISTURE DEFICIT FOR MODERATELY DRAINED SOILS AT DUBLIN AIRPORT FOR 2018 COMPARED TO THEIR 30-YEAR NORMAL (1981-2010). IN JULY SOILS WERE TWICE AS DRY AS NORMAL. 79

FIGURE 22 AVERAGE MONTHLY SOIL MOISTURE DEFICIT FOR MODERATELY DRAINED SOILS AT DUBLIN AIRPORT FOR THE PERIOD 1981-2018 INCLUSIVE. A VALUE OF -10MM REPRESENTS SOIL SATURATION, 0MM FIELD CAPACITANCE, 110MM ABSENCE OF MOISTURE. JULY 2018 IS THE HIGHEST SMD (DRIEST) MONTH OVER THIS 38-YEAR PERIOD. 79

FIGURE 23 GRAPHICAL ABSTRACT OF CHAPTER 6 81

FIGURE 24 STUDY AREA AND LOCATION OF VINEYARDS CHARACTERISED BY GRAPE VARIETY. WHITE DOTS INDICATE THE POSITIONS OF METEOROLOGICAL STATIONS 82

FIGURE 25 500 HPA GEOPOTENTIAL HEIGHT MAPS FOR (A) SUMMER 2017, (B) AUTUMN 2017, (C) SUMMER 2018 AND (D) AUTUMN18. THE DATA WERE DOWNLOADED FROM ECMWF'S ERA REANALYSIS ARCHIVE WHERE THE 06 Z AND 18 Z ANALYSIS FIELDS WERE RETRIEVED AND AVERAGED OVER EACH 3-MONTH PERIOD REPRESENTING THE RELEVANT SEASON. 85

FIGURE 26 CORRELATION BETWEEN DROUGHT INDICES (SPI, SPEI) AND CUMULATIVE GPP FOR THE BARBERA (BAR-1 AND BAR-2), MOSCATO BIANCO (MOB) AND NEBBIOLO (NEB-1 AND NEB-2) GRAPE VARIETIES. THE YEARS 2016-2018 ARE SHOWN WHERE LANDSAT 8 (A) AND SENTINEL-2 DATA (B) ARE USED TO COMPUTE GPP. DARK GREY AREAS SHOW THE 95% CONFIDENCE LEVEL INTERVAL FOR PREDICTIONS FROM THE LINEAR MODEL (RED LINE). 97

FIGURE 27 GPP INDEX TREND (TOP ROW) AND CUMULATIVE GPP TREND (BOTTOM ROW) FOR THE BARBERA (BAR-1 AND BAR-2), MOSCATO BIANCO (MOB) AND NEBBIOLO (NEB-1 AND NEB-2) GRAPE VARIETIES, FOR THE YEARS 2016-2018 DURING THE VEGETATIVE PERIOD FROM APRIL TO OCTOBER. 97

FIGURE 28 EVOLUTION OF GPP INDEX DURING THE VEGETATIVE AND REPRODUCTIVE SEASONS FOR THE YEARS 2016 TO 2018 IN FIVE OF THE MOST REPRESENTATIVE VINEYARDS FOR EACH AREA. 99

FIGURE 29 SCATTER PLOT, INCLUDING REGRESSION LINE, OF PREDICTED VS OBSERVED GRAPE PRODUCTION IN THE 5 AREAS OF PIEDMONT. THE PREDICTED GRAPE PRODUCTION VALUES (F(GRPR) WERE CALCULATED USING THE MULTIPLE LINEAR REGRESSION MODEL GIVEN IN EQ. 8, WHILE THE OBSERVED GRAPE PRODUCTION VALUES (GRPR) WERE BASED ON DATA OBTAINED FROM THE AGRICULTURAL AND LIVESTOCK PRODUCTION SECTOR OF THE PIEDMONT REGION, AGRICULTURE DIRECTORATE. THE VEGETATIVE PERIOD FROM APRIL TO OCTOBER FOR 2016 TO 2018 WAS USED. 99

FIGURE 30 GEOGRAPHICAL DISTRIBUTION OF THE METEOROLOGICAL STATIONS USED IN THIS STUDY, DISPLAYING THE BEGINNING AND FINAL YEARS OF DATA COLLECTION. 139

FIGURE 31 CHANGE IN GLOBAL AVERAGE TEMPERATURE RELATIVE TO THE 1986-2005 REFERENCE PERIOD. [SOURCE: GOVERNMENT OF CANADA] 142

FIGURE 32 ANNUAL TOTAL PRECIPITATION OF MONCTON STATION, DURING THE PERIOD 1939-2018. 142

FIGURE 33 ANNUAL TOTAL PRECIPITATION IN BOUCTOUCHE (A), MONCTON (B), REXTON (C) AND SUMMERSIDE (D) STATIONS, IN TWO FUTURE SCENARIOS (A2 RED LINE, AND B1 BLUE LINE), DURING THE PERIOD 1971-2100. ANNUAL TOTAL PRECIPITATION IN MONCTON STATIONS, IN TWO FUTURE SCENARIOS (A2 RED LINE, AND B1 BLUE LINE), DURING THE PERIOD 1971-2100. 143

FIGURE 34 ANNUAL TOTAL PRECIPITATION FORECAST IN THE COCAGNE WATERSHED, IN TWO FUTURE SCENARIOS RCP4.5 (A) AND RCP88.5 (B), DURING THE PERIOD 2071-2100. SPATIAL RESOLUTION: 50M. 144

FIGURE 35 ANNUAL NUMBER OF DAYS WHEN PRECIPITATION VALUES WERE GREATER THAN OR EQUAL TO 10MM (A), 20MM (B) AND 30MM (C), RECORDED IN MONCTON STATION DURING THE PERIOD 1939-2018. 145

FIGURE 36 ANNUAL TOTAL RAIN DAYS IN BOUCTOUCHE (A), MONCTON (B), REXTON (C) AND SUMMERSIDE (D) STATIONS IN TWO FUTURE SCENARIOS (A2 RED LINE, AND B1 BLUE LINE), DURING THE PERIOD 1971-2100. 146

FIGURE 37 ANNUAL DIFFERENCE BETWEEN MEAN TEMPERATURE (T_M) AND BASE TEMPERATURE (T_B), WHERE T_B IS A LOCATION-SPECIFIC BASE TEMPERATURE (10 °C IN THE GRAPH), AND T_M IS GREATER THAN T_B, RECORDED IN MONCTON STATION DURING THE PERIOD 1939-2018. 147

FIGURE 38 GROWING DEGREE DAYS FORECAST, CALCULATED WITH A T_B THRESHOLD GREATER THAN 5 °C IN BOUCTOUCHE (A), MONCTON (B), REXTON (C) AND SUMMERSIDE (D) STATIONS, IN TWO FUTURE SCENARIOS (A2 RED LINE, AND B1 BLUE LINE), DURING THE PERIOD 1971-2100. 147

FIGURE 39 ANNUAL NUMBER OF DAYS BETWEEN THE FIRST OCCURRENCE OF 6 CONSECUTIVE DAYS WITH MEAN TEMPERATURE (T_M) GREATER THAN 5 °C AND THE FIRST OCCURRENCE OF 6 CONSECUTIVE DAYS WITH MEAN TEMPERATURE (T_M) LOWER THAN 5 °C, RECORDED IN MONCTON STATION DURING THE PERIOD 1939-2018. 148

FIGURE 40 NUMBER (A), MAGNITUDE (B), AMPLITUDE (C), DURATION (D), AND FREQUENCY (E) OF THE HEATWAVE EVENTS, RECORDED IN MONCTON STATION DURING THE PERIOD 1939-2018. 150

FIGURE 41 STANDARDIZED PRECIPITATION INDEX, SPI AT DIFFERENT TIME SCALES: 3-MONTH (A), 6-MONTH (B), 12-MONTH (C), AND 24-MONTH (D), RECORDED IN MONCTON STATION DURING THE PERIOD 1939-2018. 151

FIGURE 42 STANDARDIZED PRECIPITATION EVAPOTRANSPIRATION INDEX, SPEI AT DIFFERENT TIME SCALES: 3-MONTH (A), 6-MONTH (B), 12-MONTH (C), AND 24-MONTH (D), RECORDED IN MONCTON STATION DURING THE PERIOD 1939-2018. 152

LIST OF ACRONYMS

a.s.l.	above sea level
BAR	Barbera grape variety
CAP	Common Agricultural Policy
CMIP3	Coupled Model Intercomparison Project
CRM	Coefficient of Residual Mass
DSS	Decision-Support Systems
DTR	Diurnal Temperature Range
EC	European Commission
ECS	EOSDIS Core System
EF	Efficiency Index
EHF	Excess Heat Factor
EHI	Excess Heat Indices
EOS	Earth project Observing System
ESA	European Space Agency
ET	Evapotranspiration
ET_0	Potential Evapotranspiration
ET_a	Daily Actual Evapotranspiration
ET_c	Crop evapotranspiration under standard conditions
EVI	Enhanced Vegetation Index
FAO	Food and Agriculture Organization
$FPAR_{chl}$	Fraction of Light Actually Absorbed by the chlorophyll pigments
GDD	Growing Degree Days
GDP	Gross Domestic Product
GPP	Gross primary production
GPRS	General Packet Radio Service
GPS	Global Positioning System
GSL	Growing Season Length
HDF	Hierarchical Data Format
IoT	Internet of Things
IPCC	Intergovernmental Panel on Climate Change
IQR	Interquartile Range
IVINE	Italian Vineyard Integrated Numerical model for Estimating physiological values
K_c	Crop coefficient
L8	Landsat 8
LAI	Leaf Area Index
LDCM	Landsat Data Continuity Mission
LP DAAC	Land Processes Distributed Active Archive Centre
LUE	Light-Use Efficiency

MOB	Moscato Bianco grape variety
MOD13Q1	MODIS/TERRA Vegetation Indices 16-Day L3 Global 250m
MODIS	Moderate Resolution Imaging Spectroradiometer
MSI	MultiSpectral Imager
NASA	National Aeronautics and Space Administration
NDMI	Normalized Difference Moisture Index
NDVI	Normalized Difference Vegetation Index
NEB	Nebbiolo grape variety
NIR	Near-Infrared
OIV	International Organisation of Vine and Wine
OLI	Operational Land Imager
P	Precipitation
P_a	Normal precipitation for the corresponding month in the 30-year period
PAR	Photosynthetically Active Radiation
PNI	Percent of Normal Index
prectot	Total annual precipitation
QC	Quality Control
r95p	Total annual precipitation from heavy rain days
RADAR	Radio Detection and Ranging
RAM	Regional Agrometeorological Network
RAS	Hydrographic Sector of Sardinia Region
RCP2.6	Representative Concentration Pathway based on low global emission scenarios (RCP2.6)
RCP4.5	Representative Concentration Pathway based on moderate global emission scenarios (RCP4.5)
RCP8.5	Representative Concentration Pathway based on high global emission scenarios (RCP8.5)
RF	Random Forests
rRMSE	Relative Root Mean Square Error
S2	Sentinel-2
SCP	Semi-Automatic Classification (QuantumGIS Plugin)
SDG	Sustainable Development Goals
SDG1	Sustainable Development Goals: no poverty
SDG15	Sustainable Development Goals: life on land
SDG2	Sustainable Development Goals: zero hunger
SDG3	Sustainable Development Goals: good health and well-being
SIMN	Italian Hydrographic Mareographic Service
SMD	Soil Moisture Deficit
SPEI	Standardised Precipitation Evapotranspiration Index
SPI	Standardised Precipitation Index
SPOT	Satellite Pour l'Observation de la Terre
SWIR	Short-Wave Infrared
T_b	Base temperature in GDD equation

TIRS	Thermal Infrared Sensor
T_m	Daily mean temperature
T_n	Daily minimum temperature
T_N	Minimum cardinal temperature
T_N90_p	Amount of hot nights
TOA	Top Of Atmosphere
T_{opt}	Optimal cardinal temperature
T_x	Daily maximum temperature
T_X	Maximum cardinal temperature
T_X90_p	Amount of hot days
UTC	Coordinated Universal Time
VU	Vineyard Units
VI	Vegetation Index
WGS84	World Geodetic System 1984
WMO	World Meteorological Organization

PUBLICATIONS AND PRESENTATIONS

The following publications were derived from this thesis:

- **Full papers (published / accepted for publication / submitted)**

Falzoi S., Gleeson E., Green S., Borgogno Mondino E.C., Spanna F., Fratianni S. (under review). Analyses of drought in north-western Italy, and effects on wine production, using Landsat and Sentinel imagery.

Moirano G., Zanet S., Giorgi E., Battisti E., **Falzoi S.**, Acquaotta F., Fratianni S., Richiardi L., Ferroglio E., Maule M. (under review). Integrating environmental, entomological, animal and human data to model the *Leishmania infantum* transmission risk in a new endemic area in Northern Italy.

Falzoi S., Acquaotta F., Pulina M.A., Fratianni S. 2019. Hydrological drought analysis in Continental Temperate and Mediterranean environment during the period 1981-2017. *Italian J. Agromet.*, 3: 13-23. doi: 10.13128/ijam-798

Falzoi S., Gleeson E., Lambkin K., Zimmermann J., O'Hara R., Marwaha R., Green S., Fratianni S. 2019. Analysis of the severe drought in Ireland in 2018. *Weather*, 74(11): 368-373. DOI: 10.1002/wea.3587

The following conference communications were derived from this thesis:

- **Oral presentations**

Falzoi S., Spanna F., Borgogno Mondino E.C., Green S., Fratianni S. 2019. Gross Primary Production analysis in Piedmontese vineyards by using remote sensing techniques. *XXII Convegno Nazionale di Agrometeorologia*, Book of abstract, Napoli, 11th-13th June.

Cassardo C., Andreoli V., **Falzoi S.**, La Iacona T., Spanna F. 2019. Midterm behaviour of surface layer and soil parameters in selected Piedmontese vineyards. *XXII Convegno Nazionale di Agrometeorologia*, Book of abstract, Napoli, 11th-13th June.

Falzoi S., Gleeson E., Lambkin K., Zimmermann J., O'Hara R., Marwaha R., Green S., Fratianni S. 2019. An analysis of drought during the Irish summer in 2018. *Met Éireann External Lecture Series*, 6th June.

Falzoi S., Gleeson E., Lambkin K., Zimmermann J., O'Hara R., Marwaha R., Green S., Fratianni S. 2019. An analysis of drought during the Irish summer in 2018. *29th Irish Environmental Researchers Colloquium*, Carlow, 15th-17th April.

Baronetti A., Acquaotta F., **Falzoi S.**, Garzena D., Guenzi D., Spanna F., Fratianni S. 2017. Assessment of daily rainfall data recorded by two different networks in Piedmont (North-West Italy). *European Conference for Applied Meteorology and Climatology*, Book of abstract, Dublin, 3rd-8th September.

Baronetti A., **Falzoi S.**, Acquaotta F., Spanna F., Fratianni S. 2017. Caratterizzazione degli eventi estremi di precipitazione e siccità in Piemonte. *XXXII Congresso Geografico Italiano*, Book of abstract.

- **Poster presentations**

Falzoi S., Fratianni S., Borgogno Mondino E.C. 2019. Multitemporal analyses of drought in north-western Italy, and effects on wine production, using Landsat and Sentinel imagery. *3rd Agriculture and Climate Change Conference*, Budapest, 24th-26th March.

Falzoi S., Gleeson E., Spanna F. 2017. Phenological modelling of trees in Alpine regions of north-western Italy. *European Conference for Applied Meteorology and Climatology*, Book of abstract, Dublin, 3rd-8th September.

Pulina M.A., Acquaotta F., **Falzoi S.**, Fratianni S. 2017. Analyse de la sécheresse hydrologique en milieu continental tempéré et en milieu Méditerranéen en Italie, pendant la période 1981-2010. *XXXème colloque de l'Association Internationale de Climatologie*, Book of abstract.

- **Related publications**

Finn J., **Falzoi S.**, Green S., Ruelle E. 2018. Dealing with drought. *TResearch (research and innovation news at Teagasc)*, vol. 13, n. 3, 14-15.

Furthermore, the following periods as a visiting scholar:

- **Research internship**

Visiting the Department of Agrifood Business and Spatial Analysis, Teagasc Food Research Centre, Dublin, Ireland, from May to August 2019.

Visiting the Geomatics Laboratory, Department of History and Geography, University of Moncton, New Brunswick, Canada, from October to December 2018.

Visiting the Department of Agrifood Business and Spatial Analysis, Teagasc Food Research Centre, Dublin, Ireland, from May to August 2018.

Visiting the Department of Agrifood Business and Spatial Analysis, Teagasc Food Research Centre, Dublin, Ireland, from May to August 2017.

CHAPTER 1: INTRODUCTION

1.1. Context and Research Aims

Drought is not an instantaneous phenomenon; its effects often take weeks or months to appear. Drought by itself is not a disaster, it is a natural weather phenomenon that occurs in all climates. Whether it becomes a disaster depends on its impact on local people, economies, agriculture, and the environment, and the ability of these social and natural factors to cope with and recover from drought (Magno, 2014). Therefore, it is important to monitor and analyse the potential impact of drought in order to identify areas that are more vulnerable (Tadesse, 2004).

Compared to other extreme weather events, drought is unusual in the slow speed and incremental rate at which it develops. This creates a challenge for detecting the beginning and end of drought episodes. Drought is one of the most important consequences of climatic change for natural and socioeconomic systems. The impact of drought on water resources and agriculture is a complex process influenced by different factors, including temperature, wind and relative humidity. The effects are also very difficult to predict both at spatial and temporal scale, and it needs specific tools and different environmental data to be recognized. Many agricultural indices and studies have been developed by using meteorological data, which cannot provide a dataset continuous in time and space. On the other hand, satellite remote sensing observations provide long term, continuous data for a wide range of indices.

Drought always begins with a precipitation deficit, but can be categorized into four general types: 1) meteorological (precipitation deficit), 2) agricultural (meteorological drought with consequences for agriculture), 3) hydrological (meteorological drought with reduced surface/sub-surface water supply), and 4) socio-economic (drought combined with excess demand on the available supply of water, with consequences for society) (Wilhite and Glantz 1985). Different indicators and recommended management practices are associated with each type, with relevance for addressing the social, economic, and environmental impacts of drought in a timely and effective manner. The four categories of drought, and their parameters, will be discussed in greater detail in Chapter 2.

1.1.1. Agriculture and drought

Compared to all other natural hazards the impact of drought has the greatest consequences in terms of the number of people affected, directly, i.e. by water scarcity, and indirectly, e.g. due to famine and consequent food shortages (FAO, 2018). Moreover, the amount of people affected by drought is rising rapidly, more than doubling in the past 40 years. Climate change is a major contributing factor to the worsening of drought, and severity of the impacts of drought (FAO, 2018).

This study focuses in particular on agricultural drought, with consideration of the meteorological drought conditions that contribute to agricultural drought, and the socio-economic impact of agricultural drought.

Agriculture is an industry with a global reach, which employs approximately 1.4 billion people, comprising 18% of the global population (Spinoni *et al.*, 2014). The impact of drought in agriculture has far-reaching effects, resulting in reduction in global food supplies, but also the capacity of farmers to receive a return on their investment and labour, and the capacity of smallholder farms, who may be directly dependent on the farm as a food source, to achieve adequate nutrition (Hlavinka *et al*., 2009; Páscoa *et al.*, 2017; Smit *et al*., 2008). In developing countries, agriculture is severely affected by drought, bearing up to 80% of direct impacts, with implications for access to water, food production and food security, and rural livelihoods (Portmann *et al*., 2010). In turn these compromise the capacity of nations to work towards sustainable development, e.g. improvements in relation to the Sustainable Development Goals (SDG), particularly SDG1 (no poverty), SDG2 (zero hunger), SDG3 (good health and well-being), and SDG15 (life on land) and can even reverse gains made in food security and poverty reduction (Meza *et al.*, 2019). The impacts of drought are also significant in developed economies, where the capacity to monitor and respond to drought may be greater. For example, in USA, drought is considered to result in an annual loss of $6-8 billion for the agricultural sector (Dai *et al.*, 2020)

Drought cannot be prevented, but it can be monitored and managed. Policy instruments, e.g. concerning water use for domestic and commercial purposes, can mitigate and reduce the impact of drought (FAO, 2018). New crop varieties, for example, are being developed with greater heat-tolerance and resilience to water deficit (Grayson, 2013; van Leeuwen and Destrac-Irvine, 2017). Advances in technological capacity have contributed to improvements in the forecasting of drought, in some cases up to a month in advance, but implementation of these technological

advances can be limited by resource constraints (Grayson, 2013). This provides farmers with greater capacity to respond to the onset of drought and minimize the impact of drought for their crops and livestock. The research undertaken in this study concentrates on the development of technological capacity to monitor drought and predict drought impacts by using diverse information sources, in order to facilitate improvements in drought management and prediction.

1.1.2. Agriculture and climate change

Agriculture is inextricably linked with climate change, both as a contributing factor and an aspect of social activity that will be profoundly affected by changes in climate (Betts *et al.*, 2018; Grillakis *et al.*, 2016; Koutroulis *et al.*, 2018). Negative impacts of climate change are already being felt across Europe. Extreme weather, including recent heatwaves in many parts of the Europe, are already causing economic losses for farmers and for the Europe's agriculture sector (Teuling, 2018). Climate impacts have led to poorer harvests and higher production costs, affecting price, quantity and the quality of farmed products in parts of Europe. Potential positive effects related to increased temperatures are expected mostly in northern Europe, while a reduction in crop productivity and an increased risk for livestock are projected in large parts of southern Europe (EEA, 2017). According to projections of a high emission scenario, yields of non-irrigated crops like wheat and corn are projected to decrease in southern Europe by up to 50% by 2050 (EC, 2017). This could result in a substantial drop in farm income by 2050.

Despite the carbon storage capacity of plants cultivated for agricultural purposes, the agricultural sector is a significant producer of greenhouse gases that contribute to climate change, e.g. carbon dioxide, methane and nitrous oxides (Agovino *et al.*, 2019). Crop production practices, animal husbandry practices, and land use change in response to agricultural demand can all contribute to the greenhouse gas production of the agricultural sector (Smith *et al.*, 2014).

At a global level, cultivation and animal husbandry practices have developed in response to prevailing climatic conditions, and must adjust to changes in these conditions (Ciais *et al.*, 2005). There is a lag-time between farmer decision-making, e.g. planting and breeding decisions, and the onset of meteorological events that influence the productivity of the crop or livestock being managed. Thus, changes in the expected pattern

and parameters of meteorological conditions have a substantial impact on the successful cultivation of crops and rearing of livestock, at a local but also global scale (FAO, 2018). Future climate change might also have some positive effects due to longer growing seasons and more suitable crop conditions, but these effects will be outweighed by the increase in extreme events negatively affecting the sector. In Europe, for example, for a number of cereal crops' flowering and harvest dates are occurring earlier in the season than expected, due to an increase in air temperatures. This might allow new crops to be cultivated in some areas, e.g. northern Europe, but may also reduce the viability of crop production in southern Europe, where increased air temperature has been accompanied by extreme heat events and water deficit. While there is the possibility for farmers to shift their production to other times of the year, in response to climatic changes, in some areas, e.g. western France and south-eastern Europe, the transition to hot, dry summers has not been accompanied by suitable winter-growing conditions for traditional summer crops (FAO, 2018).

Changing climatic conditions also creates changes in the conditions under which pests and diseases affecting crops and livestock can survive and reproduce, with the potential to exacerbate existing pest management challenges and introduce others as the viable range of pests and diseases increases (FAO, 2018). The incidence of extreme weather events and the increased challenge for farmers to develop and implement cultivation and livestock management systems that are resilient to extreme events and climatic changes (e.g. heat- and drought-resilient crops, rotating crops to match water availability) is also expected to contribute to annual variation in agricultural productivity, e.g. crop yields (García-Herrera *et al*., 2010).

1.2. Study goal and focus regions

The main goal of this study is to collect data and improve and develop instruments to provide decision-making support services to farmers, e.g. winemakers, agricultural technicians and advisory services, and policymakers, in the context of the changing global climate. The study considers agriculture in two different climatic environments, the Continental-Temperate climate and Temperate Oceanic. In addition, two further climatic environments, Mediterranean climate and Humid Continental climate are considered, in order to contribute to the development of climate analysis tools that can strengthen the analysis of drought, including agricultural drought. The predominant agricultural

activities differ, in the two climatic regions in which agricultural drought is the explicit focus. Hence, the study considers the impact of agricultural drought on one of the primary agricultural activities, winemaking, in Piedmont, the Continental Temperate region studied. The study also considers the impact of agricultural drought on grass pasture, the predominant crop cultivated in Ireland, the Temperate Oceanic region studied. The role of these two crop types for the agricultural sector in the respective regions, and the impact of climate change on production and management of those crops, is described below.

The whole Mediterranean region is sensitive to actual and projected climate changes, as established by many studies through the use of climate model simulations (Barredo *et al.*, 2019; Lefebvre *et al.*, 2019; Pausas and Millán, 2019). The inclusion of this sensitive region in this study therefore contributes to the validity and robustness of the climate analysis tools used in the study of the regions which are the main focus of the thesis research. In addition, the incorporation of Humid Continental climate, a climate region with contrasting prevailing conditions to the two focal regions, and the application of climate analysis tools to the study of extreme precipitation events there, strengthens the applicability of these tools to diverse and contrasting precipitation conditions.

1.2.1. Viniculture, drought and climate change in Piedmont

The North-West of Italy, which includes the region of Piedmont, is characterized by intense agricultural activities mostly related to wine production of high quality. The vinicultural sector plays a key role in the economy of the Piedmont region of Northern Italy. According to the regional technical report (Vigasio *et al.*, 2018), about 45,000 hectares of agricultural area was cultivated with vineyards in 2018, mainly located in the Langhe-Roero and Monferrato areas (south-east of the region), in the central hills of Torino and in the provinces of Vercelli and Novara (north of the region). Eighteen thousand farms and 54 cooperative wineries were involved, producing about 2.5 million hectolitres (5% of Italian national production) and an export of one billion euros (18% of Italian national wine exports).

In this context, determining the vegetative and reproductive development of the vine, and therefore the maturation and quality of grapes, is one of the most valuable topics from both a scientific and economic perspective. These processes are strictly regulated by environmental conditions, and

the quality of the final product is determined both by meteorological and climatic variables, and by pedological and geomorphological characteristics (Figure 1). Additionally, changes in the current climate are causing an unpredictable instability and a significant climatic difference between the years. Over the past 30 years, the temperature in Piedmont increased by 0.7 °C (Fratianni *et al.*, 2015). Some consequences of these climatic changes are already being experienced. For example, due to the drought episode that occurred during the summer and autumn of 2017, one of the driest years of the last 60 years, Piedmontese wine production experienced a reduction in productivity of 30%, compared to 2018 (Vigasio *et al*., 2018).

While the Piedmontese region can be considered a distinct winegrowing region, in this study the heterogeneity between wine cultivation areas and even between vineyards is given explicit consideration, enabled by the data collection and analysis tools applied, i.e. meteorological and remote sensing techniques. These differences between areas and between vineyards arise as a consequence of geomorphological differences within and between areas, e.g. the slope, elevation, and aspect of the cultivated land, and the soil characteristics. It must be noted that the winegrowing regions occur in areas characterised by diverse, hilly topography. In addition, the characteristics of the wine resulting from the grapevine crop, including quality, is closely linked to the climate (Biancotti, 2003). Different grape varieties are cultivated in Piedmont, which vary in their response to climatic and geomorphological conditions, and the cultivation practices which are prescribed for optimal productivity, i.e. the effect of *terroir*. Using meteorological and remote sensing techniques, this study considers the effect of climate, and particularly drought conditions, on three different grape varieties prevalent in Piedmont: Barbera, Moscato Bianco, and Nebbiolo; within five different production areas: the Langhe, Roero, Monferrato, central hills of Torino, and northern Piedmont areas.

In the following paragraphs, the Barbera, Moscato Bianco and Nebbiolo grape varieties are described.

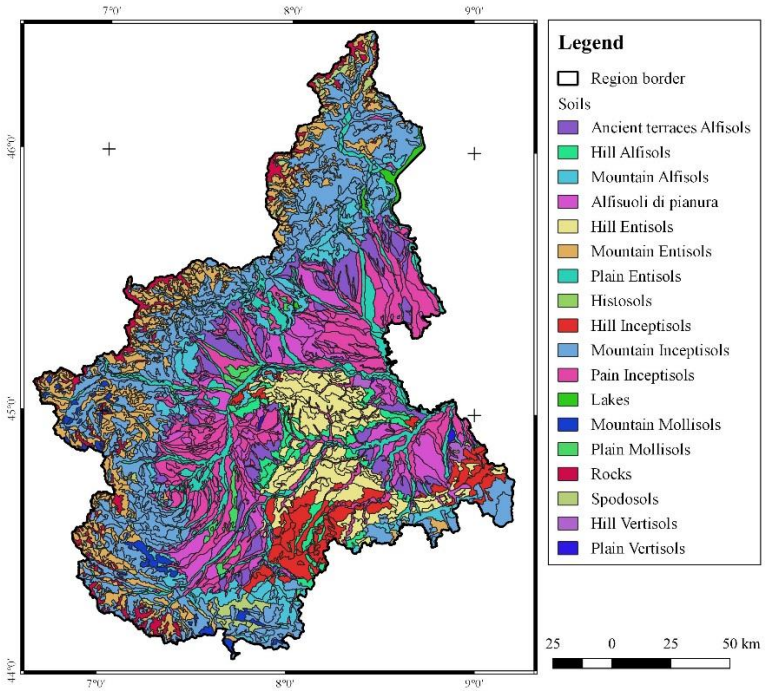

Figure 1 General soil types map of Piedmont region, spatial resolution 250m.

1.2.2. Barbera cultivar

Barbera is the most widespread grape variety in the Piedmont region; the wine-growing area extends from the Langhe and Roero areas to Monferrato and the hills of Torino. The ripening period normally occurs in the first half of October. Barbera can adapt to a wide range of vineyard soils but tends to thrive most in less fertile calcareous soils and clay loam. Sandy soils can help limit the vigour and yields. The grape rarely thrives in very alkaline or saline soils.

The southern area has two varieties, *Barbera d'Alba* and *Barbera d'Asti*, which can give rise to a varied typology of products. The origin area of *Barbera d'Alba* extends to the right and to the left of the Tanaro river, in the area of the Langhe and Roero. The *Barbera d'Alba* has an important presence in about fifty hill municipalities. The origin area of *Barbera d'Asti* is rather large, between the provincial administration of Asti and Alessandria.

The origin area of *Barbera del Monferrato* is wider than *Barbera d'Asti* and involves 118 municipalities of Asti and 99 municipalities of

Alessandria. The whole territory is hilly and in the whole viticultural area, between 85 and 100% contains *Barbera del Monferrato*. There are two types of this denomination, *Barbera del Monferrato* Doc (controlled designation of origin) and *Barbera del Monferrato Superiore* Docg (controlled and guaranteed designation of origin), with different aging obligations.

1.2.3. Moscato Bianco cultivar

The Moscato Bianco cultivar is considered one of the oldest grapes grown in Piedmont and is the most renowned and widespread aromatic berry cultivar in the region. Its cultivation extends indicatively in the hilly area between the Tanaro and Bormida rivers, in 52 municipalities between the provinces of Alessandria, Asti and Cuneo, for a total of 9,593 ha. In this area, three sub-areas have been delimited, Santa Vittoria d'Alba, Canelli and Strevi, where *Moscato d'Asti* is produced.

The Moscato Bianco grows in a dry climate, with annual precipitation ranging from 800mm to 1,100mm, and tolerates frequent water shortage episodes during the summer. The grape variety develops on hilly territories characterized by calcareous-clayey and sub-acid soils and with a moderate fertility. The harvest period normally happens in the second half of September.

1.2.4. Nebbiolo cultivar

The Nebbiolo cultivar is a vine with a cultivation area extended over the whole of Piedmont, although it is very sensitive to *terroir* (see section 1.2.5, below) and its cultivation is limited to the most suitable areas, such as vineyards with optimal exposure. It is most widespread in the Langhe and the Roero to the south, the hills of the Alto Vercellese and the Alto Novarese in the north, and the Canavese and Carema areas.

In the Nebbiolo cultivation areas, leaf removal and cluster thinning are two cultural practices used to improve cluster health and to reduce yield respectively (for production of many Italian wines, crop load is controlled by law) (Guidoni *et al.*, 2008).

The Nebbiolo cultivar grows in a dry climate with annual precipitation ranging from 800mm to 1,100mm, although it tolerates greater total annual

precipitation, typical of northern Piedmont. Acid soil are particularly favourable for the cultivation of the Nebbiolo grape variety.

It is a vine characterized by high vigour and very variable productivity depending on the clone and the health status (presence or absence of virosis), and with early budding and late ripening (first - second half of October). The Nebbiolo cultivar is characterized by reduced berry skin colour. In its original area, it is used to produce high-quality aged wines such as Barolo and Barbaresco, which have problems in colour stability during aging (Guidoni *et al.*, 2008).

1.2.5. Terroir

Terroir is a (cultivated) ecosystem, in a given place, in which the vine interacts with the natural environment and, in particular, soil and climate. Gérard Seguin's definition (1986) underlines the multidisciplinary approach to understanding the interaction between abiotic factors that play a key role in the ecosystem in which grapevines are cultivated.

More recently, the International Organization of Vine and Wine (2010) used this idea and defined the concept of the vitivinicultural terroir as an area in which collective knowledge of the interactions between the identifiable physical and biological environment and applied vitivinicultural practices are developed, providing distinctive characteristics for the products originating from this area. In other words, wine quality depends on the environmental characteristics of where the grapes are grown, and many characteristics of their physical properties can be quantified and mapped.

The main climatic parameters include temperature, rainfall and reference evapotranspiration. These can be used to calculate crop parameters for example, vine phenology and grape ripening, which are mainly driven by air and soil temperature. Moreover, considering all of the climatic conditions, macroclimate, mesoclimate, and microclimate represent a scale of the different influence of climate in the vineyard, and hence the vineyard management (Gómez-Miguel, 2011). Macroclimate is the main limiting factor for the cultivation of the vine with an effect at a regional level. The mesoclimate is characteristic of a specific topographic and landscape location where a set of vine plants in a given geomorphological area is equally affected by similar climatic variations. The microclimate refers to the vine, leaves and clusters playing an influence in the biological

cycle, such as the individual grape ripening stage. Quality grape characteristics, like sugar content, acidity and polyphenolics are analysed and regularly controlled, using the three climatic levels.

Geomorphological factors, such as topography, and soil characteristics (composition, type and depth), interact with climatic conditions, such as the meteorological variables. For example, from the soil the vine receives water and minerals, particularly nitrogen.

Many recent scientific publications on the concept of terroir consider the inter-relating elements of the environment such as temperature (Zhang *et al.*, 2015), water status (Costa *et al.*, 2016), light (de Olivera *et al.*, 2016), geology (Martínez and Gomez-Miguel, 2017), soil (van Leeuwen *et al.*, 2018) with the response of the vine.

Finally, cultural practices are highly influential on the characteristics of wine. The winemakers and their activities play an important role in terroir expression, managing vineyards by appropriate viticultural practices and choosing plant material, but these are themselves ultimately dependent upon the local environment.

All these factors act and interact, and they must be considered simultaneously, making a link between wine attributes and the environment (Ubalde *et al.*, 2010; Zsófi *et al.*, 2011). If each terroir factor is studied separately, studies remain highly descriptive and fail to explain the sensory diversity of wine. There is, therefore, a requirement for high quality contiguous spatial data of the physical elements of the environment for terroir analysis.

1.2.6. Grape Phenology

Phenology is the study of periodic plant and animal life cycle events and how seasonal and inter-annual variations in climate, as well as habitat factors, influence organism development. In the context of viticulture, phenology is the study of the growth cycle of grape vines from season to season. Grape phenology also considers cultivation decisions, climate, and soil conditions, as the events that can affect the stages of growth of grapevines. Temperature is the main driver of grapevine phenology (Gladstones, 2011; Bock *et al.*, 2011).

The typical growth season of a vine is from spring to late summer/early autumn. The growth cycle of a grape vine begins with the initiation of a

growth event and is completed with the full development of the fruit. Timing of the ripening period is critical in the production of terroir wines. The perfect range to reach full ripeness is between the beginning of September to half of October (in the northern hemisphere). In this window, grape quality is affected. In late ripening, grapes are characterized by a high acidity level with difficulties to complete the fruit development, particularly in regions where the temperatures drop quickly during October. On the contrary, in early ripening the sugar/acid balance, aromatic ripeness and phenolic ripeness are uncoupled.

Soil temperature is another important factor that influencing the timing of phenology. A warm soil can quicken phenology and can be an asset in a cool climate, while it can have an undesirable effect on early ripeness in a warm climate.

Hence, the knowledge of the climate and soil conditions allows vineyard managers to make decisions in the vineyard applying growing practices, including vine density, fertilization, rootstock management, pest control, pruning and irrigation. Understanding the environmental factors is fundamental, especially in a higher temperature scenario where future climate simulations of the phenology of grapevines indicate shorter growing seasons, earlier occurrence of phases and shorter phase duration (Alikadic *et al*., 2019).

In this study I took into consideration four phenological phases (Bud burst, Flowering, Veraison, Harvest) of three grape varieties, Barbera, Moscato Bianco, and Nebbiolo.

1.2.7. Agriculture, drought and climate change in Ireland

The agri-food sector contributes approximately 6% of total value added to the Irish economy (O'Donoghue and Hennessy, 2015), and engages 13% of the total number of people in employment in the Republic of Ireland (Ireland) (Central Statistics Office, 2018). In 2016 there were 137,500 farms in Ireland, with an average farm size of 32.4 ha (Central Statistics Office, 2018), and similar to the Piedmontese region, the Irish agricultural area is characterised by considerable geomorphological heterogeneity (Figure 2), which interacts with climatic conditions to produce variation in agricultural conditions across the nation. The predominant agricultural activities involve livestock production (89.7%), particularly specialist beef cattle (57%), dairy (11.7%), and sheep production (11%) (Central

Statistics Office, 2018). These activities rely on grass pasture as the main source of livestock fodder, and accordingly grass pasture is the most widely cultivated crop in Ireland, accounting for 92% of arable land cover (Central Statistics Office, 2018). The main effects of climate change for agriculture in Ireland are projected to involve increased incidence of extreme precipitation-related events, particularly flooding and drought (Nolan, 2015). The implications of these events will differ on a regional basis, depending on the geomorphological and agricultural context within which they occur. As in Piedmont, these effects are already being experienced, for example, during the summer drought of 2018 in Ireland which had a substantial effect on grass productivity (Falzoi *et al*., 2019) and subsequently livestock production and economic returns for farmers (Dillon *et al*., 2018).

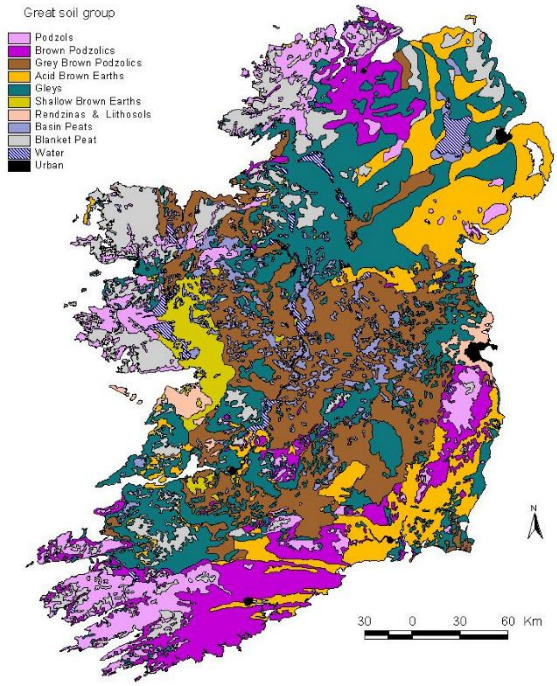

Figure 2 General soil types map of Ireland (Teagasc, 2001).

1.3. Remote sensing principles

Remote sensing is the science of acquiring information about the Earth's surface without actually coming in contact with it. This is done by recording energy, which is either reflected or emitted from the Earth's surface. Remote sensing includes techniques that allow information to be drawn from a place located at a known distance from the sensor. Remote sensing is divided into *passive* and *active*.

Passive remote sensing is based on the principle that everything with a temperature above absolute zero emits electromagnetic radiation of amplitude and wavelength depending on the thermal characteristics of the object itself. Each "place" can reflect, absorb and transmit an incident radiation in different percentages depending on its structural, chemical, chromatic qualities: radiance constitutes the information that reaches the sensors from the objects placed on the Earth's surface. In passive remote sensing the source of light energy can be considered to be the sun.

In *active* remote sensing, the sensor can emit electromagnetic energy: the sensor becomes both an emitter and an energy receptor. The principles used in this area are those of the RADAR in which the signal is emitted and the return signal is subsequently recorded to determine distance (Gomarasca, 2004).

Since, no direct information on the environment is collected with remote sensing, electromagnetic information must be converted, through the creation of appropriate multidisciplinary models and algorithms, to extract environmental parameters from the continuum of optical-spectral data collected by the sensors and by comparison with ground monitoring. So, the information recorded are processed and analysed, and can be used to obtain various layers of information about soil and crop conditions. Information about growth, vigour, and their dynamics remotely sensed from terrestrial vegetation can provide extremely useful insights for applications in environmental monitoring, biodiversity conservation, agriculture, forestry, urban green infrastructures, and other related fields (Xue and Su, 2017).

Also, this technology allows detection and characterization of an object or the landscape by using aerial or satellite imaging to sense crop vegetation and identify crop stresses and injuries, or pest infestation, in order to produce maps and predict yield potentials on large areas.

In this research, only passive remote sensing techniques have been used.

1.4. Satellite characteristics

Satellites have several characteristics particularly suitable for remote sensing of the Earth's surface.

Orbit is the track followed by the satellite and it depends on the sensor's purpose on board the spacecraft. Orbit changes in terms of altitude above the Earth's surface, orientation, and rotation relative to the Earth. Geostationary orbits, at altitudes of approximately 36,000 kilometres, are followed by satellites which always view the same portion of the Earth's surface. Their revolution speed is equal to that of the Earth. This enables continuous observation and collection of information, such as weather and communication, over specific areas.

On the contrary, near-polar orbits (so named for the inclination of the orbit relative to a line running between the North and South poles) allows the satellites to cover most of the Earth's surface over a certain period. The satellite travels northwards on one side of the Earth (ascending passes) and then toward the southern pole on the second part of its orbit (descending passes). Many of these satellites are also sun-synchronous, they cover each area at a constant local time, so the position of the sun is constant within the same season, which guarantees consistent illumination conditions.

Swath is the width of land imaged by the satellite. Generally, it varies between tens and hundreds of kilometres wide. The rotation of the Earth and the satellite's orbit allow complete coverage of the Earth's surface by the spacecraft swath.

The revisit period is the time elapsed between observations of the same point on Earth by a satellite, and it depends on the satellite's orbit, location, and swath of the sensor. Areas at high latitudes are imaged more frequently than the equatorial zone due to the increasing overlap in adjacent swaths as the orbit paths come closer together near the poles.

1.4.1. MODIS

The Moderate Resolution Imaging Spectroradiometer (MODIS) sensor instrument operates on *Terra* and *Aqua* satellites. Both the spacecrafts are multi-national NASA scientific research satellites in sun-synchronous orbit around the Earth. Figure 3 shows the entire surface of the Earth acquired by MODIS.

The MODIS Land products are freely distributed from Land Processes

Distributed Active Archive Centre (LP DAAC) and they are produced at various temporal resolutions, based on the instruments' orbital cycle: Daily, 8-Day, 16-Day, Monthly, Quarterly, and Yearly. Grids are divided into fixed-area tiles of approximately 10 degrees x 10 degrees in size. Each tile is assigned a horizontal (h) and vertical (v) coordinate ranging from 0 to 35 and 0 to 17 respectively. Products are stored in Hierarchical Data Format (HDF), the standard data storage format selected by the EOSDIS Core System (ECS). MODIS filenames follow a naming convention which gives information regarding the specific product:

- Product Short Name (e.g. MOD13Q1)
- Julian Date of Acquisition (A-YYYYDDD)
- Tile Identifier (horizontalXXverticalYY)
- Collection Version
- Julian Date of Production (YYYYDDDHHMMSS)
- Data Format (HDF-EOS)

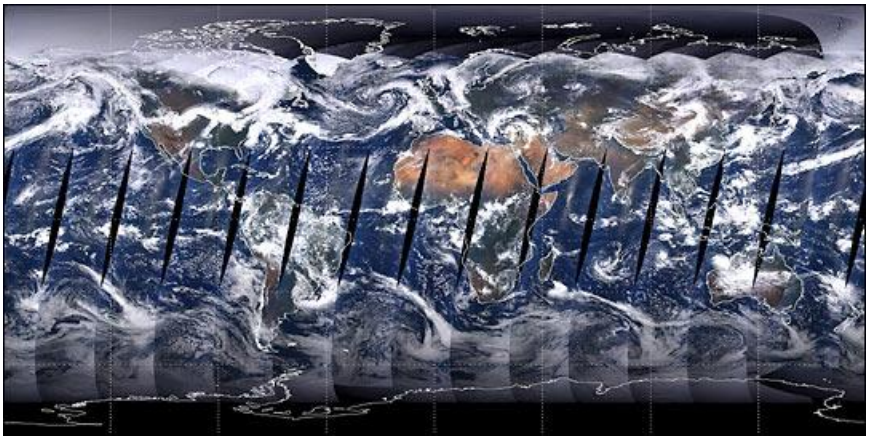

Figure 3 Global browse image for MODIS

Global MOD13Q1 data were provided by MODIS, a 36-band spectroradiometer (Table 1) equipped on board the Terra satellite which is part of the NASA-centred international Earth project Observing System (EOS). The sensor acquires data at three spatial resolutions: 250m, 500m, and 1,000m.

BAND	RANGE (nm) Reflected	RANGE (um) Emitted	KEY USE
1	620–670		Absolute Land Cover Transformation, Vegetation Chlorophyll
2	841–876		Cloud Amount, Vegetation Land Cover Transformation
3	459–479		Soil/Vegetation Differences
4	545–565		Green Vegetation
5	1230–1250		Leaf/Canopy Differences
6	1628–1652		Snow/Cloud Differences
7	2105–2155		Cloud Properties, Land Properties
8	405–420		Chlorophyll
9	438–448		Chlorophyll
10	483–493		Chlorophyll
11	526–536		Chlorophyll
12	546–556		Sediments
13h	662–672		Atmosphere, Sediments
13l	662–672		Atmosphere, Sediments
14h	673–683		Chlorophyll Fluorescence
14l	673–683		Chlorophyll Fluorescence
15	743–753		Aerosol Properties
16	862–877		Aerosol Properties, Atmospheric Properties
17	890–920		Atmospheric Properties, Cloud Properties
18	931–941		Atmospheric Properties, Cloud Properties
19	915–965		Atmospheric Properties, Cloud Properties
20		3.660–3.840	Sea Surface Temperature
21		3.929–3.989	Forest Fires & Volcanoes
22		3.929–3.989	Cloud Temperature, Surface Temperature
23		4.020–4.080	Cloud Temperature, Surface Temperature
24		4.433–4.498	Cloud Fraction, Troposphere Temperature
25		4.482–4.549	Cloud Fraction, Troposphere Temperature
26	1360–1390		Cloud Fraction (Thin Cirrus), Troposphere Temperature
27		6.535–6.895	Mid Troposphere Humidity
28		7.175–7.475	Upper Troposphere Humidity
29		8.400–8.700	Surface Temperature
30		9.580–9.880	Total Ozone
31		10.780–11.280	Cloud Temperature, Forest Fires & Volcanoes, Surface Temp.
32		11.770–12.270	Cloud Height, Forest Fires & Volcanoes, Surface Temperature
33		13.185–13.485	Cloud Fraction, Cloud Height
34		13.485–13.785	Cloud Fraction, Cloud Height
35		13.785–14.085	Cloud Fraction, Cloud Height
36		14.085–14.385	Cloud Fraction, Cloud Height

Table 1 MODIS spectral bands

1.4.2. Landsat 8

Landsat 8 satellite was launched on February 11th, 2013. It is the most recent satellite in the Landsat Data Continuity Mission (LDCM). It is collecting valuable data and imagery used in agriculture, education, business, science, and government. The Landsat Program provides repetitive acquisition of high-resolution multispectral data of the Earth's surface on a global basis. The data from Landsat spacecraft constitute the longest record of the Earth's continental surfaces.

The Landsat 8 satellite orbits the Earth in a sun-synchronous, near-polar orbit at an altitude of 705km, inclined at 98.2 degrees, and circles the Earth every 99 minutes. The satellite has a 16-day repeat cycle with an equatorial crossing time at 10:00 a.m. +/- 15 minutes. Landsat 8 data are acquired with swath overlap varying from 7% at the Equator to a maximum of approximately 85% at extreme latitudes. The scene size is 170km x 185km.

The Landsat 8 satellite has two main sensors: the Operational Land Imager (OLI) and the Thermal Infrared Sensor (TIRS).

OLI collects images using nine spectral bands (Table 2) in different wavelengths of visible near-infrared (NIR), and shortwave light (SWIR) to observe a 185km wide swath of the Earth in 15-30 metre resolution, covering wide areas of the Earth's landscape.

TIRS measures the water resource data and tracks the consumption of land and water. The sensor continues the data collection of the two previous satellites, Landsat 5 and Landsat 7, to provide information for farmers and water resource managers.

Data products of Landsat 8 OLI/TIRS scenes were downloaded from Earth Explorer (https://earthexplorer.usgs.gov/).

No.	Band name	Wavelength [µm]	Resolution [m]
Band 1	Ultra-Blue (coastal/aerosol)	0.435 - 0.451	30
Band 2	Blue	0.452 - 0.512	30
Band 3	Green	0.533 - 0.590	30
Band 4	Red	0.636 - 0.673	30
Band 5	NIR	0.851 - 0.879	30
Band 6	SWIR 1	1.566 - 1.651	30
Band 7	SWIR 2	2.107 - 2.294	30
Band 8	Panchromatic	0.503 - 0.676	15
Band 9	Cirrus	1.363 - 1.384	30
Band 10	Thermal 1	10.60 - 11.19	100* (30)
Band 11	Thermal 2	11.50 - 12.51	100* (30)

Table 2 List of spectral bands of Landsat 8 Operational Land Imager (OLI) and Thermal Infrared Sensor (TIRS), with range of wavelength and spatial resolution.

1.4.3. Sentinel-2

Sentinel-2A is a European optical imaging satellite launched on 23rd June 2015. It is the first Sentinel-2 satellite launched as part of the European Space Agency's Copernicus Programme. On 7th March 2017 the Sentinel-2A was joined in orbit by its similar satellite, Sentinel-2B.

The Copernicus Sentinel-2 mission provides the Global Monitoring for Environment and Security program, jointly implemented by the European Commission (EC) and European Space Agency (ESA) services related to land management, agricultural production and forestry, monitoring of natural disasters management, and humanitarian operations.

The Sentinel-2 mission comprises a constellation of two polar-orbiting satellites placed in the same sun-synchronous orbit, phased at 180° to each other. The two satellites provide high resolution optical imagery every 10 days at the equator with one satellite, and every 5 days with both satellites, under cloud-free conditions. This results in 2-3 days at mid-latitudes. They also provide continuity for the current SPOT and Landsat missions regarding global coverage of the Earth's land surface. It was designed specifically to deliver a wealth of data and imagery with the aim to monitor variability in land surface conditions by using a wide swath width (290km)

and high revisit time. The coverage limits are between latitudes 56° south and 84° north. The orbit has an average height of 785km.

The satellites are equipped with an opto-electronic wide swath multispectral sensor, the MultiSpectral Imager (MSI) instrument, that offers high-resolution optical imagery. The S2 MSI samples 13 spectral bands (Table 3), which ensures the capture of differences in vegetation state, including temporal changes, and also minimizes impact on the quality of atmospheric photography: visible and near infrared (NIR) at 10 metres, red edge and short-wave infrared (SWIR) spectral zones at 20 metres, and atmospheric bands at 60 metres spatial resolution. It provides data suitable for assessing state and change of vegetation, soil, land and detecting changes in water cover.

No.	Band name	Central wavelength [nm]	Bandwidth [nm]	Resolution [m]
Band 1	Coastal aerosol	443.9	27	60
Band 2	Blue	496.6	98	10
Band 3	Green	560	45	10
Band 4	Red	664.5	38	10
Band 5	Vegetation Red Edge	703.9	19	20
Band 6	Vegetation Red Edge	740.2	18	20
Band 7	Vegetation Red Edge	782.5	28	20
Band 8	NIR	835.1	145	10
Band 8a	Narrow NIR	864.8	33	20
Band 9	Water vapor	945	26	60
Band 10	SWIR – Cirrus	1373.5	75	60
Band 11	SWIR	1613.7	143	20
Band 12	SWIR	2202.4	242	20

Table 3 List of spectral bands of Sentinel-2, with central wavelength, bandwidth and spatial resolution.

Figure 4 shows the comparison of L8 and Landsat 7 spectral bands with S2 spectral bands.

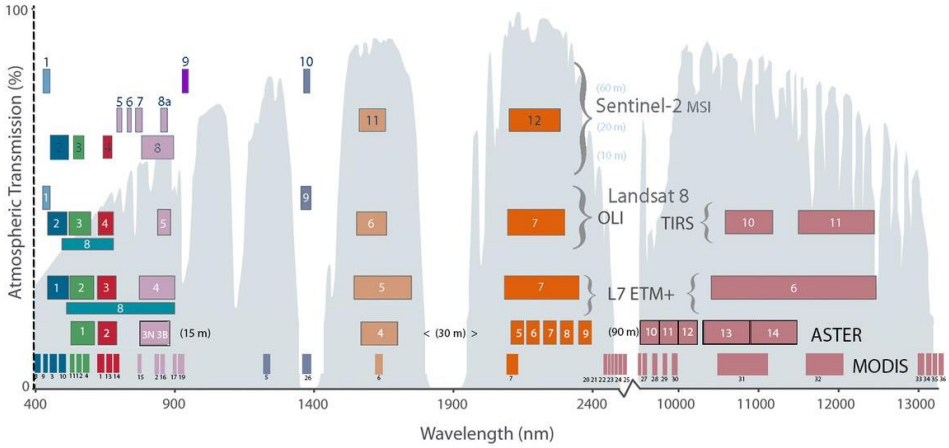

Figure 4 Comparison of Landsat 8 and Landsat 7 spectral bands with Sentinel-2 spectral bands (NASA 2018)

1.5. Study aims and objectives

The aim of this study is focused on the effects of drought and water supply in agriculture analysing in three different environmental conditions, combining weather data and satellites imagery.

In particular, the main objectives of this study are:

i) identifying the spatial and temporal distribution of major drought episodes (length and severity) in three different climatic conditions: Continental Temperate, Mediterranean and Temperate Oceanic;

ii) evaluating the effects of water shortage and drought on the productivity of the most important crop cultivated in Ireland, grass pasture;

iii) evaluating the effects of drought in the most important vineyards of Piedmont (north-western Italy), evaluating the consequences of water shortage on vineyard production in the three main grape varieties: Barbera, Moscato Bianco and Nebbiolo;

iv) to contribute to the development of a near-real-time decision support service to support winemakers in the management of vineyards.

1.6. Thesis Structure

This dissertation is divided into seven chapters and presented as a series of results chapter (chapters 4, 5 and 6) with chapters 1, 2 and 3 containing further information and description.

This **first chapter** contains the research context, aims and objectives. Piedmontese vineyards, grape varieties and wine phenology are also described. Moreover, the chapter explains the principles of remote sensing, describing three satellites, Terra (MODIS), Landsat and Sentinel.

Chapters 4, 5 and 6 are structured with Introduction, Methods, Results, Discussion and Conclusion sections. Chapters have the title of the manuscript, journal name, and a short preamble at the beginning of each chapters has been included to "set the scene" regarding the specific study.

Chapter 4 and 5 are published in peer reviewed journals. Chapter 6 has been submitted to peer reviewed journal and is under review.

Chapter 2 provides information about the context and main themes of the study, while Chapter 3 provides information about the materials and methods used. The results Chapter (4, 5 and 6) provide the results of analysis undertaken in four different climatic zones, which are Continental Temperate climate (Piedmont), Mediterranean climate (Sardinia) and Temperate Oceanic (Republic of Ireland). The final chapter discusses the strengths and limitations of the methods applied, findings of the analyses, main conclusions of the study, and recommendations for future research in this topic.

The main topics of each chapters are as follows and schematically shown in Figure 5):

Chapter 2 - focuses on drought, its definition, types, causes, effects and methods of investigation. A further description is given of the impacts of drought, early warning systems and future climate scenarios.

Chapter 3 – describes the concepts, techniques, materials and methods applied in four case studies related to the main topic of this research and reported entirely in chapters 4, 5, 6 and Appendix 2. Three sections are dedicated to the description of weather stations, quality control of meteorological data and drought indicators. A brief

concept of evapotranspiration is provided and equations to evaluate it. Subsequently, the chapter describes the remote sensing data obtained by the three satellites, Terra (MODIS), Landsat and Sentinel, and indices based on remote sensing. Finally, a machine learning algorithm and a methodology to provide gross production maps are illustrated.

Chapter 4 – presents the results of the climatic analysis in three different climatic environments by using the *ClimPACT2* software. The Continental Temperate climate is analysed in Piedmont at regional level and compared with the Mediterranean climate, studied in Sardinia to provide an analysis of the hydrological drought episodes. The water shortage events were investigated analysing the trends of the Standardised Precipitation Index (SPI) and Standardised Precipitation Evapotranspiration Index (SPEI), during the period 1981-2017.

Chapter 5 – presents a case study of a drought episode that occurred in Republic of Ireland during the summer of 2018, and provides a comprehensive, national-scale evaluation of climate conditions comparing a variety of indicators and indices. The indicators and indices are further evaluated for their efficacy, contributing to the strength of this approach for research and as a potential information service.

Chapter 6 – presents a methodology for estimating the gross primary production in the most important vineyards of Piedmont and determining its variation over time and space, using meteorological data and remote sensing techniques. The chapter shows the main results of the multi-temporal analyses about drought episodes, in particular the effect of water shortage conditions that occurred in 2017, on productivity of the Barbera, Moscato Bianco and Nebbiolo grape varieties.

Chapter 7 – draws on all the research work with a discussion of research finding, highlighting where new knowledge has been generated, discussing implications.

Additional information are presents in the Appendices (Appendix 1, 2, 3 and 4).

In Appendix 1, a case study of an adaptation plan to climate change is presented. The study was conducted in the Cocagne watershed in the south eastern cost of New Brunswick in Canada, in order to analyse the recent climate variability and trends, to identify the various climatic risks at the watershed scale and mapping the most vulnerable areas.

A list of meteorological data and remote sensing imagery is presented in Appendix 2 and 3, respectively.

Finally, all scholarly articles and reports consulted in the composition of the thesis are included in the reference list.

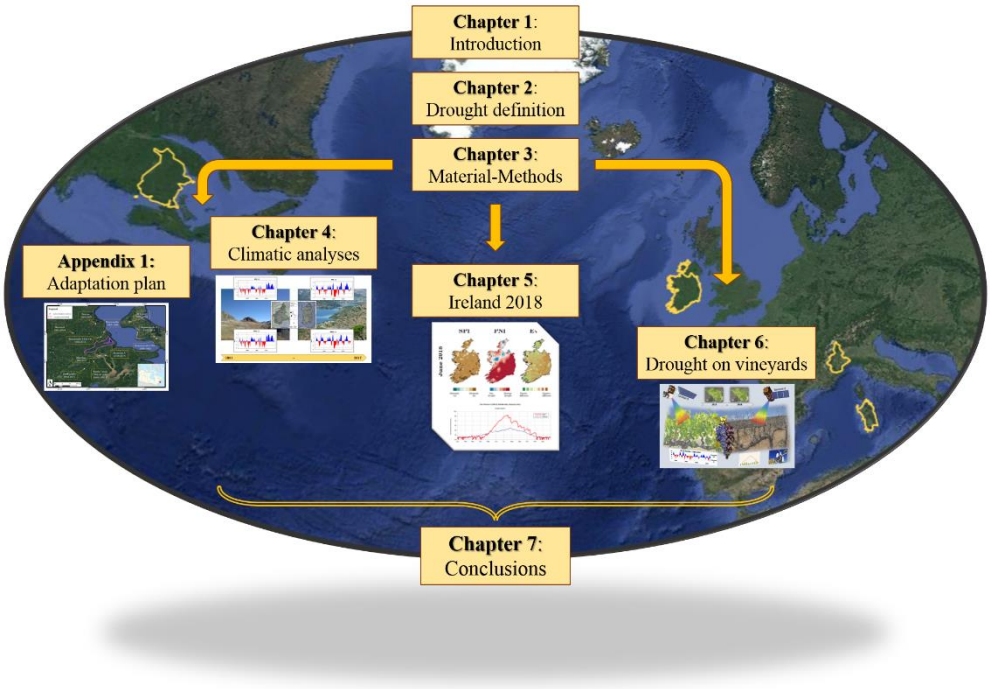

Figure 5 Diagram of thesis structure

CHAPTER 2: DROUGHT

This chapter focuses on drought, its definition, types, causes, effects, and methods of investigation. A further description is given to the impacts of drought.

2.1. Definition of Drought

According to the WMO (2006) definition, drought is an insidious natural hazard characterized by lower than expected or lower than normal precipitation that is insufficient to meet the demands of human activities and the environment, when extended over a season or longer period.

Alternatively, drought can be defined as a temporary and recurring reduction of rainfall in a specific area. In contrast to aridity, which is a measure of long-term average climatic conditions, drought is not a permanent climatic phenomenon (Maliva and Missimer, 2012); it is characterized by water supplies lower than those considered normal and considered as an expected event of recurrent features of the climate cycle.

Drought is a complex, multifaceted issue, but is a normal feature of climate and its recurrence is inevitable. It is characterized by its duration, intensity and spatial extent, and is influenced by different factors, including low precipitation, high temperature, strong wind, solar radiation and relative humidity. Moreover, drought is not restricted to dryland, but occurs both in dryland and humid areas (Wilhite *et al*., 2014) and almost every climatic zone might experience drought.

Drought is difficult to quantify and since its effects often accumulate slowly over a considerable period and may delay for years after the termination of the event, determining the onset and end of drought is problematic (Wilhite, 2000). In fact, it takes several months for a region to accumulate enough precipitation deficits to begin a drought, whereas a drought end can come within one month to one season (Mo, 2011). There are many studies (Dai and Zhao, 2017; Lena *et al.*, 2015; Schwalm *et al*., 2017; Zandalinas *et al*., 2018) on the maintenance of drought, but the onset and end of drought are not fully understood.

2.2. Types of Drought

Drought has been grouped by type as follows: meteorological, hydrological, agricultural, and socioeconomic (Wilhite and Glantz 1985). Figure 6 explains the relationship between these various types of drought and the duration of the event.

2.2.1. Meteorological drought

Meteorological drought is expressed solely by the degree of dryness and defined by rainfall deficiency (Wilhite, 2000). The intensity is often in comparison to some normal or average amount, while the duration of the dry period lasts between 1 to 3 months. Normal rainfall is assumed to be the mean rainfall for a certain period (month, season or year). Some studies criticize the definition of drought as deviations from normal conditions, because the calculation of normal precipitation is often based on a period too short (e.g. thirty years) to represent long-term variations (Deo *et al*., 2017; Barker *et al*., 2016; Hisdal and Tallaksen, 2000). Usually, meteorological drought relates to actual precipitation departures from average amounts on monthly, seasonal or annual time scale.

Meteorological drought must be considered as region-specific since climate regimes influence the atmospheric conditions that result in precipitation deficiencies. For example, calculating meteorological drought based on the number of days with precipitation less than some specified threshold instead of the magnitude of the deficiency over a period, is not correct in regions where precipitation distribution is seasonal and extended periods without rainfall are common.

2.2.2. Agricultural drought

Agriculture is usually the first economic sector to be affected by drought because soil moisture supplies are often quickly depleted, especially if the period of moisture deficiency is associated with high temperatures and windy conditions (Wilhite, 2000). Indeed, agricultural drought happens when soil moisture is insufficient and results in a lack of crop growth and production. Impacts in agriculture are the key way to evaluate agricultural droughts, which normally last between 1 to 6 months. Agricultural planning can often reduce the risk of drought on crops by changing crops, genotype, planting date and cultivation practices (Winkler *et al*., 2017).

The impacts of drought vary through the year. Growing season is the most critical moment and a change in precipitation during that period could help or destroy a whole crop (Anderson *et al*., 2016). Hence, forage yields may be normal or above normal during a drought if rainfall coincides with critical phenological stages and is characterized by low intensity and high soil infiltration rate.

The impacts of drought depend on different stages of crop development, which show variation in susceptibility. Moreover, the effects of drought are specific to crops because the phenological phases most sensitive to atmospheric agents vary between crops. High temperature stress that occurs in association with dry conditions can have different effects on ripening periods, that vary between crops and locations.

Agricultural drought links crop water demand with various characteristics of meteorological drought, such as precipitation shortages, differences between actual and potential evapotranspiration (ET_0), and soil water deficits (Wilhite, 2000). The prevailing weather conditions are the main influence on variation in plant water demand. Biological characteristics of plants, their stage of growth and the physical and biological properties of the soil also play a crucial role. In fact, in an early growth stage, deficient moisture in the subsoil can have no impact on final crop yield if topsoil moisture is enough to meet early growth requirements.

In a contest of climate change, the impact on yields of non-irrigated crops like wheat, corn and sugar beet are projected to decrease by up to 50% by 2050 in southern Europe (EC, 2017). This could result in a substantial drop in farm income by 2050, with large regional variations. In a similar scenario, farmland values are projected to decrease in parts of southern Europe by more than 80% by 2100, which could result in land abandonment (EC, 2017).

Moreover, the European agriculture sector is highly regulated by European policies, in particular the Common Agricultural Policy (CAP). The focus of previous CAP strategy, adopted in 2013, was the adaptation to climate change. The adaptation promoted the implementation of technical measures for both mitigation and adaptation at farm level in order to reach the specific objectives in the CAP. However, the specific actions to improve the resilience of the sector are still limited and the agriculture sector is still one of the sectors most vulnerable to climate change impacts.

2.2.3. Hydrological drought

Hydrological drought conditions are related to the effect of the absence of precipitation on water resources hydrological when there is a lack of water in the hydrological system (i.e., streamflow, reservoir and lake levels, groundwater). They are associated with the effects of periods of lack of precipitation on the surface or subsoil water supply, rather than precipitation deficiencies. The effects occur after 6 months and can continue over two years. Hydrological droughts are generally out of phase or delay the onset of meteorological and agricultural droughts and are detected in retrospect.

The frequency and severity of hydrological drought is defined at the river basin scale, comparing the actual flow with the long-term runoff threshold to consider the progression of the drought (Wilhite, 2000).

The impacts on hydrological system and storage systems, such as dam, reservoirs and groundwater, influence several economic sectors, since water is used for multiple purposes, such as agriculture, hydrological power production and transportation.

The complexity and connections of hydrological systems spread the impacts on the entire catchment. Hydrological drought in an upstream part of a river basin can extend downstream since a reduced flow can lead to lower groundwater levels in the downstream positions.

2.2.4. Socio-economic drought

Socio-economic drought occurs when the demand for water exceeds the supply (Ziolkowska, 2016). Considering the existing water system formed by water conveyances, reservoirs for surface storage, and aquifers, socio-economic droughts can be defined as failures in water supply when demands are not satisfied. It associates the supply and demand of some economic good or services with elements of meteorological, hydrological, and agricultural drought. Human activities modify the hydrological processes underlying drought propagation. Therefore, socio-economic drought occurs when the demand for a service exceeds the supply due to a shortage of supply linked to weather conditions. The temporal and spatial processes of supply and demand are the two key concepts.

Our society is characterized by both population growth and per capita consumption, and since most economic goods depend on weather

conditions (i.e. agriculture, hydroelectric generation), the incidence of drought could increase. There is a strong symbiosis between drought and human activities and variations in physical events associated with a change in social vulnerability to water shortages, causing an increase in drought impacts. Anthropogenic changes to the land surface alter hydrological processes including evapotranspiration, infiltration, surface runoff, and storage of water and in this way affect the development of drought (Van Loon A.F. *et al.*, 2016). In several countries, poor land-use practices and extreme land consumption increase soil erosion, which exacerbates impacts and vulnerability to droughts (Wilhite, 2000).

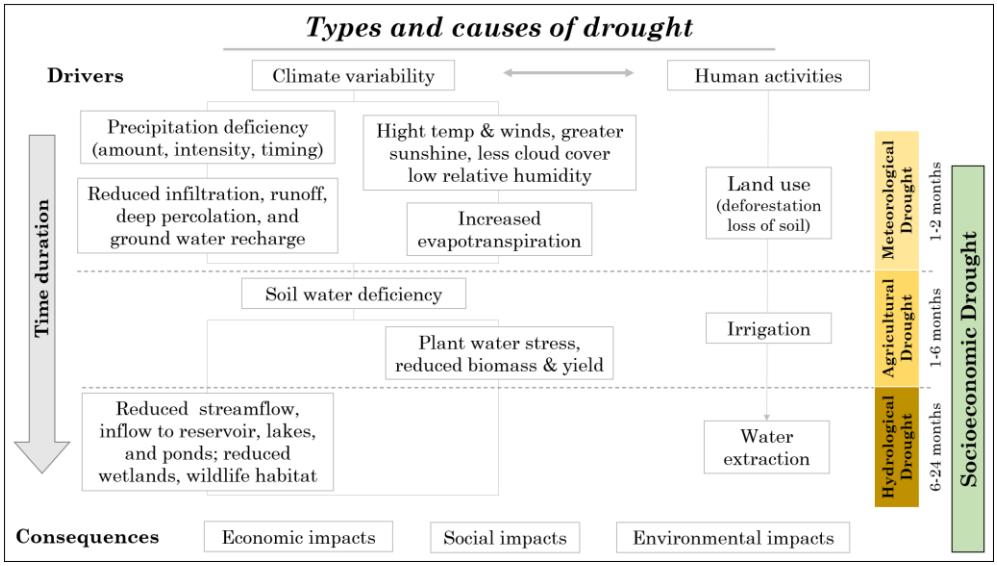

Figure 6 Relationship between various types of drought and duration of drought events (Wilhite, 2000).

2.3. Impact and vulnerability

Droughts are considered the most costly natural disaster (Ross and Lott, 2003) and can arise virtually everywhere on the globe (Schubert *et al.*, 2016). Droughts are a recurrent feature of climate and their impact on the environment and human activities depends on the interaction between this natural event and water demand for several purposes, from agriculture to civil and industrial needs. In fact, droughts can affect both ecosystems and society in multiple ways by, on the one hand, being main drivers for land

degradation and desertification and, on the other hand, involving socio-economic impacts such as crop failure, food shortages, famine, malnutrition, deaths and mass migration (Masih *et al.*, 2014).

It is important to analyse droughts at the regional or continental scale since droughts may persist for long periods and affect large areas, unlike many other natural extreme events. Heat waves, forest fires and vegetation stress are potential processes that increase droughts with impacts on a large scale. Therefore, it would be incorrect and misleading to focus the study of the drought event exclusively on a single area or local communities, that must face in the worst scenario, starvation and migration with repercussions also on the surrounding territories.

Agriculture and food production are the primary sectors affected by drought due to high water demands by farming. The impact of drought on water resources and agriculture is a complex process, it responds to the particular characteristics of a region and its effects can vary greatly from region to region (Renza *et al*., 2010). Agricultural activity itself, including water flow regulation and irrigation practices, may also lead to reduced water availability and, thus, conditions of agricultural drought (Jaramillo and Destouni, 2015). Conservation agriculture increases the capacity of agriculture to adapt to the impacts of drought. Integrated crop, soil and water management measures can be employed to reduce soil degradation and increase the resilience of agricultural production systems. Crop diversification and adoption of drought-tolerant crops, reduced tillage, adoption of improved irrigation techniques (i.e. drip irrigation), moisture conservation methods and maintaining vegetation can reduce the negative effects of water shortage. A healthy agricultural system and so a stable food production guarantee food security, while an unstable food production because of drought and others extreme weather events, can have dramatic impacts on society, safety, and stability between countries.

Drought impacts also have severe environmental and socio-economic impacts and depend upon human and ecosystem demands for water, available water-resource management capabilities and practices, and the meteorological and hydrological characteristics of the drought (Loucks and Gladwell, 1999). They are controlled to a large degree by the duration of droughts, rather than their severity, because recovery from the cumulative damage of consecutive drought years is more difficult (Cook *et al*., 2007).

Societal development and organisation are impacted by drought in different levels depending on density of the rural population and its per

capita GDP. Many societies do not have the economic resources to overcome single drought or multiple-year droughts, particularly in water-stressed regions where resources are inadequate to meet local needs even during normal years. Especially in the context of climate change, the recurrent nature of droughts requires pro-actively planned policy instruments both to be well-prepared to respond to droughts when they occur, and to undertake ex-ante actions to mitigate their impacts by strengthening the societal resilience to drought (Gerber and Mirzabaev, 2017).

The adaptive capacity of the water system and the gap between average water use and the safe yield of a system are the main factors to influence the vulnerability to droughts, especially when water supplies are already under pressure to meet demands during normal hydrologic conditions. Moreover, urban areas depending on surface water are more vulnerable to drought because the impacts of reduced precipitation are more immediate. Desalination water systems may reduce vulnerability to drought (Wilhite, 2000). The undefined onset of drought events increases the difficulties of planning for, and adapting to, this phenomenon. Droughts are usually recognized only when the water shortage conditions are already established. Moreover, the undefined end of drought creates more difficulties with taking defensive actions (Pereira *et al.* 2002).

2.4. Early warning system

Coping strategies for responding to and preparing for drought became strongly necessary and imperative both from an environmental and socio-economic point of view, since drought is a normal feature of climate and their recurrence is inevitable. Drought is context-dependent, but its impacts are diffuse, both direct and indirect, short-term and long-term. Although we cannot influence the occurrence of the natural event, and drought is a highly complex natural hazard for which it is difficult to precisely identify the start and end (Wilhite and Pulwarty, 2017), we can reduce vulnerability through more reliable forecasts, improved early warning systems, and appropriate and timely mitigation and preparedness measures. These systems are numerous, range from individual or household level to national level, and attempt to identify the precise characteristics and thresholds that define the onset, continuation, and termination of drought episodes as well as their severity.

National climate and meteorological services provide climate and drought information in order to assist decision-making by individuals and organisations. This information can be used by planners, emergency managers, policymakers and decision-makers to implement programs and policies that will help to reduce the risk associated with the hazard (Wilhite, 2000). Monitoring climate, soil, ecological factors, and biodiversity, integrated with socio-economic aspects, provides a basis for better vulnerability prediction and assessment (Vogt *et al*., 2011). Monitoring and early warning refers to activities at all levels of the onset of drought.

Data collection and analysis, including the use of indices to track current drought conditions and to view them in a historical context, and the communication of data, are some activities that form the basis of early warning techniques.

A useful approach for a comprehensive drought-monitoring system includes the collection of climatological data as well as hydrological data (i.e., streamflow, reservoir, groundwater levels, and soil moisture), but also remotely sensed data (Wilhite, 2000). Using this information allows the development of drought preparedness plans, which provide relief measures, including drought insurance, to forecasts of agricultural and hydrological drought.

Vulnerability is increasing globally despite dramatic technological advances and the availability of large financial resources. The diversity and complexity of drought impacts will be exacerbated by an increase in extreme climatic events, described below in section 2.5.

2.5. Trend and Scenarios

Global warming effects are already having negative and unpredictable consequences. Mainly, increases in heat waves and droughts that contribute to desertification and decline of crop yields, but also floods, cyclones and wildfires which reveal the significant vulnerability of many ecosystems and some human systems to current climate variability. In urban areas, climate change is projected to increase human risks, while alteration of ecosystems due to extreme weather-related events has been recorded in many parts of the world. Impacts of such climate-related extremes also include disruption of food production and water supply, damage to infrastructure and settlements, human illness and mortality, and

consequences for mental health and human well-being. A changing climate leads to changes in the frequency, intensity, spatial extent, duration, and timing of extreme weather and climate events, and can result in unprecedented extreme weather and climate events.

Droughts, as described in previous sub-chapters, occur naturally, but climate change has generally accelerated the hydrological processes to increase the speed of their onset, and the magnitude of their intensity, with many consequences (Mukherjee *et al*., 2018). Future climate projection models (Fischer *et al.*, 2007, Lorenz *et al.*, 2012) suggest that drought will be more frequent in the future due to global climate change, which is expected to cause increases in temperature (and heat wave events) and changes in precipitation. In fact, even though global rainfall is projected to increase, the activities contributing to global warming will influence the extent to which drought is triggered. This is due to the variation in precipitation characteristics (amount, frequency, intensity, duration, type) and extremes events (Trenberth *et al.*, 2003) which cause flooding and erosion, with a substantial impact on the hydrological cycle in determinate areas throughout the world, especially in the tropics and subtropics regions (Dai, 2011). For example, for the near future (next 15-20 years), Perini *et al*. (2011) predicted a strong decrease in winter and spring precipitation in Northern and Southern Italy, and a reduction of summer rainfall in Southern Italy and the islands. While, by the 2100s, a general temperature increase of about 3 °C is expected in all seasons across the whole of Italy, peaks of 4 °C are projected for the Po Valley in winter and over the whole north-west region in summer (Bucchignani *et al.*, 2016), according to the RCP4.5 scenario, with increasingly frequent and long-lasting heat waves, which will extend to more than thirty days over the entire summer season (Collins *et al*., 2013; Drumond *et al*., 2017; González-Hidalgo *et al*., 2018). On the contrary, the RCP8.5 scenario predicts a strongly significant reduction in precipitation in spring and summer in the Alpine area with a negative anomaly from 0.1 to 0.4mm day^{-1} (Bucchignani *et al*. 2016). The future projections of climate change over the 21st century also predict a reduction of renewable surface water and groundwater resources in most dry subtropical regions, intensifying competition for water among sectors. According to the RCP8.5 scenario, the frequency of droughts will likely increase by the end of the 21st century in presently dry regions, while in contrast, water resources are projected to increase at high latitudes.

In this context of climate change, Sheffield and Wood (2008) found that models in the third phase of the Coupled Model Intercomparison Project

(CMIP3) simulate large-scale droughts in the 21st century reasonably well, and the Mediterranean area and mountain regions, considered "hot spots" of climate change, will consistently be affected by droughts more frequently (Ronchi *et al*., 2007; Capra and Scicolone, 2012).

Future climate projections for Ireland based on an ensemble of high-resolution regional climate projections indicate that the number of extended dry periods is expected to increase substantially during summer and autumn by the middle of the century. Summers are projected to be worst affected, with dry periods increasing by 12 and 40% for the medium- to low- emission and high- emission scenarios, respectively. Drought will be driven mainly by a decrease in mean precipitation and a rising of mean annual temperature. By mid-century, the rainfall amount is expected to reduce during spring and especially during summer, with a reduction ranging from 3 to 20%, while mean annual temperatures will rise by 1-1.6 °C, with the largest changes seen in the east of the country (Nolan, 2015).

Furthermore, human activities can exacerbate the impacts of drought. Over-exploitation of aquifers, excessive agricultural activity, excessive irrigation, deforestation, and loss of soil covers or vegetation due to inadequate land use, may aggravate the drought conditions and adversely impact the ability of the land to capture and hold water (Changnon *et al.*, 1996; IPCC, 2012). Moreover, the interaction of increased temperatures and pollutant loadings from heavy rainfall which increases the concentration of pollutants during drought, will reduce raw water quality and pose risks to drinking water quality. Future increase in the demand for water will be most critical in periods of severe and extensive droughts (Hisdal and Tallaksen, 2000).

Climate change is already affecting the food and agriculture sectors, and these effects are projected to grow, along with global average temperatures, especially when the shortage of precipitation during the growing season imposes on crop production or ecosystem function in general (due to soil moisture drought). Responses to decreased food production and quality and adaptation options for agriculture include technological responses, and developing new crop varieties adapted to changes in CO_2, temperature, and drought; enhancing the capacity for climate risk management; and offsetting economic impacts of land use change. Improving financial support and investing in the production of small-scale farms can also provide benefits.

CHAPTER 3: MATERIAL AND METHODS

This chapter describes concepts, techniques, materials, data and statistical analyses applied in four case studies related to the main topic of this research and reported entirely in Chapters 4, 5 and 6.

3.1. Weather stations

The meteorological data were collected from four weather station networks, in the region of Piedmont, in the region of Sardinia, in the Republic of Ireland (Ireland) and in the state of New Brunswick.

3.1.1. Weather data: Piedmont

Two different networks of meteorological stations were used for the Piedmont region in two different studies, described in more detail in Chapters 4 and 6.

In the first study described in Chapter 4, daily weather data in the Piedmont region were collected from thermo-pluviometric stations of the Italian Hydrographic Mareographic Service (SIMN). The stations considered were Alessandria, Asti, Cuneo, Oropa, Torino, Varallo Sesia and Vercelli (see Chapter 4, Table 5). These are uniformly distributed in the region (see Chapter 4, Figure 8) with an altitude range between 90m and 1,180m a.s.l. Meteorological stations above the limit of 1,200m a.s.l. were excluded from the analysis.

Daily precipitation (P) and maximum (T_x) and minimum (T_n) daily temperature data were considered for all stations during the period 1981-2010, which is the current climatological standard 30-year period (WMO, 2017).

An additional seven years (2011-2017) were collected for the station of Torino resulting in a total of 37 years of data. The additional series of data (1981-2017), in the most representative station of the territory, was analysed in order to compare the most recent trend.

In the second study (see Chapter 6), the climate data were obtained by the Regional AgroMeteorological network (RAM) of Piedmont. The network currently consists of 120 electronic weather stations and has been operating continuously since the second half of the 1990s. Most of the stations have a climatic historical series of over 15-20 years, that is valuable for capillary climatological analysis and interpretation of the atmospheric, agricultural and phytosanitary phenomena. The RAM stations are uniformly distributed between 100 and 800m a.s.l. in the Piedmontese agricultural area, characterized by vineyards, orchards rice and cereal crops.

The RAM stations are equipped with a thermometer and hygrometer sensors, and use a tipping-bucket rain gauge, SIAP UM 7525, with a calibrated mouth (1000cm^2). Any movement of the lever corresponds to 20g of water, equivalent to 0.2mm of rain. The mouth is at a height of 2m from the ground.

The electronic instruments transmit the information in real time via GPS or GPRS to the operative centre in Torino (Piedmont) for collection and storage of the meteorological data in order to realize a consistent agrometeorological database. In fact, European and national regulations underline the fundamental importance of these monitoring networks and information distribution systems as support for the agricultural sector and the production processes management.

The meteorological data collected are subject to validation and possible reconstruction of missing data to provide continuity. Finally, the data are published daily on the web in an hourly and daily format. The surveys of the last 30 hours and of the last 30 days are freely available.

In this study, twenty-four weather stations were selected in the vineyard area (see Chapter 6, Figure 24 and Table 8), throughout the period from 2003 to 2018.

3.1.2. Weather data: Sardinia

In the Sardinia region, daily temperature and precipitation data were obtained from the Hydrographic Sector of Sardinia Region (RAS) and the weather stations considered were Desulo, Mandas, San Giovanni Coghinas, Santa Giusta and Villanova Monteleone. These were supplemented by the addition of Cagliari/Elmas station from the Italian

Air Force meteorological station network (see Chapter 4, Table 5). The altitude range of the stations (see Chapter 4, Figure 8 and Table 5) is between 10 and 920m a.s.l.. Their location is representative of the different geographical and topographical conditions of the island.

Daily precipitation (P) and maximum (T_x) and minimum (T_n) daily temperature data were considered for all stations during the period 1981-2010, which is the current climatological standard 30-year period (WMO, 2017).

An additional seven years (2011-2017) were collected for the station of Cagliari/Elmas resulting in a total of 37 years of data. The additional series of data (1981-2017), in the most representative station of the territory, was analysed in order to compare the most recent trend.

3.1.3. Weather data: Republic of Ireland

The observation network in Ireland is managed and maintained by Met Éireann, the Irish Meteorological Service (see Chapter 5 and Appendix 2). The network gathers weather data for use in weather forecasting, numerical weather prediction models, reanalyses, climate applications, forecast verification and for use by a wide range of stakeholders, including those in the agricultural sector. Met Éireann's network currently consists of four different types of weather station, differentiated according to the range of instruments at each station and the measurement interval.

The network includes five airports which are manned stations where staff record meteorological elements each hour. There are also 20 automatic (synoptic) stations which record data at 1-min resolution. Both the manned and automatic stations record air temperature, precipitation, atmospheric pressure, wind speed and direction, relative humidity, cloud type, visibility, sunshine, soil and earth temperatures, and past and present weather. As in the United Kingdom, Met Éireann also has a network of 60 climatological stations run by voluntary observers and state agencies who record a set of measurements at 0900 UTC each day. Each of these stations reports air temperature and precipitation, but some also record grass temperature, soil and earth temperatures, sunshine duration and cloud cover, wind speed and direction, visibility and present weather. The final suite of stations run by Met Éireann, as well as voluntary observers and state agencies, is an extensive network of approximately 500 rainfall stations. This wide network is necessary in order to capture rainfall in

Ireland, which has a high degree of spatial variability. There are daily and monthly stations in the rainfall network where 'daily' implies that the readings are taken once a day at 0900 UTC while at 'monthly' stations the readings are taken at 0900 UTC on the first day of the month.

A number of stations have been either recently installed, discontinued, or have significant gaps in their recording history. To include the maximum number of continuously recording stations in the calculations of the parameters of interest, two time periods were selected.

3.1.4. Weather data: New Brunswick

Daily climatic data around the Cocagne watershed (New Brunswick, Canada) were collected from thermo-pluviometric stations of the Environment Canada meteorological network (see Appendix 1).

The weather stations considered for the New Brunswick area were Bouctouche, Harcourt, Moncton, Parkindale, Rexton and Turtle Creek, shown in Appendix 1, Figure 12. O'Leary and Summerside stations were considered for the Prince Edward Island province, as shown in Appendix 1, Table 11).

Distance from the watershed (less than 80km), percentage of missing data (less than 20%), and number of years of collecting data (more than 20 years), were the main criteria for choosing the meteorological stations.

Turtle Creek station is close to the watershed and was chosen because of the large number of years recorded, although the percentage of missing data is higher than 20% for both temperature and precipitation data, as shown in Table 12.

On the other hand, Baltimore station was not considered because of the short period of years recorded, despite its watershed proximity.

During the study period, three stations were relocated within a few metres of the initial location, Bouctouche CDA, Moncton A and Summerside A. The historical and current dataset were merged to ensure the historical continuity of the three stations.

3.2. Quality Control: *ClimPACT2* software

A Quality Control (QC) analysis was conducted on the daily data series by using the R software *ClimPACT2* package (Alexander and Herold, 2016) to identify gaps, outliers and erroneous values (Acquaotta *et al*., 2019).

This algorithm detects incorrect values, such as Precipitation < 0mm or $T_x < T_n$, and provides a series of graphical representations in the form of box diagrams in a monthly and annual scale, to evaluate discontinuities present in the series (Acquaotta *et al*., 2016). Outlier values are identified through the calculation of the estimated thresholds on the series statistical characteristics (Fortin *et al*., 2016).

The correction of data is an essential step to ensure there are no outliers and that no more than 20% of the data is missing. The software provides a database and graphs of the daily time-series of minimum temperature (T_n), maximum temperature (T_x), diurnal temperature range (DTR) and precipitation, and identifies parts of the series which could be problematic. The boxplot graphs identify potential outliers based on the interquartile range (IQR), which is defined as the difference between the 75^{th} and the 25^{th} percentiles. The boxplots flag temperature and precipitation data as outliers, if temperature values fall outside the range defined by the 25^{th} IQR -3 interquartile ranges (lower bound) and the 75^{th} IQR +3 interquartile ranges (upper bound).

3.3. Drought indicators

Monitoring different aspects of the hydrological cycle requires a variety of indicators and indices. No single indicator or index can be used to determine appropriate actions for all types of droughts. Hence, the use of different combinations of inputs with various thresholds characterising all four meteorological, agricultural, hydrological, and socio-economic drought types is a preferred approach to provide complete information. Percent of Normal Index (PNI) and Standardised Precipitation Index (SPI) are based on precipitation data, and the former can characterise the four types of drought. Standardised Precipitation Evapotranspiration Index (SPEI) adds the evapotranspiration value to the SPI equation, while Soil Moisture Deficit (SMD, based on soil moisture data) characterises agricultural drought These drought indicators are described in the following subsections.

3.3.1. Percent of Normal Index (PNI)

The simplicity of the Percent of Normal Index (PNI) calculation (Werick *et al.*, 1994) makes the index useful for comparing any time period and location, to identify and monitor various impacts of droughts. The index can be calculated for time scales ranging from a single month to a group of months representing a particular season. PNI is calculated by dividing the actual precipitation (P) for the month under consideration by the normal precipitation for the corresponding month in the 30-year period (P_a) and multiplying the ratio by 100.

3.3.2. Standardised Precipitation Index (SPI)

The Standardised Precipitation Index (SPI) (McKee *et al.*, 1993) is an index based on monthly cumulative precipitation and classifies the accumulated precipitation of the month under consideration with respect to the long-term average monthly accumulated precipitation for the same month (or other time scales). SPI quantifies a deficit or surplus of precipitation over mean values at different time scales (1, 3, 6, 12, 24 and 48 months) using a probabilistic approach. A rainfall time series is transformed so that it can be described by a statistical gamma distribution, and further transformed into a standardised normal distribution. The index can be used to describe the four types of drought, and the classification of the values range from very wet to very dry drought conditions.

3.3.3. Standardised Precipitation Evapotranspiration Index (SPEI)

Standardised Precipitation Evapotranspiration Index (SPEI) is a multiscalar drought index designed to consider both precipitation and potential evapotranspiration (ET_0). SPEI looks at long-term rainfall at different timescales and compares it with expected demand as indicated by potential evapotranspiration. The ET_0 could be estimated with the Thornthwaite (Thornthwaite, 1948), Hargreaves (Hargreaves and Samani, 1985) or Penman-Monteith (Allen *et al*., 1998) equations. Further information is provided in the next section.

The *SPEI-CRAN* Package was used for the analysis (Beguería and Vicente-Serrano, 2017).

3.3.4. Soil Moisture Deficit (SMD)

The Soil Moisture Deficit (SMD) (Schulte *et al.* 2005), measured in millimetres of water, is the amount of rain needed to bring the soil moisture content back to field capacity. Field capacity is the amount of water that the soil can hold against gravity (e.g. the maximum amount of water you can add to a potted plant before the water leaks out). A positive SMD indicates a water deficit. A higher SMD value implies higher water deficit and therefore drier soil. A negative SMD indicates a water surplus. This surplus will drain away in time through surface runoff and/or percolation.

3.4. Evapotranspiration

The evapotranspiration (ET) provides a link between energy and water balance in the hydrological cycle. ET is defined as the transfer of liquid water to the atmosphere as water vapor from bare soil and water bodies such as rivers and lakes (evaporation), as well as vegetated surfaces through plants' leaves (transpiration) (Allen *et al.,* 1998). ET is a critical component of the water and energy balance of climate-soil-vegetation interactions and can account for a water loss of about 90% in arid regions (Lu *et al*., 2019).

The ET is divided in reference (or potential) evapotranspiration (ET_0), and crop evapotranspiration under standard conditions (ET_C). The ET_0 is the evapotranspiration rate from a hydrated reference surface and expresses the evaporating power of the atmosphere at a specific location and time of the year. The reference surface is the *Festuca arundinacea* lawn with specific characteristics, such as a well-watered grass of uniform height of 0.12m, actively growing and completely shading the ground. The fixed surface resistance of $70sm^{-1}$ and an albedo of 0.23 implies a moderately dry soil surface resulting from a weekly irrigation frequency. ET_0 does not consider the crop characteristics and soil factors.

The ET_0 multiplied by a crop coefficient K_c, that is a function of the cultivation, determines the crop evapotranspiration under standard conditions (ET_C). ET_C is defined as the quantity of water lost in the unit of time by evaporation and transpiration from a crop in real conditions. ET_C estimates the water requirements of a crop according to location, soil conditions and agronomic technique of the cultivation. ET_C is influenced by leaf anatomy, stomatal characteristics and aerodynamic properties,

while K_c for a given crop changes from sowing to harvest due to variations in the crop characteristics throughout its growing season.

On the other hand, in natural vegetation, this indicator can be used to characterize water stress conditions.

3.4.1. Thornthwaite

This methodology has been used to evaluate the reference evapotranspiration ET_0 in the equation of SPEI, in the studies described in Chapter 4. Thornthwaite equations (Thornthwaite, 1948) are a temperature-based method that uses only mean monthly temperature and latitude of the site to estimate potential evapotranspiration. Monthly average temperature and cumulative precipitation values were used to calculate SPEI.

3.4.2. Penman-Monteith

The FAO (Food and Agriculture Organization) Penman-Monteith formula (Allen *et al*., 1998) is used to calculate the daily reference evapotranspiration. The equation uses standard climatological records of solar radiation (sunshine), air temperature, humidity and wind speed. Actual evapotranspiration is derived from ET_0 as per Schulte *et al*. (2005). This methodology is used to describe the impact of drought in Irish agriculture (see Chapter 5), with meteorological data recorded at synoptic weather stations of Met Éireann network.

3.4.3. Hargreaves

The Hargreaves equation (Hargreaves and Samani, 1985) is another method recommended by the FAO as an alternative technique for estimating reference evapotranspiration if insufficient meteorological data are available for the Penman-Monteith method.

The Hargreaves equation is a simple evapotranspiration model that only requires a few easily accessible parameters: minimum, maximum and mean temperature, and extra-terrestrial radiation. Nonetheless, the Hargreaves equation overestimates the potential evapotranspiration under

conditions of high relative humidity, and underestimates the potential evapotranspiration under high wind conditions (over $3ms^{-1}$).

3.5. Data production and grape varieties

Data about the quantity of grapes harvested were obtained from the Agricultural and Livestock Production Sector of the Piedmont Region, Agriculture Directorate. The data concern the harvest periods from 2016 to 2018.

The organization of the data is based on the concept of vineyard and vineyard units (VU). The vineyard represents a certain area and is composed of an aggregation of VU that belong to the same wine company which produces a single grape variety, independent of the geographical location of the parcels. Therefore, the quantity of grapes of a specific grape variety harvested by a wine company, expressed as a single average data, is obtained from the sum of the quantities of grapes harvested for the total VU.

The Piedmontese viticultural environments show a considerable alternation of climatic and cultural situations, alongside a moderately accentuated pedological variability, characterized principally by marly limestone soils, rich in clay. The form of vine-growing in Piedmont follows the traditional practice realized by Charles Guyot in the 1860s, that is a cane-pruned system with spurs. The cane buds grow into shoots that produce the yield in the following season, while the spur buds produce shoots that can be used as canes the following year, thus preventing the vine from sprawling too far along the trellis. The Piedmontese vineyards are structured by a vertically shoot-positioned trellising system, spur-pruned cordon with a bud-load of about 8-12 nodes per metre of row length. The vine spacing is 2.20m x 1.15m (inter- and intra-row) and the cordon is raised to 0.50m from the ground with three pairs of surmounting catch wires for a canopy extending 1.40m above the cordon. In each vineyard, the plant density is less than 4,000 vines per hectare.

3.6. Remote sensing data

The MOD13Q1 products used in Chapter 5 are the result of a temporal composition designed to select the best observation of reflectance recorded over 16 days on a given surface. Hence, a total of 23 products containing the respective bands of the concerned indices were obtained for each year. The data and products acquired by the sensors at 250-metre spatial resolution are available on the NASA Earth Data website on the MODIS Rapid Response System page (https://earthexplorer.usgs.gov/). Blue, red, and near-infrared reflectances measured by the spectroradiometer are used to determine the MODIS daily vegetation indices (such as: Normalized Difference Vegetation Index – NDVI, Rouse *et al.*, 1974; Enhanced Vegetation Index – EVI, Huete *et al.*, 1997) that provide spatial and temporal comparisons of vegetation conditions.

An automatic procedure has been realized to acquire all data and products of MODIS from the EOS archives. The Irish area is located within the tiles identified as h17v03 of the Earth's surface of EOS system (identificative tile: 51017003). Subsequently, all the products have been cropped by selecting the Irish area and geo-referenced using the international reference system WGS84 (World Geodetic System 1984).

In Table 14 (see Appendix 3, 8.3.1) are presented the metadata about each single MODIS imagery used in the study. The algorithm package used to analyse the imagery is MOD_PR13A1 version 6 and the imagery are provided in two version of HDF, 2.17 and 2.19.

In Chapter 6, imagery from the Landsat 8 (L8) and Sentinel-2 (S2) satellites were retrieved from April to October for the vegetative and reproductive periods of vines from 2016 to 2018.

A total of 292 L8 imagery (see Appendix 3, 8.3.2) and 97 S2 imagery (see Appendix 3, 8.3.3) that corresponded with the Piedmont region area were selected. The imagery were identified by the codes 194028, 194029, 195028 and 195029 for L8, and T32TMQ and T32TMR for S2. The imagery were analysed with a pre-processing procedure using the QuantumGIS Semi-Automatic Classification Plugin, SCP (version 6.2.9) (Congedo, 2018). SCP converts satellite imagery from numbers into top of atmosphere (TOA) reflectance and applies dark object subtraction i.e. an image-based atmospheric correction.

3.7. Remote sensing indices

The geometric co-registration of all the bands of a multispectral image, i.e. the fact that they all refer to the same reference system and occupy the same geographic space, allows the pixels of generic coordinates *x,y* belonging to each band to overlap. The transformation of multi-band images through combinations of two or more spectral bands generates new images with the aim of obtaining data whose characteristics are more suitable for certain purposes.

In this context a Vegetation Index (VI) is a spectral transformation of two or more bands designed to enhance the contribution of vegetation properties. VI enables the acquisition of ecological information from satellite data through the analysis of multi- or hyperspectral imagery bands. The reflectance of light changes with chlorophyll content, plant type, water content, sugar content within tissues, and other factors. Due to this fact, the spectral reflectance responses captured by satellite imagery can reflect the interaction and coupling of carbon, nitrogen, and water cycles (Chang *et al*., 2016; Xue *et al*., 2017).

Several remote sensing indices have been calculated in the literature (Huete, 1988; Jordan, 1969; Rousse *et al*., 1974). In this research two indices were selected and described in the following sections: the Enhanced Vegetation Index (EVI) (Huete *et al.*, 1997) and Normalized Difference Moisture Index (NDMI) (Gao, 1986, Wilson *et al*., 2002).

3.7.1. Enhanced Vegetation Index (EVI)

This index optimises the vegetation signal and reduces the effects of the atmosphere and soil, because it is more sensitive to the structural parameters of the canopy, the type of coverage, and plant architecture than other indices. The equation for EVI is as follows (eq. 1):

$$EVI = G \times \frac{NIR - RED}{NIR + C1 \times RED - C2 \times BLUE + L} \qquad \textit{eq. 1}$$

where *NIR*, *RED* and *BLUE* are the spectral reflectance of the near-infrared, and red and blue visible regions, respectively. *L* is the correction for plant cover background (undergrowth, litter, soil) that determines

transmittance through vegetation in *NIR* and *RED* wavelengths. *C1* and *C2* are aerosol correction coefficients, which use the blue band to correct the aerosol effects in the red band. *G* is the Gain factor.

3.7.2. Normalized Difference Moisture Index (NDMI)

The NDMI is a satellite-derived index from the Near-Infrared (NIR) and the Short-Wave Infrared (SWIR) channels and describes the water content of the vegetation. The NIR reflectance is influenced by leaf internal structure and leaf dry matter content, while the SWIR reflectance reflects changes in both the spongy mesophyll structure in vegetation canopies and the amount of water content in the internal leaf structure. The combination of the NIR with the SWIR removes variation induced by leaf internal structure and leaf dry matter content, improving the accuracy in retrieving the vegetation water content. The amount of water available in the internal leaf structure largely controls the spectral reflectance in the SWIR interval of the electromagnetic spectrum. SWIR reflectance is therefore negatively related to leaf water content. The index ranges from 1 (no water stress) to -1 (completely barren). The equation for NDMI is as follows (eq. 2):

$$NDMI = \frac{NIR - SWIR}{NIR + SWIR} \qquad \textit{eq. 2}$$

3.8. Random Forest missing data algorithm

Random forests (RF) are a combination of tree predictors such that each tree depends on the values of a random vector sampled independently and with the same distribution for all trees in the forest (Breiman, 2001).

RF are an ensemble learning method. They have the properties of being able to handle mixed types of missing data. RF are adaptive to interactions and nonlinearity, and they have the potential to scale to high dimensions while avoiding overfitting. RF are based on machine learning algorithms that build multiple decision trees and merge them together to get a more accurate and stable prediction. After a large number of trees is generated, they select the most popular class.

In a practical way, RF add additional randomness to the model while growing the trees and searching for the best feature among a random subset

of features. Therefore, only a random subset of the features is taken into consideration by the algorithm for splitting a node.

A machine learning procedure was applied to monthly averaged remote sensing data in order to deal with missing data and to solve the gaps in the data due to excessive cloudiness. The *randomForest* R-package, based on the RF missing data algorithm of Breiman (2001), was used in the research and described in Chapter 6.

3.9. Gross Primary Production

Gross primary production (GPP) of vegetation is the first and most important flux of the terrestrial carbon cycle (Xiao *et al.*, 2014; Xiao *et al.*, 2004; Ruimy *et al.*, 1996). GPP is the rate at which primary producers create chemical energy and accumulate biomass by light absorption and carbon fixation processes in plant photosynthesis that occur within the chloroplasts of plant leaves. In the light absorption process, chlorophyll absorbs photosynthetically active radiation (PAR, mostly visible spectrum) from sunlight. While the carbon fixation process is the absorption of energy then used to combine water and CO_2 to produce sugar (Xiao *et al.*, 2011). There is no direct instrument-based measurement of plant photosynthesis at the canopy and landscape scales. The combination of meteorological data with remote sensing techniques provides an estimation of the GPP at canopy level (Dold *et al.*, 2019; Delgado *et al.*, 2018, Pau *et al.*, 2018; Xiao *et al.*, 2011).

The satellite indices and weather data were used to estimate the GPP, based on the light-use efficiency (LUE) approach, in which only the fraction of light actually absorbed by the chlorophyll pigments ($FPAR_{chl}$) is selected. The LUE equation is the following (eq. 3):

$$GPP = \varepsilon_g \times FPAR_{chl} \times PAR \qquad \textit{eq. 3}$$

where ε_g is the efficiency of light [µmol m^{-2} s^{-1}], eq. 4 influenced by temperature (T_{scalar}, eq. 5), water (W_{scalar}, eq. 6) and phenology (P_{scalar}, eq. 7); $FPAR_{chl}$ is equivalent to EVI; PAR is photosynthetically active radiation, estimated according to Duffie and Beckman (1991).

$$\varepsilon_g = \varepsilon_0 \times T_{scalar} \times W_{scalar} \times P_{scalar} \qquad \textit{eq. 4}$$

where ε_0 is the maximum light efficiency [µmol m^{-2} s^{-1}].

$$T_{scalar} = \frac{(T - T_n) \times (T - T_x)}{(T - T_n) \times (T - T_x) - (T - T_{opt})^2} \qquad \textit{eq. 5}$$

where T is the daily average temperature over 10 days prior to the acquisition of the satellite image; T_n, T_x, and T_{opt} representing the minimum (12 °C), the maximum (33 °C) and the optimal (25 °C) cardinal temperatures, respectively, for the grapevine (Mariani *et al.*, 2013).

$$W_{scalar} = \frac{1 + NDMI}{1 + NDMI_x} \qquad \textit{eq. 6}$$

where $NDMI_x$ is the maximum value of each pixel considered during the vegetative period.

$$P_{scalar} = \begin{cases} \dfrac{1 + NDMI}{2} & \text{Burst bud} \\ 1 & \text{Complete leaf development} \end{cases} \qquad \textit{eq. 7}$$

The GPP index was calculated at two different spatial resolutions, 30m and 10m, using the L8 and S2 imagery, respectively. Multi-temporal and spatial analyses were conducted using the R-project software R-3.5.0 statistical software.

CHAPTER 4: APPLICATION OF *ClimPACT2* SOFTWARE IN TWO DIFFERENT CLIMATIC ENVIRONMENTS

In this chapter, the results of the climatic analysis will be presented analysing two different climatic environments by using the *ClimPACT2* software.

The Continental Temperate climate is analysed in Piedmont region in the North-western of Italy and compared with the Mediterranean climate, studied in Sardinia, the second largest region of Mediterranean. The daily data of 13 meteorological stations were examined and the trends of the Standardised Precipitation Index (SPI) and Standardised Precipitation Evapotranspiration Index (SPEI) have been evaluated. The similarities and differences between the indices of the two regions were then considered.

4.1. Hydrological drought analysis in Continental Temperate and Mediterranean environment during the period 1981-2017

Figure 7 shows the graphical abstract of the study presented in the following paragraphs, where the effects of hydrological drought is analysed comparing two different environments: Continental Temperate and Mediterranean climate.

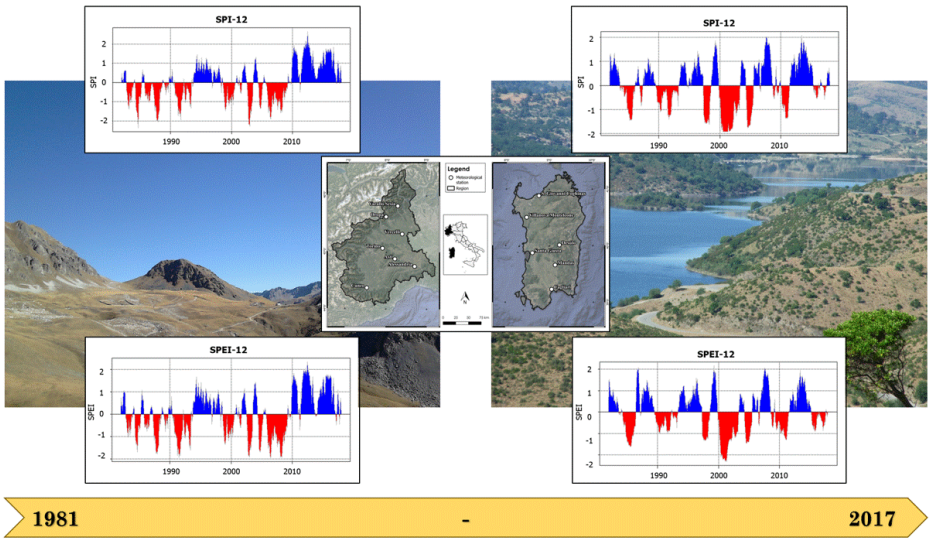

Figure 7 Graphical abstract of the study in Continental Temperate (on the left) and Mediterranean (on the right) environments.

Falzoi S., Acquaotta F., Pulina M.A., Fratianni S. 2019. Hydrological drought analysis in Continental Temperate and Mediterranean environment during the period 1981-2017. *Italian J. Agromet*., 3: 13-23. doi: 10.13128/ijam-798

4.2. Introduction

Drought is a natural hazard caused by a lower-than-average reduction of precipitation. When the phenomenon occurs for the duration of a season or for extended periods of time, it creates insufficient conditions to supply human and environmental demands (WMO, 2006). In contrast to aridity, which is defined as a permanent condition, drought is a temporary climate

phenomenon that typically begins as a dry spell or a period of abnormally dry weather.

A drought can alternatively be broadly defined as a temporary, recurring reduction in the precipitation in an area, and is considered as one of the most important climate change impacts on natural and socio-economic systems. Few extreme events are as economically and ecologically disruptive as drought, which affects millions of people in the world each year (Dai, 2011). Its effects occur after long periods without precipitation, therefore it is difficult to objectively quantify its characteristics in terms of intensity, amplitude, duration and spatial extent (Bordi *et al*., 2009*;* Vicente-Serrano *et al*., 2010; Bevan *et al.*, 2014). In recent years, drought has become more intense and frequent, which has a negative impact on the socio-economic balance of the countries concerned. For example, in recent years the Californian government had to limit water use for irrigation and domestic use (Dettinger and Cayan, 2014); in 2012 an increase in food price was caused by a simultaneous drought in USA and Russia (Van Loon, 2015); in 2011, a mass migration in the Horn of Africa was caused by drought (Viste *et al*., 2012); and in 2010, drought affected food production in large parts of China (Lu *et al*., 2011).

Mountain regions and the Mediterranean basin, considered "hot spots" of climate change, are susceptible to drought situations and are heavily impacted by extreme events (Ronchi *et al.*, 2007; Capra and Scicolone, 2012). Over the past 30 years, the temperature in Piedmont increased by 0.7 °C (Fratianni *et al.*, 2015), and July of 2015 was the hottest month on record, while the period from July to October of 2017 was one of the driest in the last 60 years, with the main Piedmontese river Po always below the average flow. While no significant variation was recorded in the annual amount of precipitation, the seasonal distribution has changed with a decrease during the winter season of -1.5mm $year^{-1}$ in the north of Italy, and -7.7mm $year^{-1}$ in the central part (Fratianni and Acquaotta, 2017). Extreme drought years have been reported in Sardinia since 1981, with a greater frequency in the last decade, especially in the springtime, at the beginning of the vegetative season, and in the South of the island (Pulina, 2012). Temperature and extreme events are expected to increase at the end of the century, according to future climate projections. For example, for the near future (next 15-20 years), Perini *et al.* (2011) predicted a strong decrease in winter and spring precipitation in Northern and Southern Italy, and a reduction of summer rainfall in Southern Italy and in the Islands. While, by the 2100s, a general temperature increase of about 3 °C is

expected in all seasons across the whole of Italy, peaks of 4 °C are projected for the Po Valley in winter and over the whole north-west region in summer (Bucchignani *et al.*, 2016), according to the RCP4.5 scenario, with increasingly frequent and long-lasting heat waves, which will extend to more than thirty days over the entire summer season (Collins *et al.*, 2013; Drumond *et al.*, 2017; González-Hidalgo *et al.*, 2018). On the contrary, the RCP8.5 scenario predicts a strongly significant precipitation reduction in spring and summer in the Alpine area with a negative anomaly from 0.1 to 0.4mm day^{-1} (Bucchignani *et al.* 2016). In these future climate scenarios, drought events will become increasingly common, more intense and less predictable, especially in vulnerable environments such as Alps and Mediterranean.

Although numerous climatic and biological classifications have been proposed for aridity and drought conditions (e.g. De Martonne, 1926; Thornthwaite, 1948; Palmer, 1965; Agnew and Anderson, 1992; Pashiardis and Michaelides, 2008; Hannaford *et al.*, 2011; Nastos *et al.*, 2013; Beguéria *et al.*, 2014; Beguéria *et al.*, 2018), it is still difficult to define wetness limits precisely and delineate the boundary between different degrees or levels of aridity/drought or the opposite, humidity. In 2009, the World Meteorological Organization, recommended that the Standardised Precipitation Index, SPI (McKee *et al.*, 1993) be used around the world to characterize meteorological droughts. Cheval *et al.* (2014), analysed the spatial and temporal variability of meteorological drought in Romania by using SPI and distinguished winter and summer driving factors of the drought spells. SPI was also investigated in six regions of southern South America in order to observe the duration of dry sequences (Minetti *et al.*, 2010). Furthermore, SPI is a useful index to analyse and compare time series of monthly precipitation in the past with the ongoing time series (Rana *et al.*, 2016). Temperature, wind and relative humidity are also important factors to include in characterizing drought, and most recently, Vicente-Serrano *et al.* (2010) proposed a further index which combines precipitation, temperature and evapotranspiration, called Standardised Precipitation Evapotranspiration Index (SPEI). SPI and SPEI were both used to characterize the summer 2015, which ranks as the hottest and climatologically driest summer since 1950 over extended regions in eastern Europe (Ionita *et al.*, 2017).

The aims of this work are *i*) to analyse the hydrological drought conditions, which are related to the effect of the absence of precipitation on water resources, in two different Italian climatic regions: Continental Temperate

climate in Piedmont region and Mediterranean climate in Sardinia region; *ii*) to compare the two above-mentioned standardised indices (SPI and SPEI) to delineate drought conditions between two different environments, and *iii*) to verify potential drought trends during a period of 37 years (1981-2017), in an ongoing climate change scenario.

4.3. Materials and methods

4.3.1. Study area

The study was conducted in two Italian regions, Piedmont and Sardinia (Figure 8), with a marked climatic difference (Figure 9).

Piedmont region is located in the continental area at the base of the Western Alps, between 44°02'N and 46°26'N and between 06°49'E and 08°32'E. Although the region is relatively small, it is characterised by a varied topography with a predominance of mountains. The Alps, where most peaks are over 2,500m, mark the border with France to the West and Switzerland to the North. The hilly areas which border the western part of the Po Valley complete the physical boundaries of the region. The altitudinal gradient (from about 100m to 4,000m a.s.l.) strongly influences the regional climate, which experiences great variation in temperature and precipitation over a short distance (Nigrelli *et al.*, 2018). The climate is Continental Temperate, "*Cf* ", according to Köppen's classification (Fratianni and Acquaotta, 2017). The average annual temperature varies between 11-12 °C in the lowlands area and it does not exceed 1 °C in mountainous areas above 2,400m a.s.l. Annual precipitation rate varies from 500-700mm in the plains to 2,000mm in the interior Alpine valleys. The rainfall pattern is characterized by a classic bimodal trend, with two peaks in spring and autumn, and a minimum in winter (Bandini, 1931; Baronetti *et al.*, 2018).

Sardinia region is the second largest island in the Mediterranean Sea and is located between 38°53'N and 41°15'N and between 8°08'E and 9°48'E. The topography is mainly characterized by hills and plateaus, but also by flat areas in the West and mountainous areas in the East, with peaks higher than 1,300m a.s.l. The average altitude is 334m a.s.l. The climate is typically Mediterranean, "*Csa*", according to Köppen's classification, with mild and relatively rainy winters and hot, dry summers. Mean annual temperatures are strongly influenced by the distance from the sea and by the orography; the values range from 16-17 °C in the western plains

(Campidano and Nurra) to 10-12 °C in the eastern highlands (Gennargentu, Limbara). The average annual precipitation is less than 500mm in the lowlands area, while it exceeds 1,300mm on the highest peaks. The maximum rainfall is normally recorded in December, with average values exceeding 200mm in the mountainous areas (Pulina, 2015).

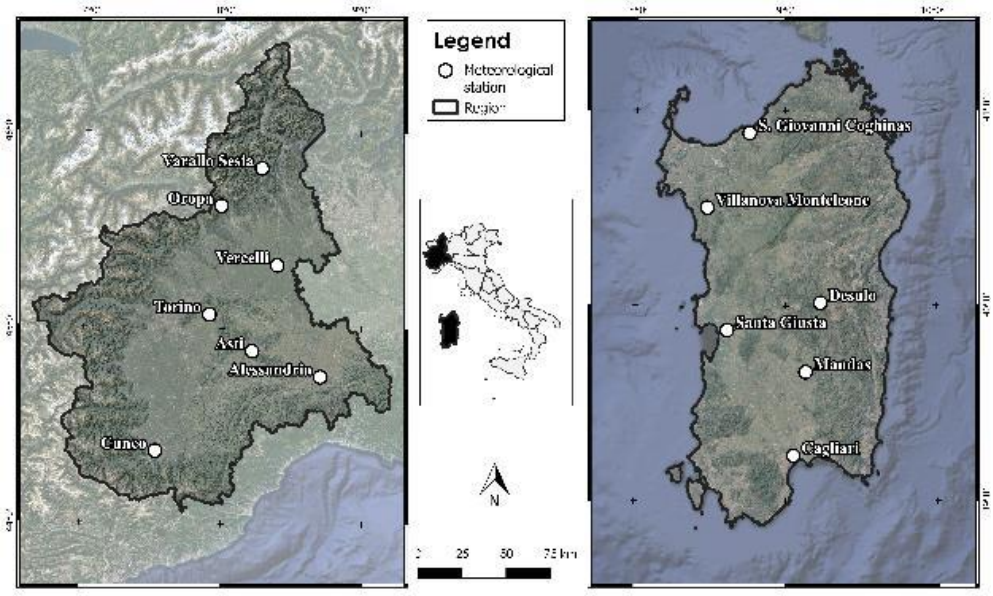

Figure 8 Study area: Piedmont region on the left, Sardinia region on the right; white dots indicate positions of meteorological stations.

4.3.2. Meteorological data

Daily weather data in Piedmont region were collected from thermo-pluviometric stations of the Italian Hydrographic Mareographic Service (SIMN). Alessandria, Asti, Cuneo, Oropa, Torino, Varallo Sesia and Vercelli were the stations considered (Table 5). These are uniformly distributed in the region (Figure 8) with an altitude range between 90m and 1,180m a.s.l. Meteorological stations above the limit of 1,200m a.s.l. were excluded from the analysis in order to standardise the measurements with the Sardinian stations.

In the Sardinia region, daily temperature and precipitation data were obtained from the Hydrographic Sector of Sardinia Region (RAS) and

Desulo, Mandas, San Giovanni Coghinas, Santa Giusta and Villanova Monteleone were the weather stations considered. These were supplemented by the addition of Cagliari/Elmas station from the Italian Air Force meteorological station network (Table 5). The altitude range of the stations (Figure 8 and Table 5) is between 10 and 920m a.s.l.. Their location is representative of the different geographical and topographical conditions of the island.

Daily precipitation (P) and maximum (T_x) and minimum (T_n) daily temperature data were considered for all stations during the period 1981-2010, which is the current climatological standard 30-year period (WMO, 2017).

An additional seven years (2011-2017) were collected for the stations of Torino and Cagliari/Elmas, in Piedmont and Sardinia region respectively, resulting in a total of 37 years of data. The two additional series of data (1981-2017), in the most representative stations of the two territories, were analysed in order to compare the most recent trends in two different areas. Figure 9 shows the thermo-pluviometric diagrams of the two stations.

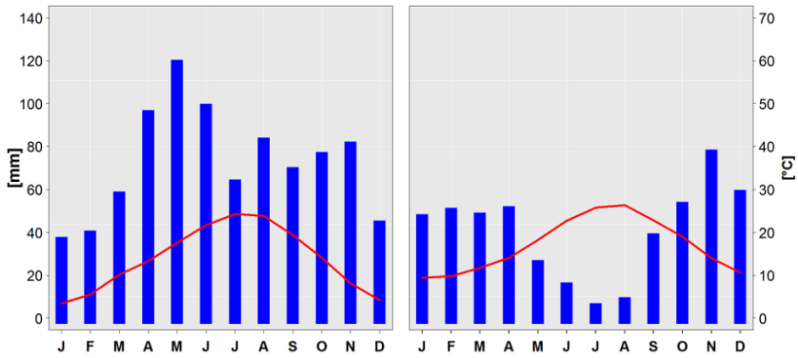

Figure 9 Thermo-pluviometric diagram for Torino data series (on the left) and Cagliari/Elmas (on the right) during the period 1981-2017.

4.3.3. Method

A Quality Control (QC) analysis was conducted on the daily data series by using the R software *ClimPACT2* package (Alexander and Herold, 2016) to identify gaps, outliers and erroneous values (Acquaotta *et al.*, 2019). This algorithm detects incorrect values, such as $P < 0$ mm or $T_x < T_n$ and

provides a series of graphical representations in the form of box diagrams in a monthly and annual scale, to evaluate discontinuities present in the series (Acquaotta *et al.*, 2016).

Outlier values are identified through the calculation of the estimated thresholds on the statistical characteristics of the series (Fortin *et al.*, 2016).

After the QC, on the T_x and T_n series, we carried out two homogenization tests, HOMER (Mestre *et al.*, 2013) and SLIDHOM (Mestre *et al*., 2011) to identify and to correct the breaks or discontinuities (Acquaotta and Fratianni, 2014). HOMER was applied on monthly scale to identify the breaks, while the SPLIDHOM was carried out on the daily series to correct the inhomogeneities.

In order to characterize the hydrological drought in both regions, we used two derived indices: Standardised Precipitation Index - SPI (McKee *et al.*, 1993) and Standardised Precipitation Evapotranspiration Index - SPEI (Vicente-Serrano *et al.*, 2010). The two drought indices have been calculated for every meteorological station and subsequently represented as a single average value for each region.

SPI is an index based on monthly cumulative precipitation and classifies the accumulated precipitation of the month under consideration with respect to the long-term average monthly accumulated precipitation for the same month (or other time scales). SPI quantifies a deficit or surplus of rain over mean values, using a probabilistic approach for the precipitation event. The rainfall series is adapted to a gamma distribution, then transformed into a normal distribution having a null mean and a standard deviation equal to 1. SPI indicates the number of standard deviations by which a particular event exceeds from mean conditions.

SPEI is a multiscalar drought index designed to consider both precipitation and potential evapotranspiration (ET_0). SPEI looks at long-term rainfall at different timescales and compares it with expected demand as indicated by potential evapotranspiration. The ET_0 has been estimated with the Thornthwaite equations (Thornthwaite, 1948), a temperature-based method that uses only mean monthly temperature and latitude of the site to estimate potential evapotranspiration. The monthly average temperature and cumulative precipitation values were used to calculate SPEI.

Classification of wet and dry periods based on SPI and SPEI indices as shown in Table 4.

Category	**SPI and SPEI values (dimensionless)**
Extremely wet	≥ 2.00
Severely wet	1.5 – 1.99
Moderately wet	1.00 – 1.49
Close to normal	-0.99 – 0.99
Moderately dry	-1.49 – -1.00
Severely dry	-1.99 – -1.50
Extremely dry	≤ -2.00

Table 4 Classification of the wet and drought periods of SPI and SPEI, according to McKee et al. (1993) and Vicente-Serrano et al. (2010), respectively. SPI and SPEI indices are dimensionless.

On the annual scale (12-months) we calculated the trends of SPI and SPEI and then we compared the results with the annual trend of four climate indices, total annual P (*prectot*) for days with P ≥ 1.0 mm, total annual P from heavy rain days (*r95p*) with annual sum of daily P > 95th percentile, amount of hot days (T_X90p) percentage of days when T_X > 90th percentile, and amount of hot nights (T_N90p) percentage of days when T_N > 90th percentile (Table 5). The trend was computed by a linear least square and statistical significance was calculated at 95% confidence level using F test, for both indices, in each station (Table 5) of the two regions (Figure 10 and Figure 11). A negative trend value means an increase of drought spells, and the statistical significance of the trend was verified by using the non-parametric test of Mann-Kendall (p value < 0.05) (Giaccone *et al.*, 2015).

Furthermore, the SPI and SPEI trends were calculated for the Torino and Cagliari/Elmas meteorological data on a timescale of 12 and 24 months, based on the period from 1981 to 2017.

4.4. Results and discussion

The Standardised Precipitation Index for the seven stations of Piedmont region showed no homogeneous trend (Table 5). The series of Cuneo, Torino and Vercelli stations showed a statistically significant upward trend. At these locations, increasing trends were observed in two climate indices of precipitation, *prectot* and *r95p*. Neither of the two indices were statistically significant according to the Mann-Kendall test. The trend was downward and statistically significant for Oropa site where the precipitation indices show decreasing trends and statistically significant for *r95p*. The series of Alessandria, Asti and Varallo Sesia stations, as well as the average SPI for those three stations showed no trend. Also, the trends of precipitation indices are not statistically significant, and the coefficients do not identify important variations. They range between 1.83 mm $year^{-1}$ to 4.17mm $year^{-1}$ for *prectot* and between -4.87mm $year^{-1}$ to 0.94mm $year^{-1}$ for *r95p* (Table 5).

The period with the greatest number of consecutive wet months (SPI > 0) (Figure 10) ranged from July 1992 to April 1997, a total of 58 months, while the period with the greatest number of consecutive dry months (SPI < 0) ranged from December 2004 to June 2008, 43 months. On average, wet periods alternated with dry periods of six months in this region.

On the other hand, the trend of SPEI is decreasing and is statistically significant in all the Piedmontese stations considered (Table 5). The maximum decrease (-0.004), is calculated for the Oropa station, followed by Asti and Cuneo (-0.003). The behaviour of this index is well correlated with the behaviour of temperature index, T_X90p. The trend of T_X90p is increasing and is statistically significant in most of the stations. The trends range between 0.67% $year^{-1}$, calculated in Oropa, to 0.33% $year^{-1}$, calculated in Alessandria (Table 5).

The average SPEI among stations shows a downward trend (-0.002), but not statistically significant. The longest wet period observed was between July 1992 and April 1997, 58 months, while the longest dry period lasted from November 2004 to November 2008, 49 months (Figure 10).

	Station	Alt. m a.s.l.	Lat N	Lon E	SPI	SPEI	prectot	r95p	T_X90p	T_N90p
Piedmont Region	Alessandria	90	4955808	476651	0	**-0.002**	1.83	1.47	**0.33**	0.16
	Asti	117	4970569	437876	0	**-0.003**	3.41	0.94	**0.40**	**-0.32**
	Cuneo	575	4914085	382681	**0.002**	**-0.003**	3.98	4.05	0.62	0.10
	Oropa	1180	5053196	420664	**-0.003**	**-0.004**	-18.77	**-17.17**	**0.67**	0.14
	Torino	239	4991497	413680	**0.003**	**-0.001**	7.00	3.42	0.43	-0.11
	Varallo Sesia	453	5074366	443680	0	**-0.001**	1.40	-4.87	**0.55**	-0.04
	Vercelli	135	5019297	452240	**0.002**	**-0.002**	4.17	3.12	**0.58**	0.09
Sardinia Region	Cagliari	21	4342672	504315	0	0	-0.47	0.87	**0.20**	**0.24**
	Desulo	920	4429509	519699	**0.002**	**0.002**	4.71	-0.09	**-0.37**	-0.17
	Mandas	491	4390215	511294	0	0	-0.99	0.39	**0.22**	**0.26**
	S. Giovanni Coghinas	210	4526143	479570	0	**-0.003**	-0.95	-0.20	**0.36**	0.08
	Santa Giusta	10	4414049	466626	**0.002**	0	1.30	-0.16	**0.21**	0.01
	Villanova Monteleone	567	4483757	455470	0	**-0.002**	-0.88	-2.39	0.06	-0.05

*Table 5 Weather stations list analysed in Piedmont and Sardinia regions for the reference period 1981-2010, with their values of Elevation (Alt. m a.s.l.), coordinates (Lat N; Lon E), the calculated SPI and SPEI annual trends (year^{-1}) at 12 months, annual total wet-day (*prectot*), total annual P from heavy rain days (*r95p*), amount of hot days (*T_X90p*), and amount of hot nights (*T_N90p*) at 12- month time scale. Statistically significant trends with a p value ≤ 0.05 are indicated in bold.*

Regarding Sardinia region, the SPI (Table 5) showed an increasing and statistically significant (0.002) trend only in 2 of the 6 stations considered (Santa Giusta and Desulo). The SPI calculated for the other stations and the average SPI for those stations showed no significant trend during the considered period. The trends on precipitation indices are not statistically significant in Santa Giusta e Desulo, with an increasing trend as for *prectot* while is decreasing for *r95p*. Also, in the other stations the trends are not statistically significant but for *prectot* the slopes are negative and near to zero, ranging between -0.99mm year^{-1} to -0.47mm year^{-1} (Table 5). The average SPI value over stations (Figure 11) remained consistently above 0 for a maximum of 34 months, from April 1984 to January 1987 and for 30 consecutive months, from October 2003 to March 2006. Values were less than zero for a total of 40 months from September 1997 to December 2000,

and for 25 consecutive months from November 1988 to November 1990. According to the classification of McKee *et al.* (1993), which evaluates the severity of drought, there were nine months considered "*Severely dry*", and two months "*Extremely dry*" (from January to March 2002), during the period 1981-2010.

The trend of SPEI (Table 5) is statistically significant in three of the six Sardinian stations considered. A positive trend was observed for Desulo station (0.002), and negative trend for the stations of Villanova Monteleone (-0.002) and San Giovanni Coghinas (-0.003). These behaviours are well correlated with the behaviour of temperature indices, in particular with maximum temperature, T_X90p. The T_X90p trend in Desulo is decreasing and statistically significant, -0.37% year^{-1}, while in San Giovanni Coghinas and Villanova Monteleone the trends increase, but only in San Giovanni Coghinas the slope is statistically significant, 0.36% year^{-1} (Table 5).

The average of SPEI shows a downward trend (< -0.001), but this is not statistically significant. The analysis of the trend of the average SPEI values (Figure 11) showed the longest wet period was from May 1984 to January 1987 (33 months), and the longest dry period was from December 1997 to December 2000 (37 months in total).

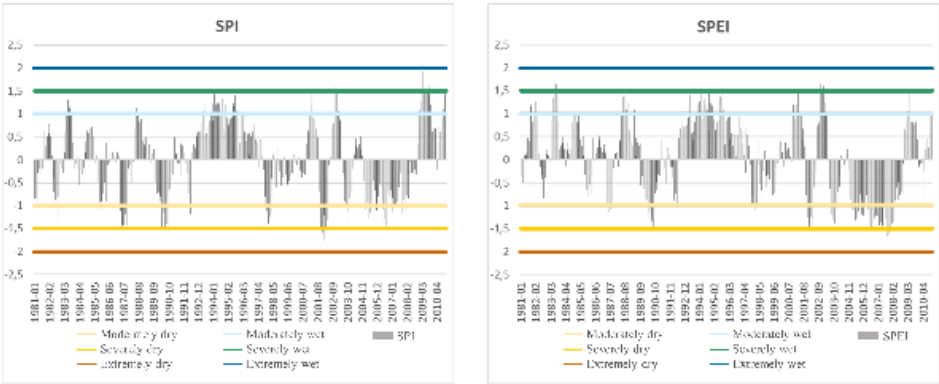

Figure 10 Average of SPI (on the left) and SPEI (on the right) values for the stations of Piedmont region. The yellow/brown and blue/green coloured lines indicate the critical values of the indices in dry and wet conditions, respectively.

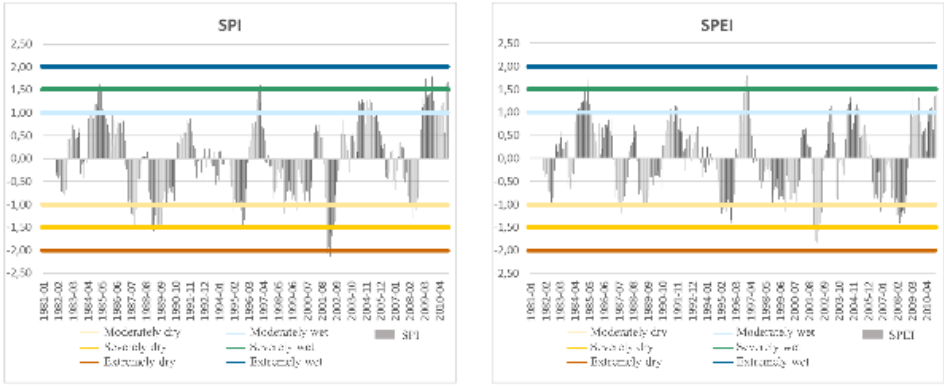

Figure 11 Average of SPI (on the left) and SPEI (on the right) values for the stations in Sardinia region. The yellow/brown and blue/green coloured lines indicate the critical values of the indices in dry and wet conditions, respectively.

Figure 12 and Figure 13 show the trend of the SPI and SPEI values calculated in the station of Torino and Cagliari/Elmas respectively, during the period 12 and 24 months.

In the last seven years in Torino, the SPI-24 and SPEI-24, as much as in the 12 months time scale, show a more humid trend with a remarkable increase of precipitation, which contrasts with the period 1981-2010 in the same region, in which dry events were prevalent. From 1993 to 1998 the second longest wet period was recorded, clearly highlighted by the 24-month graph (Figure 12).

From a general point of view, the SPEI exhibits the difference between the dry and wet months better than the SPI. This is evident in the comparison between SPI-12 and SPEI-12. The wet episodes before 1990 are clearly shown in the SPEI-12 but are absent on the SPI-12 (Figure 12).

In contrast to the trend experienced by Torino, the trend in Cagliari/Elmas is more regular with a clear alternation between drought and humid periods, as shown in the 24 month graphs (Figure 13), with an exception during the period 2000-2006, during which the dry period lasted longer and no wet episodes were recorded. SPI-12 and SPI-24 recorded "*Moderately wet*" periods in the years between 2012 and 2015. SPI shows values greater than zero in the last two years in contrast to the SPEI, which shows smaller values for the same periods.

As described by Vicente-Serrano *et al*. (2010), the influence of ET_0 on drought conditions is difficult to estimate. In this analysis it is possible to compare the extent of drought indicated by both SPI, which is a precipitation-based index in which ET_0 is not included, and SPEI, in which ET_0 is included, for the same time period. This comparison illustrates the different and sometimes contrasting outcomes regarding the evaluation of drought when ET_0 is included in the analysis. For example, at the end of the time series in Cagliari/Elmas, SPI-12 and SPI-24 indicate a wet period while SPEI-12 and SPEI-24 indicate a continuation of drought condition (Figure 13).

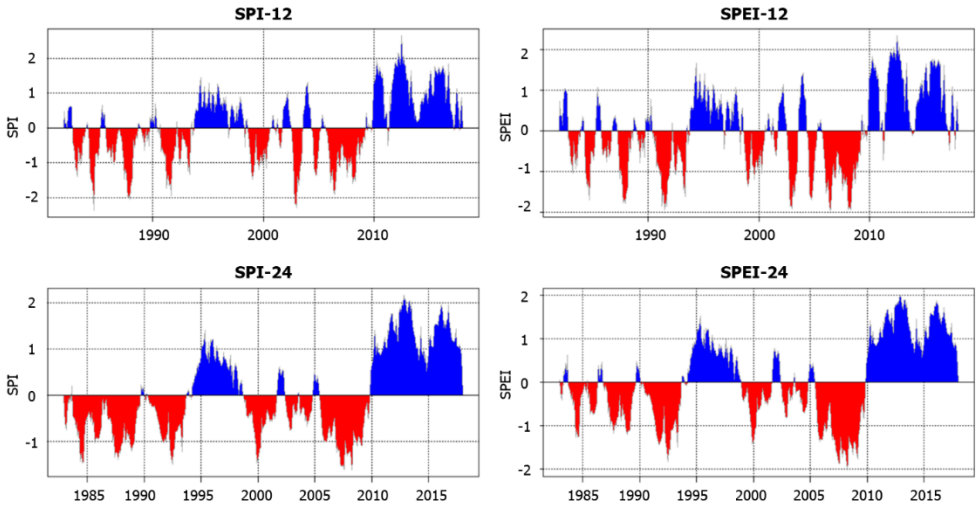

Figure 12 SPI (on the left) and SPEI (on the right) values for the Torino station in Piedmont region, calculated on the period of 12, 24 months.

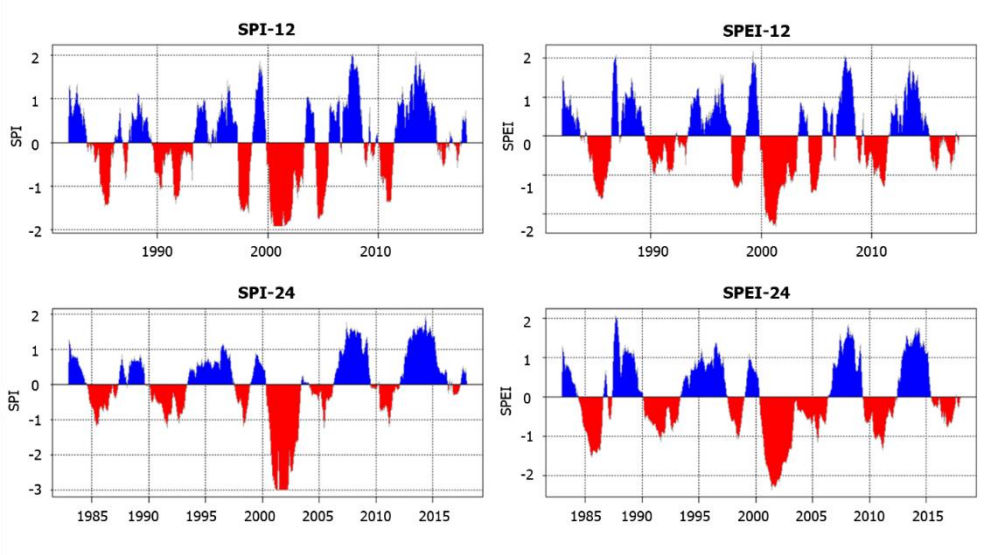

Figure 13 SPI (on the left) and SPEI (on the right) values for the Cagliari/Elmas station in Sardinia region, calculated on the period of 12, 24 months.

4.5. Conclusion

The trend analysis of hydrological drought in two different environments, Continental Temperate climate and Mediterranean climate, was conducted using the thermo-rainfall series of seven stations in Piedmont region and six stations in Sardinia region, during the period 1981-2017. The Standardised Precipitation Index, SPI, and the Standardised Evapotranspiration Precipitation Index, SPEI, were calculated for each station, and average indices were also calculated for both regions.

Similarities and differences were detected between the two environments. Index trends were more defined in Piedmont region. In particular, the SPEI trend is significantly negative in all the stations considered, while the SPI trend is statistically significant with a positive correlation in three of the seven stations. Meanwhile, indices in Sardinia region showed a clear trend in only half of the stations considered. However, the trends of the average index values for all stations are not significant in either of the two climatic environments considered. Probably because of uncertainties in the SPEI drying trends might be overestimated due to the use of Thornthwaite ET_0 estimation in this analysis. The use of this method is a limitation of the SPEI, as Thornthwaite ET_0 is less physically realistic than other estimation techniques such as Hargreaves or Penman-Monteith equation.

On an annual level, no significant variations in precipitation quantity are recorded in either region, as confirmed by the Fratianni and Acquaotta (2017), and other studies did not show significant changes in annual precipitation in the Mediterranean basin (Coll *et al.*, 2017). On the contrary, in recent years the distribution of rainfall has changed due to the increase in extreme events.

According to Vicente-Serrano *et al*. (2010), both drought indices respond mainly to variability in precipitation, which is the main explanatory variable for drought. Nevertheless, trends of the drought indices in both regions are well correlated with the trends shown by the climate indices, in particular the temperature indices, such as the amount of hot days (T_X90p) and the amount of hot nights (T_N90p). A greater variation is calculated in Piedmont for both the precipitation pattern (*prectot*) and its manifestation as short but intense events (*r95p*). Meanwhile, the climate indices calculated in Sardinia for the rain series do not show significant change. However, there is a significant increase in temperatures classified as hot (T_X90p), in both regions. This trend impacts the performance of the SPEI, for which decreasing, and statistically significant trends were calculated in most cases.

The average duration of the wet period was longer in Piedmont region, where we calculated 58 consecutive months with SPI values greater than zero (from July 1992 to April 1997), compared to 34 consecutive months in Sardinia (from April 1984 to January 1987). The duration of dry periods was almost the same in both regions, 43 months with SPI values less than zero in Piedmont (from December 2004 to June 2008) and 40 consecutive months in Sardinia (from September 1997 to December 2000).

An increase in drought for most of the twenty-first century is predicted by future climate projections. Ecosystems and human activities could be profoundly impacted by the projected drying trends, while observed drying trends are having an effect on social-ecological systems, e.g. reduction in vineyard yield in Piedmont in 2017, accompanied by an increase in alpine wildfire. Concerted political and practical action to conserve water is necessary to minimize the impact of future drought, such as appropriate water management policies, and climate-smart agriculture practices.

CHAPTER 5: ANALYSIS OF THE SEVERE DROUGHT IN IRELAND IN 2018

This chapter presents a case study and investigates the severe drought episode occurred in Ireland during the summer 2018 (Figure 14).

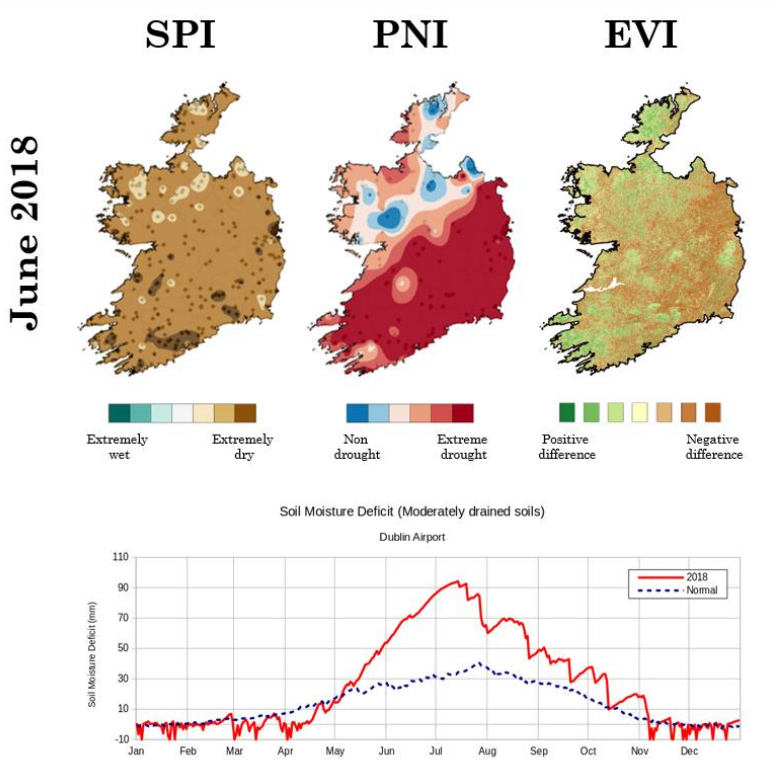

Figure 14 Graphical abstract of chapter 5

Drought episodes can happen under any conditions and environment.

The progress of the drought recorded in the summer 2018 in Ireland has been analysed using four meteorological and satellite indicators: Standardised Precipitation Index (SPI), Percent of Normal Index (PNI), Soil Moisture Deficit (SMD) and Enhanced Vegetation Index (EVI). An ordinary kriging interpolation was applied to estimate the national

coverage of drought based on those indices in order to show local variations in impacts on agriculture as determined through changes in biomass production and compared to long-term means.

Falzoi S., Gleeson E., Lambkin K., Zimmermann J., O'Hara R., Marwaha R., Green S., Fratianni S., 2019. Analysis of the severe drought in Ireland in 2018. *Weather*, 74(11): 368-373. DOI: 10.1002/wea.3587

5.1. Introduction

The World Meteorological Organization defines drought somewhat broadly as an insidious natural hazard characterised by lower than expected or lower than normal precipitation that, when extended over a season or longer period of time, is insufficient to meet the demands of human activities and the environment (WMO, 2006; Parry *et. al.*, 2013; West *et al.*, 2018). The concept of drought therefore depends on the perspective of the water resource user, and it can generally be classified into four types: meteorological (1-3 months), defined on the basis of rainfall deficiency; agricultural (1-6 months), when soil moisture is insufficient and results in a lack of crop growth and production; hydrological (6-24 months), when there is a lack of water in the hydrological system; and socio-economic, when the demand for water exceeds the supply (Kendon *et. al.*, 2013; Van Loon, 2015; Ziolkowska, 2016).

During the summer of 2018, a significant meteorological drought was recorded in Ireland, with 25th June marking the first official day of drought after a cold winter/ spring (Met Éireann, 2018a,b). Between 28th February and 4th March one of the most significant snowfall events of recent years occurred, dubbed the '*Beast from the East*', with temperatures struggling to rise above freezing as bitterly cold easterly winds swept over the country (Met Éireann, 2019). These two extreme climate-stress events highlighted the agricultural vulnerability of the country. Almost all of Ireland was negatively affected, and in particular eastern agricultural regions produced between 5 and 10% less grass than normal in 2018 – equivalent to about 1 ton ha^{-1} less (Figure 15). Figure 16 shows the colour of the vegetation in Ireland in July 2017 compared to July 2018, as measured by NASA's TERRA satellite. The fields that were green in July 2017 were desiccated

and brown in July 2018, which resulted in a reduction in agricultural production.

Agriculture is one of the main economic activities in Ireland, and this study therefore focuses on the agricultural drought. Agriculture is mainly influenced by climate conditions and soil quality. Ireland's climate is defined as Temperate Oceanic (*Cfb*) according to Köppen's climate classification system (Köppen, 1918).

Figure 15 Effects of drought in Co. Tipperary 17th July 2018 (Photo credit: Alison Maloney, Teagasc)

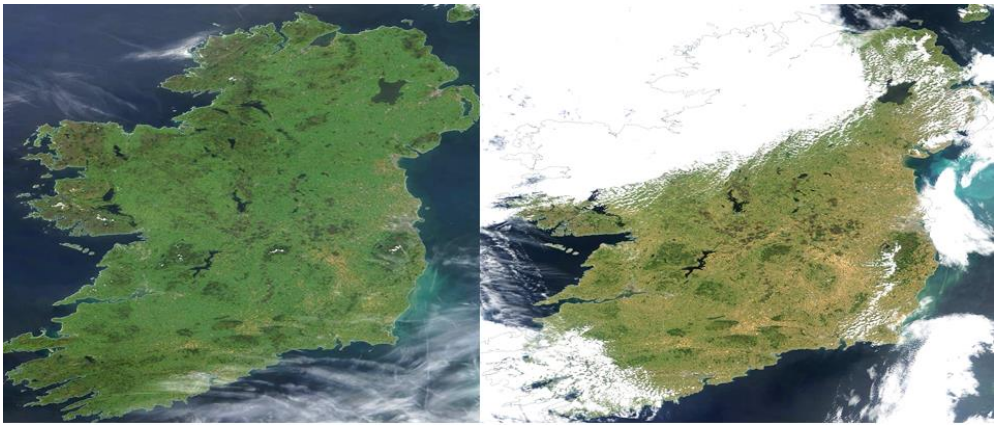

Figure 16 The NASA TERRA satellite MODIS true colour imagery for the (left) 17th July 2017 and the (right) 10th July 2018

The country lies in the north-eastern Atlantic Ocean, where the effect of North Atlantic Ocean currents mostly guarantees cool summers and mild winters. Although rainfall in Ireland is generally distributed evenly throughout the year, droughts can still occur. Between 1850 and 2015 Ireland suffered seven major drought-affected periods, the previous being between 1969 and 1977 (Wilby *et al.*, 2016; Noone *et al.*, 2017; Murphy *et. al.*, 2018). In fact, Wilby *et. al.* (2016) provide a complete report of the occurrence and persistence of meteorological droughts in Ireland since 1850 using the homogeneous Island of Ireland Precipitation network. In total, 45 individual drought events were identified in Ireland during that period. Of these, 22 were shorter than 10 months, 19 had durations of between 10 and 20 months, and four lasted longer than 20 months. Drought is a regional phenomenon and its characteristics differ from one climate to another. Climate model projections suggest that the frequency, duration, and severity of droughts are expected to increase due to rising temperatures and changes in the amount, intensity, and seasonal distribution of precipitation (Park *et al.*, 2013). Effective drought monitoring and impact mitigation are therefore urgent research priorities, not only for mitigation of agricultural impacts but also as an early warning system for socioeconomic effects (Ault *et al.*, 2014; Baronetti *et al.*, 2018; Liu *et al.*, 2016). An example of an early warning system is the monitoring of the reduction in water levels in the reservoir. Figure 17 shows the retreat of the water in Blessington Lake, one of the main reservoirs for the Greater Dublin area, following the drought in 2018 compared to a more normal summer. The image was produced using ESA (European Space Agency) Sentinel-1 Synthetic Aperture Radar products.

Meteorological data recorded at Met Éireann's networks of stations were used to calculate the Standardised Precipitation Index (SPI; McKee *et al.*, 1993), the Percent of Normal Index (PNI; Werick *et al.*, 1994) and the Soil Moisture Deficit (SMD; Schulte *et al.* 2005), where the SPI is used to assess the four types of drought. In addition, a time series of Enhanced Vegetation Index (EVI; Huete *et al.*, 1997) was calculated based on Moderate resolution Imaging Spectroradiometer (MODIS) on board the TERRA satellite.

The aim of the paper is to assess the severe drought of 2018 and, in particular its effect on agriculture, as determined through changes in biomass production compared to the long-term mean.

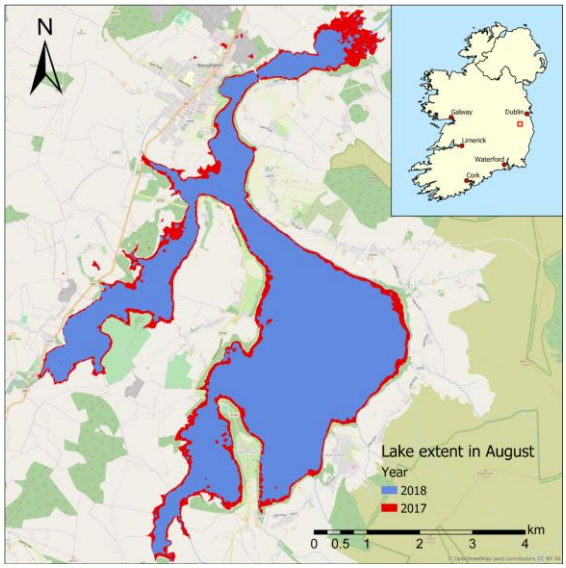

Figure 17 Images were pre-processed using Radiometric calibration, Speckle Filtering, and Terrain Correction. The respective acquisition dates were the 2nd and 4th August 2017 and 2018

5.2. Datasets

5.2.1. Meteorological data

Met Éireann manages and maintains an observation network in Ireland that gathers weather data for use in weather forecasting, numerical weather prediction models, reanalyses, climate applications, forecast verification and for use by a wide range of stakeholders, including those in the agricultural sector. Met Éireann's network currently consists of four different types of weather station, differentiated according to the range of instruments at each station and the measurement interval.

The network includes five airports which are manned stations where staff record meteorological elements each hour. There are also 20 automatic (synoptic) stations which record data at 1-min resolution. Both the manned and automatic stations record air temperature, precipitation, atmospheric pressure, wind speed and direction, relative humidity, cloud type, visibility, sunshine, soil and earth temperatures and past and pre- sent weather. As in the UK, Met Éireann also has a network of 60 climatological stations run by voluntary observers and state agencies who record a set of measurements at 0900 UTC each day. Each of these stations

reports air temperature and precipitation, but some also record grass temperature, soil and earth temperatures, sunshine duration and cloud cover, wind speed and direction, visibility and present weather. The final suite of stations run by Met Éireann, as well as voluntary observers and state agencies, is an extensive network of approximately 500 rainfall stations. This wide network is necessary in order to capture rainfall in Ireland, which has a high degree of spatial variability. There are daily and monthly stations in the rainfall network where 'daily' implies that the readings are taken once a day at 0900 UTC while at 'monthly' stations the readings are taken at 0900 UTC on the first day of the following month.

A number of stations have been either recently installed, discontinued, or have significant gaps in their recording history. To include the maximum number of continuously recording stations in the calculations of the parameters of interest, two time periods were selected. Initially, the SPI was calculated based on a 20-year dataset spanning from 1998 to 2018, which is the minimum period required to calculate the index (WMO, 2012). Data from a total of 262 meteorological stations were available for this calculation (30 from the climatological network, 221 from the rainfall network, and 11 from the synoptic network as shown in Figure 18a).

In order to compare the precipitation amounts in 2018 with the current climatological standard normal 30-year period 1981-2010 (WMO, 2017), a set of 116 meteorological stations were available for use (11 from the climatological network, 95 from the rainfall network, and 10 from the synoptic network, see Figure 18b). The PNI index was used for this purpose.

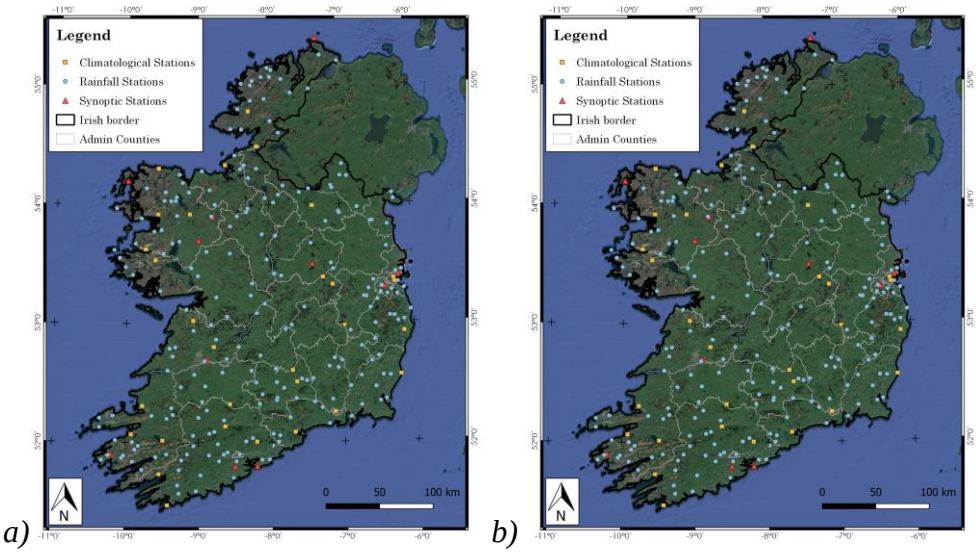

Figure 18 The meteorological stations used for the calculation of (a) SPI and (b) PNI.

5.3. Drought indicators

Monitoring different aspects of the hydrological cycle requires a variety of indicators and indices. No single indicator or index can be used to determine appropriate actions for all types of droughts. Hence, the use of different combinations of inputs with various thresholds characterising all four meteorological, agricultural, hydrological, and socio-economic drought types is a preferred approach to provide complete information. SPI and PNI are based on precipitation data, and the former can characterise the four types of drought; SMD (based on soil moisture data) characterises agricultural drought, and EVI, a vegetation index, is used to show the effects of drought on vegetation. These drought indicators are described in the following subsections.

5.3.1. Standardised Precipitation Index (SPI)

The SPI (McKee *et al.*, 1993) is an index based on monthly cumulative precipitation and classifies the accumulated precipitation of the month under consideration with respect to the long-term average monthly accumulated precipitation for the same month (or other time scales). SPI quantifies a deficit or surplus of precipitation over mean values at different time scales (1, 3, 6, 12, 24 and 48 months) using a probabilistic approach.

A rainfall time series is transformed so that it can be described by a statistical gamma distribution, and further transformed into a standard normal distribution. The index can be used to describe the four types of drought, and the classification of the values range from very wet to very dry drought conditions as shown in Table 6. The *SPEI-CRAN* Package was used for the analysis (Beguería and Vicente-Serrano, 2017).

Category	**SPI criterion (dimensionless)**
Extremely wet	≥ 2.00
Severely wet	1.5 – 1.99
Moderately wet	1.00 – 1.49
Close to normal	-0.99 – -0.99
Moderately dry	-1.00 – -1.49
Severely dry	-1.50 – -1.99
Extremely dry	≤ -2.00

Table 6 Classification of wet and drought periods based on SPI index (McKee et al.,1993).

5.3.2. Percent of Normal Index (PNI)

The simplicity of the PNI (Werick *et al.*, 1994) calculation makes the index useful for comparing any time period and location when identifying and monitoring various impacts of droughts. The index can be calculated for timescales ranging from a single month to a group of months representing a particular season. The PNI value is calculated by dividing the actual precipitation (P) for the month under consideration by the normal precipitation for the corresponding month in the 1981-2010 30-year period (Pa) and multiplying the ratio by 100.

The six categories of PNI are shown in Table 7.

Category	PNI criterion (% of normal precipitation)
Non drought	> 100
Normal	80 – 100
Slight drought	70 – 80
Moderate drought	55 – 70
Severe drought	40 – 55
Extreme drought	< 40

Table 7 Classification of wet and drought periods based on PNI index, (Werick et al., 1994).

5.3.3. Soil Moisture Deficit (SMD)

The SMD (Schulte *et al.* 2005), measured in millimetres of water, is the amount of rain needed to bring the soil moisture content back to field capacity. Field capacity is the amount of water that the soil can hold against gravity (e.g. the maximum amount of water you can add to a potted plant before the water leaks out). A positive SMD indicates a water deficit. A higher SMD value implies a higher water deficit and therefore drier soil. A negative SMD indicates a water surplus. This surplus will drain away in time through surface runoff and/or percolation.

Met Éireann runs an SMD model based on research by Schulte *et al.* (2005). In this model an SMD value of 0mm signifies field capacity, while the minimum value of SMD allowed by the model is -10mm, which indicates saturation. The maximum SMD allowed by the model is 110mm, indicating extremely dry soil which is almost devoid of moisture. The parameter values for the drainage class were derived indirectly, as no soil moisture tension was measured on soils classified as moderately drained.

To approximate the diversity of soil drainage types in Ireland, the model accounts for three simplified soil drainage types. These are well drained, moderately drained, and poorly drained soil types. The Soil Moisture Deficit (SMD) is calculated as follows (eq. 8):

$$SMD_t = SMD_{t-1} - Rain + ET_a + Drain \qquad \textit{eq. 8}$$

where SMD_t and SMD_{t-1} are the SMD values on day *t* and day *t-1* respectively (mm), *Rain* is the daily precipitation (mm day^{-1}), ET_a is the daily actual evapotranspiration (mm day^{-1}), and *Drain* is the amount of water drained daily by surface runoff and/or percolation (mm day^{-1}).

In Met Éireann, the FAO (Food and Agriculture Organization) Penman-Monteith formula (Allen *et al.*, 1998) is used to calculate the daily potential evapotranspiration, using meteorological data recorded at synoptic weather stations. Actual evapotranspiration is derived from potential evapotranspiration as per Schulte *et al*. (2005).

5.3.4. Enhanced Vegetation Index (EVI)

Global 'MOD13Q1' data are available from MODIS, a 36-band spectroradiometer on board the NASA Terra satellite. The MOD13Q1 products are temporal composites which use the best observation of reflectance recorded over 16 days on a given surface. The data and products acquired by the sensors allow for the construction of time series of vegetation indices (VIs), which are used for monitoring the spatio-temporal variability of vegetation. In this study we used the Enhanced Vegetation Index (EVI) (Huete *et al*., 1997) which is obtained from specific spectral reflectance in the visible region of the electromagnetic spectrum. The EVI product's time series has a spatial resolution of 250m and span the years 2001 to 2018. EVI shows the type and architecture of canopies and variations in canopy structure that can be associated with stress and changes related to drought. The index ranges from 1 (very lush green pasture) to 0 (completely barren). Supporting information is available in Appendix 4.

The Irish area is located within the tiles identified as h17v03 of the Earth's surface in the EOS system. All the products have been geo-referenced using the international reference system WGS84 (World Geodetic System 1984). The monthly average growth rate (i.e. the difference between the EVI values of two consecutive months) was calculated each year using the MODIS- TERRA products during the period from December to August. Subsequently, the monthly values of 2018 were compared with the monthly average values based on the period from 2001 to 2017, in order

to show how drought affects vegetation health and how the landscape copes with the water stress situation.

5.3.5. Spatial interpolation

As the meteorological indices are calculated for a limited set of stations, ordinary kriging, a simple spatial interpolation method (Oliver and Webster, 1990), was applied to estimate the national coverage of SPI and PNI. Ordinary kriging uses semi-variance, a statistical model of the spatial dependency of two measurements, to estimate values on a given grid based on multiple point measurements.

5.4. Results

Here we consider time frames from January to April (period 1) and from May to August (period 2). Figure 19 (top row) shows the SPI analysis, which is as effective in analysing wet periods as it is in analysing dry periods. At the beginning of the year, February and March were "*Moderately dry*" in the southeast and northwest, respectively, while January and April were "*Near normal*" and "*Moderately wet*". The driest SPI values were recorded during May to July, with June categorised as "*Severely dry*" over the whole country and some southern areas classified as "*Extremely dry*".

The PNI record (Figure 19, middle row), which compares monthly rainfall totals for 2018 with the climatological standard normal 30-year period 1981-2010, shows that whilst January and April were "*Non drought*", low rainfall amounts were recorded during subsequent months (from May to July). "*Extreme drought*" conditions were recorded in June in the southerneast part of Ireland. Although the PNI values reported "*Non drought*" and "*Normal*" conditions during the months of April and August, respectively, a cumulative deficit in precipitation remained. (Figure 19, middle row).

MODIS Satellite imagery shows the impact of the drought by measuring the greenness of the country. This is expressed as an Enhanced Vegetation Index as shown in Figure 19 (bottom row). The greatest difference between the EVI in 2018 and the average EVI over the long-term period (2001-2017) was recorded in March. The below normal anomalies which occurred in May and June were concentrated in the southeast of the country. Due to a persistent lack of rain, the reduction in vegetation growth

spread throughout the whole country in July, effectively turning the usually green "*Emerald Isle*" to a browner shade.

The difference in the timing of the drought occurred because the northwest is characterised by heavy soils, which have the advantage of being able to hold moisture for much longer, allowing plants to take advantage of the higher temperatures. However, these soils can't hold out continually, and as the drought progresses, growth becomes hindered in these regions too.

This analysis of climatological conditions across Ireland during the drought event, which peaked in June 2018, shows considerable regional variability: vegetation growth was well below normal in the south and east (well-drained soils), but was actually above normal in the north and west (poorly drained soils).

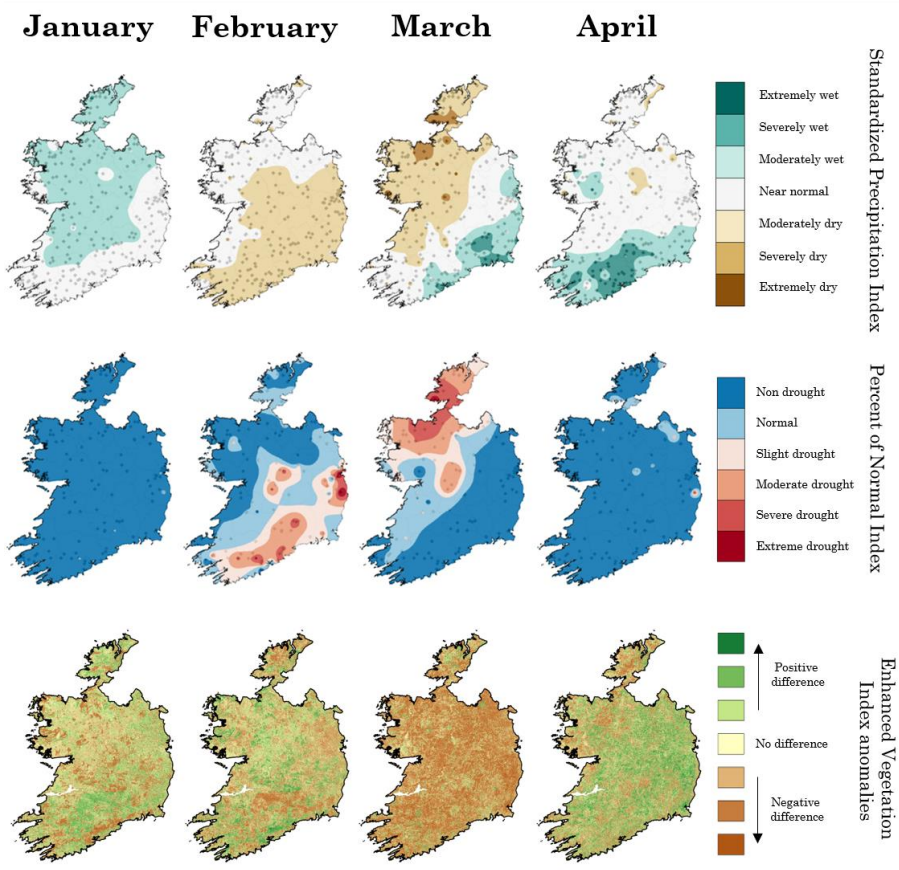

a)

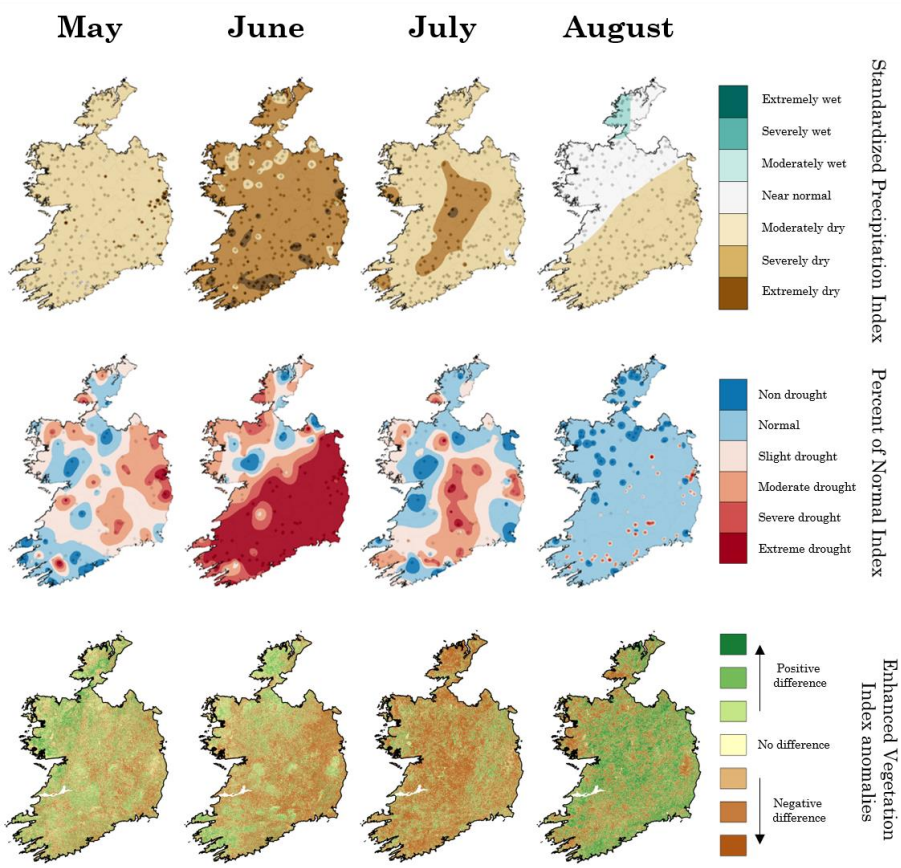

b)

Figure 19 Monthly SPI (row 1), PNI (row 2) and anomalies of monthly growth (2018 vs. (2000-2017) based on MODIS-EVI (row 3) for (a) January to April 2018 and (b), May to August 2018.

A much more detailed picture of climatic conditions can be obtained by examining the thermo-pluviometric regime (Figure 20), which indicates the seasonal variability of the climate. Figure 20 shows the pluviometric and thermal trends for Ireland, based on data from the synoptic and climatological weather station networks for 2018 (Figure 20a) and the climatological standard normal 30-year period 1981-2010 (Figure 20b). Compared to the reference period, surface air temperatures in 2018 were 2-3 °C higher than normal during the months of May to July, while precipitation in June was reduced by two thirds.

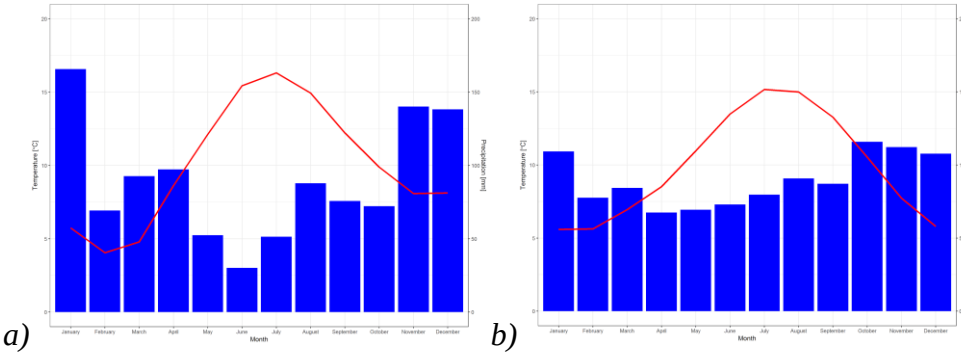

Figure 20 Thermo-pluviometric diagram in Ireland for (a) 2018 and (b) the reference period 1981–2010. The blue bars represent the monthly amount of precipitation, and the red line shows the average monthly trend.

Of the 23 operational synoptic weather stations (including airports) that calculate SMD, eight have long term records that enable a comparison to normal over the period 1981-2010. By way of an example, let us examine the moderately drained soil class of the SMD model at Dublin Airport, a representative station.

Figure 21 shows the daily SMD of moderately drained soils at Dublin Airport for 2018. While April started off with slightly wetter soils than normal, these continued to dry out during May and June, peaking on 14th July with a soil moisture deficit of 94.3mm, close to the maximum possible deficit.

While it is clear that these soils are much drier than normal, we need to look back over a longer period to see how unusual this was. Figure 22 shows the SMD of moderately drained soils at Dublin Airport for the period 1981 to 2018 inclusive. While the annual drying of soils in summer is expected and observed, the 2018 drought stands out as the driest soil on record over this period.

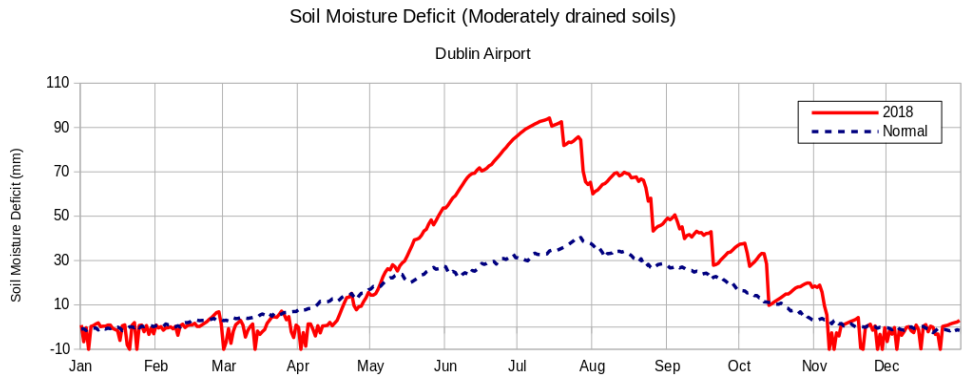

Figure 21 Daily soil moisture deficit for moderately drained soils at Dublin Airport for 2018 compared to their 30-year normal (1981-2010). In July soils were twice as dry as normal.

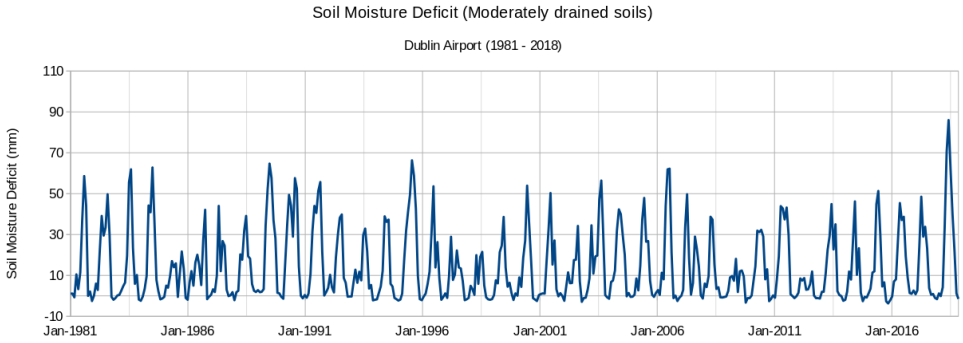

Figure 22 Average monthly soil moisture deficit for moderately drained soils at Dublin Airport for the period 1981-2018 inclusive. A value of -10mm represents soil saturation, 0mm field capacitance, 110mm absence of moisture. July 2018 is the highest SMD (driest) month over this 38-year period.

5.5. Discussion

Using climatological indices and satellite data we can assess the progress of 2018's extreme drought event and its consequences for Irish agriculture. The monitoring of conditions across the country shows that, whilst the drought occurred on a national scale, the impacts varied locally due to the different types of soil. In fact, while eastern regions reported a significant reduction on harvest this year, the uplands of the west and bogs of the midlands produced more biomass than normal, as they are less constrained by water shortages and benefit from higher temperature and increased solar irradiance.

Droughts may become the most important hazards to agriculture in the future. Future climate projections for Ireland based on an ensemble of high-resolution regional climate projections indicate that the number of extended dry periods is expected to increase substantially during summer and autumn by the middle of the century. Summers are projected to be worst affected, with dry periods increasing by 12 and 40% for the medium- to low- emission and high- emission scenarios, respectively. Drought will be driven mainly by a decrease in mean precipitation and a rising of mean annual temperature. By mid-century, the rainfall amount is expected to reduce during spring and especially during summer, with a reduction ranging from 3 to 20%, while mean annual temperatures will rise by 1-1.6 °C, with the largest changes seen in the east of the country (Nolan, 2015).

5.6. Conclusion

The aim of this study was to analyse the drought that occurred in Ireland in summer 2018 and its effects on agriculture as determined through changes in biomass production. Four drought indicators (SPI, PNI, SMD and EVI) were selected and evaluated using meteorological data recorded by Met Éireann and remote sensing imagery from the MODIS-TERRA satellite.

The four indicators show the evolution of the drought during 2018. In particular, analysis of the SMD index illustrated that the drought in 2018 was the most severe over the period 1981 to 2018 and reached a maximum value of 94.3mm on 14th July at Dublin Airport. According to the SPI and PNI, the driest months were May, June and July. The impact depended on soil type and local effects driven by soil drainage capacity. Therefore, although the drought occurred at a national scale, local conditions varied widely.

Monitoring the recurrence and persistence of drought using different sources of information enables the estimation of drought probabilities that could contribute to planning strategies for the mobilisation and management of water resources.

CHAPTER 6: ANALYSIS OF DROUGHT IN NORTH-WESTERN ITALY AND ITS EFFECTS ON WINE PRODUCTION USING LANDSAT AND SENTINEL SATELLITE IMAGERY

This chapter presents a study of agricultural drought applied to a crop of high value, wine production, in the region of Piedmont. The research evaluated the effects of drought in some of the most important vineyards in Piedmont, and the impacts of drought on production of three main grape varieties, Barbera, Moscato Bianco, and Nebbiolo, in the years 2016-2018. This study also combined meteorological data from the regional network with satellite data (Landsat 8 and Sentinel-2), in order to calculate indices for the evaluation of drought duration and impact on water availability and crop performance (Figure 23).

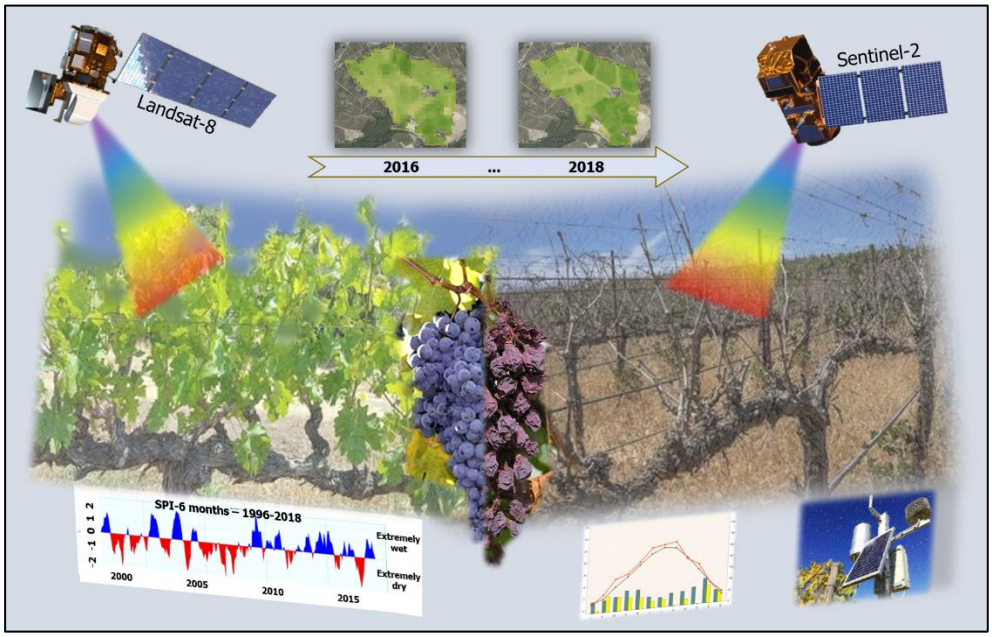

Figure 23 Graphical abstract of chapter 6

Falzoi S., Gleeson E., Green S., Borgogno Mondino E.C., Spanna F., Fratianni S., (under review). Analysis of Drought in Northwestern Italy and its Effects on Wine Production using Landsat and Sentinel Satellite Imagery.

6.1. Introduction

The wine sector plays a key role in the economy of the Piedmont region in northwest Italy. According to Vigasio *et al*. (2018) about 45 thousand hectares of agricultural land were cultivated with vineyards in 2018. These were mainly located in the Langhe-Roero and Monferrato areas (in the southeast of the Piedmont region), in the central hills of Torino and in the provinces of Vercelli and Novara (north of the Piedmont region) (see Figure 24). 18,000 farms and 54 cooperative wineries produced about 2.5 million hectolitres (5% of the Italian national production) of wine in 2018 which had an export value of around 1 billion Euro (18% of the Italian national wine exports).

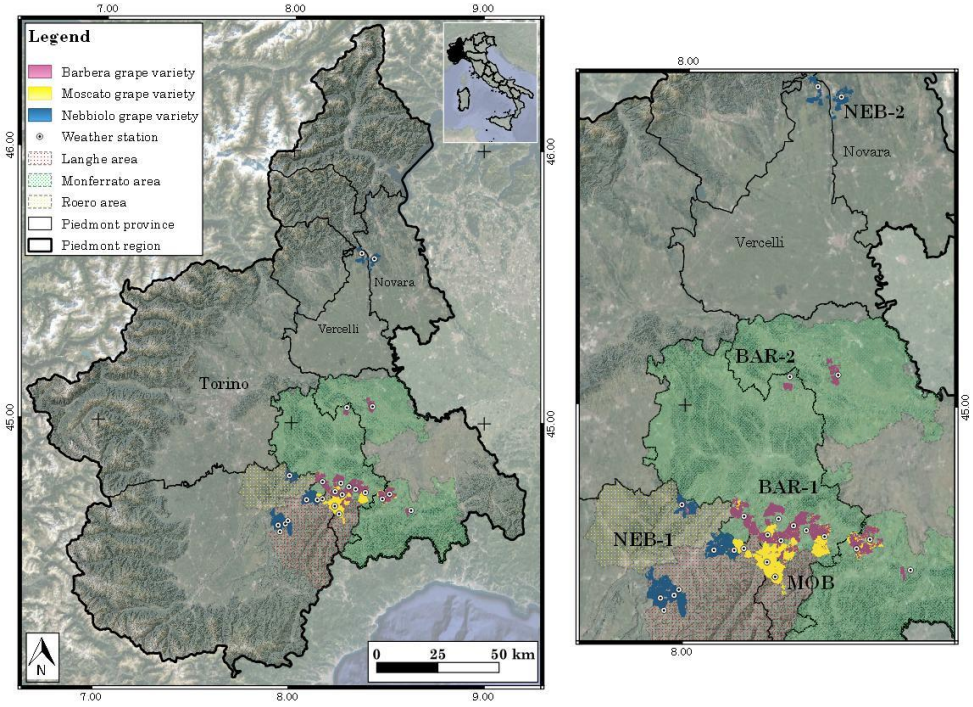

Figure 24 Study area and location of vineyards characterised by grape variety. White dots indicate the positions of meteorological stations

In this context, determining the vegetative and reproductive development of vines, and therefore the maturity and quality of the grapes, is of extreme value from both a scientific and an economic perspective. The development processes of vines are heavily influenced by environmental

conditions. The quality of the final product is determined by the climate and pedological and geographical factors (Lulli *et al*., 1989; Panont and Comolli, 1998; Scienza *et al*., 1990; Val Leeuwen, 1998). Vineyards are established in areas where soil temperatures (relative to air temperatures), soil water holding capacity (relative to rainfall and potential evapotranspiration) and soil nitrogen availability are optimum for the type of wine which is intended to be produced (van Leeuwen *et al*., 2018). Hence, a vineyard can be linked to a cultivated ecosystem, in which the vines interact with the natural environment such as the soil and climate. Such an environment is termed a Terroir. The most recent definition of a vitivini-cultural terroir according to the International Organisation of Vine and Wine (OIV, 2010) is an area in which collective knowledge develops on the interactions between the physical and biological environment and the applied vitivini-cultural practices which give the distinctive characteristics to the products originating from the area. This highlights the multidisciplinary approach to understanding the interaction between the abiotic factors, principally climate and soil, that play a key role in the ecosystem in which grapevines are cultivated (Seguin, 1986).

The quality and characteristics of any wine are tightly connected to the climate (Biancotti, 2003). The main climate parameters that affect grape production and quality are temperature, precipitation, humidity and evapotranspiration. Numerous bioclimatic indices have been suggested by Cola *et al*. (2013), Fregoni (2003), Huglin (1978) and Winkler (1962) based on weather data, but these are no longer sufficient to predict the interactions of all environmental factors. According to future climate projections, temperatures and extreme events are expected to increase significantly. This warmer and drier future scenario will change the quality of grapes and wine, for example by modifying the acidity of the grapes (Caffarra *et al*., 2011; Dalla Marta *et al*., 2010; Jones *et al*., 2005). In fact, vines are particularly sensitive to climate change because their management and adaptation must be anticipated well in advance (van Leeuwen *et al*., 2004, Carey *et al*., 2008). A changing climate will push the plants to their limits, impacting on the quality and quantity of yields (Fraga *et al*., 2016).

Weather station data are usually only representative of the particular location of the station and cannot be interpolated in space. Therefore, alternative data sources are needed to accurately estimate and predict seasonal fluctuations in grape quality. Remote sensing techniques involving satellite observations can provide long-term, continuous and

uniformly distributed data, in the form of imagery (Anderson *et al*., 2016; Gu *et al*., 2007; Renza *et al*., 2010) that are freely accessible and provided by various space agencies, including the US (NASA) and the European (ESA) space agencies. Several studies show strong relationships between satellite-based vegetation indices and vine development (Borgogno-Mondino *et al*., 2018; Sun *et al*., 2017). Satellite data can be used to predict the phenolic acid content and colour of the grapes (Ledderhof *et al*., 2016; Garcìa-Estévez *et al.*, 2017; Zarco-Tejada *et al*., 2013) and to distinguish different varieties within vineyards (Rey-Caramés *et al*., 2015).

Using remote sensing techniques in combination with meteorological data increases the potential for developing more accurate decision-support systems (DSS) which can be adapted for both decision makers and agricultural technicians, who are interested in near real-time crop growth during the growing season (Falzoi *et al*., 2019a).

The gross primary production (GPP) of vegetation is an index derived using a combination of meteorological and remote sensing data and is the most important measure of the carbon mass flux of the terrestrial carbon cycle (Nuarsa *et al*., 2018; Ruimy *et al*., 1996; Xiao *et al*., 2011; Xiao *et al*., 2004). In other words, GPP defines the rate at which primary producers create chemical energy and accumulate biomass by light absorption and carbon fixation processes in plant photosynthesis, that occur within the chloroplasts of plant leaves. In the light absorption process, chlorophyll receives photosynthetically active radiation (PAR, mostly in the visible part of the electromagnetic spectrum) from sunlight. The carbon fixation process involves the absorption of energy used to combine water with CO_2 to produce sugar (Xiao *et al*., 2011). Because there are no direct instrument-based measurements of plant photosynthesis at canopy or landscape scales (Delgado *et al*., 2018; Pau *et al*., 2018; Xiao *et al*., 2011) the estimation of GPP can reduce this lack of information. Previous studies on GPP in the Italian Mediterranean forest (Maselli *et al*., 2009), the Amazon forest (Danelichen *et al.*, 2015), and in corn-soybean and maize crops plantations (Dold *et al*., 2019; Madugundu *et al*., 2017) have been documented. However, to our knowledge, changes in GPP in vineyards as a result of climate variations have not been reported in previous studies.

GPP is strictly influenced by climate and extreme events, in particular drought episodes, and varies from year to year. The variation is clearer in unpredictable climates where there are significant differences between years. Considering the future changing climate, drought events are projected to become increasingly common, more intense and less

predictable in the coming decades, especially in vulnerable environments such as mountain areas and the Mediterranean basin, with considerable repercussions for water resources and agriculture (Bindi and Olesen, 2011). In the near future (the next 10-15 years), Perini *et al*. (2011) predicts a strong decrease in winter and spring precipitation in Northern Italy (including the Piedmont region). Over the past 30 years, the temperatures in Piedmont increased by 0.7 °C (Fratianni *et al*., 2015). In Turin, the capital of Piedmont, October 2017 was the 4th warmest October since 1753, with an average temperature of 16.2 °C (2.1 °C above the 1981-2010 normal) (Bo *et al*., 2019). The period from July to October 2017 was one of the driest in the past 60 years with 31 weeks of severe drought (Baronetti *et al*., 2020; Falzoi *et al*., 2019b) caused by positive surface pressure anomalies due to persistent anticyclonic conditions in the euro-mediterranean region (Kotsias *et al*., 2020) (Figure 25). No significant variations have been recorded in the annual amount of precipitation in the Piedmont region. However, the seasonal distribution has changed with a decrease of 1.5mm per year during winter in the north of Italy, and 7.7mm per year in central areas (Baronetti *et al*., 2018). Some consequences of this are already evident.

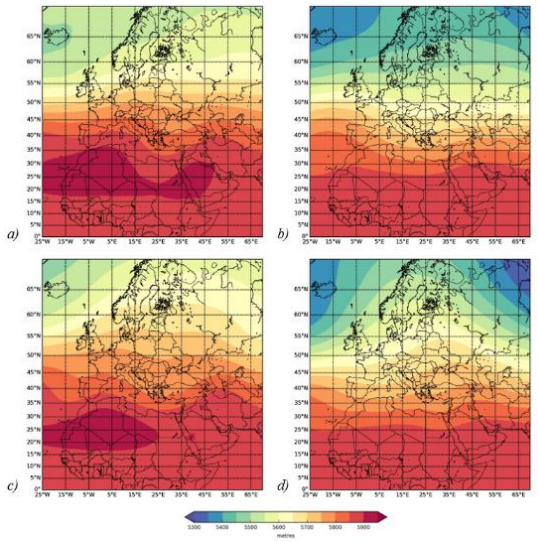

Figure 25 500 hPa geopotential height maps for (a) Summer 2017, (b) Autumn 2017, (c) Summer 2018 and (d) Autumn18. The data were downloaded from ECMWF's ERA reanalysis archive where the 06 Z and 18 Z analysis fields were retrieved and averaged over each 3-month period representing the relevant season.

In this study we:

i. estimate the GPP in the most important vineyards of Piedmont, and determine its variation in time and space using meteorological data and remote sensing techniques;
ii. analyse the effect of water shortages on the productivity of the Barbera, Moscato Bianco and Nebbiolo grape varieties;
iii. predict the productivity of grapevines in five vineyard areas.

6.2. Materials and Methods

6.2.1. Study area

The area analysed in this work falls within the Piedmont region (north-western Italy) and consists of mountains (43%), hills (30%) and plains (27%). The hilly section, where most of the wine terroir are located, has a Continental Temperate climate (*Cfa*) with hot summers (Fratianni and Acquaotta, 2017). Twenty-four vineyards in the Piedmont region were selected for this study with each having a nearby meteorological station (Table 8). Each vineyard is divided into sub areas in which information about the quantity of grapes produced [kg ha^{-1}] was recorded. Data on the quantity of grapes harvested from 2016 to 2018 were obtained from the Agricultural and Livestock Production Sector of the Piedmont Region, Agriculture Directorate.

The vineyards are mainly located in the Langhe-Roero and Monferrato areas (south and southeast of the region), in the central hills of Torino (Turin) and in the north of the region in the Novara and Vercelli provinces (Figure 24). They are generally found at heights between 100 and 700m a.s.l. The hilly vineyard area is surrounded to the south, west and north by the western Alps, where most peaks are over 2,500m. The altitude gradient (from 100m to 4,000m a.s.l.) strongly influences the regional and microclimate, which experiences great variations in temperature and precipitation over short distances (Nigrelli *et al.*, 2018).

The Langhe area extends along the Tanaro river. It has a dry climate where annual precipitation varies between 800mm and 1,100mm, and is characterised by frequent water shortages during the summer. The territory is hilly with calcareous and sub-acid type soils, and the vineyards are mainly cultivated with Nebbiolo (NEB-1) and Moscato Bianco (MOB) grapes. MOB is considered to be one of the oldest grapes grown in

Piedmont and is the most renowned and widespread aromatic berry cultivar in the region. The harvest period normally happens in the second week of September.

The hilly area of Roero extends to the north of the Langhe area, where NEB-1 and Barbera (BAR-1) are the main grape varieties. The Nebbiolo cultivar is very sensitive to the terroir and its cultivation is limited to suitable areas, such as vineyards with optimal exposure. In the Nebbiolo cultivation area, leaf removal and cluster thinning are two practices used to improve cluster health and to reduce yield (Guidoni *et al*., 2008). It is characterised by early budding and late ripening (first - second week of October) and in its original area it is used to produce high-quality aged wines such as Barolo and Barbaresco.

In the east, the Monferrato area is characterised by strong annual temperature variations between summer and winter, with low amounts of precipitation compared to the rest of the Piedmont region. The main grape varieties are BAR-1 and MOB, that are cultivated in vineyards with slopes of over 20% and south or southwest exposure. In the northern region of Monferrato the main grape variety is Barbera (BAR-2). Barbera is the most widespread grape variety in the Piedmont region. The ripening period normally occurs in the first week of October.

The northern hilly area of Piedmont is characterised by higher annual precipitation and acidic soil. This area is particularly favourable for the cultivation of Nebbiolo (NEB-2) grape variety.

The Piedmontese vineyards contain a vertical shoot-positioned trellising system and a spur-pruned cordon with a bud-load of about 8-12 nodes per meter of row length. The vine spacing is 2.20x 1.15m (inter- and intra-row) and the cordon is raised 0.50m above the ground with three pairs of surmounting catch wires for a canopy extending 1.40m above the cordon. In each vineyard, the plant density is less than 4,000 vines per hectare.

6.2.2. Weather data

Data from twenty-four weather stations in the vineyard area (Figure 24) was selected for the period 2003 to 2018. The climate data was obtained from the Regional Agrometeorological Network (RAM) of Piedmont that currently consists of 120 electronic weather stations and has been operating continuously since the second half of the 1990s. Most of the stations have a historical series of over 15-20 years of data valuable for

climatological analysis and interpretation of atmospheric, agricultural and phytosanitary phenomena. The RAM stations are uniformly distributed between 100 and 800m a.s.l. in the agricultural Piedmontese area, characterised by vineyards, orchards, rice and cereal crops. The stations are equipped with a thermometer and hygrometer sensors, and use a tipping-bucket rain gauge, SIAP UM 7525, with a calibrated mouth ($1000cm^2$). The mouth is at a height of 2m above the ground. The electronic instruments transmit information in real-time to the operation centre in Turin (Piedmont) for collection and storage.

The meteorological data collected are subjected to validation and possible reconstruction of missing data in order to provide continuity.

Vineyard	Area	Grape Varieties	Altitude [m]	Latitude	Longitude
Agliano	Monferrato	BAR-1	217	44°46'47"	8°15'36"
Cassine	Monferrato	BAR-1	200	44°44'27"	8°30'42"
Calosso	Monferrato	BAR-1	241	44°44'54"	8°13'51"
Nizza Monferrato	Monferrato	BAR-1	177	44°45'28"	8°20'12"
Costigliole Asti	Monferrato	BAR-1	256	44°47'04"	8°09'56"
Castel Boglione	Monferrato	BAR-1	275	44°44'45"	8°23'13"
San Marzano Oliveto	Monferrato	BAR-1	175	44°46'00"	8°18'06"
Canelli	Monferrato	BAR-1	263	44°44'15"	8°16'03"
Ricaldone	Monferrato	BAR-1	320	44°43'21"	8°28'29"
Carpeneto	Monferrato	BAR-1	291	44°40'53"	8°37'23"
Rosignano	Northern Monferrato	BAR-2	165	45°03'42"	8°25'15"
Moncalvo	Northern Monferrato	BAR-2	219	45°03'28"	8°17'16"
Santo Stefano Belbo	Langhe	MOB	334	44°41'42"	8°13'46"
Coazzolo	Langhe	MOB	240	44°43'16"	8°09'56"
Loazzolo	Langhe	MOB	406	44°39'59"	8°15'08"
La Morra	Langhe	NEB-1	314	44°37'24"	7°56'21"
Barbaresco	Langhe	NEB-1	287	44°43'03"	8°05'01"
Serralunga d'Alba	Langhe	NEB-1	263	44°38'22"	7°59'18"
Canale	Roero	NEB-1	264	44°48'20"	7°59'40"
Castiglione Falletto	Langhe	NEB-1	306	44°37'42"	7°58'34"
Barolo	Langhe	NEB-1	362	44°35'55"	7°56'55"
Neive	Langhe	NEB-1	276	44°43'04"	8°08'06"
Ghemme	Northern Piedmont	NEB-2	295	45°36'17"	8°25'29"
Gattinara	Northern Piedmont	NEB-2	360	45°37'28"	8°21'32"

Table 8 List of vineyards and their grape variety

6.2.3. Drought indices

In order to characterise agricultural drought in the study area, we used two derived indices: Standardised Precipitation Index - SPI (McKee *et al*., 1993) and Standardised Precipitation Evapotranspiration Index - SPEI (Vicente-Serrano *et al*., 2010). These indices were computed using data recorded at each meteorological station.

SPI is an index based on monthly cumulative precipitation and classifies the accumulated monthly precipitation with respect to the long-term average monthly accumulated precipitation for the same month (also possible on other time scales). SPI quantifies a deficit or surplus of rain for a particular event or period over mean values, using a probabilistic approach. The rainfall series is fitted to a gamma distribution, then transformed into a standard normal distribution. SPI indicates the number of standard deviations by which a particular event exceeds mean conditions.

SPEI is a multiscalar drought index designed to take into account both precipitation and potential evapotranspiration (ET_0). SPEI looks at long-term rainfall at different timescales and compares it with expected demand as indicated by normal evapotranspiration, and gives a single number which indicates conditions. ET_0 was estimated using the Hargreaves equations (Hargreaves and Samani, 1985), a temperature-based method that uses maximum and minimum air temperatures, and solar radiation to estimate evapotranspiration. Monthly average temperatures and cumulative precipitation are used to calculate SPEI.

The SPEI-CRAN package was used for the analysis (Beguería and Vicente-Serrano, 2017). The classifications of wet and drought periods based on SPI and SPEI indices are given in Table 9.

Category	SPI and SPEI values (dimensionless)
Extremely wet	≥ 2.00
Severely wet	1.5 – 1.99
Moderately wet	1.00 – 1.49
Close to normal	-0.99 – 0.99
Moderately dry	-1.49 – -1.00
Severely dry	-1.99 – -1.50
Extremely dry	≤ -2.00

Table 9 SPI and SPEI classification of wet and drought periods according to McKee et al. (1993) and Vicente-Serrano et al. (2010), respectively. SPI and SPEI indices are dimensionless.

6.2.4. Remote Sensing data

A time series of Landsat 8 (Landsat.gsfc.nasa.gov; L8) and Sentinel-2 (European Space Agency, 2015; S2) multispectral images were retrieved for April to October 2016 to 2018 for the vegetative and reproductive periods of vines in the Northern Hemisphere.

A total of 292 L8 imagery and 97 S2 imagery were selected which corresponded to the study area. The imagery was identified by the codes 194028, 194029, 195028 and 195029 for L8, and T32TMQ and T32TMR for S2. Initially, the imagery was assessed visually and all images obscured by cloud cover were excluded. The imagery was analysed with a pre-processing procedure using the QuantumGIS *Semi-Automatic Classification Plugin*, SCP (version 6.2.9) (Congedo, 2018). SCP converts satellite imagery from numbers to top of atmosphere (TOA) reflectance, and applies a dark object subtraction technique which is an image-based atmospheric correction.

The spectral indices Enhanced Vegetation Index - EVI (Huete *et al*., 1997, eq.1) and Normalized Difference Moisture (Water) Index - NDMI (or NDWI) (Gao, 1986, Wilson *et al*., 2002, eq. 2) were examined.

The EVI is obtained from specific spectral reflectances in the visible region of the electromagnetic spectrum, and shows the type and architecture of canopies and variations in canopy structure that can be associated with stress and changes related to drought. The index ranges

from 1 (very lush green pasture) to 0 (completely barren) and is as follows (eq. 9)

$$EVI = G \times \frac{NIR - RED}{NIR + C1 \times RED - C2 \times BLUE + L} \qquad \textit{eq. 9}$$

where NIR, RED and BLUE represent the spectral reflectance of near-infrared, red and blue wavelengths, respectively. L is a correction for plant cover background (undergrowth, litter, soil) that determines transmittance through vegetation in the NIR and RED wavelength bands. *C1* and *C2* are aerosol correction coefficients, where the blue band is used to correct aerosol effects in the red band. G is the gain factor. In this study, the values for *L*, *C1*, *C2* and *G* were equivalent to those adopted in the actual MODIS EVI product, i.e. 1, 6, 7.5, and 2.5, respectively.

NDMI is a satellite-derived index from the NIR and shortwave infrared (SWIR) channels which describes the water content of the vegetation. NIR reflectance is influenced by the internal structure and dry matter content of the leaves, while SWIR reflectance reflects changes in both the spongy mesophyll structure in vegetation canopies and the water content in the internal leaf structure. The index ranges from 1 (no water stress) to -1 (completely barren) and is as follows (eq. 10).

$$\text{NDMI} = \frac{\text{NIR - SWIR}}{\text{NIR + SWIR}} \qquad \textit{eq. 10}$$

The L8 and S2 wavelength range bands are shown in Table 10.

	BLUE	**RED**	**NIR**	**SWIR**
L8	B2 0.452-0.512	B4 0.636-0.673	B5 0.851-0.879	B6 1.567-1.651
S2	B2 0.439-0.535	B4 0.646-0.685	B8 0.848-0.881	B11 1.539-1.681

Table 10 BLUE, RED, near-infrared (NIR) and shortwave infrared (SWIR) wavelength bands in the instruments carried on board the Landsat 8 (L8) and Sentinel-2 (S2) satellites.

For each weather station and each vegetation index map, a 60m squared area around the station was selected and the average value of the pixels inside this area was calculated. The same set of pixels were used for calculation throughout the growing season. We assume that the pixels are also representative of the entire vineyard.

6.2.5. Gross Primary Production, GPP

The satellite indices and weather data were used to estimate the GPP, based on the light-use efficiency (LUE) approach, in which only the Fraction of Absorbed Photosynthetically Active Radiationabsorbed by the chlorophyll pigments ($FPAR_{chl}$) is selected. The equation for GPP is as follows (eq. 11):

$$GPP = \varepsilon_g \times FPAR_{chl} \times PAR \qquad \textit{eq. 11}$$

where εg is the efficiency of light use in vegetation [μmol m^{-2} s^{-1}] (eq. 12) which is influenced by temperature (T_{scalar}, eq. 13), water (W_{scalar}, eq. 14) and phenology (P_{scalar}, eq. 15); $FPAR_{chl}$ is equivalent to EVI; PAR is photosynthetically active radiation, estimated according to Duffie and Beckman (1991).

$$\varepsilon_g = \varepsilon_0 \times T_{scalar} \times W_{scalar} \times P_{scalar} \qquad \textit{eq. 12}$$

where ε_0 is the maximum light efficiency [μmol m^{-2} s^{-1}].

$$T_{scalar} = \frac{(T - T_n) \times (T - T_x)}{(T - T_n) \times (T - T_x) - (T - T_{opt})^2} \qquad \textit{eq. 13}$$

where T is the daily average temperature over 10 days prior to the acquisition of the satellite image; T_n, T_x, and T_{opt} representing the minimum (12 °C), the maximum (33 °C) and the optimal (25 °C) cardinal temperatures, respectively, for the grapevine (Mariani *et al.*, 2013).

$$W_{scalar} = \frac{1 + NDMI}{1 + NDMI_x} \qquad \textit{eq. 14}$$

where $NDMI_x$ is the maximum value of each pixel considered during the vegetative period.

$$P_{scalar} = \begin{cases} \dfrac{1 + NDMI}{2} & \text{Burst bud} \\ 1 & \text{Complete leaf development} \end{cases} \qquad \textit{eq. 15}$$

The GPP index was calculated at two different spatial resolutions, 30m and 10m, using the L8 and S2 imagery, respectively. Multi-temporal and spatial analyses were conducted using the R-project software R-3.5.0 statistical software.

6.2.6. Statistical analysis

A machine learning procedure based on the *Random Forest* (RF) missing data algorithm of Breiman (2001) was applied to monthly averaged remote sensing data in order to deal with missing data and solve cloud gaps. RF is an ensemble learning method where a combination of tree predictors such that each tree depends on the values of a random vector sampled independently and with the same distribution for all trees in the forest (Breiman, 2001). In a practical way, RF adds additional randomness to the model while growing the trees and searching for the best feature among a random subset of features. After a large number of trees is generated, they select the most popular class. The *randomForest* R-package was used (Liaw and Wiener, 2002).

The agreement between the observed grape production and estimated values of GPP was evaluated using the relative root mean square error (rRMSE; Jørgensen *et al*. 1986), the efficiency index (EF; Nash and Sutcliffe 1970), and the coefficient of residual mass (CRM; Loague and Green 1991) index.

The rRMSE index measures how close predictions are to the observed data. The EF index identifies inefficient models. Negative values indicate that the mean of the observations is a better predictor than the model used. The CRM shows whether the model tends to overestimate (if negative) or underestimate (if positive) GPP compared to the observed data.

Combining satellite and weather information with geographical factors we estimated a model (eq. 16) to predict total grape production (f(grPr). The model, based on RF techniques, considers the 5 regions collectively and uses a digital elevation model (DEM) with a spatial resolution of 10m to provide the slope and aspect values of the vineyard locations. The aspect values were grouped into 8 categories, representing 8 equal proportions of the aspect range (0° - 360°), which were then used in the model. Furthermore, we evaluated the model using observed grape production (grPr) obtained from the Agricultural and Livestock Production Sector of the Piedmont Region, Agriculture Directorate.

$$f(\text{grPr}) = \text{GPP} + \text{DEM} + \text{slope} + \text{aspect} \qquad \textit{eq. 16}$$

6.3. Results

2016 mean temperatures were not significantly different to the average temperature of the reference period (2013-2018). However, accumulated rainfall was a third of the precipitation average during the months of April and September, which contrasts the increased rainfall recorded in the summer and in the months of February and November.

2017 was characterised by high temperatures of up to 2-3° C above average and a reduction in precipitation, resulting in a dramatic dry event in the months of August, September and October. Contrasting thermal conditions recorded at the beginning of spring initially favoured the early development of vegetation. Subsequently, the processes were interrupted by temperature drops and late frosts that occurred in April, which caused considerable damage to the agricultural sector. The effects of water

shortages that began in May, associated with high temperatures, caused a drastic reduction in GPP throughout the season.

On the contrary, 2018 was characterised by higher precipitation than the average of the reference period 2003-2018, mainly due to positive pressure anomalies recorded in spring and autumn 2018. Temperatures, which were below average in February and March, were 1-2 °C above average for the rest of the year. Above average temperatures are favourable for the vegetative and productive processes of the vines, in particular for the ripening phase. For example, due to drought during the summer and autumn of 2017 Piedmontese wine production was reduced by 30% compared to 2018. Also, in 2017 many intense climate anomalies strongly influenced the trend in vegetative and productive processes of agricultural crops in Piedmont. On the contrary, 2018 was characterised by higher than normal rainfall quantities mainly caused by a spring anomaly, while the above normal temperatures were favourable for the vegetative and productive processes of the vines and the ripening phase.

The Spearman correlations between the SPI and SPEI drought indices and cumulative GPP for the Barbera (BAR-1 and BAR-2), Moscato Bianco (MOB) and Nebbiolo (NEB-1 and NEB-2) grape varieties are calculated in order to evaluate the relationship between the drought indices (SPI and SPEI) and grapevine GPP. The results are shown in Figure 26. Four agricultural drought indices, which were computed using the rolling average of 6-month and 12-month periods (SPI-6, SPI-12, SPEI-6 and SPEI-12), were compared with the cumulative GPP for the respective periods. The best results of this analysis, in terms of the Spearman correlation, were selected and shown in Figure 26.

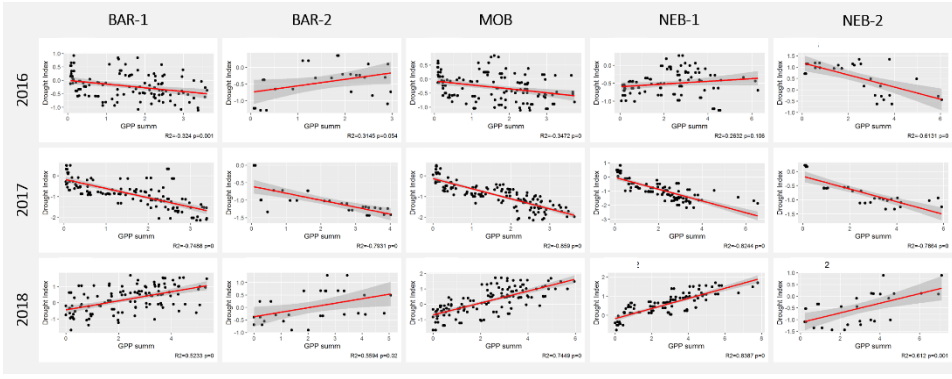

a)

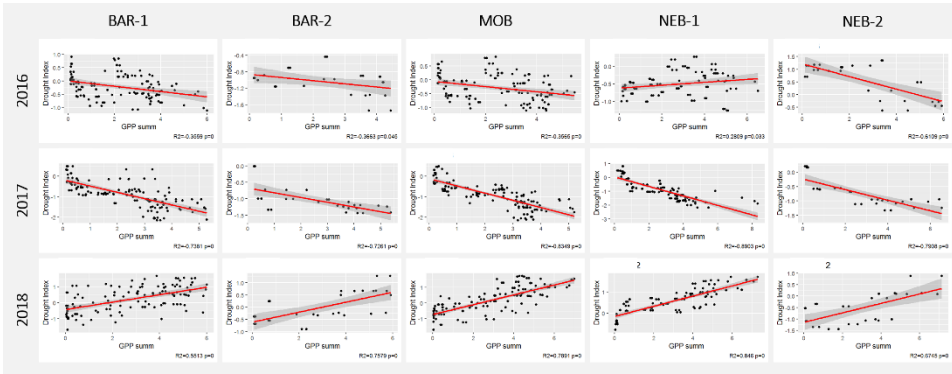

b)

Figure 26 Correlation between drought indices (SPI, SPEI) and cumulative GPP for the Barbera (BAR-1 and BAR-2), Moscato Bianco (MOB) and Nebbiolo (NEB-1 and NEB-2) grape varieties. The years 2016-2018 are shown where Landsat 8 (a) and Sentinel-2 data (b) are used to compute GPP. Dark grey areas show the 95% confidence level interval for predictions from the linear model (red line).

Since the L8 and S2 data are comparable, we created a single dataset by taking the average values of the data from both satellites every 15 days. In Figure 27 (top row) we calculated the trend in GPP index from April to October for each grape variety. We also calculated the cumulative value of the GPP index (Figure 27, bottom row) for each grape variety. Figure 27 shows 2018 as the year with the highest cumulative GPP, while 2016 and 2017 show opposite behaviour in the vegetative periods before and after July.

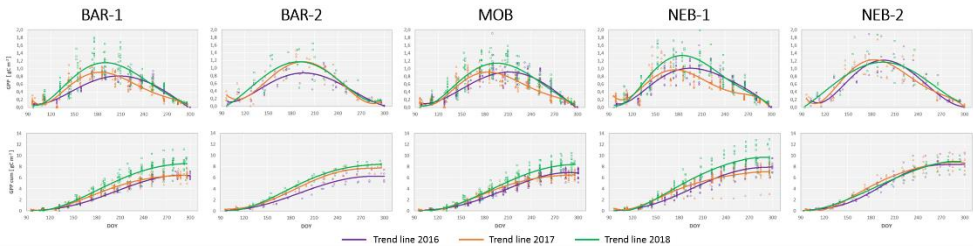

Figure 27 GPP index trend (top row) and cumulative GPP trend (bottom row) for the Barbera (BAR-1 and BAR-2), Moscato Bianco (MOB) and Nebbiolo (NEB-1 and NEB-2) grape varieties, for the years 2016-2018 during the vegetative period from April to October.

Five representative vineyards were chosen for each area in order to show the evolution of GPP index throughout the season, from bud burst in spring to the harvest in autumn (Figure 28).

Due to cloud cover, a comparison between both satellites for the first half of 2016 is not possible nor is it possible to compare this period, during which bud burst and flowering takes place, to the corresponding period in 2017 and 2018. Nonetheless, due to the relatively "normal" meteorological conditions during 2016, this year provides a useful comparison point for the GPP of 2017 and 2018.

Despite an increase of precipitation during the spring of 2018 the vegetation restart was slow and partially conditioned by the drought effects of the previous year. In fact, the budding phase was recorded at the end of April in all 5 vineyards under examination. During the reproductive period, the vineyards took advantage of the high temperatures, higher than the average, and of the abundant water. This allowed greater development of the plants which is highlighted by a more intense green colour in the Veraison maps, in particular for BAR-1 and BAR-2 (Figure 28). The high GPP values recorded during the harvest confirmed the excellent production of grapes in 2018.

Figure 29 shows a strong positive correlation (R^2= 0754, $p < 0.01$) between the observed grape production (grPr) obtained from the Agricultural and Livestock Production Sector of the Piedmont Region, Agriculture Directorate, and predicted total grape production (f(grPr) calculated using eq. 16). This highlights the reliability of the model in predicting grape production (rRMSE= 34.47%). The CRM (-0.003) was negative and close to the optimum value of 0, which indicates that the model provides a better estimation than the average value. The EF (0.815) was positive and close to the optimum value of 1.

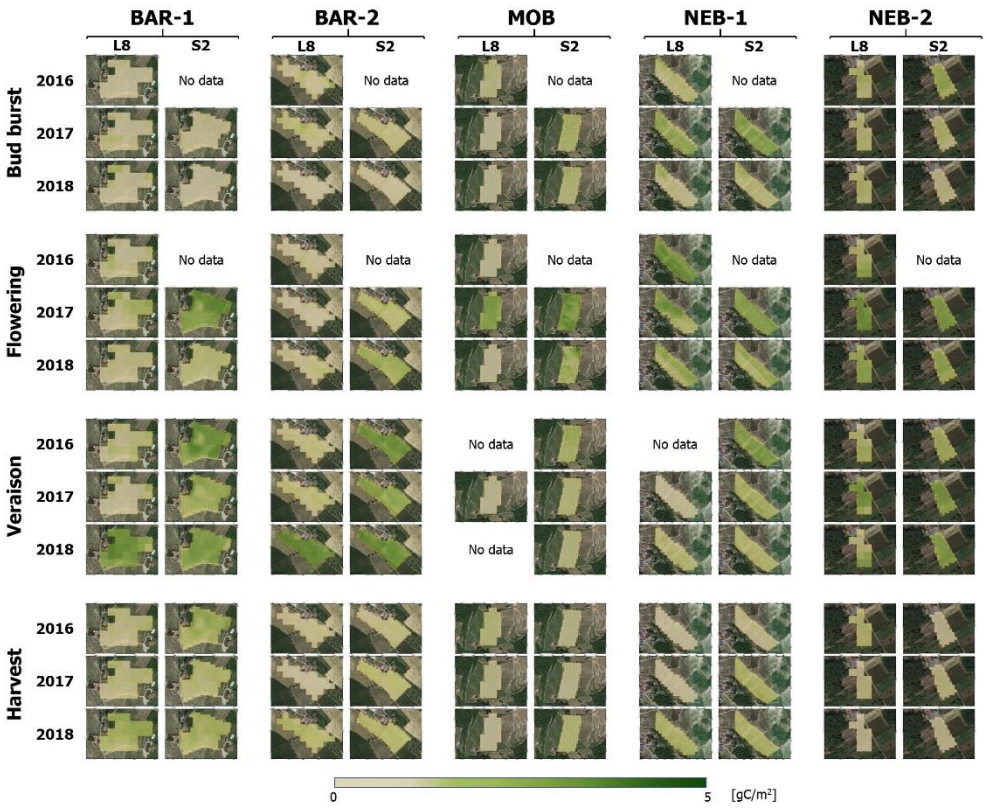

Figure 28 Evolution of GPP index during the vegetative and reproductive seasons for the years 2016 to 2018 in five of the most representative vineyards for each area.

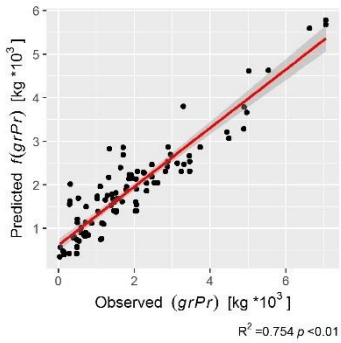

Figure 29 Scatter plot, including regression line, of predicted vs observed grape production in the 5 areas of Piedmont. The predicted grape production values (f(grPr) were calculated using the multiple linear regression model given in eq. 8, while the observed grape production values (grPr) were based on data obtained from the Agricultural and Livestock Production Sector of the Piedmont Region, Agriculture Directorate. The vegetative period from April to October for 2016 to 2018 was used.

6.4. Discussion

The chosen index for evaluating and monitoring the impact of drought on grape vine productivity, GPP, proved to serve multiple functions for the analysis. Cumulative GPP computed using Landsat 8 (Figure 26*a*) and Sentinel-2 (Figure 26*b*) data showed comparable results. These results were strengthened by comparison with SPI and SPEI drought indices. The results concerning the effects of drought on grape vine productivity varied by year and by grape variety.

The effects of the drought that occurred in 2017 were confirmed by the strong negative correlation between the GPP for L8 (R^2= -0.749; -0.859, p< 0.05) and S2 (R^2= -0.726; -0.890, p< 0.05) and the SPI and SPEI drought indices (Figure 26*a,b*, middle row). On the contrary, the correlation was positive in 2018 for all 5 grape varieties, which implies that the water supply to the vineyard was sufficient in the 5 study areas (Figure 26*a,b*, bottom row). The R^2 values for L8 ranged between 0.523 and 0.839 (p< 0.05) and for S2 between 0.551 and 0.846 (p< 0.05). Regarding 2016 the results depended on the grape variety produced by different vineyards (Figure 26*a,b*, top row). The correlation was negative for BAR-1, MOB and NEB-2 (p< 0.05, for both satellites), while it was positive for BAR-2 and NEB-2 (p< 0.05 for S2, p> 0.05 for L8). The statistical significance of these results was influenced by the availability of data, which in some cases was limited by the low ratio of meteorological stations to vineyards, e.g. in the case of BAR-2 and NEB-2 because there were few vineyards growing these varieties of grape.

In Figure 27 (top row) we calculated the trend in GPP index from April to October for each grape variety. Consistent with the favourable climate conditions, the highest values of the GPP index were calculated in 2018 (green line) with peaks of 1.2 gC m^{-2} for 4 vines. Similar to the analysis of the relationship between drought indices and GPP, the trend analysis also highlighted variation in GPP by grape variety. NEB-1 had the highest estimated GPP of 1.4 gC m^{-2}. The highest values were recorded in June (DOY= 180-210). 2016 (purple line) showed a constant trend throughout the vegetative period, although with slightly lower GPP values compared to 2018. The exception to this was the northern Piedmont area (NEB-2) where higher GPP values of 1.2 gC m^{-2} were estimated. BAR-1 and MOB recorded the highest values in July (DOY= 210-240). The increase in performance of the GPP index in 2017 was greater (orange line) than in 2016 and 2018, indicating higher production of vegetation.

The GPP trend analysis provided a means to track the progression of grapevine response to drought episodes. 2016 was considered a "normal year", especially during the growing season. However, rainfall quantities were about 10-20% lower than average and mean temperatures were higher than normal, especially in September. This provided a reference point for monitoring the impact of drought over the course of the growing season in 2017. In the first part of the vegetative period in 2017, the vines were able to take advantage of the favourable temperatures, increasing their GPP. In 2017 budding began at the beginning of April, almost two weeks earlier than in the other two years, as clearly noticed in the BAR-2 and NEB-1 varieties (Figure 27). The favourable weather conditions continued until the end of the spring, where high GPP values were calculated during the flowering period. Despite higher values in May, water scarcity associated with high temperatures caused a drastic reduction in primary production during the Veraison period and the effects are clearly visible from the images of both satellites that show a reduction in GPP from the second half of July. The southern area recorded more damage compared to the North of Piedmont (NEB-2). The lack of rainfall from July then drastically reduced the GPP thereafter, which was reduced in all 5 varieties of vine by the end of the season.

The results of this paper highlighted the vulnerability of the MOB vine variety to drought conditions, particularly the extreme drought of 2017, compared with NEB-1 and BAR-1 which showed greater resilience to extreme water deficit. This result is surprising as the literature describes MOB as a variety with good drought tolerance, historically, and underlines the complexity of drought conditions, e.g. intensity and duration, and their impacts on vine growth. The continued monitoring of the response of different varieties to a changing climate can provide more accurate knowledge about the tolerance of different varieties to events such as water shortages (Belfiore *et al*., 2019; Giordano *et al*., 2016).

The technique described in this work allowed the primary productivity trend of a vineyard to be followed over the course of the year, and indicated the areas in which the vegetative development of the vineyard is compromised, compared with the rest of the vineyard. GPP was found to be strongly correlated with classic drought indices such as SPI and SPEI, which are limited in that they only provide discrete information valid at the site of the weather station. Furthermore, comparison with a historical archive of GPP trends (Figure 27) provided a useful indication for estimating the final wine production of the vintage. The long series of

satellite data provided by the National Aeronautics and Space Administration, NASA, and the Landsat mission programme started in 1972, are a starting point for implementing historical data, but the spatial resolution is limited in terms of the analysis outcomes. GPP, based in part on satellite data, provided productivity information that clearly showed how the response to water scarcity can vary both between climatically different areas and also within the same vineyard, as shown by the maps produced for the 5 reference vineyards (Figure 28). From a management point of view, the possibility of providing maps in near-real time allows winegrowers to focus the management decisions in certain areas of the vineyard, i.e. those most affected by drought, which would result in a significant saving in terms of time and material used.

Increasing the number of variables, and considering a greater number of environmental forcing effects on vine growth, would lead to an improvement of the model (eq. 16) for estimating the final grape production quantity. Andreoli *et al*. (2019) implemented a model, called Italian Vineyard Integrated Numerical model for Estimating physiological values (IVINE), in which vine development processes are estimated, such as the leaf area index (LAI), phenological phases and the berry sugar content. Their model was applied to some vineyards located in southern Piedmont. The inclusion of the IVINE variables in the model described by eq. 16 could strengthen its predictive capacity.

In addition to the optimisation of grapevine management strategies, increased knowledge of the tolerance of different grapevine varieties to variations in meteorological conditions, can contribute to better decision-making about which grapevine and rootstock varieties to choose under different meteorological and soil conditions. Van Leeuwen and Destrac-Irivne (2017) outline the economic importance of selecting the best plant material for the prevailing agronomic conditions, as well as for ensuring optimal grape quality. This is particularly relevant for drought conditions. The drought-tolerance of both rootstock and vines is important to consider. Efforts are already being taken to enhance understanding of the resistance of different rootstock varieties to drought, e.g. the *GreffAdapt* project in France (van Leeuwen and Destrac-Irvine, 2017), and the combinations of cultivars which can enhance the climate resilience of wine-growing regions (Morales-Casilla *et al*., 2019). Such efforts can be extended in an interdisciplinary fashion, incorporating remote sensing, meteorological and agronomic research, to improve the decision-making capacity of winemakers and support the climate resilience of the industry. The

economic value of the vines must also be considered in order to support vineyard adaptation to climate change, e.g. yield reduction is a water deficit management strategy recommended by van Leeuwen and Destrac-Irvine (2017), but is only practical for grape varieties or vineyards with high value, e.g. Nebbiolo. Additionally, interaction of vine management strategies and meteorological conditions can result in further production challenges for vineyards, e.g. increased salinity in vineyards in Australia and Argentina due to irrigation under low winter rainfall conditions (van Leeuwen and Destrac-Irvine, 2017). The utility of water to meet competing social, economic and environmental demands must also be balanced, and consequently some drought management strategies such as irrigation may not be possible, e.g. in California, Australia and South Africa (Hannah *et al*., 2013)

6.5. Conclusions

Grape productivity was examined in relation to environmental variables by estimating the gross primary production (GPP) of grapes in the most important vineyards of Piedmont for the years 2016 to 2018, and determined its variation in time and space using meteorological data and remote sensing techniques. The effect of water shortages in 2017 on the productivity of the Barbera, Moscato Bianco and Nebbiolo grape varieties was also analysed, providing spatially and temporally explicit information about the negative impact of the 2017 drought on vineyard GPP. This study used a combination of meteorological, satellite, and regional data about grape production, to cross-validate GPP estimates. The results highlighted the importance of using different data sources and the reliability of using remote sensing techniques, combined with weather data, to evaluate and manage agricultural crop productivity GPP. This can support the preparation of farmers, agricultural advisory services, and regional and national policymakers and decision-makers regarding climate change, and adds to decision support capacity on the implementation of wine growing best practices, particularly in relation to water resource management.

In this study we contributed to the capacity to predict grapevine productivity through the development and testing of remote sensing techniques to monitor grape development, and the evaluation of drought impacts on grape productivity using meteorological and remotely sensed indices as in the model described by eq. 16. The study identified limitations in knowledge required to enable accurate prediction of grapevine

productivity under changing climate conditions. This includes insufficient knowledge about the relationship between crop phenology and the remotely-sensing indices of EVI and NDMI. We suggest that future research to support decision-making capacity in the wine production sector should focus on addressing this knowledge gap, in order to enable near-real-time decision support systems and timely implementation of appropriate climate change adaptation strategies on different scales.

Finally, the results described above clearly apply to the Piedmontese wine region, but also have implications for many of the world's winegrowing regions. The challenge of drought management, and monitoring drought conditions in the wine sector is particularly acute in regions where water stress also impacts drinking water availability. Considering the results of this paper, it is evident that winemakers must evaluate the environmental and economic factors which will influence the productivity of their vines in order to be prepared for the expected changes in climate. Clearly, there is a great need for interdisciplinary decision-making support and appropriate vine management in such situations, and the contribution to be made through improved application of remote sensing techniques is large.

CHAPTER 7: DISCUSSION AND CONCLUSIONS

This study focused on drought, a challenging phenomenon ecologically, socially, and economically. The specific focus of the study was on agricultural drought, and the development of novel information sources and improvement of existing instruments to provide support for the management and detection of agricultural drought, in the context of climate change. The goal of this study was thus to enhance the quality of decision-making support services available for farmers, e.g. winemakers, agricultural technicians and advisory services, and policymakers. The study aimed to analyse the effects of drought and water supply in four different climatic conditions, represented by four distinct regions, combining meteorological data and satellite imagery using remote-sensing techniques.

Not all of the regions examined experience drought conditions as a major challenge to the agricultural sector, but they were selected to enhance the validity and robustness of the techniques applied in this study and the subsequent results. In two regions, Piedmont (Italy) and Ireland, representing the Continental Temperate climate and Temperate Oceanic climate respectively, the study focused in detail on the analysis of agricultural drought, and decision-making support. In two further regions, Sardinia (Italy) and New Brunswick (Canada), representing the Mediterranean climate and Humid Continental climate respectively, the study assessed the application of the tools used to examine agricultural drought conditions, in the context of other water supply challenges, including hydrological drought (Sardinia) and flood risk (New Brunswick). Chapter 4 has described in detail the comparison of findings from the application of drought indices in Piedmont and Sardinia.

The main objectives of this study were to *i*) identify the spatial and temporal distribution of major drought episodes (length and severity) in three different climatic conditions: Continental Temperate, Mediterranean and Temperate Oceanic; *ii*) evaluate the effects of water shortage and drought on the productivity of the most important crop cultivated in Ireland, grass pasture; *iii*) evaluate the effects of drought in the most important vineyards of Piedmont (north-western Italy), and the consequences of water shortage on vineyard production in the three main grape varieties: Barbera, Moscato Bianco and Nebbiolo; and iv) contribute to the development of a near-real-time decision support service to support

winemakers in the management of vineyards. This final chapter provides a discussion of the findings of the research undertaken in this study, final conclusions, and suggestions for future research.

7.1. Discussion of methods, findings, and limitations

The research undertaken in this study described the development of methods for combining data sources to evaluate meteorological events, particularly precipitation events, and tools to evaluate the impacts of these events on agriculture and the environment. The research also described the application of these methods and tools in four different regions, representing four climate zones, and the findings of those studies have been described in chapters 4-6 and Appendix 1. Furthermore, the study identified some limitations associated with the methods and tools implemented in the study, and the findings regarding the studies of the four regions, which have implications for future research and implementation of meteorological and satellite data for decision-making support in agriculture. These aspects of the study are described in greater detail below.

7.1.1. Combining meteorological and satellite data to support decision-making

Chapter 1 underlined the relevance of monitoring and analysing the impacts of drought, and the challenges faced in predicting agricultural drought at relevant spatial and temporal scales. This study endorsed the value of agricultural drought indices that utilise both meteorological data, and by the long-term continuous data provided by satellite remote-sensing observations. The combination of these different data sources with phenological and agronomic knowledge can strengthen the capacity to identify drought conditions, monitor their effects, and appropriately inform management decisions undertaken by farmers. The strength of this interdisciplinary and evolving approach for evaluating and monitoring drought is best illustrated by the studies described in Chapters 5 and 6. For example, the application of indices that make use of satellite data enabled a comprehensive evaluation of the drought situation in 2018 in Ireland (Ch. 5), and 2017 in Piedmont (Ch. 6), which was strengthened by cross-

validation with meteorological data, but could not have been achieved with meteorological data alone.

7.1.2. Strengthening tools for monitoring and analysing drought effects

As described in section 7.1.1, the combination of meteorological and satellite data can strengthen the validity of analysis of meteorological events, and the conclusions which can be drawn from such analysis. This capacity contributes to more relevant information for decision-makers who rely on accurate analysis of meteorological and climatic conditions. The reliability of the tools which made use of this data was also considered in this study, and as a result, two climate zones with divergent characteristics, Mediterranean and Humid Continental, were chosen for the application of the R software *ClimPACT2* package, in addition to the Continental Temperate zone represented by Piedmont. The Mediterranean climate, represented by Sardinia, is dry and hot in the summer with a mild and relatively rainy winter, which is considered a climate change "hot-spot" with high vulnerability. The Humid Continental climate, represented by New Brunswick, is subject to warm to hot summers, and cold winters, with rainfall evenly distributed throughout the year. The Continental Temperate climate meanwhile experiences mild temperatures with cold winters and hot summers, and a bimodal rainfall distribution in Piedmont. Using the *ClimPACT2* package to evaluate precipitation trends and significant precipitation events (i.e. drought and flooding) in these three different climate zones contributed to greater understanding of the applicability of this analysis tool in disparate circumstances. For example, the study described in Chapter 4 found that the two drought indices, SPI and SPEI, were correlated with classical meteorological indices such as the number of hot days and hot nights in the year. Additionally, the application of *ClimPACT2* in New Brunswick (Appendix 1) confirmed that the climate projections regarding precipitation events had good accuracy in a high precipitation region with less vulnerability to climate change and extreme events than the Mediterranean region.

The study also sought to involve stakeholder organisations and local and regional decision-makers where possible, in order to enhance the relevance of the analyses undertaken and findings communicated for the regions under study. The value of this approach for the appropriate selection of analytical tools to evaluate climate change impacts, including

precipitation impacts, was evident in the New Brunswick study, which involved the largest network of stakeholders, with input during the planning, analysis, and communication phases of the study. This input increased the applicability of the findings for the local region, and in this way strengthened the knowledge of the *ClimPACT2* package and its analytical capacity and limitations for research including applied and participatory research.

7.1.3. Impact of drought on agriculture characterised by local variation

This study focused on water deficit events and their impact on agriculture in two regions, Ireland and Piedmont, and regarding two different crops, grass pasture (Ireland) and grapevines (Piedmont). While the regions represent two different climate zones and the crops and cultivation practices are different, both regions are characterised by geomorphological heterogeneity, which interacts with climatic conditions and cultivation practices to produce variation in crop productivity.

In both studies, significant, severe drought episodes affecting the whole region under study were examined. In Ireland this episode took place in 2018, and this episode was the focus of the study described in Chapter 5. In Piedmont, a severe drought occurred in 2017, and the preceding year and subsequent year were also studied to provide comparison points for the evaluation of the impact of this drought on wine making.

The drought analyses in both regions highlighted the need for meteorological analysis on micro-, meso-, and macro-scales in order to accurately identify the incidence of drought at a local and regional level, and analyse the impacts for the crop under consideration at different spatial scales. This is of particular relevance in geomorphologically diverse regions, such as those studied. For example, in Ireland in 2018, the analysis of drought found that while the drought occurred on a regional scale, the impacts depended on soil type and drainage capacity, resulting in local variation in drought effects and the management responses required by farmers and regional managers. Consideration of the scales at which drought effects are experienced are not only relevant for geomorphological variation, or spatial scales, however. The temporal scale on which drought occurs is also relevant for evaluating the severity of drought impacts, and

assessing the effects on different crops, crop varieties, and cultivation regimes, as well as geomorphological conditions.

In Piedmont in 2017, the grape varieties Barbera, Moscato Bianco and Nebbiolo all experienced reduced productivity on account of severe, prolonged drought. The drought experienced in some areas where Nebbiolo is cultivated (northern Piedmont) was shorter in duration, and therefore less severe, than in the other areas studied, and the effects of drought on Nebbiolo production in this region (NEB-2, Chapter 6) were therefore less. In addition, visual assessment of the GPP index for all varieties during four different phenological phases indicates that in areas experiencing similar drought conditions, one variety, Moscato Bianco (MOB) was more affected by the severe, prolonged drought than the other two studied. This last result highlights the sensitivity of different crop varieties to drought, and the relevance of the spatial and temporal scale at which drought manifests for accurate evaluation of drought impacts on agriculture. These findings align with the literature concerning drought effects on different crop types, and crop varieties, including in the wine making industry (van Leeuwen and Destrac-Irvine, 2017; Morales-Casilla *et al*., 2019).

Both studies highlighted the relevance of drought analysis using multiple data sources such as meteorological data, satellite data, and crop production data, and relevant climate analysis tools such as *ClimPACT2* package, to evaluate the spatial and temporal variation in water availability in the context of changing climate. This can support the preparation of farmers, agricultural advisory services, and regional and national policymakers and decision-makers for climate change.

7.1.4. Limitations

This research aimed to combine different forms of data relevant to the analysis of drought, i.e. meteorological data, satellite data, and crop production data; and to further develop drought analysis methodologies by studying four different climate zones, in order to strengthen the validity and reliability of the findings, and the relevance for agricultural and water resource decision-makers. The analyses undertaken in this study were nonetheless limited by inherent characteristics of the data and methodology used. These limitations are described below.

Different data types and sources were used, each with their own strengths and limitations. Meteorological data was sourced from weather station networks in the regions under study, satellite data was collected from three satellites: MODIS-Terra, Landsat 8 and Sentinel-2, while crop production data was collected from regional agricultural authorities (Agricultural and Livestock Production Sector of the Piedmont Region, Agriculture Directorate).

Meteorological networks are inherently limited by the fact that they can only provide information about the area immediately surrounding the weather stations in the network. Thus, in any network, gaps will exist between the weather stations for which meteorological conditions must be estimated. A network with more stations (dense) will have less gaps, and more reliable data than one with less stations (dispersed). The meteorological networks of the four regions studied (Piedmont, Sardinia, Ireland, and New Brunswick), differed in the density of their meteorological data. The networks of Piedmont, Sardinia, and Ireland were more dense, and therefore comprehensive, than that of New Brunswick. Variation in data quality and quantity also existed within the networks. The meteorological stations within the network can be limited by technical issues, which can cause the meteorological station to stop collecting data, resulting in information gaps. The continuity of the database therefore depends on regular maintenance of the meteorological stations, and statistical reconstruction of the missing data, e.g. by Quality Control Analysis (Chapters 3 and 4 and Appendix 1). These limitations affected the validity of the analysis for some regions, e.g. New Brunswick, more than others, but the analysis of all four regions, and use of reliable statistical methods for data reconstruction, e.g. Quality Control Analysis, reduced the impact of these limitations on the external validity of the study.

The satellite data contributed to the management of limitations associated with the use of meteorological data, and one of the main contributions of this study was the combined use of satellite data and meteorological data to evaluate and analyse drought, minimising the weaknesses of both data types. Satellite data has an advantage over meteorological data in that it covers a wide spatial range. However, the individual data files for each tile are large, and require resources in terms of time to acquire the data from data sources such as NASA and ESA, and space to store the data. The wide spatial range covered by each tile also requires additional labour resources compared to meteorological data, in terms of selection of the specific areas

being studied on the tile. In the study of agricultural activity, this additional labour demand will vary depending on the agricultural activity under study, e.g. crop type, and how the cultivation is organised, e.g. as multiple, dispersed fields of grapevines owned by a single vineyard as in Piedmont, or substantial connected areas of grass pasture as in Ireland. These resource demands limited the extent of analysis applied to the regions and crops studied. A final limitation of this data was the presence of cloud cover, which renders analysis of the meteorological conditions and agricultural productivity unfeasible. Cloud cover was more frequent in Ireland than in Piedmont. Nonetheless, the incorporation of data from meteorological networks in both regions facilitated robust analysis even when cloudy days prevented inclusion of some satellite images.

The data about agricultural productivity collected from regional authorities was useful for the evaluation of drought impacts on grapevine productivity. This data was cross-validated with productivity indices, such as GPP, calculated from the satellite imagery. In some cases, the productivity data from the regional authorities and that of the satellite imagery did not match, e.g. in the analysis of grape vine productivity in Piedmont (Chapter 6). This issue indicates weakness in the dataset used, when applied to the monitoring of individual vineyards. It is not clear if this weakness is a result of human error in data calculation or entry, or a mis-match in the areas included for each vineyard in the regional authority dataset and the satellite data analysis. However, the cross-validation of these two data types, and inclusion of remotely-sensed and classical meteorological indices, has minimised the impact of this limitation on the validity of the analysis undertaken.

The data collected was used in the calculation of remotely sensed and classical meteorological indices, including with the climate prediction R-project software package, *ClimPACT2*, in order to identify and monitor drought events, and evaluate the agricultural impact of drought. The *ClimPACT2* was of great value for the study, with robust results as demonstrated in Chapter 4 and Appendix 1 by the application of this package in three very different climate zones, Continental Temperate, Mediterranean, and Humid Continental, regarding extremes of water deficit and water surplus (i.e. drought and flooding). However, this software also demanded substantial time resources, as it required manual entry of data for each meteorological station in each meteorological network. The repercussions of this resource demand resulted in less available time for further analysis of the conditions within and between

each region. The use of this software could be substantially improved by automation of the data entry procedure, i.e. by changing the software code to be more user-friendly.

The research found a good correlation between remotely-sensed, such as EVI and NDMI, and meteorological indices, such as SPI and SPEI. The knowledge contributed by this study about the relationship between EVI, NDMI, SPI, and SPEI has strengthened the evidence supporting drought monitoring and evaluation of effects, such as described in this study. However, EVI and NDMI are also strongly linked with the behaviour of the plants under study, in addition to meteorological conditions. As a consequence, it is challenging to predict these indices, and in this study they were used for the purpose of monitoring drought effects, but not predicting drought effects. Further knowledge about the relationship between these indices and plant phenology would enhance the predictive capacity of additional indices used to measure drought impacts, e.g. GPP, and enable better decision-making support in the agricultural and water management context. Improvement in the accuracy of GPP calculations can also enhance the capacity to evaluate regional impacts of cultivation practices on agricultural productivity over time and inform best-practices in aspects of agricultural management beyond water management, e.g. nutrient cycling (Dold *et al*., 2019).

7.2. Conclusions

This study combined meteorological data and satellite imagery to provide a robust analysis of the effects of variation in water supply, including drought, in four different climate zones. Combining these different data sources strengthened the reliability of the findings, and the validity of the analysis was further enhanced by the application of similar analytical techniques, using similar data sources, in the four different case study regions which represented the climate zones. By contributing to knowledge about methods of combining meteorological, satellite, and agricultural production data, and generating reliable and relevant information about the effects of water supply in the agricultural context, this study has contributed to the quality of decision-making support services for farmers, agricultural technicians and advisory services, and policy-makers, concerning the management of agricultural drought, particularly in the context of wine production. The study had four primary

objectives, and the conclusions regarding each of those objectives are described below.

7.2.1. The spatial and temporal distribution of major drought episodes in Continental Temperate, Mediterranean, and Temperate Oceanic climates

In order to contribute to greater knowledge about the identification of spatial and temporal distribution, i.e. length and severity, of major drought episodes, two main studies were undertaken involving three climate zones, Continental Temperate, Mediterranean and Temperate Oceanic, represented by Piedmont, Sardinia, and Ireland regions respectively. The first was a trend analysis of hydrological drought in Piedmont and Sardinia, described in greater detail in Chapter 4. Indices evaluated included the SPI and SPEI, which were calculated using meteorological data from regional meteorological networks. The study found that the average duration of the wet period was longer in Piedmont region, while the duration of dry periods was almost the same in both regions. The analysis highlighted limitations in the methods used, e.g. use of Thornthwaite equation for the calculation of SPEI, which could be overcome by using alternative estimation techniques such as Hargreaves.

The second study (Chapter 5) addressing this objective involved an analysis of a severe drought episode in Ireland, that took place in the summer of 2018. In this analysis, meteorological data from regional meteorological networks and satellite imagery from the MODIS-Terra satellite were combined, and the data were used to calculate four drought indicators: SPI, PNI, SMD, and EVI. These indicators provided valuable insights into the evolution of the drought, and the SMD index proved particularly useful, demonstrating that the 2018 drought episode was the most severe since 1981. SPI and PNI identified that the driest months were May, June and July. These indices also indicated spatial heterogeneity in the impact of drought, even while the drought occurred at a national scale. The use of satellite imagery in combination with meteorological data in this study enhanced the capacity to identify and evaluate spatial variation of drought, compared with the use of meteorological data alone in the hydrological drought trend analysis in Piedmont and Sardinia.

7.2.2. The effects of water shortage and drought on the productivity of grass pasture in Ireland

In order to evaluate the effects of water deficit and drought on agriculture in Ireland, one crop was examined, grass pasture, which accounts for 92% of the farmed area of Ireland (Central Statistics Office, 2018). This evaluation took place as part of the study of the drought episode in 2018 (Chapter 5), described in point 7.2.1 above, and used the same data and analytical methods. As described above, the SPI and PNI highlighted spatial heterogeneity in the impact of drought, including in grass pasture. The variation in the drought impact measured by SPI and PNI was associated with variation in soil type, accounting for regional differences, and driven by soil drainage capacity, accounting for local variation. These impacts were borne out in recorded productivity, e.g. eastern regions of Ireland reported reduced productivity, while the uplands of the west produced more biomass, as indicated by the EVI index.

This study underlined the contribution of drought monitoring using different sources of information to effective planning for water resource management and agricultural planning, e.g. assessing the impacts on pasture and the need to supplement livestock with other fodder sources.

7.2.3. The effects of drought in vineyards in Piedmont and consequences of water shortage on production of Barbera Moscato Bianco and Nebbiolo grape varieties

The study of agricultural drought was applied to a second crop of high value, wine production, in the region of Piedmont (Chapter 6). The study evaluated the effects of drought in some of the most important vineyards in Piedmont, and the impacts of drought on production of three main grape varieties, Barbera, Moscato Bianco, and Nebbiolo, in the years 2016-2018. This study also combined meteorological data from the regional network with satellite data (Landsat 8 and Sentinel-2), in order to calculate indices for the evaluation of drought duration and impact on water availability and crop performance. In addition, the study used regional grape production data, to contribute to the evaluation of drought impacts on crop productivity. GPP was calculated using a combination of all of these data sources, providing a comprehensive index of drought impacts on grape vine productivity for each vineyard and each grape variety. The results of the analysis showed that the vineyards were strongly affected by drought

in 2017, but the crops recovered very well in 2018 to achieve or surpass the "normal" productivity levels observed in 2016. While this study displayed the strength of combined data sources, particularly when used collectively in a comprehensive index such as GPP, the study also identified some knowledge gaps related to GPP, which can be addressed in future research to enhance drought management capacity, e.g. the relationship between crop phenology and the EVI and NDMI indices that are utilised in the calculation of GPP.

7.2.4. Data collection and technology development for near-real-time decision support services for winemakers

The analysis of hydrological drought in the Piedmont and Sardinia regions in Chapter 4 highlighted the impact of changing climatic conditions on weather and extreme weather events, e.g. drought. Future climate projections indicate that droughts will increase in many regions over the course of this century. For many individuals and organisations with a role to play in the management of water, but particularly for farmers, near-real-time maps of drought evolution and projected impacts could result in more efficient and effective management decisions. The results of Chapters 4, 5 and 6 highlighted the value of remote sensing techniques, combined with weather data, for the evaluation of drought and its effects, particularly in relation to agriculture. In Chapter 6 this approach enabled a comprehensive evaluation of the gross primary production of grape vines, according to climatic conditions. The analysis procedure described in Chapter 6, particularly the evaluation using GPP, constitutes a method that could be applied to different geographical situations to predict vegetative activity and productivity for many agricultural crops. This method can be translated as a near-real-time service, that could be easily updated each year with new data observations. Such a service can add to the decision support services available to farmers, such as winemakers, who must cope with, and adapt to, changing climate conditions and extreme events.

However, the study identified some knowledge gaps which limit the capacity to accurately predict agricultural productivity in the context of climate change. As described in section 7.2.3 above, this includes information about crop phenological stages, and their relationship with the indices examined, particularly the remotely sensed indices EVI and NDMI. In order to facilitate better decision support systems for the

agricultural sector, and adoption of scale-appropriate climate change adaptation strategies, it is necessary to address these knowledge gaps.

7.3. Recommendations

The results presented in this study provided data and technological tools to advance the capacity to detect, monitor, and respond to drought conditions in the context of changing climatic conditions. The greatest contribution of this study was to the development of monitoring and analysis tools. Based on the findings of this study, it is recommended that future research focuses on drought response measures that can enhance the resilience of agricultural production to extreme and unexpected drought events, which are predicted to increase in many climate regions in future climate change projections. Additionally, research to develop drought response measures should consider measures that enable farmers such as wine growers to rapidly respond to acute drought situations, to prevent severe production impacts, which can be particularly useful when improved drought detection techniques are employed such as those developed in this study. Following the recommendations of Shukla *et al*. (2019) these response measures should be integrated, in order to achieve resilient agricultural systems that can tolerate other effects of climate change, e.g. other unexpected weather events such as heavy rainfall. Such measures include strategic production decisions such as crop diversification, adoption of drought-tolerant crops, reduced tillage, and maintenance of vegetation and mulch cover, and measures that can enable more rapid response, such as improved irrigation techniques (e.g. drip irrigation) and moisture conservation methods (e.g. rainwater harvesting) (Shukla *et al*., 2019).

Moreover, valuable novel technologies and analysis techniques have been developed around the wine supply chain. The digital platforms technologies analyzes the vineyard in its whole complexity by using advanced instrumentation, that include new, low-cost and extensive sensor networks. The interconnection of these objects enables advanced services, allowing the creation of an intelligent and complete ecosystem, where such objects collect different types of data from the environment in which they are inserted. The analysis of this data allows the generation of knowledge about those environments, comparison between historical data, and, consequently, better resource utilization. In particular, the sensors transport data to a cloud-based service to manage a wide range of Internet

of Things (IoT) applications, that is defined as a network that connects things, or intelligent objects, to the internet. As many other sectors, the wine industry is investigating the potential of the IoT for collection and processing of sensor data from a vineyard environment in order to give more accurate information to the wine producers. The sensors are designed to measure a variety of environmental factors, including air humidity, temperature, soil humidity and solar intensity, and to monitor micro-climate in vineyards. All the data collected within the vineyard can also be combined with the expertise of the winemakers to significantly improve the quality of the grapes, and so the final wine product. This new application, called Internet of Grapes, provides real-time access to the vineyard conditions, allowing the wine makers to plan the allocation of resources and specify the precise necessary actions in advance, e.g. to predict the optimum time for harvest, increasing the yield and minimizing risk to the grapes; to define the optimal time and location for fertilization and use of fungicides, and to minimize negative environmental impacts. Furthermore, in the climate change condition, early intervention can limit drought impact and provide information in assessing compensation claims for losses from insurance bodies or government.

The research undertaken in this thesis has highlighted the need for greater knowledge about drought management measures such as those listed above, e.g. optimal crop diversification strategies within the wine industry and drought tolerance of crops and crop varieties under extreme climate conditions.

The findings of this research described the occurrence and impact of unexpected weather events, e.g. drought in Ireland in 2018 (Chapter 5) and drought in Piedmont in 2017 (Chapter 6), in addition to the worsening of climatic conditions in climate-sensitive and vulnerable regions, e.g. the Alpine region in Piedmont and the Mediterranean region of which Sardinia is a part (Chapter 4). The severity of the climate change risk for agriculture and the environment, on a local, regional and global scale, is clear in the findings of these studies. This research indicates that future research and regional and national policy decisions should continue to address the mitigation of greenhouse gas emissions from agriculture, and other sectors, in order to manage the severity of climate change risk. In addition, the research highlights the relevance of incorporating climate monitoring at appropriate spatial and temporal scales with climate change adaptation measures in agriculture, in order to ensure adequate preparation by regions and farmers for chronic and acute weather events that impact agricultural

productivity, and the characteristics of which are expected to change over time as the global climate changes.

REFERENCES

Acquaotta F., Baronetti A., Bentivenga M., Fratianni S., Piccarreta M., 2019. Estimation of rainfall erosivity in Piedmont (North West Italy) by using 10-minute fixed-interval rainfall. *Időjárás*, 123(1), DOI:10.28974/idojaras.2019.1

Acquaotta F., Fratianni S., 2014. The importance of the quality and reliability of the historical time series for the study of climate change. *Revista Brasileira de Climatologia*, 14: 20-38, ISSN: 1980-055X.

Acquaotta F., Fratianni S., Venema V., 2016. Assessment of parallel precipitation measurements networks in Piedmont, Italy. *Int. J. Climatol.*, 36: 3963-3974.

Agnew C., Anderson W., 1992. Water in the arid realm. *Routledge*, London.

Agovino M., Casaccia M., Ciommi M., Ferrara M., Marchesano K., 2019. Agriculture, climate change and sustainability: The case of EU-28. *Ecol. Indic.*, 105: 525-543. doi.org/10.1016/j.ecolind.2018.04.064

Alexander L., Herold N., 2016. *ClimPACT2* Indices and software. User manual available online.

Alikadic A., Pertot I., Eccel E., Dolci C., Zarbo C., Caffarra A., De Filippi R., Furlanello C., 2019. The impact of climate change on grapevine phenology and the influence of altitude: A regional study. *Agric For Meteorol.*, 271: 73-82.

Allen R.G., Pereira L.S., Raes D., Smith M., 1998. Crop evapotranspiration. Guidelines for computing crop water requirements. FAO irrigation and drainage paper, 56: 227.

Anderson M.C., Zolin C.A., Sentelhas P.C., Hain C.R., Semmens K., Yilmaz M.T., Gao F., Otkin J.A., Tetrault R., 2016. The Evaporative Stress Index as an indicator of agricultural drought in Brazil: An assessment based on crop yield impacts. *Remote Sens. Environ.*, 174:82-99. https://doi.org/10.1016/j.rse.2015.11.034

Andreoli V., Cassardo C., La Iacona T., Spanna F., 2019. Description and Preliminary Simulations with the Italian Vineyard Integrated Numerical Model for Estimating Physiological Values (IVINE). *Agronomy*, 9: 94. doi:10.3390/agronomy9020094

Ault T.R., Cole J.E., Overpeck J.T., Pederson G.T., Meko D.M., 2014. Assessing the risk of persistent drought using climate model simulations and paleoclimate data. *J. of Climate*, 27(20): 7529-7549.

Bandini A., 1931. Tipi pluviometrici dominanti sulle regioni italiane. Tech. report, Roma: Ministero dei Lavori Pubblici.

Barker L.J., Hannaford J., Chiverton A., Svensson C., 2016. From meteorological to hydrological drought using standardised indicators. *Hydrol. Earth Syst. Sci*., 20: 2483-2505. doi.org/10.5194/hess-20-2483-2016

Baronetti A., Acquaotta F., Fratianni S. 2018. Rainfall variability from a dense rain gauge network in north-western Italy. *Clim. Res*., 75(3): 201-213. doi: 10.3354/cr01517

Baronetti A., González-Hidalgo J.C., Vicente-Serrano S.M., Acquaotta F., Fratianni S., 2020. A weekly spatio-temporal distribution of drought events over the Po Plain (North Italy) in the last five decades. *Int. J. Climatol*., 1-14. doi: 10.1002/joc.6467

Barredo J.I., Mauri A., Caudullo G., Dosio A., 2019. Assessing shifts of Mediterranean and arid climates under RCP4.5 and RCP8.5 Climate Projections in Europe. In: Vilibic I., Horvath K., Palau J. (eds) Meteorology and Climatology of the Mediterranean and Black Seas. Pageoph Topical Volumes. Birkhäuser, Cham.

Beguería S., Serrano-Notivoli R., Tomas-Burguera M., 2018. Computation of rainfall erosivity from daily precipitation amounts. *Sci. Total Environ.,* 637: 359-373.

Beguería S., Vicente-Serrano S.M., 2017. SPEI: Calculation of the Standardised Precipitation-Evapotranspiration Index, R package version 1.7.

Beguería S., Vicente-Serrano S.M., Reig F., Latorre B., 2014. Standardized precipitation evapotranspiration index (SPEI) revisited: parameter fitting, evapotranspiration models, tools, datasets and drought monitoring. *Int. J. Climatol*., 34 (10): 3001-3023.

Belfiore N., Vinti R., Lovat L., Chitarra W., Tomasi D., de Bei R., Meggio F., Gaiotti F., 2019. Infrared Thermography to Estimate Vine Water Status: Optimizing Canopy Measurements and Thermal Indices for the Varieties Merlot and Moscato in Northern Italy. *Agronomy*, 9(12): 821. doi.org/10.3390/agronomy9120821.

Betts R.A., Alfieri L., Bradshaw C., Caesar J., Feyen L., Friedlingstein P., Gohar L., Koutroulis A., Lewis K., Morfopoulos C., Papadimitriou L., Richardson K.J., Tsanis I., Wyser K., 2018. Changes in climate extremes, fresh water availability and vulnerability to food insecurity projected at 1.5 °C and 2 °C global warming with a higher-resolution global climate model. *Phil. Trans. R. Soc. A*., 376, p. 20160452, 10.1098/RSTA.2016.0452.

Bevan S.L., Los S.O., North P.R.J., 2014. Response of vegetation to the 2003 European drought was mitigated by height. *Biogeosciences*, 11(11): 2897-2908.

Biancotti A., 2003. Physical geography's contribution to studying terroir. In: Spaces, environments and landscape of terroirs. Ed. BEM sas, pp. 166.

Bindi M., Olesen J.E. 2011. The responses of agriculture in Europe to climate change. *Reg. Environ. Change*, 11 (Suppl 1):S151-S158.

Bo M., Mercalli L., Pognant F., Cat Berro D., Clerico M, 2019. Urban air pollution, climate change and wildfires: The case study of an extended forest fire episode in northern Italy favoured by drought and warm weather conditions. *6th Int. Conf. on Energy and Environ. Res*., ICEER, 22-25 July, University of Aveiro, Portugal. doi.org/10.1016/j.egyr.2019.11.002

Bock A., Sparks T., Estrella N., Menzel A., 2011. Changes in the phenology and composition of wine from Franconia, Germany. *Res*. 50: 69–81.

Bordi I., Fraedrich K., Sutera A., 2009. Observed drought and wetness trends in Europe: an update. *Hydrol. Earth Syst. Sci*., 13: 1519-1530.

Borgogno-Mondino E., Novello V., Lessio A., Tarricone L., de Palma L., 2018. Intra-vineyard variability description through satellite derived spectral indices as related to soil and vine water status. *Acta Hortic*., 1197: 59-67. doi 10.17660/ActaHortic.2018.1197.8

Breiman L., 2001. Random Forests. Machine Learning, 45, 5-32. doi:10.1023/A:1010933404324

Bucchignani E., Montesarchio M., Zollo A.L., Mercogliano P., 2016. High-resolution climate simulations with COSMO-CLM over Italy: performance evaluation and climate projections for the 21st century. *Int. J. Climatol*., 36: 735-756.

Caffarra A., Eccel E., 2011. Projecting the impacts of climate change on the phenology of grapevine in a mountain area. *Aust. J. Grape Wine Res*., 17: 52-61. doi.org/10.1111/j.1755-0238.2010.00118.x

Capra A., Scicolone B., 2012. Spatiotemporal variability of drought on a short-medium timescale in the Calabria region (Southern Italy). *Theor. Appl. Climatol*., 116: 371-384.

Carey V.A., Archer E., Barbeau G., Saayman D., 2008. Viticultural terroirs in Stellenbosch, South Africa. II. The interaction of Cabernet-Sauvignon and Sauvignon blanc with environment. *J. Int. Sci. Vigne Vin*., 42(4): 185-201.

Central Statistics Office, 2018. Farm Structure Survey 2016. Cork.

Chang L., Peng-Sen S., Shi-Rong L., 2016. A review of plant spectral reflectance response to water physiological changes. *Chinese J. Plant Ecology*, 40(1): 80-91.

Changnon S.A., Kunkel K.E., Reinke B.C., 1996. Impacts and responses to the 1995 heat wave: a call to action. *Bull. Am. Meteorol. Soc.*, 77: 1497-1506.

Cheval S., Busuioc A., Dumitrescu A., Birsan M.V., 2014. Spatiotemporal variability of meteorological drought in Romania using the standardized precipitation index (SPI). *Climate Research*, 60(3): 235-248.

Ciais P., Reichstein M., Viovy N., Granier A., Ogée J., Allard V., Aubinet M., Buchmann N., Bernhofer C., Carrara A., Chevallier F., De Noblet N., Friend A.D., Friedlingstein P., Grünwald T., Heinesch B., Keronen P., Knohl A., Krinner G., Loustau D., Manca G., Matteucci G., Miglietta F., Ourcival J.M., Papale D., Pilegaard K., Rambal S., Seufert G., Soussana J.F., Sanz M.J., Schulze E.D., Vesala T., Valentini R., 2005. Europe-wide reduction in primary productivity caused by the heat and drought in 2003. Nature, 437 (2005), pp. 529-533, 10.1038/nature03972

Cola G., Mariani L., Salinari F., Civardi S., Bernizzoni F., Gatti M., Poni S., 2014. Description and testing of a weather-based model for predicting phenology, canopy development and source-sink balance in Vitis vinifera L. cv. Barbera. *Agric. For. Meteorol*., 184: 117-136.

Coll J.R., Aguilar E., Ashcroft L., 2017. Drought variability and change across the Iberian Peninsula. *Theor. Appl. Climatol*., 130: 901-916. DOI 10.1007/s00704-016-1926-3.

Collins M., Knutti R., Arblaster J., Dufresne J.L., Fichefet T., Friedlingstein P., Gao X., Gutowski W.J., Johns T., Krinner G., Shongwe M., Tebaldi C., Weaver A.J., Wehner M., 2013. Long-term Climate Change: Projections, Commitments and Irreversibility. In: Climate Change 2013: The Physical Science Basis. Contribution of Working Group I to the Fifth Assessment Report of the Intergovernmental Panel on Climate Change [Stocker T.F., Qin D., Plattner G.-K., Tignor M., Allen S.K., Boschung J., Nauels A., Xia Y., Bex V., Midgley P.M. (eds.)]. Cambridge University Press, Cambridge, United Kingdom and New York, NY, USA.

Congedo L., 2018. Semi-Automatic Classification Plugin Documentation. Release 6.0.1.1. DOI: 10.13140/RG.2.2.29474.02242/1.

Cook E.R., Seager R., Cane M.A., Stahle D.W., 2007. North American drought: Reconstructions, causes, and consequences. *Earth-Sci. Reviews*, 81(1-2): 93-134. doi.org/10.1016/j.earscirev.2006.12.002

Costa J.M., Vaz M., Escalona J., Egipto R., Lopes C., Medrano H., Chaves M.M., 2016. Modern viticulture in southern Europe: Vulnerabilities and strategies for adaptation to water scarcity. *Agricultural Water Management*. 164: 5-18. DOI: 10.1016/j.agwat.2015.08.021

Dai A., 2011. Drought under global warming: a review. *Climate Change*, 2(1): 45-65.

Dai A., Zhao T., 2017. Uncertainties in historical changes and future projections of drought. Part I: estimates of historical drought changes. *Climatic Change*, 144: 519. https://doi.org/10.1007/s10584-016-1705-2

Dai M., Huang S., Huang Q., Leng G., Guo Y., Wang L., Fang W., Li P., Zheng X., 2020. Assessing agricultural drought risk and its dynamic evolution characteristics. *Agr. Water Manage*., 231. doi.org/10.1016/j.agwat.2020.106003.

Dalla Marta A., Grifoni D., Mancini M., Storchi P., Zipoli G., Orlandini S., 2010. Analysis of the relationships between climate variability and grapevine phenology in the Nobile di Montepulciano wine production area. J. *Agric. Sci*., 148: 657-666.

Danelichen V.H.M., Biudes M., Velasque M.C.S., Machado N.G., Gomes R.S.R., Vourlitis G.L., Nogueira J.S., 2015. Estimating of gross primary production in an Amazon-Cerrado transitional forest using MODIS and Landsat imagery. *Anais da Academia Brasileira de Ciências*, 87(3): 1545-1564.

De Martonne E., 1926. Aréisme et indice aridité. *Comptes Rendus de L'Acad. Sci., Paris*, 182: 1395-1398.

de Oliveira A.F., Nieddu G., 2016. Accumulation and partitioning of anthocyanins in two red grape cultivars under natural and reduced UV solar radiation. *Aust. J. Grape Wine Res*., 22(1): 96-104. DOI: 10.1111/ajgw.12174

Delgado R.C., Pereira M.G., Teodoro P.E., dos Santos G.L., de Carvalho D.C., Magistrali I.C., Vilanova R.S., 2018. Seasonality of gross primary production in the Atlantic Forest of Brazil. *Glob. Ecol. Conserv*., 14: e00392.

Deo R.C., Byun H.R., Adamowski J.F., Begum K., 2017. Application of effective drought index for quantification of meteorological drought events: a case study in Australia. *Theor Appl Climatol*, 128: 359-379. doi:10.1007/s00704-015-1706-5

Dettinger M., Cayan D.R., 2014. Drought and the California Delta - a matter of extremes. *San Francisco Estuary and Watershed Sci*., 12(2).

Dillon E., Donnellan T., Hanrahan K., Houlihan T., Kinsella A., Loughrey J., McKeon M., Moran B., Thorne F., 2018. Outlook 2019 Economic Prospects for Agriculture. Athenry.

Dold C., Hatfield J.L., Prueger J.H., Moorman T.B., Sauer T.J.,Cosh M.H., Drewry D.T., Wacha K.W., 2019. Upscaling Gross Primary Production in corn-soybean rotation systems in the Midwest. *Remote Sens*., 11: 1688. doi:10.3390/rs11141688

Drumond A., Gimeno L., Nieto R., Trigo R.M., Vicente-Serrano S.M., 2017. Drought episodes in the climatological sinks of the Mediterranean moisture source: The role of moisture transport. *Global and Planetary Change*, 151: 4-14.

Duffie J.A., Beckman W.A. 1991. Solar Engineering of Thermal Processes. *Wiley*, Hoboken.

EC, 2017. Communication from the Commission to the European Parliament, the Council, the European Economic and Social Committee and the Committee of the Regions. The Future of Food and Farming (COM(2017) 713 final).

EEA, 2017. Climate change, impacts and vulnerability in Europe 2016 - An indicator ‐based report, EEA Report No 1/2017, European Environment Agency https://www.eea.europa.eu/publications/climate-change-impacts-and-vulnerability-2016

European Space Agency (ESA). SENTINEL-2 User Handbook; ESA: Paris, France, 2015; pp. 1–64.

Falzoi S., Acquaotta F., Pulina M.A., Fratianni S. 2019b. Hydrological drought analysis in Continental Temperate and Mediterranean environment during the period 1981-2017. *Italian J. Agrometeorol*., 3: 13-23. doi: 10.13128/ijam-798

Falzoi S., Gleeson E., Lambkin K., Zimmermann J., Marwaha R., O'Hara R., Green S., Fratianni S. 2019a. Analysis of the severe drought in Ireland in 2018. *Weather*, 74(11): 368-373. doi: 10.1002/wea.3587

FAO, 2018. The impact of disasters and crises on agriculture and food security. Retrieved from: http://www.fao.org/3/I8656EN/i8656en.pdf.

Fischer E.M., Seneviratne S.I., Lüthi D., Schär C., 2007. Contribution of land-atmosphere coupling to recent European summer heat waves. *Geophys. Res. Lett*., 34: L06707.

Fortin G., Acquaotta F., Fratianni S., 2016. The evolution of temperature extremes in the Gaspé Peninsula, Quebec, Canada (1974–2013). *Theor. Appl. Climatol*., 1-10.

Fraga H., De Cortazar Atauri I.G., Malheiro A.C., Santos J.A., 2016. Modelling climate change impacts on viticultural yield, phenology and stress conditions in Europe. *Glob. Chang. Biol*., 22: 3774-3788.

Fratianni S., Acquaotta F., 2017. The climate of Italy. In Landscapes and Landforms of Italy. *World Geomorphological Landscapes*, 29-38. doi: 10.1007/978-3-319-26194-2_4.

Fratianni S., Terzago S., Acquaotta F., Faletto M., Garzena D., Prola M.C., Barbero S., 2015. How Snow and its Physical Properties Change in a Changing Climate Alpine Context? *Eng. Geol. Soc. Territ*., 1, 57-60.

Fregoni M., 2003. L'indice bioclimatico di qualità Fregoni. Terroir Zonazione Viticoltura. *Phytoline*.

Gao B.C. 1996. NDWI : A normalized difference water index for remote sensing of vegetation liquid water from space. *Remote Sens. Environ*., 58: 257-266.

García-Estévez I., Quijada-Morín N., Rivas-Gonzalo J.C., Martínez-Fernández J., Sánchez N., Herrero-Jiménez C.M., Escribano-Bailón M.T., 2017. Relationship between hyperspectral indices, agronomic parameters and phenolic composition of Vitis vinifera cv Tempranillo grapes. *J. Sci. Food Agric*., 97(12): 4066-4074.

García-Herrera R., Díaz J., Trigo R.M., Luterbacher J., Fischer E.M., 2010. A review of the European summer heat wave of 2003. *Crit. Rev. Environ. Sci. Technol.*, 40: 267-306. 10.1080/10643380802238137

Gerber N., Mirzabaev A., 2017. Benefits of action and costs of inaction: Drought mitigation and preparedness – a literature review (No. 1). WMO, Geneva, Switzerland and GWP, Stockholm, Sweden.

Giaccone E., Colombo N., Acquaotta F., Paro L., Fratianni S., 2015. Climate variations in a high altitude Alpine basin and their effects on a glacial environment (Italian Western Alps). *Atmosfera*, 28: 117-128, ISSN: 0187-6236.

Giordano D., Provenzano S., Ferrandino A., Vitali M., Pagliarani C., Roman F., Cardinale F., Castellarin S.D., Schubert A., 2016. Characterization of a multifunctional caffeoyl-CoA O-methyltransferase activated in grape berries upon drought stress. *Plant Physiol. Biochem.*, 101: 23-32. doi.org/10.1016/j.plaphy.2016.01.015

Gladstones J.S., 2011. Wine, terroir and climate change. *Wakefield Press*, Kent Town, South Australia, 2011.

Gomarasca M.A:, 2004. Elementi di Geomatica. Ed. Associazione Italiana di Telerilevamento, 618 pp.

Gómez-Miguel V., 2011. Terroir. In: Böhm J., editor. Atlas das Castas da Península Ibérica: História, Terroir, Ampelografia. Lisboa, Portugal: Dinalivro; 2011, 104-153.

González-Hidalgo J.C., Vicente-Serrano S.M., Peña-Angulo D., Salinas C., Tomas-Burguera M., Beguería S., 2018. High-resolution spatio-temporal analysis of drought episodes in the western Mediterranean basin (Spanish mainland, Iberian Peninsula). *Acta Geophysica*, 1-12.

Grayson M., 2013. Agriculture and drought. *Nature*, 501(S1). https://doi.org/10.1038/501S1a

Grillakis M.G., Koutroulis A.G., Tsanis I.K., 2016.The 2 °C global warming effect on summer European tourism through different indices. *Int. J. Biometeorol.*, 60: 1205-1215. 10.1007/s00484-015-1115-6.

Gu Y., Brown J.F., Verdin J.P., Wardlow B. 2007. A five-year analysis of MODIS NDVI and NDWI for grassland drought assessment over the central Great Plains of the United States. *Geophys Res. Lett.*, 34, L06407.

Guidoni S., Ferrandino A., Novello V., 2008. Effects of seasonal and agronomical practices on skin anthocyanin profile of Nebbiolo grapes. *Am. J. Enol. Vitic.*, 59:1, 22-29.

Hannaford J., Lloyd-Hughes B., Keef C., Parry S., Prudhomme C., 2011. Examining the large-scale spatial coherence of European drought using regional indicators of precipitation and streamflow deficit. *Hydrol Process*, 25: 1146-1162.

Hannah L., Roehrdanz P.R., Ikegami M., Shepard A.V., Shaw M.R., Tabor G., ZHI L., Marquet P.A., Hijmans R.J., 2013. Climate change, wine, and conservation. *Proc. Natl. Acad. Sci. USA*, 110: 6907-6912.

Hargreaves G.H., Samani Z.A. 1985. Reference crop evapotranspiration from temperature. *Appl. Eng. Agric*., 1(2): 96-99.

Hisdal H., Tallaksen L.M., 2000. Drought Event Definition. Technical Report to the ARIDE project No. 6. Assessment of the Regional Impact of Droughts in Europe, pp.41.

Hlavinka P., Trnka M., Semerádová D., Dubrovsky M., Žalud Z., Možný M., 2009. Effect of drought on yield variability of key crops in Czech Republic. *Agr. Forest Meteo.*, 149: 431-442. https://doi.org/10.1023/A:1020355407821, 2009.

Huete A. R., 1988. A soil-adjusted vegetation index (SAVI). *Remote Sens. Environ.*, 25(3): 295-309.

Huete A.R., Liu H.Q., Batchily K., van Leeuwen W. 1997. A comparison of vegetation indices over a global set of TM images for EOS-MODIS. *Remote Sens. Environ*., 59: 440-451.

Huglin P., 1978. Nouveau mode d'évaluation des possibilités héliothermiques d'un milieu viticole. In: Proceedings of the Symposium International sur l'écologie de la Vigne. Ministère de l'Agriculture et de l'Industrie Alimentaire, Contança, pp. 89-98.

Ionita M., Tallaksen L.M., Kingston D.G., Stagge J.H., Laaha G., Van Lanen H.A.J., Scholz P., Chelcea S.M., Haslinger K., 2017. The European 2015 drought from climatological perspective. *Hydrol. Earth. Syst. Sci*., 21: 1397-1419.

IPCC, 2012. Summary for policy-makers, in Managing the Risks of Extreme Events and Disasters to Advance Climate Change Adaptation. A Special Report of Working Groups I and II of the Intergovernmental Panel on Climate Change, edited by Field et al., 1-19, Cambridge Univ. Press, Cambridge, U.K.

Jaramillo F., Destouni G., 2015. Local flow regulation and irrigation raise global human water consumption and footprint. *Science*, 350: 1248-1251.

Jones G.V., White M.A., Cooper O.R., Storchmann K., 2005. Climate change and global wine quality. *Clim. Change*, 73: 319-343. doi.org/10.1007/s10584- 005-4704-2

Jordan C. F., 1969. Derivation of leaf-area index from quality of light on the forest floor. *Ecology*, 50(4): 663-666.

Jørgensen S.E., Kamp-Nielsen L., Christensen T., Windolf-Nielsen J., Westergaard, B. (1986). Validation of a prognosis based upon an eutrophication model. *Ecol. Model*., 32: 165-182. doi:10.1016/0304-3800(86)90024-4

Kendon M., Marsh T., Parry S., 2013. The 2010-2012 drought in England and Wales. *Weather*, 68(4): 88-95.

Köppen W. 1918. Klassification der Klimate nach Temperatur, Niederschlag and Jahreslauf. *Petermanns Geographische Mitteilungen*, 64: 193-203, 243-248.

Kotsias G., Lolis C.J., Hatzianastassiou N., Levizzani V., Bartzokas A., 2020. On the connection between large-scale atmospheric circulation and winter GPCP precipitation over the Mediterranean region for the period 1980-2017. *Atmos. Res*., 233: 104714. doi.org/10.1016/j.atmosres.2019.104714

Koutroulis A.G., Papadimitriou L.V., Grillakis M.G., Tsanis I.K., Wyser K., Betts R.A., 2018. Freshwater vulnerability under high end climate change. a pan-European assessment. *Sci. Total Environ*., 613-614(1): 271-286. 10.1016/j.scitotenv.2017.09.074

Ledderhof D., Brown R., Reynolds A., Jollineau M., 2016. Using remote sensing to understand Pinot noir vineyard variability in Ontario. *Can. J. Plant Sci*., 96(1): 89-108.

Lefebvre G., Redmond L., Germain c., Palazzi E., Terzago S., Willm L., Poulin B., 2019. Predicting the vulnerability of seasonally-flooded wetlands to climate change across the Mediterranean Basin. *Sci. Total Environ*., 692: 546-555. doi.org/10.1016/j.scitotenv.2019.07.263.

Lena M., Tallaksen L.M., Stagge J.H., Stahl K., Gudmundsson L., Orth R., Seneviratne S.I., Van Loon A.F., Van Lanen H.A.J., 2015. Characteristics and drivers of drought in Europe; a summary of the DROUGHT-R&SPI project. Drought: Research and Science-Policy Interfacing – Andreu et al. (Eds) Taylor & Francis Group, London, ISBN 978-1-138-02779-4

Liaw A., Wiener M., 2002. Classification and Regression by randomForest. *R News* 2(3): 18-22.

Liu X., Zhu X., Pan Y., Li S., Liu Y., Ma Y., 2016. Agricultural drought monitoring: progress, challenges and prospects. *J. Geogr. Sci*., 26: 750-767.

Loague K., Green R.E., 1991. Statistical and graphical methods for evaluating solute transport models: overview and application. *J. Contam. Hydrol*., 7: 51-73. doi:10.1016/0169-7722(91)90038-3

Lorenz R., Davin E.L., Seneviratne S.I., 2012. Modeling land-climate coupling in Europe: Impact of land surface representation on climate variability and extremes. *J. Geophys. Res.*, 117. doi:10.1029/2012JD017755

Loucks D.P., Gladwell J.S., 1999. Sustainability Criteria for Water Resource Systems, Cambridge: Cambridge University Press.

Lu E., Luo Y., Zhang R., Wu Q., Liu L., 2011. Regional atmospheric anomalies responsible for the 2009-2010 severe drought in China. *J. Geophys. Res*., 116(D2114).

Lu Z., Zhao Y., Wei Y., Feng Q., Xie J., 2019. Differences among Evapotranspiration Products Affect Water Resources and Ecosystem Management in an Australian Catchment. *Remote Sens*., 11: 958.

Lulli L., Costantini E. A. C., Mirabella A., Gigliotti A., Buccelli P., 1989. Influenza del suolo sulla qualità della Vernaccia di S. Giminiano. *Vignevini*, 2: 53-62.

Madugundu R., Al-Gaadi K.A., Tola E., Kayad A.G., Jha C.S., 2017. Estimation of gross primary production of irrigated maize using Landsat-8 imagery and Eddy Covariance data. Saudi *J. of Biol. Sci*., 24(2): 410-420. doi.org/10.1016/j.sjbs.2016.10.003.

Magno R., Angeli L., Chiesi M., Pasqui M., 2014. Prototype of a drought monitoring and forecasting system for the Tuscany region. *Adv. Sci. Res*., 11: 7-10. doi:10.5194/asr-11-7-2014

Maliva R., Missimer T. 2012. Aridity and Drought. In: Arid Lands Water Evaluation and Management. Environmental Science and Engineering (Environmental Engineering). Springer, Berlin, Heidelberg. doi: 10.1007/978-3-642-29104-3_2

Mariani L., Alilla R., Cola G., Dal Monte G., Epifani C., Puppi G., Failla O. 2013. IPHEN - a real-time network for phenological monitoring and modelling in Italy. *Int. J. Biometeorol*., 57: 881-893.

Martínez A., Gomez-Miguel V., 2017. Vegetation index cartography as a methodology complement to the terroir zoning for its use in precision viticulture. *OENO One*. 51(3): 289. doi: 10.20870/oeno-one.2017.51.4.1589

Maselli F., Moriondo M., Chiesi M., Chirici G., Puletti N., Barbati A., Corona P., 2009. Evaluating the Effects of Environmental Changes on the Gross Primary Production of Italian Forests. *Remote Sens*., 1: 1108-1124. doi:10.3390/rs1041108

Masih I., Maskey S., Mussá F.E.F., Trambauer P., 2014. A review of droughts on the African continent: A geospatial and long-term perspective. *Hydrol. Earth Syst*. Sci., 18: 3635-3649.

McKee T.B., Doesken N.J., Kleist J., 1993. The relationship of drought frequency and duration to time scales. *Am. Meteorol. Soc.*, 8th Conference on Applied Climatology, 17-22 Janvier, Anaheim, 179-184.

Mestre O., Domonkos P., Picard F., Auer I., Robin S., Lebarbier E., Böhm R., Aguilar E., Guijarro J., Vertacnik G., Klancar M., Dubuisson B., Stepanek P., 2013. HOMER: a homogenization software – methods and applications. *Időjárás*, 117(1): 1-158.

Mestre O., Gruber C., Prieur C., Caussinus H., Jourdain S., 2011. SPLIDHOM: A method for homogenization of daily temperature observations. *J. Appl. Meteorol. Climatol*., 50, 2343-2358. doi: 10.1175/2011JAMC2641.1

Met Éireann Major Weather Events "Storm Emma", March 2019, 2019. https://www.met.ie/cms/assets/uploads/2019/02/EmmaReport2019.pdf

Met Éireann Past Weather Statement, February 2018. 2018a. https://www.met.ie/climate/past-weather-statements

Met Éireann Past Weather Statement, March 2018. 2018b. https://www.met.ie/climate/past-weather-statements

Meza I., Siebert S., Doll P., Kusche J., Herbert C., Eyshi Rezaei E., Nouri H., Gerdener H., Popat E., Frischen J., Naumann G., Vogt J.V., Walz Y., Sebesvari Z., Hagenlocher M., 2019. Global-scale drought risk assessment for agricultural systems. *Nat. Hazards Earth Syst. Sci*., 2019: 1-26. doi:10.5194/nhess-2019-255

Minetti J.L., Vargas W.M., Poblete A.G., de la Zerda L.R., Acuña, L.R., 2010. Regional droughts in southern South America. *Theor. Appl. Climatol*., 102(3-4): 403-415.

Mo K.C., 2011. Drought onset and recovery over the United States. *J. Geophys. Res*., 116(D20106). doi:10.1029/2011JD016168.

Morales-Castilla I., de Cortázar-Atauri I.G., Cook B.I., Lacombe T., Parker A., van Leeuwen C., Nicholas K.A., Wolkovich E.M., 2020. Diversity buffers winegrowing regions from climate change losses. *Proceedings of the National Academy of Sciences*, 117(6): 2864-2869. doi: 10.1073/pnas.1906731117

Moss R.H., Edmonds J.A., Hibbard K.A., Manning M.R., Rose S.K., van Vuuren D.P., Carter T.R., Emori S., Kainuma M., Kram T., Meehl G.A., Mitchell J.F.B., Nakicenovic N., Riahi K., Smith S.J., Stouffer R.J., Thomson A.M., Weyant J.P., Wilbanks T.J., 2010. The next generation of scenarios for climate change research and assessment. *Nature*, 463: 747-756.

Mukherjee S., Mishra A., Trenberth K.E., 2018. Climate Change and Drought: a Perspective on Drought Indices. *Curr Clim Change Rep.,* 4: 145. doi.org/10.1007/s40641-018-0098-x

Murphy C., Broderick C., Burt T.P., Curley M., Duffy C., Hall J., Harrigan S., Matthews T.K.R., Macdonald N., McCarthy G., McCarthy M.P., Mullan D., Noone S., Osborn T.J., Ryan C., Sweeney J., Thorne P.W., Walsh S., Wilby R.L., 2018. A 305-year continuous monthly rainfall series for the island of Ireland (1711-2016). *Clim. Past*., 14: 413-440.

Nairn J.R., Fawcett R.G., 2013. Defining heatwaves: heatwave defined as a heat-impact event servicing all community and business sectors in Australia (Centre for Australian Weather and Climate Research), *CAWCR Technical Report* No. 060.

Nash J.E., Sutcliffe J.V., 1970. River flow forecasting through conceptual models part I. A discussion of principles. *J. Hydrol*., 10: 282–290.

Nastos P.T., Politi N., Kapsomenakis J., 2013. Spatial and temporal variability of the aridity index in Greece. *Atmos. Res*., 119: 140-152.

Nigrelli G., Fratianni S., Zampollo A., Turconi L., Chiarle M., 2018. The altitudinal temperature lapse rates applied to high elevation rockfalls studies in the Western European Alps. *Theor. Appl. Climatol*., 131(3-4): 1479-1491.

Nolan P., 2015. Ensemble of regional climate model projections for Ireland. *Environ. Protection Agency*. No 159. ISBN: 978-1-84095-609-2.

Noone S., Broderick C., Duffy C., Matthews T., Wilby R.L., Murphy C., 2017. A 250-year drought catalogue for the Island of Ireland (1765-2015). *Int. J. Climatol*. 37(S1): 239-254.

Nuarsa I.W., As-syakur A.R., Gunadi I.G.A., Sukewijaya I.M., 2018. Changes in Gross Primary Production (GPP) over the Past Two Decades Due to Land Use Conversion in a Tourism City. ISPRS *Int. J. Geo-Inf*., 7: 57.

O'Donoghue, C., Hennessy, T., 2015. Policy and Economic Change in the Agri-Food Sector in Ireland. *Econ. Soc. Rev*. (Irel). 46: 23.

OIV, 2010. Definition of terroir. http://www.oiv.int/public/medias/400/viti-2012-1-en.pdf. Accessed September 6, 2017.

Oliver M.A., Webster R., 1990. Kriging: a method of interpolation for geographical information systems. *Int. J. Geogr. Inf. Sci.*, 4.3: 313-332.

Organization of Vine and Wine, 2010. Definición de terroir. *Vitivinícola*.

Palmer W.C., 1965. Meteorological drought. US Research Paper No. 45. US Department of Commerce Weather Bureau, Washington DC.

Panont C.A., Comolli G., 1998. La zonazione della Franciacorta: il modello viticolo della docg. *Int. Symp. Acts* "Territorio e vino", Siena 19th-24th May: 321-340.

Páscoa P., Gouveia C.M., Russo A., Trigo R.M., 2017. The role of drought on wheat yield interannual variability in the Iberian Peninsula from 1929 to 2012. *Int. J. Biometeorol*., 61(3): 439-451. doi: 10.1007/s00484-016-1224-x, 2017.

Park W.A., Allen C.D., Macalady A.K., Griffin D., Woodhouse C.A., Meko D.M., Swetnam T.W., Rauscher S.A., Seager R., Grissino-Mayer H.D., Dean J.S., Cook E.R., Gangodagamage C., Cai M., McDowell N.G., 2013. Temperature as a potent driver of regional forest drought stress and tree mortality. *Nature Climate Change*. 3: 292-297.

Parry S., Marsh T., Kendon M., 2013. 2012: from drought to floods in England and Wales. *Weather*. 68(10): 268-274.

Pashiardis S., Michaelides S., 2008. Implementation of the Standardized Precipitation Index (SPI) and the Reconnaissance Drought Index (RDI) for Regional Drought Assessment: A case study for Cyprus. *European Water*, 23/24: 57-65.

Pau S., Detto M., Kim Y., Still C.J., 2018. Tropical forest temperature thresholds for gross primary productivity. *Ecosphere*, 9(7): e02311. 10.1002/ecs2.2311

Pausas J.G., Millán M.M., 2019. Greening and Browning in a Climate Change Hotspot: The Mediterranean Basin. *BioScience*, 69(2): 143-151. doi.org/10.1093/biosci/biy157

Pereira L.S., Oweis T., Zairi A., 2002. Irrigation management under water scarcity. *Agric. Water Manag*., 57(3): 175-206. doi.org/10.1016/S0378-3774(02)00075-6.

Perini L., Salvati L., Zitti M., Bajocco S., 2011. A proposal for a meteorological index of climate change impact. *Italian J. Agrometeorol*., 1: 17-24.

Portmann F.T., Siebert S., Döll P., 2010. MIRCA2000-global monthly irrigated and rainfed crop areas around the year 2000: a new high-resolution data set for agricultural and hydrological modeling. *Glob. Biogeochem. Cycles*, 24(1). 10.1029/2008GB003435

Pulina M.A., 2012. Sécheresses et déficience hydrique des sol dans des zones agricoles de la Sardaigne durant la période 1951-2010. *Actes du colloque*, XXVème AIC, Septembre, Grenoble.

Pulina M.A., 2015. Extreme temperatures in Sardinia during the period 1951-2012. Geomorphology for Society, *5th AIGEO National Conference*, September, Cagliari.

R Core Team. 2018. R: A language and environment for statistical computing. R Foundation for Statistical Computing, Vienna, Austria.

Rana G., Muschitiello C., Ferrara R.M., 2016. Analysis of a precipitation time series at monthly scale recorded in Molfetta (south Italy) in the XVIII century (1784-1803) and comparisons with present pluviometric regime. *Italian J. Agrometeorol*, 3: 23-30.

Renza D., Martinez E., Arquero A., Sanchez J. 2010. Drought estimation maps by means of multidate Landsat fused images. In *30th EARSeL Symposium*: Remote Sens. Sci., Education, and Natural and Cultural Heritage, vol. 30.

Rey-Caramés C., Diago M.P., Martín M.P., Lobo A., Tardaguila J., 2015. Using RPAS Multi-Spectral Imagery to Characterise Vigour, Leaf Development, Yield Components and Berry Composition Variability within a Vineyard. *Remote Sens*., 7: 14458-14481. doi.org/10.3390/rs71114458.

Ronchi C., Rabuffetti D., Salandin A., Vargiu A., Barbero S., Pelosini R., 2007. Development of the Piedmont Region Hydrological Bulletin as a Support to Water Resources Monitoring and Management. In: Rossi G., Vega T., Bonaccorso B. (eds) Methods and Tools for Drought Analysis and Management. Water Science and Technology Library, vol 62.

Ross T. , Lott N., 2003. A Climatology of 1980-2003 Extreme Weather and Climate Events. *Technical Report* 2003-01. Asheville, NC : U.S. Department of Commerce NOAA/NESDIS, National Climatic Data Center.

Rouse J.W., Haas R.H., Schell J.A., Deering D.W., 1974. Monitoring vegetation systems in the Great Plains with ERTS. *Third ERTS Symp*., NASA SP-351 1: 309-317.

Ruimy A., Dedieu G., Saugier B. 1996. TURC: A diagnostic model of continental gross primary productivity and net primary productivity. *Glob. Biogeochem. Cycles*, 10: 269-285.

Schubert S.D., Stewart R.E., Wang H., Barlow M., Berbery E.H., Cai W., Hoerling M.P., Kanikicharla K.K., Koster R.D., Lyon B., Mariotti A., Mechoso C.R., Müller O.V., Rodriguez-Fonseca B., Seager R., Seneviratne S.I., Zhang L., Zhou T., 2016. Global meteorological drought: A synthesis of current understanding with a focus on sst drivers of precipitation deficits. *J. Clim*., 29: 3989-4019.

Schulte R.P.O., Diamond J., Finkele K., Holden N.M., Brereton A.J., 2005. Predicting the Soil Moisture Conditions of Irish Grasslands. *Irish J. Agr. Res.,* 44: 95-110.

Schwalm C.R., Anderegg W.R.L., Michalak A.M., Fisher J.B., Biondi F., Koch G., Litvak M., Ogle K., Shaw J.D., Wolf A., Huntzinger D.N., Schaefer K., Cook R., Wei Y., Fang Y., Hayes D., Huang M., Jain A., Tian H., 2017. Global patterns of drought recovery. *Nature*, 548: 202-205. doi:10.1038/nature23021

Scienza A., Bogoni M., Valenti L., Brancadoro L., Romano F.A., 1990. La conoscenza dei rapporti tra vitigno ed ambiente quale strumento programmatorio in viticoltura: stima della vocazionalità viticola dell'Oltrepò Pavese. *Vignevini*, suppl. n. 12: 4-62.

Seguin G., 1986. Terroirs and pedology of vinegrowing. *Experientia*, 42: 861-873.

Sheffield J., Wood E.F., 2008. Projected changes in drought occurrence under future global warming from multi-model, multi-scenario, IPCC AR4 simulations. *Clim Dyn*., 31: 79-105.

Shukla P.R., Skea J., Slade R., van Diemen R., Haughey E., Malley J., Pathak M., Portugal Pereira J. (eds.) Technical Summary, 2019. In: Climate Change and Land: an IPCC special report on climate change, desertification, land degradation, sustainable land management, food security, and greenhouse gas fluxes in terrestrial ecosystems [P.R. Shukla, J. Skea, E. Calvo Buendia, V. Masson-Delmotte, H.-O. Pörtner, D. C. Roberts, P. Zhai, R. Slade, S. Connors, R. van Diemen, M. Ferrat, E. Haughey, S. Luz, S. Neogi, M. Pathak, J. Petzold, J. Portugal Pereira, P. Vyas, E. Huntley, K. Kissick, M, Belkacemi, J. Malley, (eds.)]. In press.

Smith P., Bustamante M., Ahammad H., Clark H., Dong H., Elsiddig E.A., Haberl H., Harper R., House J., Jafari M., Masera O., Mbow C., Ravindranath N.H., Rice C.W., Robledo Abad C., Romanovskaya A., Sperling F., Tubiello F., 2014. Agriculture, Forestry and Other Land Use (AFOLU). In: Climate Change 2014: Mitigation of Climate Change. Contribution of Working Group III to the Fifth Assessment Report of the Intergovernmental Panel on Climate Change [Edenhofer, O., R. Pichs-Madruga, Y. Sokona, E. Farahani, S. Kadner, K. Seyboth, A. Adler, I. Baum, S. Brunner, P. Eickemeier, B. Kriemann, J. Savolainen, S. Schlömer, C. von Stechow, T. Zwickel and J.C. Minx (eds.)]. Cambridge University Press, Cambridge, United Kingdom and New York, NY, USA.

Smit H.J., Metzger M.J., Ewert F., 2018. Spatial distribution of grassland productivity and land use in Europe. *Agr. Syst*., 98: 208-219, doi:10.1016/j.agsy.2008.07.004, 2008

Spinoni J., Naumann G., Carrao H., Barbosa P., Vogt J., 2014. World drought frequency, duration, and severity for 1951-2010. *Int. J. Climatol*., 34: 2792-2804. 10.1002/joc.3875

Sun L., Gao F., Anderson M.C., Kustas W.P., Alsina M.M., Sanchez L., Sams B., McKee L., Dulaney W., White W.A., Alfieri J.G., Prueger J.H., Melton F., Post K., 2017. Daily Mapping of 30 m LAI and NDVI for Grape Yield Prediction in California Vineyards. *Remote Sens*., 9: 317. doi:10.3390/rs9040317

Tadesse T., Wilhite D.A., Harms S.K., Hayes M.J., Goddard S., 2004. Drought Monitoring Using Data Mining Techniques: A Case Study for Nebraska, USA. *Natural Hazards*, 33: 137-159. https://doi.org/10.1023/B:NHAZ.0000035020.76733.0b

Teuling A.J., 2018. A hot future for European droughts. Nature Clim Change 8: 364-365. https://doi.org/10.1038/s41558-018-0154-5

Thornthwaite C.W., 1948. An approach toward a rational classification of climate. *Geogr. Rev*., 38: 55-94.

Trenberth K.E., Dai A., Rasmussen R.M., Parsons D.B., 2003. The Changing Character of Precipitation. The National Center for Atmospheric Research, Boulder, Colorado. doi: 10.1175/BAMS-84-9-1205

Ubalde J.M., Sor X., Zayas A., Poch R.M., 2010. Effects of soil and climatic conditions on grape ripening and wine quality of Cabernet Sauvignon. *J. Wine Research*. 21: 1-17

van Leeuwen C., 1998. Effects of water and nitrogen uptake, and soil temperature, on vine development. Berry ripening and wine quality of Cabernet Sauvignon, Cabernet Franc and Merlot (Saint Emilion, 1997). *Int. Symp. Acts* "Territorio e vino", Siena 19th-24th May: 221-233.

van Leeuwen C., Destrac-Irvine A., 2017. Modified grape composition under climate change conditions requires adaptations in the vineyard. *OENO One*, 51(2): 147-154. doi.org/10.20870/oeno-one.2017.51.2.1647

van Leeuwen C., Friant P., Xavier C., Tregoat O., Koundouras S., Dubourdieu D., 2004. Influence of climate, soil, and cultivar on terroir. *Am. J. Enol. Vitic*., 55: 207-217.

van Leeuwen C., Roby J.P., de Resseguier L., 2018. Soil-related terroir factors: A review. *OENO One*. 52(2): 173-188. doi: 10.20870/oeno-one.2018.52.2.2208

Van Loon A.F., 2015. Hydrological drought explained. *WIREs Water*, 2(4): 359-392.

Van Loon A.F., Gleeson T., Clark J., Van Dijk A.I.J.M., Stahl K., Hannaford J., Di Baldassarre G., Teuling A.J., Tallaksen L.M., Uijlenhoet R., Hannah D.M., Sheffield J., Svoboda M., Verbeiren B., Wagener T., Rangecroft S., Wanders N., Van Lanen H.A.J., 2016. Drought in the Anthropocene. *Nature Geoscience*, 9: 89-91. doi: 10.1038/ngeo2646

Vicente-Serrano S.M., Beguería S., López-Moreno J.I., 2010. A multi-scalar drought index sensitive to global warming: The Standardized Precipitation Evapotranspiration Index-SPEI. *J. Clim*., 23: 1696-1718.

Vigasio M., Montaldo G., Tornato D., 2018. L'annata vitivinicola in Piemonte. Il clima, la maturazione delle uve, gli aspetti economici e produttivi e le tendenze di sviluppo 2018. *Anteprima vendemmia*, 1-64.

Viste E., Korecha D., Sorteberg A., 2012. Recent drought and precipitation tendencies in Ethiopia. *Theor. Appl. Climatol*., 112: 535-551.

Vogt J.V., Safriel U., Von Maltitz G., Sokona Y., Zougmore R., Bastin G., Hill J. 2011. Monitoring and assessment of land degradation and desertification: Towards new conceptual and integrated approaches. *Land Degradation & Development*, 22(2): 150-165. doi.org/10.1002/ldr.1075

Wang J.Y., 1960. A critique of the heat unit approach to plant response studies. *Ecology*, 41: 785-790.

Werick W.J., Willeke G.E., Guttman N.B., Hosking J.R.M., Wallis J.R., 1994. National drought atlas developed. *Eos, Transactions American Geophysical Union*. 75(8): 89-90.

West H., Quinn N., Horswell M., White P., 2018. Assessing vegetation response to soil moisture fluctuation under extreme drought using Sentinel-2. *Water*, 10: 838.

Wilby R.L., Noone S., Murphy C., Matthews T., Harrigan S., Broderick C., 2016. An evaluation of persistent meteorological drought using a homogeneous Island of Ireland precipitation network. *Int. J. Climatol*. 36: 2854-2865.

Wilhite D.A, Glantz M.H., 1985. Understanding: the Drought Phenomenon: The Role of Definitions. *Water Int*., 10(3): 111-120 doi.org/10.1080/02508068508686328

Wilhite D.A., 2000. Drought as a Natural Hazard: Concepts and Definit ions. in Drought: A Global Assessment, vol. I, edited by Donald A. Wilhite, chap. 1, pp. 3-18.

Wilhite D.A., Pulwarty R.S., 2017. Drought and Water Crises, Integrating Science, Management, and Policy (Second). Boca Raton, Florida: CRC Press. https://doi.org/10.1201/b22009

Wilhite D.A., Sivakumar M.V.K., Pulwarty R., 2014. Managing drought risk in a changing climate: The role of national drought policy. *Weather and Climate Extremes*, 3:B14 4-13. https://doi.org/10.1016/J.WACE.2014.01.002

Wilson E.H., Sader S.A. 2002. Detection of forest harvest type using multiple dates of Landsat TM imagery. *Remote Sens. Environ*., 80: 385-396.

Winkler A.J., 1962. General Viticulture. University of California, Berkeley, pp. 633

Winkler K., Gessner U.,Hochschild V., 2017. Identifying Droughts Affecting Agriculture in Africa Based on Remote Sensing Time Series between 2000–2016: Rainfall Anomalies and Vegetation Condition in the Context of ENSO. *Remote Sens*., 9: 831. doi:10.3390/rs9080831

World Meteorological Organization, 2006. Drought monitoring and early worming: concepts, progress and future challenges. N° 1006.

World Meteorological Organization, 2012. Standardized Precipitation Index User Guide. N° 1090

World Meteorological Organization, 2015. Guidelines on the definition and monitoring of extreme weather and climate events.

World Meteorological Organization, 2017. Guidelines on the calculation of climate normals. N° 1203.

Xiao X., Jin C., Dong J., 2014. Gross Primary Production of Terrestrial Vegetation. In: Hanes J. (eds) Biophysical Applications of Satellite Remote Sensing. Springer Remote Sensing/Photogrammetry. Springer, Berlin, Heidelberg.

Xiao X., Yan H., Kalfas J., Zhang Q., 2011. Satellite-based modeling of Gross Primary Production of terrestrial ecosystems. In: Wang QH (ed.) Advances in environmental remote sensing: sensors, algorithms, and application. Taylor & Francis Group, Boca Raton, 367-397.

Xiao X., Zhang Q., Hollinger D., Aber J., Moore B., 2004. Modelling seasonal dynamics of gross primary production of an evergreen needleleaf forest using MODIS images and climate data. *Ecol. Appl*., 15, 954-969.

Xue J, Su B. 2017. Significant Remote Sensing Vegetation Indices: A Review of Developments and Applications. *J. Sensors*, 2017(ID 1353691): 17. doi:10.1155/2017/1353691.

Zandalinas S.I., Mittler R., Balfagón D., Arbona V., Gómez-Cadenas A., 2018. Plant adaptations to the combination of drought and high temperatures. *Physiol Plantarum*, 162: 2-12. doi:10.1111/ppl.12540

Zarco-Tejada P.J., Guillén-Climent M.L., Hernández-Clemente R., Catalina A., González M.R., Martín P., 2013. Estimating leaf carotenoid content in vineyards using high resolution hyperspectral imagery acquired from an unmanned aerial vehicle (UAV). *Agric. For. Meteorol*., 171-172: 281-294. doi.org/10.1016/j.agrformet.2012.12.013

Zhang P., Barlow S., Krstic M., Herderich M., Fuentes S., Howell K., 2015. Within-vineyard, within-vine, and within-bunch variability of the rotundone concentration in berries of Vitis vinifera L. cv. Shiraz. *J. Agric. Food Chem.*, 63(17): 4276-4283. DOI: 10.1021/acs.jafc.5b00590

Ziolkowska J.R., 2016. Socio-economic implications of drought in the agricultural sector and the state economy. *Economies*, 4-19.

Zsófi Z., Tóth E., Rusjan D., Bálo B., 2011. Terroir aspects of grape quality in a cool climate wine region: relationship between water deficit, vegetative growth and berry sugar concentration. *Scientia Horticulturae*, 127: 494-499.

CHAPTER 8: APPENDICES: Supplementary data

8.1. Appendix 1. Adaptation plan: New Brunswick

A case study of an adaptation plan to climate change is presented. The study was conducted in the Cocagne watershed in the south eastern cost of New Brunswick in Canada, in order to analyse the recent climate variability and trends, to identify the various climatic risks at the watershed scale and mapping the most vulnerable areas.

8.1.1. Adaptation plan to climate change in the Cocagne watershed, New Brunswick

Drought and flood are becoming not only increasingly common, but more intense and less predictable. To deal with these extreme climatic events effectively, we need to be able to predict these risks, and provide the most complete information to the decision makers and government agencies to be adequately prepared in order to take the correct decisions for water shortages or surpluses as they occur.

A case study of an adaptation plan to climate change is presented. The study was conducted in the Cocagne watershed in the south eastern cost of New Brunswick, Canada, in collaboration of the Sustainable Group of Pays du Cocagne and the University of Moncton, and was based on:

- analysing recent climate variability and trends;
- identifying the various climatic risks at the watershed scale;
- mapping the most vulnerable areas.

Statistical approaches with Environment Canada data were used to determine climate variability and trends, and to analyse past and future climate conditions in the Cocagne watershed. The nature and magnitude of climate change from the 1970s to today were also illustrated.

Furthermore, climate model outputs using various scenarios from the 1970s to the 2100s were used to conduct risk analysis based on past and future trends, in order to assess how the watershed climate might change.

8.1.2. Materials and Methods

Daily climatic data around Cocagne watershed were collected from thermo-pluviometric stations of the Environment Canada meteorological network.

Bouctouche, Harcourt, Moncton, Parkindale, Rexton and Turtle Creek were the stations considered for New Brunswick area. O'Leary and Summerside stations were considered for the Prince Edward Island province, as shown in Table 11. Figure 30 shows the geographical distributions of the 11 meteorological stations.

Prov	ID Station	Start date	End date	Tot years	Distance [km]
NB	Bouctouche	15 Oct 1965	31 July 1999	34	10.5
NB	Bouctouche CDA	1 July 1982	31 Oct 1991	36	7.5
NB	Harcourt	1 July 1981	31 May 2004	23	36,5
NB	Moncton	10 Apr 1898	31 Dec 2011	113	11,5
NB	Moncton A	1 Dec 1939	6 June 2012	79	18
NB	Parkindale	15 May 1984	28 Feb 2017	33	32
NB	Rexton	18 Sep 1924	31 Dec 2009	85	31
NB	Turtle Creek	1 Jan 1968 P 1 Jan 1980 T	30 June 2015 June 1999	47 19	18.5
PEI	O'Leary	18 Nov 1960	31 Mar 2004	44	42
PEI	Summerside A	1 May 1942	16 Sep 1999	76	56
PEI	Summerside CDA	1 May 1936	31 Mar 1963	27	60

Table 11 List of meteorological stations (ID Station) used for this study, divided by Province (Prov.) New Brunswick, NB, and Prince Edward Island, PEI; Start date and End date are the date of starting and ending station activity, respectively; New end date is the date after joining data set; Tot years is the number of years recorded; and Distance from watershed border in km is calculated in the last column.

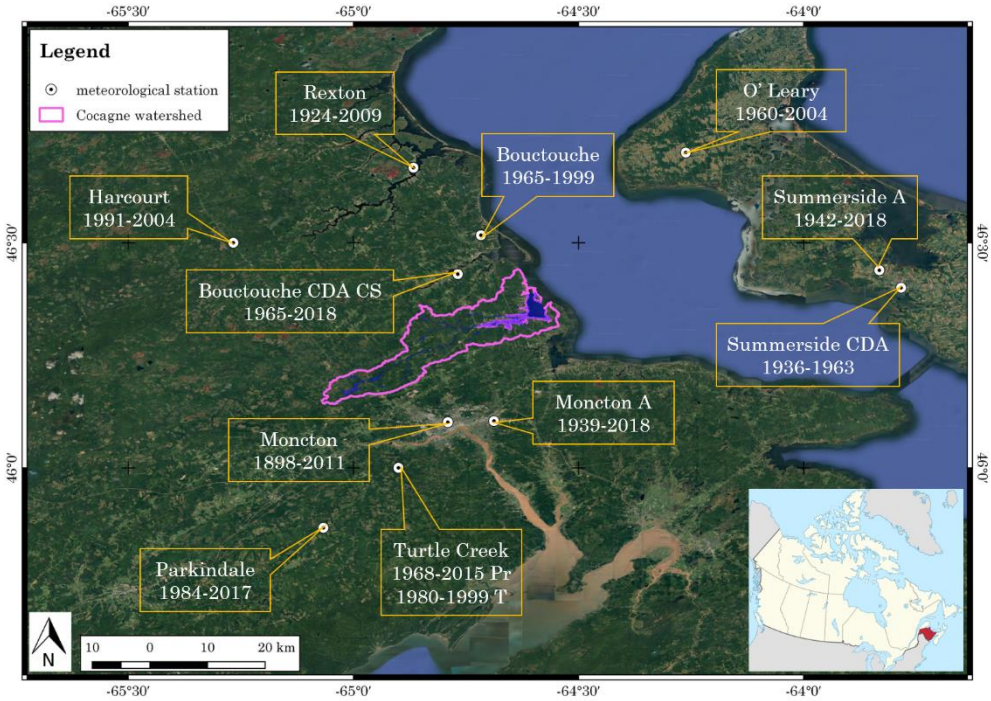

Figure 30 Geographical distribution of the meteorological stations used in this study, displaying the beginning and final years of data collection.

Distance from the watershed (less than 80km), percentage of missing data (less than 20%) and number of years of collecting data (more than 20 years) were the main criteria for choosing the meteorological stations.

Turtle Creek station is close to the watershed and we chose the dataset because of the high number of years recorded, although the percentage of missing data is higher than 20% for both temperature and precipitation data, as shown in Table 12. On the other hand, Baltimore station was not considered because of the short period of years recorded, despite its watershed proximity.

During the study period, three stations were relocated within a few meters of the initial location. The historical and current dataset were merged to ensure the historical continuity of the three stations.

ID Station	Tot %	P %	T_x %	T_n %
Bouctouche	2.67	1.13	0.79	0.75
Bouctouche CDA	7.61	3.61	2.09	1.92
Harcourt	1.08	0.07	0.54	0.47
Moncton	7.61	2.49	2.56	2.55
Moncton A	0.54	0.22	0.16	0.17
O' Leary	0.53	0.46	0.02	0.05
Parkindale	37.86	12.35	12.80	12.72
Rexton	6.10	2.39	1.43	2.29
Summerside A	16.52	5.82	5.39	5.31
SummersideCDA	6.52	5.33	0.63	0.56
Turtle Creek	144.73	25.33	59.70	59.70

*Table 12 Percentage of missing data of the meteorological stations (*ID Station*) in the study area, where* Tot % *is the percentage of missing data of the whole station dataset, and* P %, T_x %, T_n % *are the percentages of missing data concerning precipitation, maximum temperature and minimum temperature, respectively.*

A Quality Control (QC) analysis was conducted on the daily data series by using the R software *ClimPACT2* package (Alexander and Herold, 2016) to identify gaps, outliers and erroneous values.

Subsequently, the following meteorological indices were selected to climatically characterize the study area:

- annual total precipitation;
- number of very heavy rain days (10; 20; 30 mm);
- daily precipitation intensity;
- Growing Degree Days;
- Growing Season Length;
- Heatwave: Number; Magnitude; Amplitude; Duration and Frequency.

The graphs of Moncton meteorological station, which has collected data since 1939 and contains the longest and most complete dataset, are presented and used as an example to explain the meaning of the indices.

Daily minimum (T_n) and maximum temperature (T_x), and precipitation (P) are the variables used to calculate the indices. Daily mean temperature (T_m) is calculated from $T_m = (T_x + T_n) / 2$.

Each graph header includes station metadata (name, latitude and longitude of the station) and climatic index information. Additionally, a linear trend value (linear trend slope, marked as a black line), error on the calculated trend (slope error), and statistical significance are provided.

The red dotted line represents the locally weighted scatterplot smoothing, also called moving average, which is a tool used in regression analysis to create a smooth line to see the relationship between variables and foresee trends.

A future climate analysis is also presented, and the historical dataset was compared with three future periods of thirty years: 2011–2040; 2041–2070; 2071-2100. Two Representative Concentration Pathways (RCP), RCP4.5 and RCP8.5 (Moss *et al.*, 2010), were analysed. RCPs are designed to provide plausible future scenarios of human emission patterns (Figure 31). Historical simulations are for the period from 1900 to 2005. Future projections are for the period from 2006 to 2100 based on three global emission scenarios: low (RCP2.6), moderate (RCP4.5), and high (RCP8.5).

- *RCP2.6*: low emission global scenario, requires strong mitigation actions. This scenario indicates global average warming levels of 0.9 to 2.3 °C by 2090;
- *RCP4.5*: (or B1) medium global emission scenario, includes measures to limit (mitigate) climate change, and indicates global average warming levels of 1.7 to 3.2 °C by 2090;
- *RCP8.5*: (or A2) high global emission scenario indicates global average warming levels of 3.2 to 5.4 °C by 2090.

These scenarios provide a range of possible futures, based on a range of future emissions deforestation, population growth and many other factors.

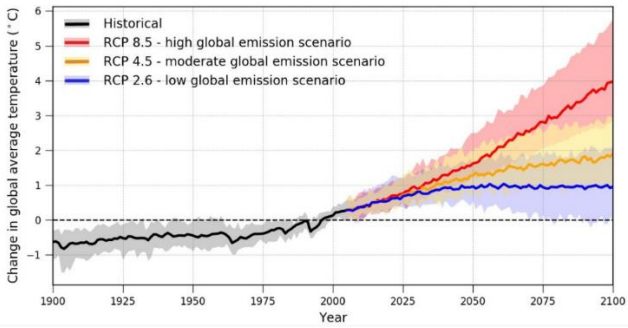

Figure 31 Change in global average temperature relative to the 1986-2005 reference period. [source: Government of Canada]

In this study, RCP4.5 and RCP8.5 were considered for the future forecast predictions.

8.1.3. Annual total precipitation

Annual total precipitation, with daily values greater than or equal to 1.0mm, is a measure of the quantity of rainfall and snowfall, (Figure 32). The index is important for water management.

A positive value of the linear trend slope indicates an increase of annual total rain in the watershed region, from about 1,000mm to over 1,250mm annually.

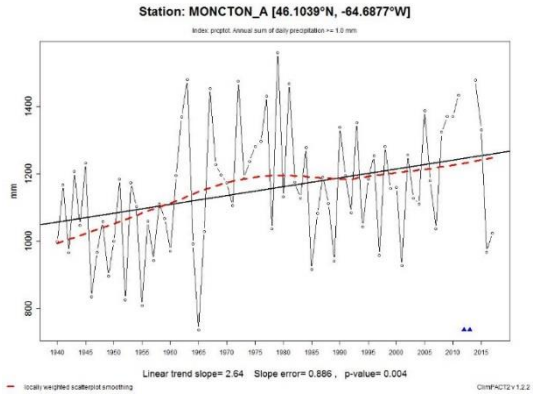

Figure 32 Annual total precipitation of Moncton station, during the period 1939-2018.

In future decades, precipitation is expected to increase across the entire watershed, by about 150mm in the RCP4.5 scenario (B1 blue line in Figure

33), and about 200mm in RCP8.5 scenario (A2 red line in Figure 33), with an incremental increase at the end of the century.

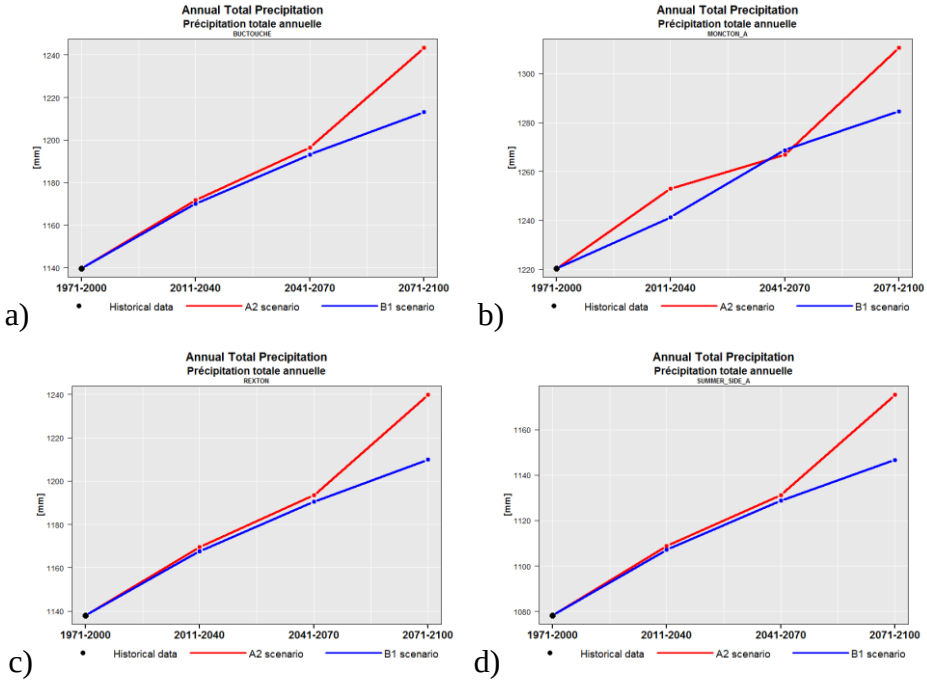

Figure 33 Annual total precipitation in Bouctouche (a), Moncton (b), Rexton (c) and Summerside (d) stations, in two future scenarios (A2 red line, and B1 blue line), during the period 1971-2100. Annual total precipitation in Moncton stations, in two future scenarios (A2 red line, and B1 blue line), during the period 1971-2100.

The interpolation geo-statistical technique enables visualization of the distribution of precipitation inside the watershed. The major increase is expected in the inland region according to the two future scenarios, with values around 1,300mm. Along the coast, the quantity of precipitation increases slightly, and values will be less than 1,100mm (Figure 34).

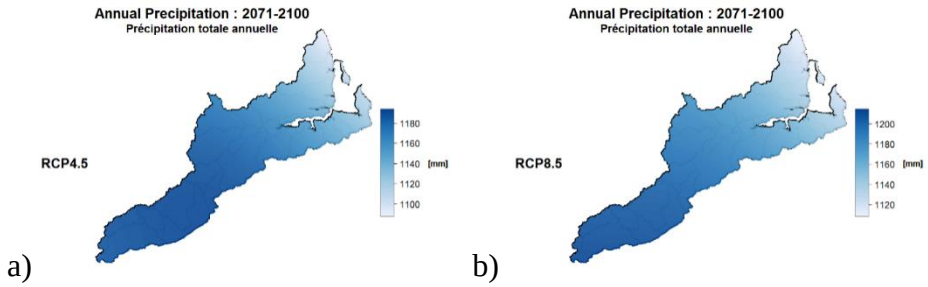

Figure 34 Annual total precipitation forecast in the Cocagne watershed, in two future scenarios RCP4.5 (a) and RCP88.5 (b), during the period 2071-2100. Spatial resolution: 50m.

Looking more in detail, a seasonal analysis allows to better understand the real impacts of the change in precipitation distribution. Precipitation is expected to increase in the Spring, Autumn and Winter seasons from 20 to 40mm, and decrease in Summer particularly towards the end of the century.

In Spring, total precipitation, which is the average total of rainfall and snowfall for the months of March, April and May, is expected to increase in both the RCP4.5 and RCP8.5 scenarios, except for the Moncton area which shows an opposite trend in the more optimistic scenario, RCP4.5.

Despite an initial slight increase, Summer total precipitation, which is the average total of rainfall and snowfall for the months of June, July and August, is expected to decrease in the last 30 years of the century. Due to the reduction of water during the growing season, it will have consequences for the environment and the agriculture sector.

Autumn total precipitation is the average total of rainfall and snowfall for the months of September, October and November, and is expected to increase in all areas. This pattern is expected to persist in the last 30 years of the century.

Higher temperature in Winter will affect precipitation characteristics. Future scenarios show a reduction of snowfall, which will be substituted by rainfall. Winter total precipitation is the average total of rainfall and snowfall for the months of December, January and February, and it is expected to increase.

8.1.4. Number of very heavy rain days (10; 20; 30 mm)

The index linear trend indicates a significant increase in the number of very heavy rain days. As shown in Figure 35, the annual number when precipitation values are greater than or equal to 10mm (a), 20mm (b) and 30mm (c) is increasing, and this pattern is also expected in the future.

In the period analysed, almost 6 more days recorded a precipitation equal to 10mm, 5 more days recorded 2 mm, and 4 more days recorded 30mm. This index is indirectly linked to the intensity of the precipitation, and because the total precipitation is expected to increase, the intensity of the rainfall will also be higher, as shown in Figure 32. In other words, it will rain more, but concentrated in a shorter number of days, with consequent reduction of soil capacity to drain water.

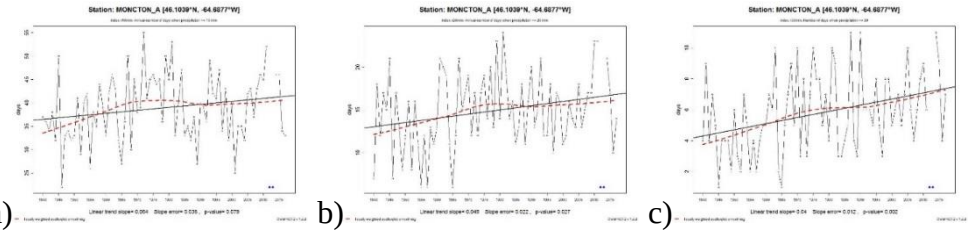

a) b) c)

Figure 35 Annual number of days when precipitation values were greater than or equal to 10mm (a), 20mm (b) and 30mm (c), recorded in Moncton station during the period 1939-2018.

In New Brunswick, the frequency of extreme rainfall events and the number of days with measurable rain show a general increase in future scenarios (Figure 36). The greatest totals are found close to southern coasts and the lowest totals in inland locations.

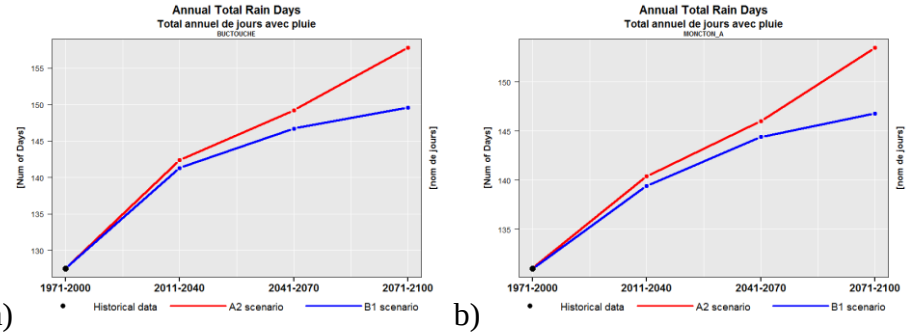

a) b)

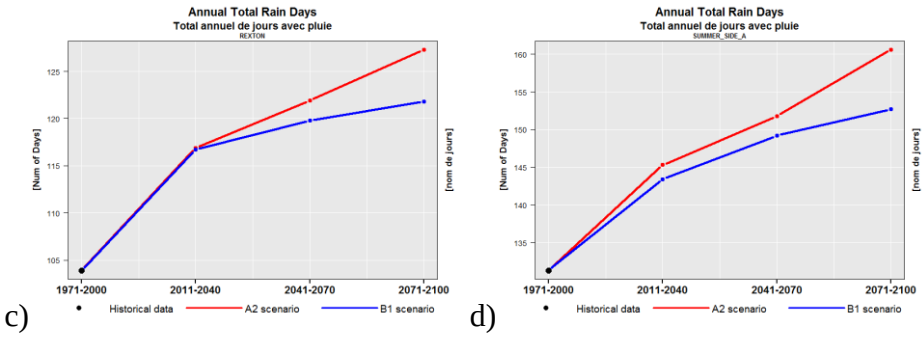

Figure 36 Annual total rain days in Bouctouche (a), Moncton (b), Rexton (c) and Summerside (d) stations in two future scenarios (A2 red line, and B1 blue line), during the period 1971-2100.

As previously described, the trend of daily precipitation intensity is increasing. The daily precipitation intensity index, calculated by dividing the annual total precipitation when the value is greater than or equal to 1.0mm by the number of wet days, increases by 1.0mm per day, in the period considered.

In addition to the volume, the frequency of rain affects tourism, outdoor events, recreation, farming, construction, and building maintenance.

Increased frequency of rainfall is likely to be accompanied by other changes. Higher temperatures may mean that wet surfaces dry more rapidly, while more intense falls may be less beneficial for many crops.

8.1.5. Growing Degree Days

The Growing Degree Days (GDD) are calculated as the cumulative sum of productive temperatures for crop growth. In other words, vegetation growth will only occur if the mean temperature exceeds a minimum development threshold called the base temperature (T_b). T_b is determined experimentally, varies with species and possibly cultivars, and likely varies with growth stage or the process being considered (Wang, 1960).

In Figure 37, the T_b value is equal to 10 °C. Hence, if the daily mean temperature is 15 °C, for example, this indicates a growing degree day total of 5 for that day. A positive linear trend means that daily mean temperature is increasing, and the difference between daily mean temperature and T_b is larger.

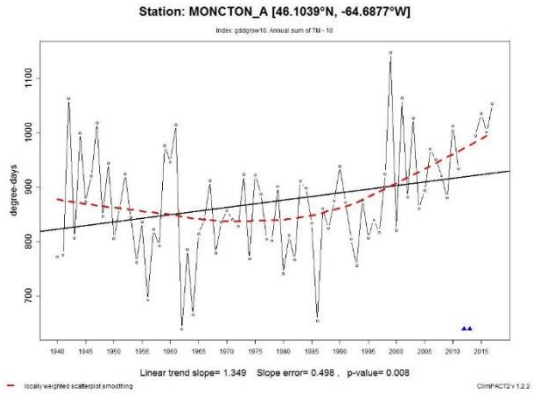

Figure 37 Annual difference between mean temperature (T_m) and base temperature (T_b), where T_b is a location-specific base temperature (10 °C in the graph), and T_M is greater than T_b, recorded in Moncton station during the period 1939-2018.

In the future predictions (Figure 38), GDD values rise everywhere and are expected to increase for both scenarios RCP4.5 (B1) and RCP8.5 (A2).

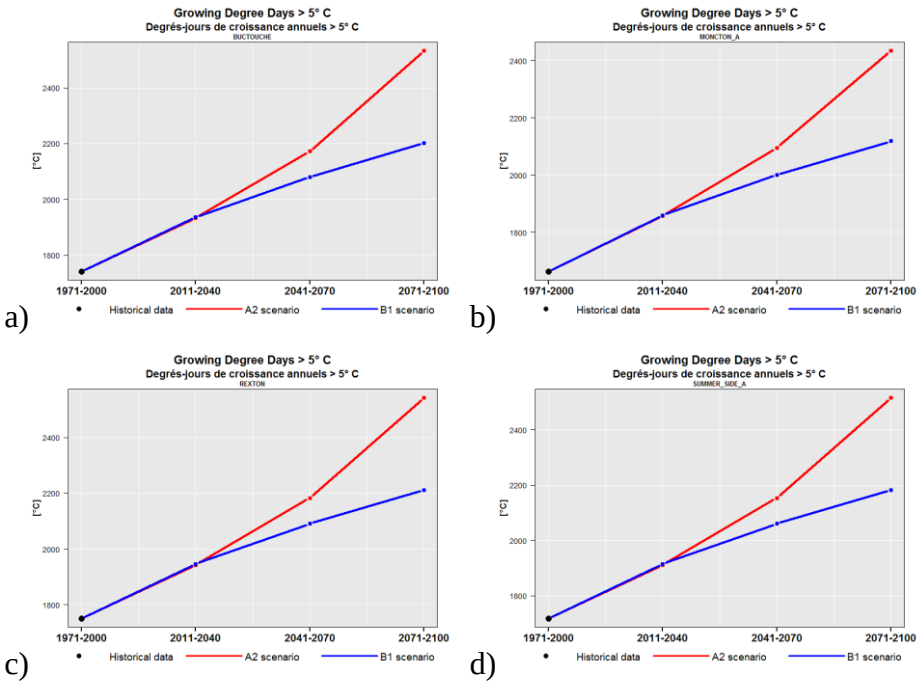

Figure 38 Growing Degree Days forecast, calculated with a T_b threshold greater than 5 °C in Bouctouche (a), Moncton (b), Rexton (c) and Summerside (d) stations, in two future scenarios (A2 red line, and B1 blue line), during the period 1971-2100.

8.1.6. Growing Season Length

Growing Season Length (GSL), which is the annual number of days between the first occurrence of 6 consecutive days with mean temperature (T_m) greater than 5 °C and the first occurrence of 6 consecutive days with T_m lower than 5 °C, is shown in Figure 39. In other words, it is the period between the beginning and end date of the growing season, characterized by the consecutive number of days with T_m greater or lower than 5 °C, respectively.

GSL is strictly related to mean temperature, with a threshold of 5 °C, and in conjunction with Growing Degree Days, adds information of interest to farmers and growers.

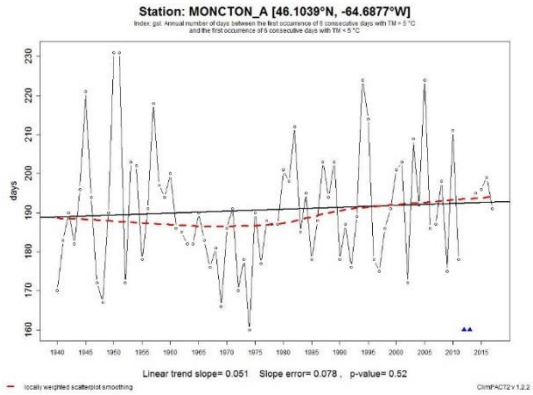

Figure 39 Annual number of days between the first occurrence of 6 consecutive days with mean temperature (T_m) greater than 5 °C and the first occurrence of 6 consecutive days with mean temperature (T_m) lower than 5 °C, recorded in Moncton station during the period 1939-2018.

In future, the GSL is expected to increase in all provinces. By the end of the century, the season in the North of New Brunswick will be longer than currently seen anywhere in the South. A significantly longer growing season is likely to offer new opportunities for farmers, horticulturists and gardeners. At the same time, growers will need to be prepared regarding how to deal with new pests, diseases, and water management methods suited to a warmer environment. Competition for water resources may be expected to increase, while simultaneously the available water resources may diminish.

8.1.7. Heatwave: Number, Magnitude, Amplitude, Duration and Frequency

A heatwave refers to a prolonged period of hot weather, which may be accompanied by high humidity. The World Meteorological Organization (2015) guidance about the definition of a heatwave is: marked unusual hot weather over a region persisting for at least two consecutive days during the hot period of the year, based on local climatological conditions, with thermal conditions recorded above given thresholds.

Heatwaves will become more frequent, drawn-out and intense due to climate change. Heat stroke, dehydration, cardiovascular disease, and other temperature-related illnesses are on the rise. Globally, the number of people exposed to heat waves between 2000 and 2016 increased by an estimated 126million.

In Figure 40 five graphs describe the heatwave index by the number, magnitude, amplitude, duration, and frequency of heatwave events, recorded by Moncton meteorological station.

a. The number of individual heatwaves that occur each summer is defined as three or more days where the Excess Heat Factor (EHF) is positive, maximum temperature (T_x) is greater than the 90^{th} percentile of T_x, and minimum temperature (T_n) is greater than the 90^{th} percentile of T_n.
b. Heatwave magnitude is defined as the mean temperature of all heatwaves identified by heatwave number.
c. Heatwave amplitude is the peak daily value in the hottest heatwave and is defined as the heatwave with the highest heatwave magnitude.
d. Heatwave duration is calculated as the length of the longest heatwave identified by heatwave number.
e. Heatwave frequency is the number of days that contribute to heatwaves as identified by heatwave number.

The EHF is the difference between two Excess Heat Indices, EHI (Nairn and Fawcett, 2013):

$$EHI_1 = [(T_{mi} + T_{mi-1} + T_{mi-2}) / 3] - [(T_{mi-3} + \ldots + T_{mi-32}) / 30]$$

$$EHI_2 = [(T_{mi} + T_{mi-1} + T_{mi-2}) / 3] - T_{m90}$$

Where T_{mi} represents the average daily temperature for day *i* and T_{m90} is the 90^{th} percentile of T_M which is calculated within a user-specified base

period, over the calendar year and using a 15-day running window. T_m is calculated via $T_m = (T_x + T_n) / 2$.

Trend recorded in the period 1939-2018 shows an increase in heatwave events in terms of number, amplitude, duration, and frequency. Since the 1980s the heatwaves in Moncton have increased, and it is expected that this trend will continue in the future.

Longer and more intense heatwaves are associated with an increase in heat-related illnesses and deaths, especially amongst vulnerable populations. Extended heat also increases the demand for cooling, which in turn increases electricity costs in summer, and the risk of food and water-borne contamination.

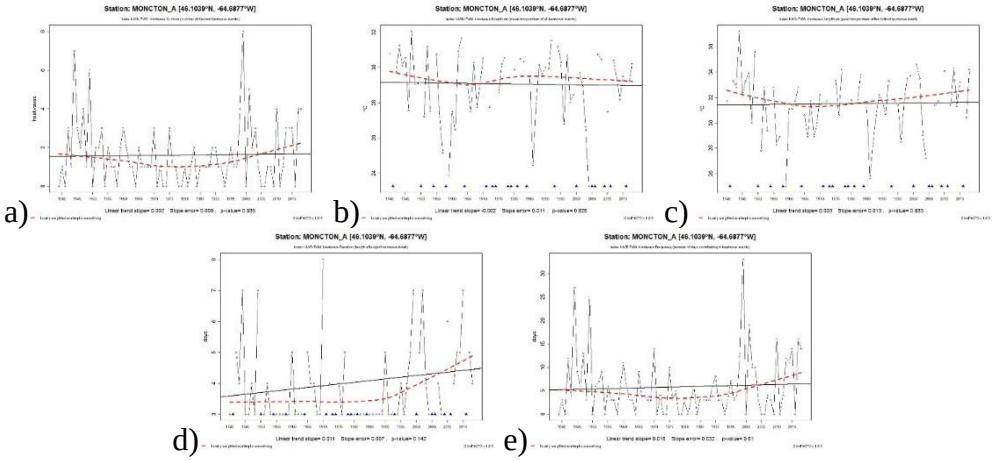

Figure 40 Number (a), magnitude (b), amplitude (c), duration (d), and frequency (e) of the heatwave events, recorded in Moncton station during the period 1939-2018.

8.1.8. Drought indices, SPI and SPEI

SPI trends recorded in Moncton station during the period 1939-2018 show progress towards a "*normal*" condition, for both the 3-month and 6-month time scales, and towards "*moderately wet*" in both the 12-month and 24-month time scales (Figure 41). While this result agrees with the increasing trend in precipitation amount, it alternates with "*moderately dry*" and "*severely dry*" conditions.

The same characteristics are observed with the SPEI. The index trend shows a future generally wet condition, alternating with dry conditions (Figure 42).

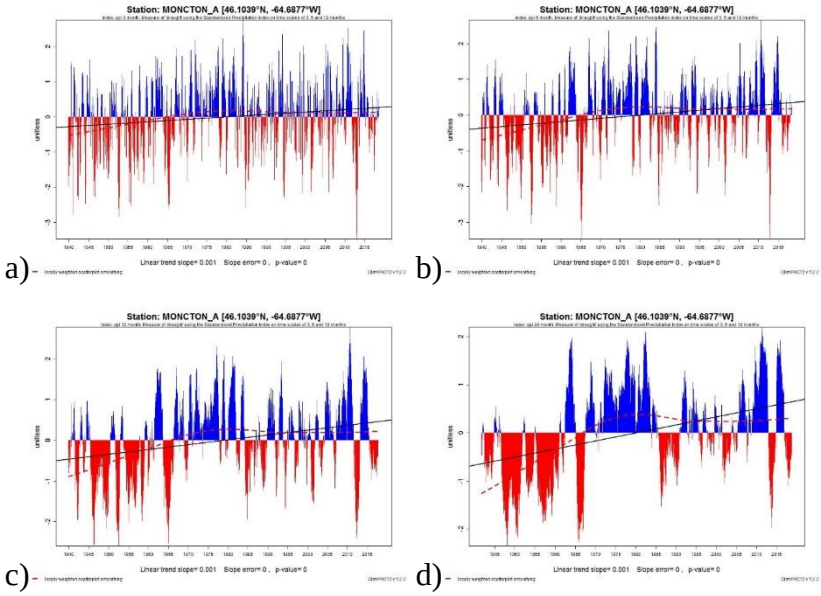

Figure 41 Standardized Precipitation Index, SPI at different time scales: 3-month (a), 6-month (b), 12-month (c), and 24-month (d), recorded in Moncton station during the period 1939-2018.

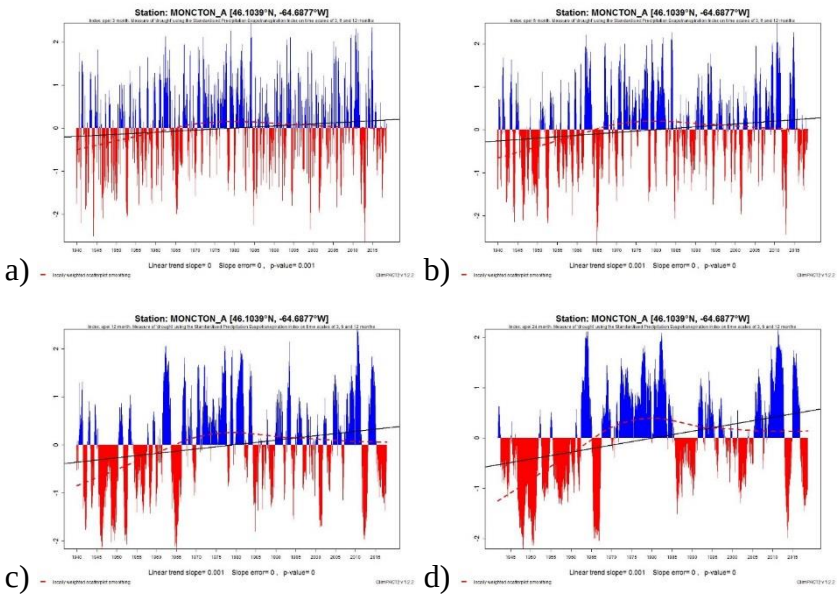

Figure 42 Standardized Precipitation Evapotranspiration Index, SPEI at different time scales: 3-month (a), 6-month (b), 12-month (c), and 24-month (d), recorded in Moncton station during the period 1939-2018.

8.1.9. Conclusion

The study was conducted in the Cocagne watershed in the south eastern cost of New Brunswick in Canada. The specific focus of this study was to analyse the recent climate variability and trends, to identify the various climatic risks at the watershed scale and mapping the most vulnerable areas in Humid Continental climate zone. The study aimed to develop novel information sources and improve of existing instruments to provide support for the management and detection of flooding in the study area. Moreover, this study enhanced the quality of decision-making support services available advisory services and policymakers.

The study assessed the application of the tools used to examine flood risk conditions. The two drought indices, Standardised Precipitation Index and Standardised Precipitation and Evapotranspiration Index, were correlated with classical meteorological indices. Application of the same tools in the region and comparison of the results strengthened the validity of the results of this study. The density of meteorological networks was identified as a shortcoming of this analysis however, highlighting the importance of using satellite data in combination with meteorological data. The study

also sought to involve stakeholder organisations and local and regional decision-makers where possible, in order to enhance the relevance of the analyses and communication of findings. The value of this approach was evident in the current study, which involved the largest network of stakeholders, with input during the planning, analysis, and communication phases of the study.

The findings provide improved decision-making support that can help advisory services and policymakers to plan for and adapt to changing climatic conditions.

8.2. Appendix 2. Meteorological Data

In Table 13 is presented the list of meteorological stations used to analyse the drought episode occurred in summer 2018 in Ireland.

ID	LAT	LON	Starting day	Number Year	Network
DUBLIN AIRPORT	53,400	-6,200	1/1/1942	76	Synoptic
VALENTIA OBSERVATORY	51,900	-10,200	1/1/1942	76	Synoptic
SHANNON AIRPORT	52,700	-8,900	1/9/1945	73	Synoptic
CLAREMORRIS	53,700	-9,000	1/1/1950	68	Synoptic
MALIN HEAD	55,400	-7,300	1/5/1955	63	Synoptic
ROCHES POINT	51,800	-8,200	1/12/1955	63	Synoptic
BELMULLET	54,200	-10,000	17/9/1956	62	Synoptic
CORK AIRPORT	51,800	-8,500	1/1/1962	56	Synoptic
CASEMENT	53,300	-6,400	1/1/1964	54	Synoptic
MULLINGAR	53,500	-7,400	8/11/1973	45	Synoptic
KNOCK AIRPORT	53,900	-8,800	1/8/1996	22	Synoptic
FOULKESMILL (Longraigue)	52,306	-6,760	1/1/1941	77	Rainfall
SHANNON AIRPORT	52,687	-8,917	1/1/1941	77	Rainfall
DUBLIN AIRPORT	53,423	-6,238	1/1/1941	77	Rainfall
KENMARE (DERREEN)	51,768	-9,775	1/1/1941	77	Rainfall
MALLOW (Hazelwood)	52,187	-8,650	1/1/1941	77	Rainfall
MEELICK (Victoria Lock)	53,167	-8,075	1/1/1941	77	Rainfall
DRUMSHANBO	54,057	-8,057	1/1/1941	77	Rainfall
PORTUMNA O.P.W.	53,088	-8,188	1/1/1941	77	Rainfall
ATHLONE O.P.W.	53,420	-7,938	1/1/1941	77	Rainfall
CASHEL (Ballinamona)	52,506	-7,924	1/1/1941	77	Rainfall
DUBLIN (Ringsend)	53,338	-6,208	1/1/1941	77	Rainfall
CARNDOLLA	53,402	-9,009	1/12/1941	77	Rainfall
KESHCARRIGAN G.S.	54,017	-7,938	15/6/1942	76	Rainfall
OMEATH	54,085	-6,254	25/3/1943	75	Rainfall
COROFIN	52,942	-9,068	1/6/1943	75	Rainfall
TULLA	52,868	-8,756	15/7/1943	75	Rainfall
KILTORMER	53,237	-8,269	21/7/1943	75	Rainfall
LOUGHGLINN	53,820	-8,553	29/3/1944	74	Rainfall
MILLTOWN	53,607	-8,889	28/4/1944	74	Rainfall
GLENAMADDY (Gortnagier)	53,592	-8,558	1/5/1944	74	Rainfall
CASTLEISLAND (Coom)	52,233	-9,353	1/6/1944	74	Rainfall
CUILCAGH MTNS.	54,160	-7,801	11/8/1944	74	Rainfall
ESKERAGH	54,107	-9,467	15/8/1944	74	Rainfall
KEENAGH BEG	54,035	-9,483	15/8/1944	74	Rainfall
DERRYHILLAGH	54,033	-9,388	16/8/1944	74	Rainfall
BALLYMORE EUSTACE D.C.W.W.	53,122	-6,603	25/9/1944	74	Rainfall
WATERVILLE OCTIVE NO.9	51,868	-10,050	1/1/1948	70	Rainfall
DONOUGHMORE	51,987	-8,737	2/2/1948	70	Rainfall
MONEYSTOWN	53,007	-6,223	1/7/1948	70	Rainfall
GREENCASTLE	55,206	-6,985	16/7/1948	70	Rainfall

CREESLOUGH (Brockagh)	55,075	-7,972	19/8/1948	70	Rainfall
CREESLOUGH (Carrownamaddy)	55,133	-7,950	1/9/1948	70	Rainfall
BALLINGEARY (Voc.Sch.)	51,850	-9,233	20/10/1948	70	Rainfall
GLENVICKEE (Caragh River Area)	51,971	-9,824	12/6/1949	69	Rainfall
CLOONE LAKE (Caragh River Area)	51,939	-9,871	13/6/1949	69	Rainfall
HACKETSTOWN (Voc.Sch.)	52,857	-6,552	5/9/1949	69	Rainfall
SNEEM	51,837	-9,902	1/11/1949	69	Rainfall
CLOGHANE	52,224	-10,174	18/10/1950	68	Rainfall
COOLE (Coolnagun)	53,674	-7,417	2/4/1951	67	Rainfall
GLEN IMAAL (FOR.STN.)	52,991	-6,539	1/5/1951	67	Rainfall
CAHIR (Voc.Sch.)	52,375	-7,918	21/11/1951	67	Rainfall
LECARROW	53,540	-8,042	21/2/1952	66	Rainfall
KINSALE (Voc.Sch.)	51,704	-8,524	25/4/1952	66	Rainfall
PETTIGO (Lough Derg)	54,604	-7,856	10/6/1952	66	Rainfall
CLOONACOOL (Lough Easkey)	54,126	-8,842	22/8/1952	66	Rainfall
CASTLEBAR (Burren)	53,909	-9,304	1/9/1952	66	Rainfall
ARDEE (St.Brigid s Hosp.)	53,854	-6,543	4/9/1952	66	Rainfall
ARDNACRUSHA (Gen.Stn.No.2)	52,704	-8,609	9/10/1952	66	Rainfall
SILVERMINES MTNS.(Curreeny)	52,733	-8,142	16/4/1953	65	Rainfall
SLIEVE BLOOM MTNS.(Nealstown)	52,989	-7,703	1/5/1953	65	Rainfall
CARRIGADROHID (Gen.Stn.)	51,892	-8,858	12/11/1953	65	Rainfall
CASEMENT	53,303	-6,437	1/1/1954	64	Rainfall
INISHCARRA (GEN.STN.)	51,900	-8,657	27/1/1954	64	Rainfall
BALLYSHANNON (Cherrymount)	54,488	-8,153	20/7/1954	64	Rainfall
NAAS (C.B.S.)	53,217	-6,655	11/5/1955	63	Rainfall
BANSHA (Aherlow W.W.)	52,404	-8,120	19/5/1955	63	Rainfall
CARRICKMACROSS (Dunoge)	53,972	-6,753	1/10/1958	60	Rainfall
MACROOM (Renaniree)	51,900	-9,157	23/7/1959	59	Rainfall
GLENASMOLE (Supt s Lodge)	53,237	-6,358	1/10/1959	59	Rainfall
COSTELLOE FISHERY	53,276	-9,536	6/10/1960	58	Rainfall
DROMAHAIR (Market St.)	54,226	-8,292	1/11/1960	58	Rainfall
CORK AIRPORT	51,842	-8,485	5/1/1962	56	Rainfall
CLONMEL (Redmondstown)	52,370	-7,654	13/2/1962	56	Rainfall
ATHLONE (Glynnwood)	53,403	-7,840	1/4/1962	56	Rainfall
DRANGAN (Moanvurrin)	52,533	-7,576	1/6/1962	56	Rainfall
KNOCKANORE	52,058	-7,886	2/9/1964	54	Rainfall
YOUGHAL (Glendine W.W.)	52,004	-7,904	1/12/1964	54	Rainfall
GLENMACNASS	53,056	-6,333	1/2/1965	53	Rainfall
MALAHIDE CASTLE	53,440	-6,157	1/12/1965	53	Rainfall
BALLYBODEN	53,272	-6,303	1/3/1967	51	Rainfall
ARDEE (Boharnamoe)	53,853	-6,568	1/7/1968	50	Rainfall
KILGARVAN (Gortnaboul)	51,901	-9,438	15/5/1969	49	Rainfall
BALLINA (Shanaghy)	54,106	-9,135	1/11/1969	49	Rainfall
LETTERKENNY (Dromore)	54,941	-7,674	6/8/1970	48	Rainfall
MONAGHAN (Castleshane)	54,235	-6,890	1/2/1971	47	Rainfall
BOYLE (Marian Road)	53,968	-8,303	1/7/1971	47	Rainfall
NEWBLISS (Drumshannon)	54,158	-7,119	1/9/1971	47	Rainfall
AUGHNASHEELAN (Miskawn)	54,084	-7,868	1/10/1971	47	Rainfall
TERMON (Goldrum)	55,057	-7,805	1/6/1972	46	Rainfall
CROLLY (Filter Works)	55,006	-8,250	1/11/1972	46	Rainfall

BAILIEBORO (Duneena)	53,940	-7,018	1/8/1973	45	Rainfall
BAILIEBORO (Leiter)	53,926	-7,008	1/8/1973	45	Rainfall
WEXFORD (Newtown W.W.)	52,338	-6,501	1/6/1974	44	Rainfall
BRITTAS (GLENARANEEN)	53,251	-6,451	1/12/1975	43	Rainfall
KILLEAGH (Monabraher)	51,973	-7,985	1/5/1976	42	Rainfall
SHANAGARRY NORTH	51,856	-8,034	1/5/1976	42	Rainfall
KILCAR (Cronasillagh)	54,639	-8,540	5/7/1976	42	Rainfall
MACROOM (Curraleigh)	51,971	-9,070	1/12/1977	41	Rainfall
CALLAN (Moonarche)	52,534	-7,419	1/3/1978	40	Rainfall
MONAGHAN (Knockroe)	54,240	-6,985	1/10/1979	39	Rainfall
TRALEE (Lisaboula)	52,224	-9,642	1/2/1980	38	Rainfall
MULLINAHONE (KILLAGHY)	52,519	-7,506	1/6/1980	38	Rainfall
CAHIR PARK II	52,354	-7,924	1/1/1981	37	Rainfall
HEADFORD O.P.W.	53,469	-9,101	1/2/1981	37	Rainfall
FENOR (Islandtarsney)	52,153	-7,206	7/2/1981	37	Rainfall
MANORHAMILTON (Amorset)	54,304	-8,176	1/3/1981	37	Rainfall
PATRICKSWELL (Dooneen)	52,590	-8,670	1/9/1981	37	Rainfall
DERRYHENNY DOOCHARY	54,876	-8,252	1/12/1981	37	Rainfall
ARDNAWARK BARNESMORE	54,704	-7,973	5/3/1982	36	Rainfall
BAWNASKEHY CASTLEISLAND	52,201	-9,436	1/4/1982	36	Rainfall
VENTRY THE BOAT SLIP	52,126	-10,356	2/4/1982	36	Rainfall
DOO-LOUGH	52,801	-9,321	5/6/1982	36	Rainfall
GORT (Derrybrien) II	53,060	-8,601	1/7/1982	36	Rainfall
MURRISK	53,776	-9,624	1/10/1982	36	Rainfall
COOLGREANY CASTLEWARREN	52,705	-7,118	1/11/1982	36	Rainfall
GLENCAR (Dreenagh)	52,002	-9,904	1/7/1983	35	Rainfall
KILLALOE DOCKS	52,806	-8,443	1/7/1983	35	Rainfall
ENNISCORTHY (Brownswood)	52,458	-6,557	1/8/1983	35	Rainfall
LAHERDANE (Cum)	54,034	-9,322	1/9/1983	35	Rainfall
CASTLEDERMOT KILKEA HOUSE	52,934	-6,888	1/11/1983	35	Rainfall
CARRICK-ON-SUIR II	52,338	-7,403	1/11/1983	35	Rainfall
PAULSTOWN (Shankill Castle)	52,686	-7,018	1/1/1984	34	Rainfall
RATHWIRE	53,505	-7,138	1/2/1984	34	Rainfall
GALTEE MOUNTAINS SKEHEENARINKY	52,323	-8,160	1/3/1984	34	Rainfall
KILLADOON	53,672	-9,885	1/4/1984	34	Rainfall
ASHFORD (Glanmore Gardens)	53,020	-6,139	6/4/1984	34	Rainfall
CARNDONAGH (Rocksmount) II	55,255	-7,237	20/5/1984	34	Rainfall
KILMIHIL (Shyan)	52,725	-9,358	1/6/1984	34	Rainfall
MULLAGH (Carrowlagan)	52,792	-9,401	1/6/1984	34	Rainfall
INISHBOFIN	53,618	-10,185	1/6/1984	34	Rainfall
BALLYVAUGHAN (Ballyconry)	53,120	-9,168	1/6/1984	34	Rainfall
ROSCREA (NEW ROAD)	52,952	-7,789	1/6/1984	34	Rainfall
KILTEALY (Askinvillar)	52,553	-6,754	1/7/1984	34	Rainfall
KILKENNY (Lavistown House) II	52,636	-7,192	1/7/1984	34	Rainfall
RATHKEALE (Duxton)	52,474	-8,907	1/7/1984	34	Rainfall
BALLINAMULT (Doon)	52,208	-7,742	1/7/1984	34	Rainfall
EMYVALE	54,338	-6,956	1/8/1984	34	Rainfall
FINTOWN (Kingarrow)	54,891	-8,054	2/8/1984	34	Rainfall
KINCASSLAGH	55,021	-8,385	2/8/1984	34	Rainfall
MULRANY (Doughbeg)	53,885	-9,805	1/9/1984	34	Rainfall

CARROWMORE LACKEN	54,256	-9,271	1/9/1984	34	Rainfall
CORK MONTENOTTE	51,903	-8,441	2/9/1984	34	Rainfall
BUNCLODY (Corragh)	52,676	-6,604	1/10/1984	34	Rainfall
COOGA LowerDoon	52,605	-8,270	1/10/1984	34	Rainfall
MULLINAVAT (GLENDONNELL)	52,358	-7,154	2/10/1984	34	Rainfall
FREEMOUNT PUMPING STATION	52,271	-8,887	1/11/1984	34	Rainfall
DINGLE (Baile na nGall)	52,202	-10,357	1/12/1984	34	Rainfall
CLEGGAN (Cloch Breac)	53,553	-10,106	1/1/1985	33	Rainfall
NEWBLISS (Crappagh)	54,137	-7,103	1/2/1985	33	Rainfall
BALLYEDMONDUFF HOUSE	53,233	-6,222	2/2/1985	33	Rainfall
BRUCKLESS	54,635	-8,385	1/4/1985	33	Rainfall
BALLINSKELLIGS THE GLEN	51,851	-10,325	1/4/1985	33	Rainfall
CLONASLEE WATERWORKS II	53,138	-7,523	1/5/1985	33	Rainfall
CLIFDEN	53,475	-10,021	1/6/1985	33	Rainfall
CRAUGHWELL (Grenage)	53,223	-8,752	1/6/1985	33	Rainfall
BALLINASLOE (Derrymullen)	53,338	-8,251	1/6/1985	33	Rainfall
BALLYCONNELL (Mullaghduff)	54,104	-7,568	1/6/1985	33	Rainfall
ROUNDSTONE	53,410	-9,917	1/7/1985	33	Rainfall
ATHEA (Templeathea)	52,467	-9,242	1/7/1985	33	Rainfall
AHERLAMORE	51,843	-8,722	1/7/1985	33	Rainfall
LOMBARDSTOWN (Drompeach)	52,091	-8,784	1/7/1985	33	Rainfall
BANTEER LYRE	52,075	-8,852	1/7/1985	33	Rainfall
KILCOOLE (Treatment Plant)	53,101	-6,043	1/8/1985	33	Rainfall
ROSSCARBERY (Froe)	51,590	-9,034	1/8/1985	33	Rainfall
TULLOW (Waterworks)	52,803	-6,739	1/8/1985	33	Rainfall
NAAS (OSBERSTOWN)	53,221	-6,689	1/8/1985	33	Rainfall
RIVERSTOWN (Glenmore Upper)	54,035	-6,236	4/12/1985	33	Rainfall
TALLOW KILMORE	52,071	-7,976	1/5/1986	32	Rainfall
MONEYPOINT E.S.B.	52,607	-9,426	1/7/1986	32	Rainfall
FRENCHPARK CALLOW	53,905	-8,457	1/7/1986	32	Rainfall
BANGOR ERRIS (Main St.)	54,140	-9,738	1/8/1986	32	Rainfall
STROKESTOWN (Carrowclogher)	53,752	-8,106	1/4/1987	31	Rainfall
TOGHER (Barmeath Castle)	53,822	-6,334	1/9/1987	31	Rainfall
BOOLAVOGUE (Knockavocca)	52,555	-6,451	1/9/1987	31	Rainfall
POLLMOUNTY FISH FARM	52,467	-6,902	1/11/1987	31	Rainfall
TOURMAKEADY (WaterTreatmentPlant	53,676	-9,369	1/12/1987	31	Rainfall
LISGLENNON WATERWORKS	54,186	-9,223	1/1/1988	30	Rainfall
DOOAGH (Water Treatment Plant)	53,969	-10,157	1/6/1988	30	Rainfall
FALCARRAGH (Lough Altan)	55,075	-8,093	8/6/1988	30	Rainfall
KNOCK AIRPORT	53,904	-8,817	1/7/1988	30	Rainfall
SKIBEREEN (WaterTreatmentPlant)	51,571	-9,269	1/8/1988	30	Rainfall
WATERGRASSHILL (Tinageragh)	52,009	-8,350	1/8/1988	30	Rainfall
CASHEL (BALLYDOYLE HOUSE)	52,457	-7,823	1/8/1988	30	Rainfall
KINSELLAGH	54,302	-8,407	1/6/1989	29	Rainfall
CROSSMOLINA (Castlehill)	54,067	-9,308	1/10/1989	29	Rainfall
BLESSINGTON (HEMPSTOWN)	53,192	-6,503	1/5/1990	28	Rainfall
CELBRIDGE Moortown	53,355	-6,551	1/5/1990	28	Rainfall
MILLSTREET (Coomlogane)	52,059	-9,074	2/5/1991	27	Rainfall
WEXFORD WILDFOWL RESERVE	52,354	-6,419	1/6/1992	26	Rainfall
BARTLEMY	52,037	-8,259	1/8/1992	26	Rainfall

KNOCKNAGOSHEL (Meinleitrim)	52,290	-9,372	8/10/1992	26	Rainfall
LOUGH GLENCAR	54,334	-8,353	1/3/1993	25	Rainfall
BELTURBET (Naughan)	54,134	-7,437	1/7/1993	25	Rainfall
COOMCLOGH	51,768	-9,267	1/8/1993	25	Rainfall
DERRIANA	51,889	-10,023	1/10/1993	25	Rainfall
CARHEENY BEG	52,991	-8,825	4/10/1993	25	Rainfall
CARNEW (Cronyhorn)	52,717	-6,507	1/11/1993	25	Rainfall
NEWMARKET (New-Street)	52,209	-9,001	1/11/1993	25	Rainfall
WESTPORT (CARRABAWN)	53,789	-9,523	7/12/1993	25	Rainfall
KINNEGAD (Mullingar Road)	53,456	-7,107	7/12/1993	25	Rainfall
KENMARE	51,876	-9,586	2/3/1994	24	Rainfall
PORTLAW-MAYFIELD II	52,288	-7,301	1/4/1994	24	Rainfall
EASKEY (Bunowna)	54,285	-8,951	1/5/1994	24	Rainfall
KILKEERAN	53,692	-9,267	1/6/1994	24	Rainfall
SPRINGFIELD CASTLE	52,343	-8,951	1/7/1994	24	Rainfall
SHANAGOLDEN OldAbbey	52,572	-9,058	1/7/1994	24	Rainfall
DUNCANNON	52,209	-6,908	1/11/1994	24	Rainfall
DRIMOLEAGUE (Angram)	51,639	-9,289	1/11/1994	24	Rainfall
GOWRAN	52,623	-7,069	1/11/1994	24	Rainfall
CLONOULTY Clogher	52,619	-7,934	1/11/1994	24	Rainfall
MONAMOLIN	52,551	-6,354	2/11/1994	24	Rainfall
BALLINEEN (Carbery)	51,725	-8,973	1/5/1995	23	Rainfall
MUSKERRY (GOLF CLUB)	51,918	-8,606	2/5/1995	23	Rainfall
KILCLOONEY MORE	54,807	-8,438	1/12/1995	23	Rainfall
BALLYMORE	53,939	-8,323	3/12/1995	23	Rainfall
GRANGE (Mountemple)	54,417	-8,484	1/1/1996	22	Rainfall
CLOYNE (LISANLEY)	51,854	-8,135	1/3/1996	22	Rainfall
LIMERICK JUNCTION (SOLOHEAD)	52,504	-8,204	1/3/1996	22	Rainfall
STRAFFAN (TURNINGS)	53,284	-6,621	2/3/1996	22	Rainfall
DEREEN	51,891	-10,237	1/4/1996	22	Rainfall
DUNFANAGHY (Murroe)	55,153	-8,006	1/6/1996	22	Rainfall
CARRIGANS (Kildrum)	54,974	-7,409	3/6/1996	22	Rainfall
ROADS	52,018	-10,137	1/10/1996	22	Rainfall
TERMONBARRY	53,738	-7,917	1/10/1996	22	Rainfall
DERRYPARK	53,590	-9,490	1/1/1997	21	Rainfall
BALLYJAMESDUFF (Kilcully)	53,855	-7,201	1/4/1997	21	Rainfall
BELLEWSTOWN (COLLIERSTOWN)	53,638	-6,356	1/4/1997	21	Rainfall
GWEEDORE WEIR	55,043	-8,225	1/5/1997	21	Rainfall
DUN LAOGHAIRE	53,285	-6,126	1/8/1997	21	Rainfall
CURRY	54,003	-8,770	1/11/1997	21	Rainfall
OLDBRIDGE (Oakview)	53,052	-6,272	1/12/1997	21	Rainfall
NEWPORT (Furnace)	53,921	-9,569	1/1/1960	58	Climatic
WATERFORD (Tycor)	52,252	-7,125	1/1/1961	57	Climatic
DERRYGREENAGH	53,388	-7,255	1/1/1961	57	Climatic
GLENTIES HATCHERY	54,788	-8,286	1/1/1961	57	Climatic
DUBLIN (Glasnevin)	53,369	-6,269	1/1/1961	57	Climatic
DUBLIN (Merrion Square)	53,338	-6,252	1/6/1965	53	Climatic
BALLYSHANNON (Cathleen s Fall)	54,492	-8,172	1/1/1966	52	Climatic
KILLARNEY (Muckross House)	52,017	-9,492	1/12/1968	50	Climatic
SHERKIN ISLAND	51,472	-9,424	1/7/1974	44	Climatic

GLENGARRIFF (Ilnacullin)	51,734	-9,541	1/4/1975	43	Climatic
ARDFERT (Liscahane)	52,307	-9,771	1/11/1980	38	Climatic
GLENEALY (Kilmacurragh Park)	52,924	-6,143	1/7/1981	37	Climatic
LITTLETON II B. NA M.	52,607	-7,700	1/7/1982	36	Climatic
CARRON	53,026	-9,073	1/8/1982	36	Climatic
DUNGARVAN (Carriglea)	52,086	-7,676	1/1/1983	35	Climatic
MAAM VALLEY	53,535	-9,605	1/1/1983	35	Climatic
STRAIDE	53,922	-9,122	1/9/1983	35	Climatic
FETHARD (PARSONSHILL)	52,509	-7,643	1/4/1985	33	Climatic
CAVAN (Drumconnick)	53,991	-7,391	1/7/1986	32	Climatic
MOUNT RUSSELL	52,324	-8,568	1/6/1990	28	Climatic
ATHY (CHANTERLANDS)	52,984	-6,972	1/7/1993	25	Climatic
DELPHI LODGE II	53,626	-9,742	1/1/1994	24	Climatic
CRAGGAUNOWEN	52,806	-8,788	1/3/1994	24	Climatic
BELDERRIG	54,306	-9,567	1/5/1994	24	Climatic
ARDTARMON	54,336	-8,620	1/6/1994	24	Climatic
EDENDERRY (BALLINLA)	53,325	-7,122	1/6/1994	24	Climatic
CAHORE (Kilmichael House)	52,558	-6,207	1/9/1995	23	Climatic
BALLINCURRIG (Peafield)	52,007	-8,200	1/7/1996	22	Climatic
MALLOW (SpaHouse)	52,137	-8,634	1/8/1996	22	Climatic
DOOKS	52,067	-9,923	1/6/1997	21	Climatic

Table 13 Meteorological stations used to analyse the drought episode during the summer 2018 in Ireland.

8.3. Appendix 3. Remote sensing imagery

8.3.1. MODIS imagery

In Table 14 are presented the metadata about each single MODIS imagery used in the study. The algorithm package used to analyse the imagery is MOD_PR13A1 version 6 and the imagery are provided in two version of HDF, 2.17 and 2.19.

LOCAL GRANULE ID	LOCAL VERSION	PGE VERSION	PRODUCTION DATE TIME
MOD13Q1.A2000049.h17v03.006.2015136104734.hdf	6.0.14	6.0.27	2015-05-16T14:47:34.000Z
MOD13Q1.A2000065.h17v03.006.2015136023014.hdf	6.0.14	6.0.27	2015-05-16T06:30:14.000Z
MOD13Q1.A2000081.h17v03.006.2015136041159.hdf	6.0.14	6.0.27	2015-05-16T08:11:59.000Z
MOD13Q1.A2000097.h17v03.006.2015136041457.hdf	6.0.14	6.0.27	2015-05-16T08:14:57.000Z
MOD13Q1.A2000113.h17v03.006.2015137035219.hdf	6.0.14	6.0.27	2015-05-17T07:52:19.000Z
MOD13Q1.A2000129.h17v03.006.2015137053104.hdf	6.0.14	6.0.27	2015-05-17T09:31:04.000Z
MOD13Q1.A2000145.h17v03.006.2015137100116.hdf	6.0.14	6.0.27	2015-05-17T14:01:17.000Z
MOD13Q1.A2000161.h17v03.006.2015137044205.hdf	6.0.14	6.0.27	2015-05-17T08:42:05.000Z
MOD13Q1.A2000177.h17v03.006.2015138072156.hdf	6.0.14	6.0.27	2015-05-18T11:21:56.000Z
MOD13Q1.A2000193.h17v03.006.2015138080658.hdf	6.0.14	6.0.27	2015-05-18T12:06:58.000Z
MOD13Q1.A2000209.h17v03.006.2015138074425.hdf	6.0.14	6.0.27	2015-05-18T11:44:25.000Z
MOD13Q1.A2000225.h17v03.006.2015138075451.hdf	6.0.14	6.0.27	2015-05-18T11:54:51.000Z
MOD13Q1.A2000241.h17v03.006.2015138080659.hdf	6.0.14	6.0.27	2015-05-18T12:06:59.000Z
MOD13Q1.A2000257.h17v03.006.2015139074046.hdf	6.0.14	6.0.27	2015-05-19T11:40:46.000Z
MOD13Q1.A2000273.h17v03.006.2015139075249.hdf	6.0.14	6.0.27	2015-05-19T11:52:49.000Z
MOD13Q1.A2000289.h17v03.006.2015139085331.hdf	6.0.14	6.0.27	2015-05-19T12:53:31.000Z
MOD13Q1.A2000305.h17v03.006.2015139075621.hdf	6.0.14	6.0.27	2015-05-19T11:56:21.000Z
MOD13Q1.A2000321.h17v03.006.2015139221934.hdf	6.0.14	6.0.27	2015-05-20T02:19:34.000Z
MOD13Q1.A2000337.h17v03.006.2015140093442.hdf	6.0.14	6.0.27	2015-05-20T13:34:42.000Z
MOD13Q1.A2000353.h17v03.006.2017285144113.hdf	6.0.33	6.0.34	2017-10-12T18:41:13.000Z
MOD13Q1.A2001001.h17v03.006.2015140084907.hdf	6.0.14	6.0.27	2015-05-20T12:49:07.000Z
MOD13Q1.A2001017.h17v03.006.2015140092224.hdf	6.0.14	6.0.27	2015-05-20T13:22:24.000Z
MOD13Q1.A2001033.h17v03.006.2015141154200.hdf	6.0.14	6.0.27	2015-05-21T19:42:00.000Z
MOD13Q1.A2001049.h17v03.006.2015142165844.hdf	6.0.14	6.0.27	2015-05-22T20:58:44.000Z
MOD13Q1.A2001065.h17v03.006.2015142182740.hdf	6.0.14	6.0.27	2015-05-22T22:27:40.000Z
MOD13Q1.A2001081.h17v03.006.2015142191528.hdf	6.0.14	6.0.27	2015-05-22T23:15:28.000Z
MOD13Q1.A2001097.h17v03.006.2015142195347.hdf	6.0.14	6.0.27	2015-05-22T23:53:47.000Z
MOD13Q1.A2001113.h17v03.006.2015142195330.hdf	6.0.14	6.0.27	2015-05-22T23:53:30.000Z
MOD13Q1.A2001129.h17v03.006.2015142065614.hdf	6.0.14	6.0.27	2015-05-22T10:56:14.000Z
MOD13Q1.A2001145.h17v03.006.2015143102242.hdf	6.0.14	6.0.27	2015-05-23T14:22:42.000Z
MOD13Q1.A2001161.h17v03.006.2015143074140.hdf	6.0.14	6.0.27	2015-05-23T11:41:40.000Z
MOD13Q1.A2001177.h17v03.006.2015143095133.hdf	6.0.14	6.0.27	2015-05-23T13:51:33.000Z
MOD13Q1.A2001193.h17v03.006.2015143124338.hdf	6.0.14	6.0.27	2015-05-23T16:43:38.000Z
MOD13Q1.A2001209.h17v03.006.2015143163908.hdf	6.0.14	6.0.27	2015-05-23T20:39:08.000Z
MOD13Q1.A2001225.h17v03.006.2015144064539.hdf	6.0.14	6.0.27	2015-05-24T10:45:40.000Z
MOD13Q1.A2001241.h17v03.006.2015144063521.hdf	6.0.14	6.0.27	2015-05-24T10:35:21.000Z
MOD13Q1.A2001257.h17v03.006.2015144063517.hdf	6.0.14	6.0.27	2015-05-24T10:35:17.000Z

MOD13Q1.A2001273.h17v03.006.2015144062351.hdf	6.0.14	6.0.27	2015-05-24T10:23:52.000Z
MOD13Q1.A2001289.h17v03.006.2015146021532.hdf	6.0.14	6.0.27	2015-05-26T06:15:32.000Z
MOD13Q1.A2001305.h17v03.006.2015146023455.hdf	6.0.14	6.0.27	2015-05-26T06:34:55.000Z
MOD13Q1.A2001321.h17v03.006.2015146032004.hdf	6.0.14	6.0.27	2015-05-26T07:20:04.000Z
MOD13Q1.A2001337.h17v03.006.2015146040355.hdf	6.0.14	6.0.27	2015-05-26T08:03:55.000Z
MOD13Q1.A2001353.h17v03.006.2015146092423.hdf	6.0.14	6.0.27	2015-05-26T13:24:23.000Z
MOD13Q1.A2002001.h17v03.006.2015146145758.hdf	6.0.14	6.0.27	2015-05-26T18:57:58.000Z
MOD13Q1.A2002017.h17v03.006.2015146124741.hdf	6.0.14	6.0.27	2015-05-26T16:47:41.000Z
MOD13Q1.A2002033.h17v03.006.2015146145536.hdf	6.0.14	6.0.27	2015-05-26T18:55:36.000Z
MOD13Q1.A2002049.h17v03.006.2015146132038.hdf	6.0.14	6.0.27	2015-05-26T17:20:38.000Z
MOD13Q1.A2002065.h17v03.006.2015147121444.hdf	6.0.14	6.0.27	2015-05-27T16:14:44.000Z
MOD13Q1.A2002081.h17v03.006.2015147125733.hdf	6.0.14	6.0.27	2015-05-27T16:57:33.000Z
MOD13Q1.A2002097.h17v03.006.2015147214322.hdf	6.0.14	6.0.27	2015-05-28T01:43:22.000Z
MOD13Q1.A2002113.h17v03.006.2015147221118.hdf	6.0.14	6.0.27	2015-05-28T02:11:18.000Z
MOD13Q1.A2002129.h17v03.006.2015147233940.hdf	6.0.14	6.0.27	2015-05-28T03:39:40.000Z
MOD13Q1.A2002145.h17v03.006.2015148102623.hdf	6.0.14	6.0.27	2015-05-28T14:26:23.000Z
MOD13Q1.A2002161.h17v03.006.2015148094906.hdf	6.0.14	6.0.27	2015-05-28T13:49:06.000Z
MOD13Q1.A2002177.h17v03.006.2015149001355.hdf	6.0.14	6.0.27	2015-05-29T04:13:55.000Z
MOD13Q1.A2002193.h17v03.006.2015149035057.hdf	6.0.14	6.0.27	2015-05-29T07:50:57.000Z
MOD13Q1.A2002209.h17v03.006.2015149181301.hdf	6.0.14	6.0.27	2015-05-29T22:13:01.000Z
MOD13Q1.A2002225.h17v03.006.2015150025449.hdf	6.0.14	6.0.27	2015-05-30T06:54:49.000Z
MOD13Q1.A2002241.h17v03.006.2015150204858.hdf	6.0.14	6.0.27	2015-05-31T00:48:58.000Z
MOD13Q1.A2002257.h17v03.006.2015151084251.hdf	6.0.14	6.0.27	2015-05-31T12:42:51.000Z
MOD13Q1.A2002273.h17v03.006.2015151082040.hdf	6.0.14	6.0.27	2015-05-31T12:20:40.000Z
MOD13Q1.A2002289.h17v03.006.2015152040227.hdf	6.0.14	6.0.27	2015-06-01T08:02:27.000Z
MOD13Q1.A2002305.h17v03.006.2015152042044.hdf	6.0.14	6.0.27	2015-06-01T08:20:44.000Z
MOD13Q1.A2002321.h17v03.006.2015152185158.hdf	6.0.14	6.0.27	2015-06-01T22:51:58.000Z
MOD13Q1.A2002337.h17v03.006.2015153070756.hdf	6.0.14	6.0.27	2015-06-02T11:07:56.000Z
MOD13Q1.A2002353.h17v03.006.2015153025421.hdf	6.0.14	6.0.27	2015-06-02T06:54:21.000Z
MOD13Q1.A2003001.h17v03.006.2015153195253.hdf	6.0.14	6.0.27	2015-06-02T23:52:53.000Z
MOD13Q1.A2003017.h17v03.006.2015154060455.hdf	6.0.14	6.0.27	2015-06-03T10:04:55.000Z
MOD13Q1.A2003033.h17v03.006.2015156053701.hdf	6.0.14	6.0.27	2015-06-05T09:37:01.000Z
MOD13Q1.A2003049.h17v03.006.2015156083048.hdf	6.0.14	6.0.27	2015-06-05T12:30:48.000Z
MOD13Q1.A2003065.h17v03.006.2015156190601.hdf	6.0.14	6.0.27	2015-06-05T23:06:01.000Z
MOD13Q1.A2003081.h17v03.006.2015156190641.hdf	6.0.14	6.0.27	2015-06-05T23:06:41.000Z
MOD13Q1.A2003097.h17v03.006.2015158152039.hdf	6.0.14	6.0.27	2015-06-07T19:20:39.000Z
MOD13Q1.A2003113.h17v03.006.2015158152355.hdf	6.0.14	6.0.27	2015-06-07T19:23:55.000Z
MOD13Q1.A2003129.h17v03.006.2015158153812.hdf	6.0.14	6.0.27	2015-06-07T19:38:12.000Z
MOD13Q1.A2003145.h17v03.006.2015158154545.hdf	6.0.14	6.0.27	2015-06-07T19:45:45.000Z
MOD13Q1.A2003161.h17v03.006.2015159143732.hdf	6.0.14	6.0.27	2015-06-08T18:37:32.000Z
MOD13Q1.A2003177.h17v03.006.2015161133259.hdf	6.0.14	6.0.27	2015-06-10T17:32:59.000Z
MOD13Q1.A2003193.h17v03.006.2015153110431.hdf	6.0.14	6.0.27	2015-06-02T15:04:31.000Z
MOD13Q1.A2003209.h17v03.006.2015153105857.hdf	6.0.14	6.0.27	2015-06-02T14:58:57.000Z
MOD13Q1.A2003225.h17v03.006.2015153114228.hdf	6.0.14	6.0.27	2015-06-02T15:42:28.000Z
MOD13Q1.A2003241.h17v03.006.2015153114010.hdf	6.0.14	6.0.27	2015-06-02T15:40:10.000Z
MOD13Q1.A2003257.h17v03.006.2015153114315.hdf	6.0.14	6.0.27	2015-06-02T15:43:15.000Z
MOD13Q1.A2003273.h17v03.006.2015153115241.hdf	6.0.14	6.0.27	2015-06-02T15:52:41.000Z
MOD13Q1.A2003289.h17v03.006.2015153121339.hdf	6.0.14	6.0.27	2015-06-02T16:13:39.000Z
MOD13Q1.A2003305.h17v03.006.2015153124757.hdf	6.0.14	6.0.27	2015-06-02T16:47:57.000Z
MOD13Q1.A2003321.h17v03.006.2015153130235.hdf	6.0.14	6.0.27	2015-06-02T17:02:35.000Z

MOD13Q1.A2003337.h17v03.006.2015153125814.hdf	6.0.14	6.0.27	2015-06-02T16:58:14.000Z
MOD13Q1.A2003353.h17v03.006.2017285165751.hdf	6.0.33	6.0.34	2017-10-12T20:57:51.000Z
MOD13Q1.A2004001.h17v03.006.2015154121223.hdf	6.0.14	6.0.27	2015-06-03T16:12:23.000Z
MOD13Q1.A2004017.h17v03.006.2015154121202.hdf	6.0.14	6.0.27	2015-06-03T16:12:02.000Z
MOD13Q1.A2004033.h17v03.006.2015154122955.hdf	6.0.14	6.0.27	2015-06-03T16:29:55.000Z
MOD13Q1.A2004049.h17v03.006.2015154125717.hdf	6.0.14	6.0.27	2015-06-03T16:57:17.000Z
MOD13Q1.A2004065.h17v03.006.2015154124839.hdf	6.0.14	6.0.27	2015-06-03T16:48:39.000Z
MOD13Q1.A2004081.h17v03.006.2015154125239.hdf	6.0.14	6.0.27	2015-06-03T16:52:39.000Z
MOD13Q1.A2004097.h17v03.006.2015154125059.hdf	6.0.14	6.0.27	2015-06-03T16:50:59.000Z
MOD13Q1.A2004113.h17v03.006.2015154125834.hdf	6.0.14	6.0.27	2015-06-03T16:58:34.000Z
MOD13Q1.A2004129.h17v03.006.2015154125727.hdf	6.0.14	6.0.27	2015-06-03T16:57:27.000Z
MOD13Q1.A2004145.h17v03.006.2015154130010.hdf	6.0.14	6.0.27	2015-06-03T17:00:10.000Z
MOD13Q1.A2004161.h17v03.006.2015154131615.hdf	6.0.14	6.0.27	2015-06-03T17:16:16.000Z
MOD13Q1.A2004177.h17v03.006.2015154132119.hdf	6.0.14	6.0.27	2015-06-03T17:21:19.000Z
MOD13Q1.A2004193.h17v03.006.2015154131841.hdf	6.0.14	6.0.27	2015-06-03T17:18:41.000Z
MOD13Q1.A2004209.h17v03.006.2015154132708.hdf	6.0.14	6.0.27	2015-06-03T17:27:08.000Z
MOD13Q1.A2004225.h17v03.006.2015154133159.hdf	6.0.14	6.0.27	2015-06-03T17:31:59.000Z
MOD13Q1.A2004241.h17v03.006.2015154134252.hdf	6.0.14	6.0.27	2015-06-03T17:42:52.000Z
MOD13Q1.A2004257.h17v03.006.2015154134224.hdf	6.0.14	6.0.27	2015-06-03T17:42:24.000Z
MOD13Q1.A2004273.h17v03.006.2015154135331.hdf	6.0.14	6.0.27	2015-06-03T17:53:31.000Z
MOD13Q1.A2004289.h17v03.006.2015154140648.hdf	6.0.14	6.0.27	2015-06-03T18:06:48.000Z
MOD13Q1.A2004305.h17v03.006.2015154140716.hdf	6.0.14	6.0.27	2015-06-03T18:07:17.000Z
MOD13Q1.A2004321.h17v03.006.2015154140830.hdf	6.0.14	6.0.27	2015-06-03T18:08:30.000Z
MOD13Q1.A2004337.h17v03.006.2015154141255.hdf	6.0.14	6.0.27	2015-06-03T18:12:55.000Z
MOD13Q1.A2004353.h17v03.006.2015154141715.hdf	6.0.14	6.0.27	2015-06-03T18:17:15.000Z
MOD13Q1.A2005001.h17v03.006.2015157040916.hdf	6.0.14	6.0.27	2015-06-06T08:09:17.000Z
MOD13Q1.A2005017.h17v03.006.2015157044742.hdf	6.0.14	6.0.27	2015-06-06T08:47:42.000Z
MOD13Q1.A2005033.h17v03.006.2015157044843.hdf	6.0.14	6.0.27	2015-06-06T08:48:43.000Z
MOD13Q1.A2005049.h17v03.006.2015157043913.hdf	6.0.14	6.0.27	2015-06-06T08:39:13.000Z
MOD13Q1.A2005065.h17v03.006.2015157045019.hdf	6.0.14	6.0.27	2015-06-06T08:50:19.000Z
MOD13Q1.A2005081.h17v03.006.2015157045435.hdf	6.0.14	6.0.27	2015-06-06T08:54:35.000Z
MOD13Q1.A2005097.h17v03.006.2015157052317.hdf	6.0.14	6.0.27	2015-06-06T09:23:17.000Z
MOD13Q1.A2005113.h17v03.006.2015157052239.hdf	6.0.14	6.0.27	2015-06-06T09:22:39.000Z
MOD13Q1.A2005129.h17v03.006.2015157052326.hdf	6.0.14	6.0.27	2015-06-06T09:23:26.000Z
MOD13Q1.A2005145.h17v03.006.2015157053216.hdf	6.0.14	6.0.27	2015-06-06T09:32:16.000Z
MOD13Q1.A2005161.h17v03.006.2015157052714.hdf	6.0.14	6.0.27	2015-06-06T09:27:14.000Z
MOD13Q1.A2005177.h17v03.006.2015157054249.hdf	6.0.14	6.0.27	2015-06-06T09:42:49.000Z
MOD13Q1.A2005193.h17v03.006.2015157054313.hdf	6.0.14	6.0.27	2015-06-06T09:43:13.000Z
MOD13Q1.A2005209.h17v03.006.2015157060040.hdf	6.0.14	6.0.27	2015-06-06T10:00:40.000Z
MOD13Q1.A2005225.h17v03.006.2015157055820.hdf	6.0.14	6.0.27	2015-06-06T09:58:20.000Z
MOD13Q1.A2005241.h17v03.006.2015157061751.hdf	6.0.14	6.0.27	2015-06-06T10:17:51.000Z
MOD13Q1.A2005257.h17v03.006.2015157060828.hdf	6.0.14	6.0.27	2015-06-06T10:08:28.000Z
MOD13Q1.A2005273.h17v03.006.2015157060450.hdf	6.0.14	6.0.27	2015-06-06T10:04:50.000Z
MOD13Q1.A2005289.h17v03.006.2015157061809.hdf	6.0.14	6.0.27	2015-06-06T10:18:09.000Z
MOD13Q1.A2005305.h17v03.006.2015157061857.hdf	6.0.14	6.0.27	2015-06-06T10:18:57.000Z
MOD13Q1.A2005321.h17v03.006.2015157063033.hdf	6.0.14	6.0.27	2015-06-06T10:30:33.000Z
MOD13Q1.A2005337.h17v03.006.2015157063312.hdf	6.0.14	6.0.27	2015-06-06T10:33:12.000Z
MOD13Q1.A2005353.h17v03.006.2015157063533.hdf	6.0.14	6.0.27	2015-06-06T10:35:33.000Z
MOD13Q1.A2006001.h17v03.006.2015161092258.hdf	6.0.14	6.0.27	2015-06-10T13:22:58.000Z
MOD13Q1.A2006017.h17v03.006.2015161112625.hdf	6.0.14	6.0.27	2015-06-10T15:26:25.000Z

MOD13Q1.A2006033.h17v03.006.2015161113857.hdf	6.0.14	6.0.27	2015-06-10T15:38:57.000Z
MOD13Q1.A2006049.h17v03.006.2015161115816.hdf	6.0.14	6.0.27	2015-06-10T15:58:16.000Z
MOD13Q1.A2006065.h17v03.006.2015161120022.hdf	6.0.14	6.0.27	2015-06-10T16:00:22.000Z
MOD13Q1.A2006081.h17v03.006.2015161120747.hdf	6.0.14	6.0.27	2015-06-10T16:07:47.000Z
MOD13Q1.A2006097.h17v03.006.2015161151343.hdf	6.0.14	6.0.27	2015-06-10T19:13:43.000Z
MOD13Q1.A2006113.h17v03.006.2015161152806.hdf	6.0.14	6.0.27	2015-06-10T19:28:06.000Z
MOD13Q1.A2006129.h17v03.006.2015161162607.hdf	6.0.14	6.0.27	2015-06-10T20:26:07.000Z
MOD13Q1.A2006145.h17v03.006.2015161162613.hdf	6.0.14	6.0.27	2015-06-10T20:26:13.000Z
MOD13Q1.A2006161.h17v03.006.2015161173742.hdf	6.0.14	6.0.27	2015-06-10T21:37:42.000Z
MOD13Q1.A2006177.h17v03.006.2015161173250.hdf	6.0.14	6.0.27	2015-06-10T21:32:50.000Z
MOD13Q1.A2006193.h17v03.006.2015161174502.hdf	6.0.14	6.0.27	2015-06-10T21:45:03.000Z
MOD13Q1.A2006209.h17v03.006.2015161192305.hdf	6.0.14	6.0.27	2015-06-10T23:23:05.000Z
MOD13Q1.A2006225.h17v03.006.2015161192918.hdf	6.0.14	6.0.27	2015-06-10T23:29:18.000Z
MOD13Q1.A2006241.h17v03.006.2015161195242.hdf	6.0.14	6.0.27	2015-06-10T23:52:42.000Z
MOD13Q1.A2006257.h17v03.006.2015161200918.hdf	6.0.14	6.0.27	2015-06-11T00:09:18.000Z
MOD13Q1.A2006273.h17v03.006.2015161201145.hdf	6.0.14	6.0.27	2015-06-11T00:11:45.000Z
MOD13Q1.A2006289.h17v03.006.2015161205540.hdf	6.0.14	6.0.27	2015-06-11T00:55:40.000Z
MOD13Q1.A2006305.h17v03.006.2015161205836.hdf	6.0.14	6.0.27	2015-06-11T00:58:36.000Z
MOD13Q1.A2006321.h17v03.006.2015161211853.hdf	6.0.14	6.0.27	2015-06-11T01:18:53.000Z
MOD13Q1.A2006337.h17v03.006.2015161213414.hdf	6.0.14	6.0.27	2015-06-11T01:34:14.000Z
MOD13Q1.A2006353.h17v03.006.2015161215348.hdf	6.0.14	6.0.27	2015-06-11T01:53:49.000Z
MOD13Q1.A2007001.h17v03.006.2015160165444.hdf	6.0.14	6.0.27	2015-06-09T20:54:44.000Z
MOD13Q1.A2007017.h17v03.006.2015161221416.hdf	6.0.14	6.0.27	2015-06-11T02:14:16.000Z
MOD13Q1.A2007033.h17v03.006.2015161221820.hdf	6.0.14	6.0.27	2015-06-11T02:18:20.000Z
MOD13Q1.A2007049.h17v03.006.2015161222530.hdf	6.0.14	6.0.27	2015-06-11T02:25:30.000Z
MOD13Q1.A2007065.h17v03.006.2015161224344.hdf	6.0.14	6.0.27	2015-06-11T02:43:44.000Z
MOD13Q1.A2007081.h17v03.006.2015161230318.hdf	6.0.14	6.0.27	2015-06-11T03:03:18.000Z
MOD13Q1.A2007097.h17v03.006.2015161233411.hdf	6.0.14	6.0.27	2015-06-11T03:34:11.000Z
MOD13Q1.A2007113.h17v03.006.2015161232858.hdf	6.0.14	6.0.27	2015-06-11T03:28:58.000Z
MOD13Q1.A2007129.h17v03.006.2015161233922.hdf	6.0.14	6.0.27	2015-06-11T03:39:22.000Z
MOD13Q1.A2007145.h17v03.006.2015161235513.hdf	6.0.14	6.0.27	2015-06-11T03:55:13.000Z
MOD13Q1.A2007161.h17v03.006.2015162000302.hdf	6.0.14	6.0.27	2015-06-11T04:03:02.000Z
MOD13Q1.A2007177.h17v03.006.2015162001734.hdf	6.0.14	6.0.27	2015-06-11T04:17:34.000Z
MOD13Q1.A2007193.h17v03.006.2015162003521.hdf	6.0.14	6.0.27	2015-06-11T04:35:21.000Z
MOD13Q1.A2007209.h17v03.006.2015164013752.hdf	6.0.14	6.0.27	2015-06-13T05:37:52.000Z
MOD13Q1.A2007225.h17v03.006.2015164160927.hdf	6.0.14	6.0.27	2015-06-13T20:09:27.000Z
MOD13Q1.A2007241.h17v03.006.2015164183846.hdf	6.0.14	6.0.27	2015-06-13T22:38:46.000Z
MOD13Q1.A2007257.h17v03.006.2015167042424.hdf	6.0.14	6.0.27	2015-06-16T08:24:24.000Z
MOD13Q1.A2007273.h17v03.006.2015167051508.hdf	6.0.14	6.0.27	2015-06-16T09:15:08.000Z
MOD13Q1.A2007289.h17v03.006.2015167192710.hdf	6.0.14	6.0.27	2015-06-16T23:27:10.000Z
MOD13Q1.A2007305.h17v03.006.2015168084602.hdf	6.0.14	6.0.27	2015-06-17T12:46:02.000Z
MOD13Q1.A2007321.h17v03.006.2015168094348.hdf	6.0.14	6.0.27	2015-06-17T13:43:48.000Z
MOD13Q1.A2007337.h17v03.006.2015169044421.hdf	6.0.14	6.0.27	2015-06-18T08:44:21.000Z
MOD13Q1.A2007353.h17v03.006.2017285170239.hdf	6.0.33	6.0.34	2017-10-12T21:02:39.000Z
MOD13Q1.A2008001.h17v03.006.2015169101054.hdf	6.0.14	6.0.27	2015-06-18T14:10:54.000Z
MOD13Q1.A2008017.h17v03.006.2015170042509.hdf	6.0.14	6.0.27	2015-06-19T08:25:09.000Z
MOD13Q1.A2008033.h17v03.006.2015170043658.hdf	6.0.14	6.0.27	2015-06-19T08:36:58.000Z
MOD13Q1.A2008049.h17v03.006.2015172132113.hdf	6.0.14	6.0.27	2015-06-21T17:21:14.000Z
MOD13Q1.A2008065.h17v03.006.2015172181625.hdf	6.0.14	6.0.27	2015-06-21T22:16:25.000Z
MOD13Q1.A2008081.h17v03.006.2015173020810.hdf	6.0.14	6.0.27	2015-06-22T06:08:10.000Z

MOD13Q1.A2008097.h17v03.006.2015173055705.hdf	6.0.14	6.0.27	2015-06-22T09:57:05.000Z
MOD13Q1.A2008113.h17v03.006.2015173162756.hdf	6.0.14	6.0.27	2015-06-22T20:27:56.000Z
MOD13Q1.A2008129.h17v03.006.2015175092227.hdf	6.0.14	6.0.27	2015-06-24T13:22:27.000Z
MOD13Q1.A2008145.h17v03.006.2015175110847.hdf	6.0.14	6.0.27	2015-06-24T15:08:47.000Z
MOD13Q1.A2008161.h17v03.006.2015176074328.hdf	6.0.14	6.0.27	2015-06-25T11:43:28.000Z
MOD13Q1.A2008177.h17v03.006.2015176075015.hdf	6.0.14	6.0.27	2015-06-25T11:50:15.000Z
MOD13Q1.A2008193.h17v03.006.2015177040500.hdf	6.0.14	6.0.27	2015-06-26T08:05:00.000Z
MOD13Q1.A2008209.h17v03.006.2015177051611.hdf	6.0.14	6.0.27	2015-06-26T09:16:11.000Z
MOD13Q1.A2008225.h17v03.006.2015178165410.hdf	6.0.14	6.0.27	2015-06-27T20:54:10.000Z
MOD13Q1.A2008241.h17v03.006.2015179220314.hdf	6.0.14	6.0.27	2015-06-29T02:03:14.000Z
MOD13Q1.A2008257.h17v03.006.2015179222818.hdf	6.0.14	6.0.27	2015-06-29T02:28:18.000Z
MOD13Q1.A2008273.h17v03.006.2015180221530.hdf	6.0.14	6.0.27	2015-06-30T02:15:30.000Z
MOD13Q1.A2008289.h17v03.006.2015180224349.hdf	6.0.14	6.0.27	2015-06-30T02:43:49.000Z
MOD13Q1.A2008305.h17v03.006.2015181144824.hdf	6.0.14	6.0.27	2015-06-30T18:48:24.000Z
MOD13Q1.A2008321.h17v03.006.2015181150037.hdf	6.0.14	6.0.27	2015-06-30T19:00:38.000Z
MOD13Q1.A2008337.h17v03.006.2015184002953.hdf	6.0.14	6.0.27	2015-07-03T04:29:53.000Z
MOD13Q1.A2008353.h17v03.006.2015186055721.hdf	6.0.14	6.0.27	2015-07-05T09:57:21.000Z
MOD13Q1.A2009001.h17v03.006.2015186061542.hdf	6.0.14	6.0.27	2015-07-05T10:15:42.000Z
MOD13Q1.A2009017.h17v03.006.2015186063500.hdf	6.0.14	6.0.27	2015-07-05T10:35:01.000Z
MOD13Q1.A2009033.h17v03.006.2015187063345.hdf	6.0.14	6.0.27	2015-07-06T10:33:45.000Z
MOD13Q1.A2009049.h17v03.006.2015187064257.hdf	6.0.14	6.0.27	2015-07-06T10:42:57.000Z
MOD13Q1.A2009065.h17v03.006.2015188085721.hdf	6.0.14	6.0.27	2015-07-07T12:57:21.000Z
MOD13Q1.A2009081.h17v03.006.2015188092042.hdf	6.0.14	6.0.27	2015-07-07T13:20:42.000Z
MOD13Q1.A2009097.h17v03.006.2015189152625.hdf	6.0.14	6.0.27	2015-07-08T19:26:25.000Z
MOD13Q1.A2009113.h17v03.006.2015189143459.hdf	6.0.14	6.0.27	2015-07-08T18:34:59.000Z
MOD13Q1.A2009129.h17v03.006.2015189212253.hdf	6.0.14	6.0.27	2015-07-09T01:22:53.000Z
MOD13Q1.A2009145.h17v03.006.2015190120330.hdf	6.0.14	6.0.27	2015-07-09T16:03:30.000Z
MOD13Q1.A2009161.h17v03.006.2015190223539.hdf	6.0.14	6.0.27	2015-07-10T02:35:40.000Z
MOD13Q1.A2009177.h17v03.006.2015191094903.hdf	6.0.14	6.0.27	2015-07-10T13:49:03.000Z
MOD13Q1.A2009193.h17v03.006.2015192141837.hdf	6.0.14	6.0.27	2015-07-11T18:18:37.000Z
MOD13Q1.A2009209.h17v03.006.2015192141853.hdf	6.0.14	6.0.27	2015-07-11T18:18:53.000Z
MOD13Q1.A2009225.h17v03.006.2015194151102.hdf	6.0.14	6.0.27	2015-07-13T19:11:02.000Z
MOD13Q1.A2009241.h17v03.006.2015194151100.hdf	6.0.14	6.0.27	2015-07-13T19:11:00.000Z
MOD13Q1.A2009257.h17v03.006.2015194225106.hdf	6.0.14	6.0.27	2015-07-14T02:51:06.000Z
MOD13Q1.A2009273.h17v03.006.2015195130713.hdf	6.0.14	6.0.27	2015-07-14T17:07:13.000Z
MOD13Q1.A2009289.h17v03.006.2015195224046.hdf	6.0.14	6.0.27	2015-07-15T02:40:46.000Z
MOD13Q1.A2009305.h17v03.006.2015196133745.hdf	6.0.14	6.0.27	2015-07-15T17:37:45.000Z
MOD13Q1.A2009321.h17v03.006.2015196201843.hdf	6.0.14	6.0.27	2015-07-16T00:18:43.000Z
MOD13Q1.A2009337.h17v03.006.2015197071733.hdf	6.0.14	6.0.27	2015-07-16T11:17:33.000Z
MOD13Q1.A2009353.h17v03.006.2015198031358.hdf	6.0.14	6.0.27	2015-07-17T07:13:58.000Z
MOD13Q1.A2010001.h17v03.006.2015198104338.hdf	6.0.14	6.0.27	2015-07-17T14:43:38.000Z
MOD13Q1.A2010017.h17v03.006.2015198195615.hdf	6.0.14	6.0.27	2015-07-17T23:56:15.000Z
MOD13Q1.A2010033.h17v03.006.2015199120758.hdf	6.0.14	6.0.27	2015-07-18T16:07:58.000Z
MOD13Q1.A2010049.h17v03.006.2015200023222.hdf	6.0.14	6.0.27	2015-07-19T06:32:22.000Z
MOD13Q1.A2010065.h17v03.006.2015206075223.hdf	6.0.14	6.0.27	2015-07-25T11:52:23.000Z
MOD13Q1.A2010081.h17v03.006.2015206075610.hdf	6.0.14	6.0.27	2015-07-25T11:56:10.000Z
MOD13Q1.A2010097.h17v03.006.2015206224856.hdf	6.0.14	6.0.27	2015-07-26T02:48:57.000Z
MOD13Q1.A2010113.h17v03.006.2015207160254.hdf	6.0.14	6.0.27	2015-07-26T20:02:55.000Z
MOD13Q1.A2010129.h17v03.006.2015207185811.hdf	6.0.14	6.0.27	2015-07-26T22:58:11.000Z
MOD13Q1.A2010145.h17v03.006.2015208151712.hdf	6.0.14	6.0.27	2015-07-27T19:17:12.000Z

MOD13Q1.A2010161.h17v03.006.2015208193606.hdf	6.0.14	6.0.27	2015-07-27T23:36:06.000Z
MOD13Q1.A2010177.h17v03.006.2015208204230.hdf	6.0.14	6.0.27	2015-07-28T00:42:30.000Z
MOD13Q1.A2010193.h17v03.006.2015209100517.hdf	6.0.14	6.0.27	2015-07-28T14:05:17.000Z
MOD13Q1.A2010209.h17v03.006.2015209152802.hdf	6.0.14	6.0.27	2015-07-28T19:28:02.000Z
MOD13Q1.A2010225.h17v03.006.2015210090855.hdf	6.0.14	6.0.27	2015-07-29T13:08:55.000Z
MOD13Q1.A2010241.h17v03.006.2015210102407.hdf	6.0.14	6.0.27	2015-07-29T14:24:07.000Z
MOD13Q1.A2010257.h17v03.006.2015211025457.hdf	6.0.14	6.0.27	2015-07-30T06:54:57.000Z
MOD13Q1.A2010273.h17v03.006.2015211142241.hdf	6.0.14	6.0.27	2015-07-30T18:22:42.000Z
MOD13Q1.A2010289.h17v03.006.2015211230007.hdf	6.0.14	6.0.27	2015-07-31T03:00:07.000Z
MOD13Q1.A2010305.h17v03.006.2015213081642.hdf	6.0.14	6.0.27	2015-08-01T12:16:42.000Z
MOD13Q1.A2010321.h17v03.006.2015213085333.hdf	6.0.14	6.0.27	2015-08-01T12:53:33.000Z
MOD13Q1.A2010337.h17v03.006.2015213174258.hdf	6.0.14	6.0.27	2015-08-01T21:42:58.000Z
MOD13Q1.A2010353.h17v03.006.2015216041403.hdf	6.0.14	6.0.27	2015-08-04T08:14:04.000Z
MOD13Q1.A2011001.h17v03.006.2015216114414.hdf	6.0.14	6.0.27	2015-08-04T15:44:14.000Z
MOD13Q1.A2011017.h17v03.006.2015216150431.hdf	6.0.14	6.0.27	2015-08-04T19:04:31.000Z
MOD13Q1.A2011033.h17v03.006.2015216132121.hdf	6.0.14	6.0.27	2015-08-04T17:21:21.000Z
MOD13Q1.A2011049.h17v03.006.2015216133132.hdf	6.0.14	6.0.27	2015-08-04T17:31:32.000Z
MOD13Q1.A2011065.h17v03.006.2015217064502.hdf	6.0.14	6.0.27	2015-08-05T10:45:02.000Z
MOD13Q1.A2011081.h17v03.006.2015217160802.hdf	6.0.14	6.0.27	2015-08-05T20:08:02.000Z
MOD13Q1.A2011097.h17v03.006.2015218081159.hdf	6.0.14	6.0.27	2015-08-06T12:12:00.000Z
MOD13Q1.A2011113.h17v03.006.2015218102946.hdf	6.0.14	6.0.27	2015-08-06T14:29:46.000Z
MOD13Q1.A2011129.h17v03.006.2015219104715.hdf	6.0.14	6.0.27	2015-08-07T14:47:15.000Z
MOD13Q1.A2011145.h17v03.006.2015219145928.hdf	6.0.14	6.0.27	2015-08-07T18:59:28.000Z
MOD13Q1.A2011161.h17v03.006.2015219192156.hdf	6.0.14	6.0.27	2015-08-07T23:21:56.000Z
MOD13Q1.A2011177.h17v03.006.2015220084052.hdf	6.0.14	6.0.27	2015-08-08T12:40:52.000Z
MOD13Q1.A2011193.h17v03.006.2015220140117.hdf	6.0.14	6.0.27	2015-08-08T18:01:17.000Z
MOD13Q1.A2011209.h17v03.006.2015221074943.hdf	6.0.14	6.0.27	2015-08-09T11:49:43.000Z
MOD13Q1.A2011225.h17v03.006.2015221114006.hdf	6.0.14	6.0.27	2015-08-09T15:40:06.000Z
MOD13Q1.A2011241.h17v03.006.2015221213234.hdf	6.0.14	6.0.27	2015-08-10T01:32:35.000Z
MOD13Q1.A2011257.h17v03.006.2015222094406.hdf	6.0.14	6.0.27	2015-08-10T13:44:06.000Z
MOD13Q1.A2011273.h17v03.006.2015222122446.hdf	6.0.14	6.0.27	2015-08-10T16:24:47.000Z
MOD13Q1.A2011289.h17v03.006.2015229094537.hdf	6.0.14	6.0.27	2015-08-17T13:45:37.000Z
MOD13Q1.A2011305.h17v03.006.2015229102943.hdf	6.0.14	6.0.27	2015-08-17T14:29:44.000Z
MOD13Q1.A2011321.h17v03.006.2015229115709.hdf	6.0.14	6.0.27	2015-08-17T15:57:10.000Z
MOD13Q1.A2011337.h17v03.006.2015229235626.hdf	6.0.14	6.0.27	2015-08-18T03:56:26.000Z
MOD13Q1.A2011353.h17v03.006.2015230014304.hdf	6.0.14	6.0.27	2015-08-18T05:43:04.000Z
MOD13Q1.A2012001.h17v03.006.2015236171001.hdf	6.0.14	6.0.27	2015-08-24T21:10:01.000Z
MOD13Q1.A2012017.h17v03.006.2015237084718.hdf	6.0.14	6.0.27	2015-08-25T12:47:18.000Z
MOD13Q1.A2012033.h17v03.006.2015237195448.hdf	6.0.14	6.0.27	2015-08-25T23:54:48.000Z
MOD13Q1.A2012049.h17v03.006.2015238134423.hdf	6.0.14	6.0.27	2015-08-26T17:44:23.000Z
MOD13Q1.A2012065.h17v03.006.2015238152529.hdf	6.0.14	6.0.27	2015-08-26T19:25:29.000Z
MOD13Q1.A2012081.h17v03.006.2015239235820.hdf	6.0.14	6.0.27	2015-08-28T03:58:20.000Z
MOD13Q1.A2012097.h17v03.006.2015240114950.hdf	6.0.14	6.0.27	2015-08-28T15:49:50.000Z
MOD13Q1.A2012113.h17v03.006.2015240193547.hdf	6.0.14	6.0.27	2015-08-28T23:35:47.000Z
MOD13Q1.A2012129.h17v03.006.2015246095519.hdf	6.0.14	6.0.27	2015-09-03T13:55:19.000Z
MOD13Q1.A2012145.h17v03.006.2015246100235.hdf	6.0.14	6.0.27	2015-09-03T14:02:35.000Z
MOD13Q1.A2012161.h17v03.006.2015247055809.hdf	6.0.14	6.0.27	2015-09-04T09:58:09.000Z
MOD13Q1.A2012177.h17v03.006.2015247081015.hdf	6.0.14	6.0.27	2015-09-04T12:10:15.000Z
MOD13Q1.A2012193.h17v03.006.2015247171002.hdf	6.0.14	6.0.27	2015-09-04T21:10:02.000Z
MOD13Q1.A2012209.h17v03.006.2015248104903.hdf	6.0.14	6.0.27	2015-09-05T14:49:03.000Z

MOD13Q1.A2012225.h17v03.006.2015248124325.hdf	6.0.14	6.0.27	2015-09-05T16:43:25.000Z
MOD13Q1.A2012241.h17v03.006.2015249122438.hdf	6.0.14	6.0.27	2015-09-06T16:24:38.000Z
MOD13Q1.A2012257.h17v03.006.2015249155031.hdf	6.0.14	6.0.27	2015-09-06T19:50:31.000Z
MOD13Q1.A2012273.h17v03.006.2015249215631.hdf	6.0.14	6.0.27	2015-09-07T01:56:31.000Z
MOD13Q1.A2012289.h17v03.006.2015251140105.hdf	6.0.14	6.0.27	2015-09-08T18:01:05.000Z
MOD13Q1.A2012305.h17v03.006.2015251162143.hdf	6.0.14	6.0.27	2015-09-08T20:21:43.000Z
MOD13Q1.A2012321.h17v03.006.2015252201040.hdf	6.0.14	6.0.27	2015-09-10T00:10:40.000Z
MOD13Q1.A2012337.h17v03.006.2015252233348.hdf	6.0.14	6.0.27	2015-09-10T03:33:48.000Z
MOD13Q1.A2012353.h17v03.006.2015253232556.hdf	6.0.14	6.0.27	2015-09-11T03:25:57.000Z
MOD13Q1.A2013001.h17v03.006.2015254154741.hdf	6.0.14	6.0.27	2015-09-11T19:47:41.000Z
MOD13Q1.A2013017.h17v03.006.2015254145811.hdf	6.0.14	6.0.27	2015-09-11T18:58:11.000Z
MOD13Q1.A2013033.h17v03.006.2015256072224.hdf	6.0.14	6.0.27	2015-09-13T11:22:24.000Z
MOD13Q1.A2013049.h17v03.006.2015256174319.hdf	6.0.14	6.0.27	2015-09-13T21:43:19.000Z
MOD13Q1.A2013065.h17v03.006.2015256181458.hdf	6.0.14	6.0.27	2015-09-13T22:14:58.000Z
MOD13Q1.A2013081.h17v03.006.2015257073759.hdf	6.0.14	6.0.27	2015-09-14T11:37:59.000Z
MOD13Q1.A2013097.h17v03.006.2015257101526.hdf	6.0.14	6.0.27	2015-09-14T14:15:26.000Z
MOD13Q1.A2013113.h17v03.006.2015260130105.hdf	6.0.14	6.0.27	2015-09-17T17:01:05.000Z
MOD13Q1.A2013129.h17v03.006.2015260163001.hdf	6.0.14	6.0.27	2015-09-17T20:30:01.000Z
MOD13Q1.A2013145.h17v03.006.2015261185531.hdf	6.0.14	6.0.27	2015-09-18T22:55:31.000Z
MOD13Q1.A2013161.h17v03.006.2015262164206.hdf	6.0.14	6.0.27	2015-09-19T20:42:06.000Z
MOD13Q1.A2013177.h17v03.006.2015262164137.hdf	6.0.14	6.0.27	2015-09-19T20:41:37.000Z
MOD13Q1.A2013193.h17v03.006.2015264062906.hdf	6.0.14	6.0.27	2015-09-21T10:29:06.000Z
MOD13Q1.A2013209.h17v03.006.2015267153435.hdf	6.0.14	6.0.27	2015-09-24T19:34:35.000Z
MOD13Q1.A2013225.h17v03.006.2015267220402.hdf	6.0.14	6.0.27	2015-09-25T02:04:02.000Z
MOD13Q1.A2013241.h17v03.006.2015268074539.hdf	6.0.14	6.0.27	2015-09-25T11:45:39.000Z
MOD13Q1.A2013257.h17v03.006.2015268080107.hdf	6.0.14	6.0.27	2015-09-25T12:01:07.000Z
MOD13Q1.A2013273.h17v03.006.2015269192124.hdf	6.0.14	6.0.27	2015-09-26T23:21:24.000Z
MOD13Q1.A2013289.h17v03.006.2015269224103.hdf	6.0.14	6.0.27	2015-09-27T02:41:03.000Z
MOD13Q1.A2013305.h17v03.006.2015270191903.hdf	6.0.14	6.0.27	2015-09-27T23:19:03.000Z
MOD13Q1.A2013321.h17v03.006.2015271103205.hdf	6.0.14	6.0.27	2015-09-28T14:32:05.000Z
MOD13Q1.A2013337.h17v03.006.2015271134944.hdf	6.0.14	6.0.27	2015-09-28T17:49:44.000Z
MOD13Q1.A2013353.h17v03.006.2018226110010.hdf	6.0.33	6.0.35	2018-08-14T15:00:10.000Z
MOD13Q1.A2014001.h17v03.006.2015272062512.hdf	6.0.14	6.0.27	2015-09-29T10:25:12.000Z
MOD13Q1.A2014017.h17v03.006.2015273225843.hdf	6.0.14	6.0.27	2015-10-01T02:58:43.000Z
MOD13Q1.A2014033.h17v03.006.2015274230621.hdf	6.0.14	6.0.27	2015-10-02T03:06:21.000Z
MOD13Q1.A2014049.h17v03.006.2015274230853.hdf	6.0.14	6.0.27	2015-10-02T03:08:53.000Z
MOD13Q1.A2014065.h17v03.006.2015276175512.hdf	6.0.14	6.0.27	2015-10-03T21:55:12.000Z
MOD13Q1.A2014081.h17v03.006.2015276221542.hdf	6.0.14	6.0.27	2015-10-04T02:15:42.000Z
MOD13Q1.A2014097.h17v03.006.2015278233534.hdf	6.0.14	6.0.27	2015-10-06T03:35:34.000Z
MOD13Q1.A2014113.h17v03.006.2015281100812.hdf	6.0.14	6.0.27	2015-10-08T14:08:12.000Z
MOD13Q1.A2014129.h17v03.006.2015281105051.hdf	6.0.14	6.0.27	2015-10-08T14:50:51.000Z
MOD13Q1.A2014145.h17v03.006.2015287233418.hdf	6.0.14	6.0.27	2015-10-15T03:34:19.000Z
MOD13Q1.A2014161.h17v03.006.2015288073333.hdf	6.0.14	6.0.27	2015-10-15T11:33:33.000Z
MOD13Q1.A2014177.h17v03.006.2015288071337.hdf	6.0.14	6.0.27	2015-10-15T11:13:37.000Z
MOD13Q1.A2014193.h17v03.006.2015289002421.hdf	6.0.14	6.0.27	2015-10-16T04:24:21.000Z
MOD13Q1.A2014209.h17v03.006.2015289032625.hdf	6.0.14	6.0.27	2015-10-16T07:26:25.000Z
MOD13Q1.A2014225.h17v03.006.2015289162859.hdf	6.0.14	6.0.27	2015-10-16T20:28:59.000Z
MOD13Q1.A2014241.h17v03.006.2015289183359.hdf	6.0.14	6.0.27	2015-10-16T22:33:59.000Z
MOD13Q1.A2014257.h17v03.006.2015291064214.hdf	6.0.14	6.0.27	2015-10-18T10:42:14.000Z
MOD13Q1.A2014273.h17v03.006.2015291111731.hdf	6.0.14	6.0.27	2015-10-18T15:17:31.000Z

MOD13Q1.A2014289.h17v03.006.2015291191340.hdf	6.0.14	6.0.27	2015-10-18T23:13:40.000Z
MOD13Q1.A2014305.h17v03.006.2015292061930.hdf	6.0.14	6.0.27	2015-10-19T10:19:30.000Z
MOD13Q1.A2014321.h17v03.006.2015292072241.hdf	6.0.14	6.0.27	2015-10-19T11:22:41.000Z
MOD13Q1.A2014337.h17v03.006.2015294144642.hdf	6.0.14	6.0.27	2015-10-21T18:46:42.000Z
MOD13Q1.A2014353.h17v03.006.2015295003808.hdf	6.0.14	6.0.27	2015-10-22T04:38:08.000Z
MOD13Q1.A2015001.h17v03.006.2015295101330.hdf	6.0.14	6.0.27	2015-10-22T14:13:30.000Z
MOD13Q1.A2015017.h17v03.006.2015295120129.hdf	6.0.14	6.0.27	2015-10-22T16:01:29.000Z
MOD13Q1.A2015033.h17v03.006.2015296123102.hdf	6.0.14	6.0.27	2015-10-23T16:31:02.000Z
MOD13Q1.A2015049.h17v03.006.2015297001700.hdf	6.0.14	6.0.27	2015-10-24T04:17:00.000Z
MOD13Q1.A2015065.h17v03.006.2015298005045.hdf	6.0.14	6.0.27	2015-10-25T04:50:45.000Z
MOD13Q1.A2015081.h17v03.006.2015298195011.hdf	6.0.14	6.0.27	2015-10-25T23:50:11.000Z
MOD13Q1.A2015097.h17v03.006.2015299005140.hdf	6.0.14	6.0.27	2015-10-26T04:51:40.000Z
MOD13Q1.A2015113.h17v03.006.2015299024003.hdf	6.0.14	6.0.27	2015-10-26T06:40:03.000Z
MOD13Q1.A2015129.h17v03.006.2015299151904.hdf	6.0.14	6.0.27	2015-10-26T19:19:04.000Z
MOD13Q1.A2015145.h17v03.006.2015301000719.hdf	6.0.14	6.0.27	2015-10-28T04:07:19.000Z
MOD13Q1.A2015161.h17v03.006.2015301073713.hdf	6.0.14	6.0.27	2015-10-28T11:37:13.000Z
MOD13Q1.A2015177.h17v03.006.2015301215450.hdf	6.0.14	6.0.27	2015-10-29T01:54:50.000Z
MOD13Q1.A2015193.h17v03.006.2015304014647.hdf	6.0.14	6.0.27	2015-10-31T05:46:47.000Z
MOD13Q1.A2015209.h17v03.006.2015304024556.hdf	6.0.14	6.0.27	2015-10-31T06:45:56.000Z
MOD13Q1.A2015225.h17v03.006.2015305194908.hdf	6.0.14	6.0.27	2015-11-02T00:49:08.000Z
MOD13Q1.A2015241.h17v03.006.2015305213843.hdf	6.0.14	6.0.27	2015-11-02T02:38:43.000Z
MOD13Q1.A2015257.h17v03.006.2015306145656.hdf	6.0.14	6.0.27	2015-11-02T19:56:56.000Z
MOD13Q1.A2015273.h17v03.006.2015307060134.hdf	6.0.14	6.0.27	2015-11-03T11:01:34.000Z
MOD13Q1.A2015289.h17v03.006.2015317212457.hdf	6.0.14	6.0.27	2015-11-14T02:24:57.000Z
MOD13Q1.A2015305.h17v03.006.2015335131645.hdf	6.0.14	6.0.27	2015-12-01T18:16:45.000Z
MOD13Q1.A2015321.h17v03.006.2015343140459.hdf	6.0.14	6.0.27	2015-12-09T19:04:59.000Z
MOD13Q1.A2015337.h17v03.006.2016004171707.hdf	6.0.14	6.0.27	2016-01-04T22:17:08.000Z
MOD13Q1.A2015353.h17v03.006.2016007181306.hdf	6.0.14	6.0.27	2016-01-07T23:13:06.000Z
MOD13Q1.A2016001.h17v03.006.2016029070523.hdf	6.0.14	6.0.27	2016-01-29T12:05:23.000Z
MOD13Q1.A2016017.h17v03.006.2016035114724.hdf	6.0.14	6.0.27	2016-02-04T16:47:24.000Z
MOD13Q1.A2016033.h17v03.006.2016050023403.hdf	6.0.14	6.0.27	2016-02-19T07:34:03.000Z
MOD13Q1.A2016049.h17v03.006.2016109133536.hdf	6.0.14	6.0.27	2016-04-18T17:35:36.000Z
MOD13Q1.A2016065.h17v03.006.2016111112509.hdf	6.0.14	6.0.27	2016-04-20T15:25:09.000Z
MOD13Q1.A2016081.h17v03.006.2016111112936.hdf	6.0.14	6.0.27	2016-04-20T15:29:36.000Z
MOD13Q1.A2016097.h17v03.006.2016114042322.hdf	6.0.14	6.0.27	2016-04-23T08:23:22.000Z
MOD13Q1.A2016113.h17v03.006.2016130115814.hdf	6.0.14	6.0.27	2016-05-09T15:58:14.000Z
MOD13Q1.A2016129.h17v03.006.2016147113013.hdf	6.0.14	6.0.27	2016-05-26T15:30:14.000Z
MOD13Q1.A2016145.h17v03.006.2016166144300.hdf	6.0.14	6.0.27	2016-06-14T18:43:00.000Z
MOD13Q1.A2016161.h17v03.006.2016184003323.hdf	6.0.14	6.0.27	2016-07-02T04:33:23.000Z
MOD13Q1.A2016177.h17v03.006.2016200095528.hdf	6.0.14	6.0.27	2016-07-18T13:55:28.000Z
MOD13Q1.A2016193.h17v03.006.2016215085155.hdf	6.0.14	6.0.27	2016-08-02T12:51:55.000Z
MOD13Q1.A2016209.h17v03.006.2016229083039.hdf	6.0.14	6.0.27	2016-08-16T12:30:39.000Z
MOD13Q1.A2016225.h17v03.006.2016243085340.hdf	6.0.14	6.0.27	2016-08-30T12:53:40.000Z
MOD13Q1.A2016241.h17v03.006.2016263150659.hdf	6.0.14	6.0.27	2016-09-19T19:06:59.000Z
MOD13Q1.A2016257.h17v03.006.2016274144931.hdf	6.0.14	6.0.27	2016-09-30T18:49:31.000Z
MOD13Q1.A2016273.h17v03.006.2016292071335.hdf	6.0.14	6.0.27	2016-10-18T11:13:35.000Z
MOD13Q1.A2016289.h17v03.006.2016306040154.hdf	6.0.14	6.0.27	2016-11-01T08:01:54.000Z
MOD13Q1.A2016305.h17v03.006.2016322051355.hdf	6.0.14	6.0.27	2016-11-17T10:13:55.000Z
MOD13Q1.A2016321.h17v03.006.2016340092657.hdf	6.0.14	6.0.27	2016-12-05T14:26:57.000Z
MOD13Q1.A2016337.h17v03.006.2016357045328.hdf	6.0.14	6.0.27	2016-12-22T09:53:28.000Z

MOD13Q1.A2016353.h17v03.006.2017010091501.hdf	6.0.14	6.0.27	2017-01-10T14:15:01.000Z
MOD13Q1.A2017001.h17v03.006.2017020214947.hdf	6.0.14	6.0.31	2017-01-21T02:49:47.000Z
MOD13Q1.A2017017.h17v03.006.2017034073715.hdf	6.0.14	6.0.31	2017-02-03T12:37:15.000Z
MOD13Q1.A2017033.h17v03.006.2017053061727.hdf	6.0.14	6.0.31	2017-02-22T11:17:27.000Z
MOD13Q1.A2017049.h17v03.006.2017066032758.hdf	6.0.14	6.0.31	2017-03-07T08:27:58.000Z
MOD13Q1.A2017065.h17v03.006.2017082120820.hdf	6.0.14	6.0.31	2017-03-23T16:08:21.000Z
MOD13Q1.A2017081.h17v03.006.2017111085102.hdf	6.0.14	6.0.31	2017-04-21T12:51:02.000Z
MOD13Q1.A2017097.h17v03.006.2017116143611.hdf	6.0.14	6.0.31	2017-04-26T18:36:11.000Z
MOD13Q1.A2017113.h17v03.006.2017131014717.hdf	6.0.14	6.0.31	2017-05-11T05:47:17.000Z
MOD13Q1.A2017129.h17v03.006.2017145233950.hdf	6.0.14	6.0.31	2017-05-26T03:39:50.000Z
MOD13Q1.A2017145.h17v03.006.2017164072204.hdf	6.0.14	6.0.31	2017-06-13T11:22:04.000Z
MOD13Q1.A2017161.h17v03.006.2017178080953.hdf	6.0.14	6.0.31	2017-06-27T12:09:53.000Z
MOD13Q1.A2017177.h17v03.006.2017194070426.hdf	6.0.14	6.0.31	2017-07-13T11:04:26.000Z
MOD13Q1.A2017193.h17v03.006.2017209235105.hdf	6.0.14	6.0.31	2017-07-29T03:51:05.000Z
MOD13Q1.A2017209.h17v03.006.2017234112605.hdf	6.0.14	6.0.31	2017-08-22T15:26:05.000Z
MOD13Q1.A2017225.h17v03.006.2017250141701.hdf	6.0.14	6.0.31	2017-09-07T18:17:01.000Z
MOD13Q1.A2017241.h17v03.006.2017262090831.hdf	6.0.14	6.0.31	2017-09-19T13:08:31.000Z
MOD13Q1.A2017257.h17v03.006.2017276132946.hdf	6.0.33	6.0.34	2017-10-03T17:29:46.000Z
MOD13Q1.A2017273.h17v03.006.2017290091109.hdf	6.0.33	6.0.34	2017-10-17T13:11:09.000Z
MOD13Q1.A2017289.h17v03.006.2017310142837.hdf	6.0.33	6.0.34	2017-11-06T19:28:37.000Z
MOD13Q1.A2017305.h17v03.006.2017325114248.hdf	6.0.33	6.0.34	2017-11-21T16:42:48.000Z
MOD13Q1.A2017321.h17v03.006.2017337222703.hdf	6.0.33	6.0.34	2017-12-04T03:27:03.000Z
MOD13Q1.A2017337.h17v03.006.2017353223911.hdf	6.0.33	6.0.34	2017-12-20T03:39:11.000Z
MOD13Q1.A2017353.h17v03.006.2018004225454.hdf	6.0.33	6.0.34	2018-01-05T03:54:54.000Z
MOD13Q1.A2018001.h17v03.006.2018017224914.hdf	6.0.33	6.0.34	2018-01-18T03:49:14.000Z
MOD13Q1.A2018017.h17v03.006.2018033224048.hdf	6.0.33	6.0.34	2018-02-03T03:40:48.000Z
MOD13Q1.A2018033.h17v03.006.2018049223512.hdf	6.0.33	6.0.35	2018-02-19T03:35:12.000Z
MOD13Q1.A2018049.h17v03.006.2018066165830.hdf	6.0.33	6.0.35	2018-03-07T21:58:30.000Z
MOD13Q1.A2018065.h17v03.006.2018082152058.hdf	6.0.33	6.0.35	2018-03-23T19:20:58.000Z
MOD13Q1.A2018081.h17v03.006.2018097234332.hdf	6.0.33	6.0.35	2018-04-08T03:43:32.000Z
MOD13Q1.A2018097.h17v03.006.2018113235016.hdf	6.0.33	6.0.35	2018-04-24T03:50:16.000Z
MOD13Q1.A2018113.h17v03.006.2018130000144.hdf	6.0.33	6.0.35	2018-05-10T04:01:44.000Z
MOD13Q1.A2018129.h17v03.006.2018151111223.hdf	6.0.33	6.0.35	2018-05-31T15:12:23.000Z
MOD13Q1.A2018145.h17v03.006.2018162005400.hdf	6.0.33	6.0.35	2018-06-11T04:54:00.000Z
MOD13Q1.A2018161.h17v03.006.2018178000133.hdf	6.0.33	6.0.35	2018-06-27T04:01:33.000Z
MOD13Q1.A2018177.h17v03.006.2018197103256.hdf	6.0.33	6.0.35	2018-07-16T14:32:56.000Z
MOD13Q1.A2018193.h17v03.006.2018210001831.hdf	6.0.33	6.0.35	2018-07-29T04:18:31.000Z
MOD13Q1.A2018209.h17v03.006.2018227125834.hdf	6.0.33	6.0.35	2018-08-15T16:58:34.000Z
MOD13Q1.A2018225.h17v03.006.2018242000129.hdf	6.0.33	6.0.35	2018-08-30T04:01:29.000Z
MOD13Q1.A2018241.h17v03.006.2018257235904.hdf	6.0.33	6.0.35	2018-09-15T03:59:05.000Z
MOD13Q1.A2018257.h17v03.006.2018282130739.hdf	6.0.33	6.0.35	2018-10-09T17:07:39.000Z

Table 14 Information and metadata about MODIS imagery (see Chapter 5).

8.3.2. Landsat 8 imagery

In Table 15 are provided the information and metadata of Landsat 8 imagery used to evaluate the effects of drought in some of the most important vineyards in Piedmont, and the impacts of drought on production of three main grape varieties, Barbera, Moscato Bianco, and Nebbiolo, in the years 2016-2018 (see Chapter 6).

Landsat 8 Product ID	File Date	Scene Centre Time	Sun Azimuth	Sun Elevation	Earth sun Distance
LC08_L1TP_194028_20160302_20170328_01_T1	2017-03-28T13:45:11Z	10:10:37.1156610Z	154,20231	33,67098	0,99122
LC08_L1TP_194028_20160318_20170328_01_T1	2017-03-28T01:18:06Z	10:10:31.8513220Z	152,95594	39,93247	0,99542
LC08_L1TP_194028_20160419_20170326_01_T1	2017-03-26T18:06:17Z	10:10:16.8746750Z	150,05675	52,04876	1,00450
LC08_L1TP_194028_20160521_20170324_01_T1	2017-03-24T16:55:15Z	10:10:19.6226290Z	144,83308	60,51207	1,01220
LC08_L1TP_194028_20160606_20170324_01_T1	2017-03-24T06:10:50Z	10:10:24.4361430Z	141,70997	62,45263	1,01487
LC08_L1TP_194028_20160622_20170323_01_T1	2017-03-23T20:42:10Z	10:10:29.2724770Z	139,55442	62,72611	1,01633
LC08_L1TP_194028_20160708_20170323_01_T1	2017-03-23T09:38:01Z	10:10:37.9899860Z	139,36505	61,49173	1,01671
LC08_L1TP_194028_20160724_20170322_01_T1	2017-03-22T22:35:53Z	10:10:43.3074130Z	141,39270	59,00108	1,01578
LC08_L1TP_194028_20160809_20170322_01_T1	2017-03-22T12:44:20Z	10:10:45.3813070Z	145,12047	55,46298	1,01376
LC08_L1TP_194028_20160825_20170322_01_T1	2017-03-22T01:53:28Z	10:10:52.2244400Z	149,74990	51,05759	1,01069
LC08_L1TP_194028_20160910_20170321_01_T1	2017-03-21T10:31:23Z	10:10:56.8747030Z	154,47275	45,95704	1,00682
LC08_L1TP_194028_20160926_20170319_01_T1	2017-03-19T15:52:48Z	10:10:57.5045390Z	158,69245	40,40605	1,00247
LC08_L1TP_194028_20161012_20170319_01_T1	2017-03-19T22:50:07Z	10:11:02.5317670Z	161,98021	34,71254	0,99784
LC08_L1TP_194028_20161231_20170314_01_T1	2017-03-14T16:22:47Z	10:10:57.3298170Z	161,46004	18,78110	0,98335
LC08_L1TP_194028_20170116_20170311_01_T1	2017-03-11T12:13:07Z	10:10:52.7842690Z	159,27682	20,50949	0,98371
LC08_L1TP_194028_20170217_20170228_01_T1	2017-02-28T21:11:51Z	10:10:39.3184080Z	155,40339	28,87474	0,98821
LC08_L1TP_194028_20170305_20170316_01_T1	2017-03-16T21:17:31Z	10:10:32.8464160Z	153,95933	34,72085	0,99191
LC08_L1TP_194028_20170406_20170414_01_T1	2017-04-14T09:37:41Z	10:10:15.8135170Z	151,41335	47,26552	1,00077
LC08_L1TP_194028_20170422_20170501_01_T1	2017-05-01T23:44:19Z	10:10:06.3341399Z	149,66040	52,95651	1,00529
LC08_L1TP_194028_20170524_20170614_01_T1	2017-06-14T12:21:10Z	10:10:15.5384359Z	144,26087	60,96139	1,01275
LC08_L1TP_194028_20170625_20170713_01_T1	2017-07-13T18:42:27Z	10:10:29.0058150Z	139,33296	62,60594	1,01651
LC08_L1TP_194028_20170727_20170810_01_T1	2017-08-10T14:00:32Z	10:10:39.3190850Z	141,89874	58,45039	1,01552
LC08_L1TP_194028_20170812_20170824_01_T1	2017-08-24T19:17:52Z	10:10:45.5906579Z	145,84985	54,75380	1,01326
LC08_L1TP_194028_20171015_20171024_01_T1	2017-10-24T15:19:50Z	10:11:01.1264780Z	162,40840	33,74051	0,99710
LC08_L1TP_194028_20171031_20171109_01_T1	2017-11-09T07:21:58Z	10:11:01.5387390Z	164,32174	28,38981	0,99269
LC08_L1TP_194028_20171116_20171122_01_T1	2017-11-22T08:53:03Z	10:10:58.0627919Z	164,99169	23,82291	0,98890
LC08_L1TP_194028_20180119_20180206_01_T1	2018-02-06T05:33:44Z	10:10:44.5132589Z	158,87392	20,98430	0,98398
LC08_L1TP_194028_20180204_20180220_01_T1	2018-02-20T22:34:41Z	10:10:35.3942080Z	156,82624	24,73199	0,98581
LC08_L1TP_194028_20180220_20180308_01_T1	2018-03-08T02:52:04Z	10:10:30.0090550Z	155,09868	29,81919	0,98882
LC08_L1TP_194028_20180308_20180320_01_T1	2018-03-20T03:07:33Z	10:10:21.7764490Z	153,70947	35,77943	0,99261
LC08_L1TP_194028_20180425_20180502_01_T1	2018-05-02T09:19:28Z	10:09:56.7956840Z	149,23352	53,83554	1,00598
LC08_L1TP_194028_20180511_20180517_01_T1	2018-05-17T11:14:47Z	10:09:47.2605400Z	146,58675	58,28872	1,00999
LC08_L1TP_194028_20180527_20180605_01_T1	2018-06-05T13:33:08Z	10:09:34.8487740Z	143,30828	61,27321	1,01317
LC08_L1TP_194028_20180628_20180704_01_T1	2018-07-04T09:52:04Z	10:09:45.3663779Z	138,90166	62,37078	1,01655
LC08_L1TP_194028_20180714_20180730_01_T1	2018-07-30T16:11:33Z	10:09:53.3256630Z	139,52128	60,68086	1,01653
LC08_L1TP_194028_20180730_20180814_01_T1	2018-08-14T02:36:37Z	10:10:00.3242860Z	142,24757	57,81696	1,01519
LC08_L1TP_194028_20180815_20180828_01_T1	2018-08-28T23:03:12Z	10:10:09.5764390Z	146,41084	53,97134	1,01283
LC08_L1TP_194028_20181002_20181010_01_T1	2018-10-10T06:10:35Z	10:10:28.4430630Z	159,78811	38,41097	1,00091

LC08_L1TP_194028_20181018_20181031_01_T1	2018-10-31T02:36:16Z	10:10:34.9962020Z	162,71843	32,76368	0,99632
LC08_L1TP_194028_20181205_20181211_01_T1	2018-12-11T16:02:46Z	10:10:37.7315390Z	164,25475	20,06262	0,98548
LC08_L1TP_194029_20160302_20170328_01_T1	2017-03-28T13:49:39Z	10:11:00.9982260Z	153,29935	34,81647	0,99122
LC08_L1TP_194029_20160318_20170328_01_T1	2017-03-28T01:15:55Z	10:10:55.7338870Z	151,87615	41,05700	0,99542
LC08_L1TP_194029_20160419_20170326_01_T1	2017-03-26T18:01:28Z	10:10:40.7530050Z	148,48253	53,12122	1,00450
LC08_L1TP_194029_20160521_20170324_01_T1	2017-03-24T16:55:27Z	10:10:43.5094310Z	142,59051	61,48413	1,01220
LC08_L1TP_194029_20160622_20170323_01_T1	2017-03-23T20:40:32Z	10:10:53.1592780Z	136,95326	63,59128	1,01633
LC08_L1TP_194029_20160724_20170322_01_T1	2017-03-22T22:36:10Z	10:11:07.1942150Z	139,17321	59,90694	1,01578
LC08_L1TP_194029_20160809_20170322_01_T1	2017-03-22T12:44:02Z	10:11:09.2681080Z	143,23954	56,44378	1,01376
LC08_L1TP_194029_20160825_20170322_01_T1	2017-03-22T01:49:51Z	10:11:16.1112410Z	148,21146	52,12454	1,01069
LC08_L1TP_194029_20160910_20170321_01_T1	2017-03-21T10:35:31Z	10:11:20.7615050Z	153,23696	47,10376	1,00682
LC08_L1TP_194029_20160926_20170319_01_T1	2017-03-19T15:56:53Z	10:11:21.3871050Z	157,69949	41,61661	1,00247
LC08_L1TP_194029_20161012_20170319_01_T1	2017-03-19T22:50:00Z	10:11:26.4185680Z	161,16728	35,96841	0,99784
LC08_L1TP_194029_20161231_20170314_01_T1	2017-03-14T16:22:50Z	10:11:21.2166190Z	160,90424	20,03226	0,98335
LC08_L1TP_194029_20170116_20170311_01_T1	2017-03-11T12:12:40Z	10:11:16.6710709Z	158,67771	21,73145	0,98371
LC08_L1TP_194029_20170217_20170228_01_T1	2017-02-28T21:15:38Z	10:11:03.2009730Z	154,61817	30,03960	0,98821
LC08_L1TP_194029_20170305_20170316_01_T1	2017-03-16T21:17:21Z	10:10:56.7289820Z	153,02884	35,86255	0,99191
LC08_L1TP_194029_20170406_20170414_01_T1	2017-04-14T09:41:24Z	10:10:39.6918470Z	150,06944	48,36275	1,00077
LC08_L1TP_194029_20170422_20170501_01_T1	2017-05-01T23:43:59Z	10:10:30.2124699Z	148,03319	54,02181	1,00529
LC08_L1TP_194029_20170508_20170515_01_T1	2017-05-15T23:42:43Z	10:10:28.1833640Z	145,35160	58,68652	1,00932
LC08_L1TP_194029_20170524_20170524_01_T1	2017-05-24T17:00:14Z	10:10:39.4252380Z	141,96374	61,92208	1,01275
LC08_L1TP_194029_20170812_20170824_01_T1	2017-08-24T19:17:12Z	10:11:09.4774610Z	144,02901	55,74874	1,01326
LC08_L1TP_194029_20171015_20171024_01_T1	2017-10-24T15:24:21Z	10:11:25.0175170Z	161,62029	35,00219	0,99710
LC08_L1TP_194029_20171116_20171122_01_T1	2017-11-22T08:43:25Z	10:11:21.9453590Z	164,39553	25,11641	0,98890
LC08_L1TP_194029_20180119_20180206_01_T1	2018-02-06T05:34:50Z	10:11:08.3958250Z	158,26410	22,20051	0,98398
LC08_L1TP_194029_20180220_20180308_01_T1	2018-03-08T02:55:15Z	10:10:53.8916210Z	154,29080	30,97928	0,98882
LC08_L1TP_194029_20180308_20180320_01_T1	2018-03-20T03:06:58Z	10:10:45.6590160Z	152,75001	36,91691	0,99261
LC08_L1TP_194029_20180425_20180502_01_T1	2018-05-02T09:17:56Z	10:10:20.6782510Z	147,55089	54,89324	1,00598
LC08_L1TP_194029_20180511_20180517_01_T1	2018-05-17T11:11:45Z	10:10:11.1388700Z	144,56645	59,29608	1,00999
LC08_L1TP_194029_20180527_20180605_01_T1	2018-06-05T13:34:58Z	10:09:58.7313399Z	140,95918	62,21628	1,01317
LC08_L1TP_194029_20180628_20180704_01_T1	2018-07-04T09:51:02Z	10:10:09.2531810Z	136,31704	63,22262	1,01655
LC08_L1TP_194029_20180714_20180730_01_T1	2018-07-30T16:11:31Z	10:10:17.2082300Z	137,11284	61,54695	1,01653
LC08_L1TP_194029_20180730_20180814_01_T1	2018-08-14T02:27:40Z	10:10:24.2110879Z	140,13832	58,74052	1,01519
LC08_L1TP_194029_20180815_20180828_01_T1	2018-08-28T23:04:02Z	10:10:33.4632419Z	144,64722	54,97693	1,01283
LC08_L1TP_194029_20181002_20181010_01_T1	2018-10-10T06:14:46Z	10:10:52.3298659Z	158,86160	39,63722	1,00091
LC08_L1TP_194029_20181018_20181031_01_T1	2018-10-31T02:38:58Z	10:10:58.8830050Z	161,95257	34,02902	0,99632
LC08_L1TP_194029_20181205_20181211_01_T1	2018-12-11T15:58:39Z	10:11:01.6098700Z	163,70313	21,34754	0,98548
LC08_L1TP_195028_20160121_20170405_01_T1	2017-04-05T11:51:34Z	10:16:59.5996630Z	158,69124	21,27158	0,98403
LC08_L1TP_195028_20160325_20170327_01_T1	2017-03-27T20:12:50Z	10:16:38.2657500Z	152,42773	42,71292	0,99738
LC08_L1TP_195028_20160410_20170326_01_T1	2017-03-26T23:05:16Z	10:16:31.4272920Z	151,04480	48,86012	1,00202
LC08_L1TP_195028_20160426_20170326_01_T1	2017-03-26T03:35:13Z	10:16:26.2747580Z	149,13101	54,32792	1,00640
LC08_L1TP_195028_20160528_20170324_01_T1	2017-03-24T12:06:19Z	10:16:33.0484040Z	143,42926	61,56995	1,01349
LC08_L1TP_195028_20160613_20170324_01_T1	2017-03-24T01:36:08Z	10:16:36.0492140Z	140,57162	62,77141	1,01564
LC08_L1TP_195028_20160629_20170323_01_T1	2017-03-23T15:07:08Z	10:16:44.2243450Z	139,19862	62,35759	1,01667
LC08_L1TP_195028_20160715_20170323_01_T1	2017-03-23T04:17:31Z	10:16:51.5869480Z	139,99713	60,54192	1,01643
LC08_L1TP_195028_20160731_20170322_01_T1	2017-03-22T19:09:50Z	10:16:55.3761260Z	142,86304	57,57093	1,01506
LC08_L1TP_195028_20160816_20170322_01_T1	2017-03-22T07:49:06Z	10:16:58.8617550Z	147,08855	53,63198	1,01249
LC08_L1TP_195028_20160901_20170321_01_T1	2017-03-21T21:05:15Z	10:17:05.6168940Z	151,84728	48,89779	1,00911
LC08_L1TP_195028_20161003_20170319_01_T1	2017-03-19T14:53:52Z	10:17:09.8675880Z	160,26195	37,90899	1,00047
LC08_L1TP_195028_20161206_20170317_01_T1	2017-03-17T15:30:24Z	10:17:13.3116890Z	164,21701	19,87160	0,98525

LC08_L1TP_195028_20161222_20170315_01_T1	2017-03-15T20:48:25Z	10:17:08.5906450Z	162,60518	18,64474	0,98367
LC08_L1TP_195028_20170107_20170311_01_T1	2017-03-11T22:38:23Z	10:17:05.9838840Z	160,51149	19,30757	0,98333
LC08_L1TP_195028_20170123_20170311_01_T1	2017-03-11T04:37:37Z	10:17:01.0494140Z	158,33537	21,83337	0,98434
LC08_L1TP_195028_20170328_20170414_01_T1	2017-04-14T02:33:43Z	10:16:30.4665120Z	152,18308	43,79134	0,99823
LC08_L1TP_195028_20170413_20170501_01_T1	2017-05-01T17:31:56Z	10:16:22.9000649Z	150,72279	49,85310	1,00275
LC08_L1TP_195028_20170429_20170515_01_T1	2017-05-15T17:48:00Z	10:16:12.1896890Z	148,74347	55,17170	1,00715
LC08_L1TP_195028_20170515_20170525_01_T1	2017-05-25T20:06:05Z	10:16:20.3910710Z	146,03736	59,30063	1,01091
LC08_L1TP_195028_20170531_20170615_01_T1	2017-06-15T21:02:11Z	10:16:30.2779520Z	142,85468	61,89108	1,01392
LC08_L1TP_195028_20170616_20170629_01_T1	2017-06-29T05:24:22Z	10:16:37.1318849Z	140,17699	62,80478	1,01587
LC08_L1TP_195028_20170718_20170727_01_T1	2017-07-27T22:21:47Z	10:16:45.5776320Z	140,33059	60,09916	1,01628
LC08_L1TP_195028_20170803_20170812_01_T1	2017-08-12T08:39:43Z	10:16:53.1570230Z	143,48141	56,94593	1,01464
LC08_L1TP_195028_20170819_20170826_01_T1	2017-08-26T12:08:28Z	10:16:58.4043519Z	147,86317	52,85996	1,01201
LC08_L1TP_195028_20170904_20170916_01_T1	2017-09-16T19:20:23Z	10:17:00.9509480Z	152,63364	48,00609	1,00838
LC08_L1TP_195028_20170920_20170930_01_T1	2017-09-30T05:46:03Z	10:17:03.8076460Z	157,10962	42,59864	1,00423
LC08_L1TP_195028_20171006_20171023_01_T1	2017-10-23T21:19:28Z	10:17:10.1163340Z	160,79935	36,91909	0,99963
LC08_L1TP_195028_20171209_20171223_01_T1	2017-12-23T08:42:15Z	10:17:03.0676080Z	163,96758	19,52641	0,98489
LC08_L1TP_195028_20171225_20180103_01_T1	2018-01-03T08:02:31Z	10:17:05.6300710Z	162,23798	18,61513	0,98353
LC08_L1TP_195028_20180211_20180222_01_T1	2018-02-22T03:54:56Z	10:16:44.1889579Z	156,02889	26,82055	0,98703
LC08_L1TP_195028_20180416_20180501_01_T1	2018-05-01T19:17:15Z	10:16:12.5862610Z	150,37387	50,82291	1,00357
LC08_L1TP_195028_20180518_20180604_01_T1	2018-06-04T22:28:08Z	10:15:52.9949760Z	145,19065	59,79216	1,01152
LC08_L1TP_195028_20180603_20180615_01_T1	2018-06-15T02:01:56Z	10:15:41.2446799Z	141,98701	62,08693	1,01430
LC08_L1TP_195028_20180619_20180703_01_T1	2018-07-03T15:06:22Z	10:15:50.6630250Z	139,52723	62,71275	1,01610
LC08_L1TP_195028_20180705_20180717_01_T1	2018-07-17T05:14:41Z	10:15:59.9140930Z	138,89425	61,79110	1,01669
LC08_L1TP_195028_20180806_20180815_01_T1	2018-08-15T00:51:20Z	10:16:15.4269580Z	143,94446	56,24523	1,01430
LC08_L1TP_195028_20180822_20180829_01_T1	2018-08-29T15:40:22Z	10:16:23.7432280Z	148,47517	52,02272	1,01143
LC08_L1TP_195028_20180907_20180912_01_T1	2018-09-12T19:02:01Z	10:16:29.6806710Z	153,27259	47,07037	1,00778
LC08_L1TP_195028_20180923_20180929_01_T1	2018-09-29T00:05:31Z	10:16:34.4529320Z	157,66890	41,60152	1,00343
LC08_L1TP_195028_20181009_20181029_01_T1	2018-10-29T23:00:06Z	10:16:42.4925040Z	161,21305	35,91763	0,99893
LC08_L1TP_195028_20181025_20181114_01_T1	2018-11-14T21:54:27Z	10:16:47.8342110Z	163,63008	30,39316	0,99436
LC08_L1TP_195028_20181212_20181226_01_T1	2018-12-26T23:00:21Z	10:16:46.7279919Z	163,66445	19,22662	0,98457
LC08_L1TP_195029_20160121_20170405_01_T1	2017-04-05T11:51:24Z	10:17:23.4822290Z	158,07497	22,48512	0,98403
LC08_L1TP_195029_20160325_20170327_01_T1	2017-03-27T20:06:12Z	10:17:02.1483150Z	151,25717	43,82826	0,99738
LC08_L1TP_195029_20160410_20170326_01_T1	2017-03-26T23:10:37Z	10:16:55.3056220Z	149,63132	49,95060	1,00202
LC08_L1TP_195029_20160426_20170326_01_T1	2017-03-26T03:34:46Z	10:16:50.1615600Z	147,41935	55,38359	1,00640
LC08_L1TP_195029_20160528_20170324_01_T1	2017-03-24T12:05:06Z	10:16:56.9352050Z	141,05403	62,51407	1,01349
LC08_L1TP_195029_20160613_20170324_01_T1	2017-03-24T01:32:21Z	10:16:59.9360160Z	137,99602	63,65732	1,01564
LC08_L1TP_195029_20160629_20170323_01_T1	2017-03-23T15:03:34Z	10:17:08.1111470Z	136,62408	63,21574	1,01667
LC08_L1TP_195029_20160715_20170323_01_T1	2017-03-23T04:17:42Z	10:17:15.4779850Z	137,61303	61,41832	1,01643
LC08_L1TP_195029_20160816_20170322_01_T1	2017-03-22T07:54:15Z	10:17:22.7485570Z	145,36016	54,65036	1,01249
LC08_L1TP_195029_20160901_20170321_01_T1	2017-03-21T21:00:25Z	10:17:29.5036960Z	150,44788	50,00117	1,00911
LC08_L1TP_195029_20161003_20170319_01_T1	2017-03-19T14:49:40Z	10:17:33.7543900Z	159,35515	39,14180	1,00047
LC08_L1TP_195029_20161206_20170317_01_T1	2017-03-17T15:30:16Z	10:17:37.1900190Z	163,66802	21,15623	0,98525
LC08_L1TP_195029_20161222_20170315_01_T1	2017-03-15T20:49:02Z	10:17:32.4732110Z	162,06012	19,91011	0,98367
LC08_L1TP_195029_20170107_20170311_01_T1	2017-03-11T22:42:47Z	10:17:29.8706859Z	159,94059	20,54625	0,98333
LC08_L1TP_195029_20170123_20170311_01_T1	2017-03-11T04:41:53Z	10:17:24.9319800Z	157,70711	23,04189	0,98434
LC08_L1TP_195029_20170328_20170414_01_T1	2017-04-14T02:34:04Z	10:16:54.3490779Z	150,97423	44,90246	0,99823
LC08_L1TP_195029_20170413_20170501_01_T1	2017-05-01T17:27:46Z	10:16:46.7826310Z	149,26149	50,93804	1,00275
LC08_L1TP_195029_20170429_20170515_01_T1	2017-05-15T17:48:03Z	10:16:36.0764910Z	146,97269	56,21916	1,00715
LC08_L1TP_195029_20170515_20170525_01_T1	2017-05-25T20:05:42Z	10:16:44.2778730Z	143,92505	60,29636	1,01091
LC08_L1TP_195029_20170531_20170531_01_RT	2017-05-31T17:14:19Z	10:16:54.1647550Z	140,43294	62,82372	1,01392

LC08_L1TP_195029_20170616_20170629_01_T1	2017-06-29T05:27:11Z	10:17:01.0144510Z	137,58671	63,68257	1,01587
LC08_L1TP_195029_20170718_20170720_01_RT	2017-07-20T00:40:13Z	10:17:09.4601979Z	137,99431	60,98249	1,01628
LC08_L1TP_195029_20170819_20170826_01_T1	2017-08-26T12:12:46Z	10:17:22.2911550Z	146,19371	53,89271	1,01201
LC08_L1TP_195029_20170904_20170916_01_T1	2017-09-16T19:19:06Z	10:17:24.8377500Z	151,28596	49,12271	1,00838
LC08_L1TP_195029_20170920_20170930_01_T1	2017-09-30T05:45:20Z	10:17:27.6944480Z	156,02916	43,78626	1,00423
LC08_L1TP_195029_20171006_20171023_01_T1	2017-10-23T21:13:57Z	10:17:33.9989010Z	159,92307	38,15905	0,99963
LC08_L1TP_195029_20171022_20171107_01_T1	2017-11-07T01:12:35Z	10:17:36.5082030Z	162,66683	32,60542	0,99515
LC08_L1TP_195029_20171209_20171223_01_T1	2017-12-23T08:51:49Z	10:17:26.9459389Z	163,42122	20,80805	0,98489
LC08_L1TP_195029_20171225_20180103_01_T1	2018-01-03T08:07:18Z	10:17:29.5126370Z	161,69060	19,87595	0,98353
LC08_L1TP_195029_20180211_20180222_01_T1	2018-02-22T03:53:54Z	10:17:08.0715240Z	155,29053	27,99513	0,98703
LC08_L1TP_195029_20180416_20180501_01_T1	2018-05-01T19:16:36Z	10:16:36.4688280Z	148,86292	51,90155	1,00357
LC08_L1TP_195029_20180518_20180604_01_T1	2018-06-04T22:26:13Z	10:16:16.8733060Z	143,01999	60,77252	1,01152
LC08_L1TP_195029_20180603_20180615_01_T1	2018-06-15T02:03:07Z	10:16:05.1314820Z	139,52012	63,00199	1,01430
LC08_L1TP_195029_20180619_20180703_01_T1	2018-07-03T15:07:01Z	10:16:14.5455920Z	136,92672	63,57708	1,01610
LC08_L1TP_195029_20180705_20180717_01_T1	2018-07-17T05:22:23Z	10:16:23.8008959Z	136,36609	62,64331	1,01669
LC08_L1TP_195029_20180721_20180731_01_T1	2018-07-31T07:07:08Z	10:16:30.7729490Z	138,19546	60,44481	1,01607
LC08_L1TP_195029_20180806_20180815_01_T1	2018-08-15T00:46:21Z	10:16:39.3137600Z	141,98490	57,20298	1,01430
LC08_L1TP_195029_20180822_20180829_01_T1	2018-08-29T15:37:59Z	10:16:47.6300300Z	146,86126	53,06670	1,01143
LC08_L1TP_195029_20180907_20180912_01_T1	2018-09-12T19:04:29Z	10:16:53.5674740Z	151,97246	48,19754	1,00778
LC08_L1TP_195029_20180923_20180929_01_T1	2018-09-29T00:07:16Z	10:16:58.3397350Z	156,62568	42,79733	1,00343
LC08_L1TP_195029_20181009_20181029_01_T1	2018-10-29T23:04:28Z	10:17:06.3793070Z	160,36384	37,16328	0,99893
LC08_L1TP_195029_20181025_20181114_01_T1	2018-11-14T21:53:16Z	10:17:11.7252489Z	162,91771	31,67021	0,99436

Table 15 Landsat 8 imagery metadata used to evaluate the effects of drought in some of the most important vineyards in Piedmont (see Chapter 6).

8.3.3. Sentinel-2 imagery

In Table 16 are provided the information and metadata of Sentinel-2 imagery used to evaluate the effects of drought in some of the most important vineyards in Piedmont, and the impacts of drought on production of three main grape varieties, Barbera, Moscato Bianco, and Nebbiolo, in the years 2016-2018 (see Chapter 6). All the imagery used are in Level-1C.

Name ID is composed and provide different information:

MMM_CCCC_MSI_YYY_ZZ_KKK_YYYYMMDDTHHMMSS_SYYYYMMDDTHHMMSS Nxx.yy

Mission Identifier (MMM) and File Class (CCCC) are as per the product naming convention.

The File Category comprises 3 characters and an ending underscore "_". For Granules this value is set to Multi-Spectral Instrument "MSI". The Semantic Descriptor (YYY_ZZ) where YYY may be "L0_" for Level-0, "L1A" for Level-1A, "L1B" for Level-1B, "L1C" for Level-1C and ZZ may be "GR" for Granule, "DS" for Data strip, "TL" for Tile, "TC" for True Color Image, or "CO" for Consolidated.

For Top of Atmosphere reflectances in cartographic geometry -Level-1C, the granules, also called tiles, are 100x100 km^2 ortho-images in UTM/WGS84 projection.

The starting point of the circulation data KKK. The allowed values are: SGS, MPS, MTI, EPA, UPA, CDAM, MPC.

The Applicability Start time identifies the Validity Start Time or the Data take Start Time (YYYYMMDDTHHMMSS_SYYYYMMDDTHHMMSS).

The Processing Baseline Number (Nxx.yy) identifies the current processing baseline where x and y may be a digit ranging from 0 to 9.

Sentinel-2 Product ID	File Date	Zenith Angle	Azimuth Angle	Tile Number
S2A_OPER_MSI_L1C_DS_SGS__20160113T143043_S20160113T102400_N02.01	2016-01-13T10:30:04.844Z	67,8977	163,3706	T32TMQ
S2A_OPER_MSI_L1C_DS_SGS__20160303T192800_S20160303T102108_N02.01	2016-03-03T10:21:08.969Z	53,5701	158,3175	T32TMQ
S2A_OPER_MSI_L1C_DS_SGS__20160323T160631_S20160323T102143_N02.01	2016-03-23T10:21:43.441Z	45,6444	157,2434	T32TMQ
S2A_OPER_MSI_L1C_DS_SGS__20160711T154947_S20160711T102030_N02.04	2016-07-11T10:20:30.066Z	26,1126	144,9775	T32TMQ
S2A_OPER_MSI_L1C_DS_SGS__20160721T154816_S20160721T102059_N02.04	2016-07-21T10:20:59.926Z	27,7080	146,1771	T32TMQ
S2A_OPER_MSI_L1C_DS_SGS__20160731T154018_S20160731T102107_N02.04	2016-07-31T10:21:07.142Z	29,7458	148,1147	T32TMQ
S2A_OPER_MSI_L1C_DS_SGS__20160810T160246_S20160810T102044_N02.04	2016-08-10T10:20:44.502Z	32,1794	150,5801	T32TMQ
S2A_OPER_MSI_L1C_DS_SGS__20160919T155227_S20160919T102112_N02.04	2016-09-19T10:21:12.580Z	44,9002	161,6252	T32TMQ
S2A_OPER_MSI_L1C_DS_SGS__20161029T172901_S20161029T102445_N02.04	2016-10-29T10:24:45.668Z	59,0793	168,2386	T32TMQ
S2A_OPER_MSI_L1C_DS_SGS__20161108T154744_S20161108T102425_N02.04	2016-11-08T10:24:25.911Z	62,1401	168,7412	T32TMQ

S2A_OPER_MSI_L1C_DS_SGS__20161208T173135_S20161208T102418_N02.04	2016-12-08T10:24:18.464Z	68,3932	167,6407	T32TMQ
S2A_OPER_MSI_L1C_DS_SGS__20161218T141626_S20161218T102606_N02.04	2016-12-18T10:26:06.867Z	69,1937	166,6024	T32TMQ
S2A_OPER_MSI_L1C_DS_SGS__20161228T172936_S20161228T102428_N02.04	2016-12-28T10:24:28.463Z	69,2533	165,3756	T32TMQ
S2A_OPER_MSI_L1C_DS_SGS__20160113T143043_S20160113T102400_N02.01	2016-01-13T10:30:04.844Z	68,7740	163,4046	T32TMR
S2A_OPER_MSI_L1C_DS_SGS__20160303T192800_S20160303T102108_N02.01	2016-03-03T10:21:08.969Z	54,4249	158,4756	T32TMR
S2A_OPER_MSI_L1C_DS_SGS__20160323T160631_S20160323T102143_N02.01	2016-03-23T10:21:43.441Z	46,4939	157,4838	T32TMR
S2A_OPER_MSI_L1C_DS_SGS__20160711T154947_S20160711T102030_N02.04	2016-07-11T10:20:30.066Z	26,8814	145,8711	T32TMR
S2A_OPER_MSI_L1C_DS_SGS__20160721T154816_S20160721T102059_N02.04	2016-07-21T10:20:59.926Z	28,4861	146,9791	T32TMR
S2A_OPER_MSI_L1C_DS_SGS__20160731T154018_S20160731T102107_N02.04	2016-07-31T10:21:07.142Z	30,5384	148,8037	T32TMR
S2A_OPER_MSI_L1C_DS_SGS__20160810T160246_S20160810T102044_N02.04	2016-08-10T10:20:44.502Z	32,9893	151,1488	T32TMR
S2A_OPER_MSI_L1C_DS_SGS__20160919T155227_S20160919T102112_N02.04	2016-09-19T10:21:12.580Z	45,7700	161,8086	T32TMR
S2A_OPER_MSI_L1C_DS_SGS__20161029T172901_S20161029T102445_N02.04	2016-10-29T10:24:45.668Z	59,9702	168,2686	T32TMR
S2A_OPER_MSI_L1C_DS_SGS__20161108T154744_S20161108T102425_N02.04	2016-11-08T10:24:25.911Z	63,0321	168,7578	T32TMR
S2A_OPER_MSI_L1C_DS_SGS__20161208T173135_S20161208T102418_N02.04	2016-12-08T10:24:18.464Z	69,2827	167,6472	T32TMR
S2A_OPER_MSI_L1C_DS_SGS__20161218T141626_S20161218T102606_N02.04	2016-12-18T10:26:06.867Z	70,0804	166,6125	T32TMR
S2A_OPER_MSI_L1C_DS_SGS__20161228T172936_S20161228T102428_N02.04	2016-12-28T10:24:28.463Z	70,1364	165,3926	T32TMR
S2A_OPER_MSI_L1C_DS_SGS__20170107T153933_S20170107T102658_N02.04	2017-01-07T10:26:58.239Z	68,5604	164,0522	T32TMQ
S2A_OPER_MSI_L1C_DS_SGS__20170216T153936_S20170216T102204_N02.04	2017-02-16T10:22:04.792Z	59,1355	159,4408	T32TMQ
S2A_OPER_MSI_L1C_DS_SGS__20170226T171842_S20170226T102458_N02.04	2017-02-26T10:24:58.867Z	55,5588	158,6607	T32TMQ
S2A_OPER_MSI_L1C_DS_SGS__20170308T154001_S20170308T102514_N02.04	2017-03-08T10:25:14.905Z	51,7223	158,0219	T32TMQ
S2A_OPER_MSI_L1C_DS_SGS__20170328T170003_S20170328T102018_N02.04	2017-03-28T10:20:18.464Z	43,7546	156,9940	T32TMQ
S2A_OPER_MSI_L1C_DS_SGS__20170328T174628_S20170328T102821_N02.04	2017-03-28T10:28:21.905Z	43,7546	156,9940	T32TMQ
S2A_OPER_MSI_L1C_DS_MPS__20170413T142452_S20170407T102343_N02.04	2017-04-07T10:23:43.496Z	39,8662	156,4352	T32TMQ
S2A_OPER_MSI_L1C_DS_SGS__20170417T154145_S20170417T102334_N02.04	2017-04-17T10:23:34.672Z	36,2008	155,7117	T32TMQ
S2A_OPER_MSI_L1C_DS_SGS__20170517T154043_S20170517T102352_N02.05	2017-05-17T10:23:52.107Z	27,6323	151,6269	T32TMQ
S2A_OPER_MSI_L1C_DS_SGS__20170527T154136_S20170527T102301_N02.05	2017-05-27T10:23:01.597Z	25,8972	149,6393	T32TMQ
S2A_OPER_MSI_L1C_DS_SGS__20170606T154806_S20170606T102456_N02.05	2017-06-06T10:24:56.040Z	24,8227	147,6282	T32TMQ
S2A_OPER_MSI_L1C_DS_SGS__20170616T154459_S20170616T102331_N02.05	2017-06-16T10:23:31.068Z	24,4175	145,9294	T32TMQ
S2A_OPER_MSI_L1C_DS_SGS__20170626T154604_S20170626T102321_N02.05	2017-06-26T10:23:21.851Z	24,6559	144,8547	T32TMQ
S2B_OPER_MSI_L1C_DS_MPS__20170701T123153_S20170701T102338_N02.05	2017-07-01T10:23:38.275Z	24,9943	144,6565	T32TMQ
S2A_OPER_MSI_L1C_DS_SGS__20170706T154812_S20170706T102301_N02.05	2017-07-06T10:23:01.202Z	25,4748	144,6753	T32TMQ
S2A_OPER_MSI_L1C_DS_SGS__20170716T155056_S20170716T102324_N02.05	2017-07-16T10:23:24.845Z	26,8178	145,4242	T32TMQ
S2A_OPER_MSI_L1C_DS_SGS__20170726T154546_S20170726T102259_N02.05	2017-07-26T10:22:59.590Z	28,6316	146,9938	T32TMQ
S2A_OPER_MSI_L1C_DS_EPA__20170809T212512_S20170805T102535_N02.05	2017-08-05T10:25:35.729Z	30,8617	149,2169	T32TMQ
S2A_OPER_MSI_L1C_DS_SGS__20170815T154731_S20170815T102513_N02.05	2017-08-15T10:25:13.077Z	33,4639	151,8690	T32TMQ
S2A_OPER_MSI_L1C_DS_SGS__20170825T154912_S20170825T102114_N02.05	2017-08-25T10:21:14.964Z	36,3979	154,7190	T32TMQ
S2A_OPER_MSI_L1C_DS_SGS__20170904T154956_S20170904T102511_N02.05	2017-09-04T10:25:11.085Z	39,6087	157,5859	T32TMQ
S2A_OPER_MSI_L1C_DS_SGS__20170914T154652_S20170914T102559_N02.05	2017-09-14T10:25:59.593Z	43,0378	160,3069	T32TMQ
S2A_OPER_MSI_L1C_DS_SGS__20170924T154031_S20170924T102649_N02.05	2017-09-24T10:26:49.096Z	46,6168	162,7598	T32TMQ
S2A_OPER_MSI_L1C_DS_SGS__20171014T153939_S20171014T102235_N02.05	2017-10-14T10:22:35.950Z	53,8667	166,5700	T32TMQ
S2A_OPER_MSI_L1C_DS_SGS__20171024T140204_S20171024T102105_N02.06	2017-10-24T10:21:05.456Z	57,3467	167,7942	T32TMQ
S2A_OPER_MSI_L1C_DS_MPS__20171106T195236_S20171103T102724_N02.06	2017-11-03T10:27:24.553Z	60,5808	168,5429	T32TMQ
S2B_OPER_MSI_L1C_DS_SGS__20171118T140451_S20171118T102306_N02.06	2017-11-18T10:23:06.456Z	64,7298	168,7398	T32TMQ
S2A_OPER_MSI_L1C_DS_SGS__20171213T140708_S20171213T102656_N02.06	2017-12-13T10:26:56.987Z	68,8642	167,1763	T32TMQ
S2A_OPER_MSI_L1C_DS_SGS__20170107T153933_S20170107T102658_N02.04	2017-01-07T10:26:58.239Z	69,4391	164,0795	T32TMR
S2A_OPER_MSI_L1C_DS_SGS__20170216T153936_S20170216T102204_N02.04	2017-02-16T10:22:04.792Z	59,9956	159,5495	T32TMR
S2A_OPER_MSI_L1C_DS_SGS__20170226T171842_S20170226T102458_N02.04	2017-02-26T10:24:58.867Z	56,4153	158,8006	T32TMR
S2A_OPER_MSI_L1C_DS_SGS__20170308T154001_S20170308T102514_N02.04	2017-03-08T10:25:14.905Z	52,5756	158,1977	T32TMR
S2A_OPER_MSI_L1C_DS_SGS__20170328T170003_S20170328T102018_N02.04	2017-03-28T10:20:18.464Z	44,6028	157,2578	T32TMR
S2A_OPER_MSI_L1C_DS_MPS__20170413T142452_S20170407T102343_N02.04	2017-04-07T10:23:43.496Z	40,7116	156,7541	T32TMR
S2A_OPER_MSI_L1C_DS_SGS__20170417T154145_S20170417T102334_N02.04	2017-04-17T10:23:34.672Z	37,0423	156,0961	T32TMR
S2A_OPER_MSI_L1C_DS_SGS__20170517T154043_S20170517T102352_N02.05	2017-05-17T10:23:52.107Z	28,4497	152,2901	T32TMR
S2A_OPER_MSI_L1C_DS_SGS__20170527T154136_S20170527T102301_N02.05	2017-05-27T10:23:01.597Z	26,7012	150,4133	T32TMR
S2A_OPER_MSI_L1C_DS_SGS__20170606T154806_S20170606T102456_N02.05	2017-06-06T10:24:56.040Z	25,6124	148,5008	T32TMR
S2A_OPER_MSI_L1C_DS_SGS__20170616T154459_S20170616T102331_N02.05	2017-06-16T10:23:31.068Z	25,1942	146,8688	T32TMR
S2A_OPER_MSI_L1C_DS_SGS__20170626T154604_S20170626T102321_N02.05	2017-06-26T10:23:21.851Z	25,4240	145,8143	T32TMR
S2B_OPER_MSI_L1C_DS_MPS__20170701T123153_S20170701T102338_N02.05	2017-07-01T10:23:38.275Z	25,7607	145,6065	T32TMR
S2A_OPER_MSI_L1C_DS_SGS__20170706T154812_S20170706T102301_N02.05	2017-07-06T10:23:01.202Z	26,2413	145,6037	T32TMR
S2A_OPER_MSI_L1C_DS_SGS__20170716T155056_S20170716T102324_N02.05	2017-07-16T10:23:24.845Z	27,5900	146,2782	T32TMR
S2A_OPER_MSI_L1C_DS_SGS__20170726T154546_S20170726T102259_N02.05	2017-07-26T10:22:59.590Z	29,4159	147,7441	T32TMR
S2A_OPER_MSI_L1C_DS_EPA__20170809T212512_S20170805T102535_N02.05	2017-08-05T10:25:35.729Z	31,6621	149,8491	T32TMR
S2A_OPER_MSI_L1C_DS_SGS__20170815T154731_S20170815T102513_N02.05	2017-08-15T10:25:13.077Z	34,2822	152,3814	T32TMR
S2A_OPER_MSI_L1C_DS_SGS__20170825T154912_S20170825T102114_N02.05	2017-08-25T10:21:14.964Z	37,2336	155,1196	T32TMR

S2A_OPER_MSI_L1C_DS_SGS__20170904T154956_S20170904T102511_N02.05	2017-09-04T10:25:11.085Z	40,4600	157,8880	T32TMR
S2A_OPER_MSI_L1C_DS_SGS__20170924T154031_S20170924T102649_N02.05	2017-09-24T10:26:49.096Z	47,4910	162,9137	T32TMR
S2A_OPER_MSI_L1C_DS_SGS__20171014T153939_S20171014T102235_N02.05	2017-10-14T10:22:35.950Z	54,7534	166,6359	T32TMR
S2A_OPER_MSI_L1C_DS_SGS__20171024T140204_S20171024T102105_N02.06	2017-10-24T10:21:05.456Z	58,2366	167,8341	T32TMR
S2A_OPER_MSI_L1C_DS_MPS__20171106T195236_S20171103T102724_N02.06	2017-11-03T10:27:24.553Z	61,4724	168,5657	T32TMR
S2B_OPER_MSI_L1C_DS_SGS__20171118T140451_S20171118T102306_N02.06	2017-11-18T10:23:06.456Z	65,6218	168,7493	T32TMR
S2A_OPER_MSI_L1C_DS_MPS__20171205T155256_S20171203T102404_N02.06	2017-12-03T10:24:04.068Z	68,5839	168,0735	T32TMR
S2A_OPER_MSI_L1C_DS_MPS__20180102T123237_S20180102T102420_N02.06	2018-01-02T10:24:20.462Z	69,0177	164,7504	T32TMQ
S2A_OPER_MSI_L1C_DS_SGS__20180211T154746_S20180211T102559_N02.06	2018-02-11T10:25:59.219Z	60,8642	159,9232	T32TMQ
S2A_OPER_MSI_L1C_DS_SGS__20180313T140648_S20180313T102540_N02.06	2018-03-13T10:25:40.551Z	49,8380	157,7789	T32TMQ
S2A_OPER_MSI_L1C_DS_MPS__20180323T123106_S20180323T102021_N02.06	2018-03-23T10:20:21.456Z	45,8381	157,2747	T32TMQ
S2A_OPER_MSI_L1C_DS_SGS__20180422T141352_S20180422T102115_N02.06	2018-04-22T10:21:15.970Z	34,5673	155,2706	T32TMQ
S2A_OPER_MSI_L1C_DS_SGS__20180512T140712_S20180512T102148_N02.06	2018-05-12T10:21:48.437Z	28,7931	152,5636	T32TMQ
S2A_OPER_MSI_L1C_DS_MPS__20180601T123308_S20180601T102024_N02.06	2018-06-01T10:20:24.463Z	25,3039	148,6544	T32TMQ
S2A_OPER_MSI_L1C_DS_MPS__20180701T123211_S20180701T102404_N02.06	2018-07-01T10:24:04.535Z	24,9726	144,6678	T32TMQ
S2A_OPER_MSI_L1C_DS_MPS__20180731T123218_S20180731T102701_N02.06	2018-07-31T10:27:01.317Z	29,6445	147,9753	T32TMQ
S2A_OPER_MSI_L1C_DS_SGS__20180810T142114_S20180810T102023_N02.06	2018-08-10T10:20:23.460Z	32,0593	150,4216	T32TMQ
S2A_OPER_MSI_L1C_DS_MPS__20180830T123227_S20180830T102524_N02.06	2018-08-30T10:25:24.509Z	37,8949	156,0820	T32TMQ
S2A_OPER_MSI_L1C_DS_SGS__20180909T155923_S20180909T102205_N02.06	2018-09-09T10:22:05.087Z	41,2180	158,8975	T32TMQ
S2A_OPER_MSI_L1C_DS_MPS__20180919T123234_S20180919T102018_N02.06	2018-09-19T10:20:18.462Z	44,7286	161,5035	T32TMQ
S2A_OPER_MSI_L1C_DS_SGS__20180929T122813_S20180929T102019_N02.06	2018-09-29T10:20:19.456Z	48,3440	163,8161	T32TMQ
S2A_OPER_MSI_L1C_DS_SGS__20181009T141444_S20181009T102559_N02.06	2018-10-09T10:25:59.595Z	51,9838	165,7310	T32TMQ
S2A_OPER_MSI_L1C_DS_SGS__20181019T123546_S20181019T102029_N02.06	2018-10-19T10:20:29.464Z	55,5468	167,2009	T32TMQ
S2A_OPER_MSI_L1C_DS_SGS__20181128T122538_S20181128T102346_N02.07	2018-11-28T10:28:23.817Z	66,8113	168,4016	T32TMQ
S2A_OPER_MSI_L1C_DS_MTI__20181208T105614_S20181208T102407_N02.07	2018-12-08T10:28:24.071Z	68,3388	167,6692	T32TMQ
S2B_OPER_MSI_L1C_DS_MPS__20180117T122826_S20180117T102341_N02.06	2018-01-17T10:23:41.462Z	67,1787	162,7603	T32TMQ
S2B_OPER_MSI_L1C_DS_SGS__20180226T154425_S20180226T102050_N02.06	2018-02-26T10:20:50.534Z	55,6521	158,6650	T32TMQ
S2B_OPER_MSI_L1C_DS_MPS__20180308T123007_S20180308T102241_N02.06	2018-03-08T10:22:41.383Z	51,8208	158,0282	T32TMQ
S2B_OPER_MSI_L1C_DS_SGS__20180407T143030_S20180407T102020_N02.06	2018-04-07T10:20:20.460Z	39,9597	156,4504	T32TMQ
S2B_OPER_MSI_L1C_DS_SGS__20180417T140522_S20180417T102021_N02.06	2018-04-17T10:20:21.457Z	36,2888	155,7149	T32TMQ
S2B_OPER_MSI_L1C_DS_SGS__20180616T154713_S20180616T102021_N02.06	2018-06-16T10:20:21.460Z	24,4243	145,9370	T32TMQ
S2B_OPER_MSI_L1C_DS_MPS__20180626T123321_S20180626T102626_N02.06	2018-06-26T10:26:26.849Z	24,6424	144,8701	T32TMQ
S2B_OPER_MSI_L1C_DS_SGS__20180706T140932_S20180706T102724_N02.06	2018-07-06T10:27:24.568Z	25,4492	144,6633	T32TMQ
S2B_OPER_MSI_L1C_DS_SGS__20180726T142914_S20180726T102150_N02.06	2018-07-26T10:21:50.652Z	28,5896	146,9128	T32TMQ
S2B_OPER_MSI_L1C_DS_SGS__20180805T142133_S20180805T102019_N02.06	2018-08-05T10:20:19.462Z	30,8110	149,1158	T32TMQ
S2B_OPER_MSI_L1C_DS_SGS__20180815T161223_S20180815T102017_N02.06	2018-08-15T10:20:17.456Z	33,4091	151,7432	T32TMQ
S2B_OPER_MSI_L1C_DS_SGS__20180904T141830_S20180904T102014_N02.06	2018-09-04T10:20:14.457Z	39,5360	157,4660	T32TMQ
S2B_OPER_MSI_L1C_DS_SGS__20180914T160343_S20180914T102014_N02.06	2018-09-14T10:20:14.459Z	42,9599	160,2026	T32TMQ
S2B_OPER_MSI_L1C_DS_SGS__20180924T175930_S20180924T102602_N02.06	2018-09-24T10:26:02.807Z	46,5298	162,6920	T32TMQ
S2B_OPER_MSI_L1C_DS_SGS__20181004T141056_S20181004T102018_N02.06	2018-10-04T10:20:18.457Z	50,1676	164,8210	T32TMQ
S2B_OPER_MSI_L1C_DS_SGS__20181024T160131_S20181024T102428_N02.06	2018-10-24T10:24:28.105Z	57,2643	167,7645	T32TMQ
S2B_OPER_MSI_L1C_DS_SGS__20181203T172205_S20181203T102604_N02.07	2018-12-03T10:28:27.610Z	67,6549	168,0927	T32TMQ
S2A_OPER_MSI_L1C_DS_MPS__20180102T123237_S20180102T102420_N02.06	2018-01-02T10:24:20.462Z	69,8988	164,7718	T32TMR
S2A_OPER_MSI_L1C_DS_SGS__20180122T140448_S20180122T102323_N02.06	2018-01-22T10:23:23.459Z	67,0859	162,1777	T32TMR
S2A_OPER_MSI_L1C_DS_SGS__20180211T154746_S20180211T102559_N02.06	2018-02-11T10:25:59.219Z	61,7265	160,0172	T32TMR
S2A_OPER_MSI_L1C_DS_SGS__20180313T140648_S20180313T102540_N02.06	2018-03-13T10:25:40.551Z	50,6902	157,9733	T32TMR
S2A_OPER_MSI_L1C_DS_MPS__20180323T123106_S20180323T102021_N02.06	2018-03-23T10:20:21.456Z	46,6877	157,5127	T32TMR
S2A_OPER_MSI_L1C_DS_SGS__20180402T155007_S20180402T102435_N02.06	2018-04-02T10:24:35.002Z	42,7281	157,0511	T32TMR
S2A_OPER_MSI_L1C_DS_SGS__20180422T141352_S20180422T102115_N02.06	2018-04-22T10:21:15.970Z	35,4065	155,6907	T32TMR
S2A_OPER_MSI_L1C_DS_SGS__20180512T140712_S20180512T102148_N02.06	2018-05-12T10:21:48.437Z	29,6164	153,1700	T32TMR
S2A_OPER_MSI_L1C_DS_MPS__20180701T123211_S20180701T102404_N02.06	2018-07-01T10:24:04.535Z	25,7391	145,6185	T32TMR
S2A_OPER_MSI_L1C_DS_MPS__20180731T123218_S20180731T102701_N02.06	2018-07-31T10:27:01.317Z	30,4360	148,6706	T32TMR
S2A_OPER_MSI_L1C_DS_SGS__20180810T142114_S20180810T102023_N02.06	2018-08-10T10:20:23.460Z	32,8681	150,9966	T32TMR
S2A_OPER_MSI_L1C_DS_SGS__20180820T143312_S20180820T102358_N02.06	2018-08-20T10:23:58.925Z	35,6525	153,6506	T32TMR
S2A_OPER_MSI_L1C_DS_MPS__20180830T123227_S20180830T102524_N02.06	2018-08-30T10:25:24.509Z	38,7383	156,4339	T32TMR
S2A_OPER_MSI_L1C_DS_SGS__20180909T155923_S20180909T102205_N02.06	2018-09-09T10:22:05.087Z	42,0757	159,1585	T32TMR
S2A_OPER_MSI_L1C_DS_MPS__20180919T123234_S20180919T102018_N02.06	2018-09-19T10:20:18.462Z	45,5978	161,6901	T32TMR
S2A_OPER_MSI_L1C_DS_SGS__20180929T122813_S20180929T102019_N02.06	2018-09-29T10:20:19.456Z	49,2220	163,9440	T32TMR
S2A_OPER_MSI_L1C_DS_SGS__20181009T141444_S20181009T102559_N02.06	2018-10-09T10:25:59.595Z	52,8680	165,8150	T32TMR
S2A_OPER_MSI_L1C_DS_SGS__20181019T123546_S20181019T102029_N02.06	2018-10-19T10:20:29.464Z	56,4351	167,2533	T32TMR
S2A_OPER_MSI_L1C_DS_MTI__20181118T105544_S20181118T102312_N02.07	2018-11-18T10:28:11.516Z	65,5596	168,7817	T32TMR
S2A_OPER_MSI_L1C_DS_SGS__20181128T122538_S20181128T102346_N02.07	2018-11-28T10:28:09.207Z	67,7026	168,4078	T32TMR
S2A_OPER_MSI_L1C_DS_MTI__20181208T105614_S20181208T102407_N02.07	2018-12-08T10:28:09.464Z	69,2283	167,6757	T32TMR

S2B_OPER_MSI_L1C_DS_SGS__20180226T154425_S20180226T102050_N02.06	2018-02-26T10:20:50.534Z	56,5085	158,8043	T32TMR
S2B_OPER_MSI_L1C_DS_MPS__20180308T123007_S20180308T102241_N02.06	2018-03-08T10:22:41.383Z	52,6741	158,2032	T32TMR
S2B_OPER_MSI_L1C_DS_SGS__20180417T140522_S20180417T102021_N02.06	2018-04-17T10:20:21.457Z	37,1303	156,0979	T32TMR
S2B_OPER_MSI_L1C_DS_MPS__20180626T123321_S20180626T102626_N02.06	2018-06-26T10:26:26.849Z	25,4106	145,8299	T32TMR
S2B_OPER_MSI_L1C_DS_SGS__20180726T142914_S20180726T102150_N02.06	2018-07-26T10:21:50.652Z	29,3732	147,6666	T32TMR
S2B_OPER_MSI_L1C_DS_SGS__20180805T142133_S20180805T102019_N02.06	2018-08-05T10:20:19.462Z	31,6107	149,7517	T32TMR
S2B_OPER_MSI_L1C_DS_SGS__20180815T161223_S20180815T102017_N02.06	2018-08-15T10:20:17.456Z	34,2266	152,2594	T32TMR
S2B_OPER_MSI_L1C_DS_SGS__20180904T141830_S20180904T102014_N02.06	2018-09-04T10:20:14.457Z	40,3867	157,7711	T32TMR
S2B_OPER_MSI_L1C_DS_SGS__20180914T160343_S20180914T102014_N02.06	2018-09-14T10:20:14.459Z	43,8236	160,4247	T32TMR
S2B_OPER_MSI_L1C_DS_SGS__20180924T175930_S20180924T102602_N02.06	2018-09-24T10:26:02.807Z	47,4037	162,8475	T32TMR
S2B_OPER_MSI_L1C_DS_SGS__20181004T141056_S20181004T102018_N02.06	2018-10-04T10:20:18.457Z	51,0490	164,9254	T32TMR
S2B_OPER_MSI_L1C_DS_SGS__20181024T160131_S20181024T102428_N02.06	2018-10-24T10:24:28.105Z	58,1540	167,8049	T32TMR
S2B_OPER_MSI_L1C_DS_SGS__20181203T172205_S20181203T102604_N02.07	2018-12-03T10:28:13.003Z	68,5455	168,0985	T32TMR

Table 16 Sentinel-2 imagery metadata used to evaluate the effects of drought in some of the most important vineyards in Piedmont (see Chapter 6).

8.4. Appendix 4.

This index optimises the vegetation signal and reduces the effects of the atmosphere and soil, because it is more sensitive to the structural parameters of the canopy, the type of coverage and plant architecture than other indices. The equation for EVI is as follows:

$$EVI = G \times \frac{NIR - RED}{NIR + C1 \times RED - C2 \times BLUE + L}$$

where NIR, RED and BLUE are the spectral reflectance of the near-infrared, and red and blue visible regions, respectively. L is the correction for plant cover background (undergrowth, litter, soil) that determines transmittance through vegetation in NIR and RED wavelengths. C1 and C2 are aerosol correction coefficients, which use the blue band to correct the aerosol effects in the red band. G is the Gain factor.